Universidade de Aveiro Departamento de Biologia
2016

Verónica Isabel Correia Bastos

As nanopartículas de prata induzem citotoxicidade e genotoxicidade nas linhas celulares da pele, fígado e sangue?

Do silver nanoparticles induce cytotoxicity and genotoxicity to skin, liver and blood cell lines?

Universidade de Aveiro Departamento de Biologia
2016

Verónica Isabel Correia Bastos

As nanopartículas de prata induzem citotoxicidade e genotoxicidade nas linhas celulares da pele, fígado e sangue?

Do silver nanoparticles induce cytotoxicity and genotoxicity to skin, liver and blood cell lines?

Tese apresentada à Universidade de Aveiro para cumprimento dos requisitos necessários à obtenção do grau de Doutor em Biologia, realizada sob a orientação científica da Doutora Maria da Conceição Santos, Professora Catedrática do Departamento de Biologia da Faculdade de Ciências da Universidade do Porto e co-orientação científica da Doutora Helena Cristina Correia de Oliveira, Estagiária de Pós-doutoramento do Centro de Estudos do Ambiente e do Mar e Departamento de Biologia da Universidade de Aveiro.

Apoio financeiro da Fundação para a Ciência e Tecnologia (FCT) – bolsa de investigação FCT SFRH/BD/81792/2011 e do FSE no âmbito do III Quadro Comunitário de Apoio. Apoio financeiro do POCTI no âmbito do III Quadro Comunitário de Apoio. Este trabalho foi ainda financiado pelo Fundo Europeu de Desenvolvimento Regional (FEDER) e Programa Operacional Fatores de Competitividade (COMPETE) CICECO (Ref. FCT UID/CTM/50011/2013), CESAM (Ref. FCT UID/AMB/50017/2013), FCOMP-01-0124-FEDER-021456 (Ref. FCT PTDC/SAU-TOX/120953/2010); e da Universidade de Aveiro.

“Chegará o tempo em que o homem conhecerá o íntimo de um animal e nesse dia todo crime contra um animal será um crime contra a humanidade.”
Lenardo da Vinci

o júri

Presidente

Professor Doutor João Manuel da Costa e Araújo Pereira Coutinho
Professor Catedrático do Departamento de Química da Universidade de Aveiro

Professora Doutora Eduarda das Graças Rodrigues Fernandes
Professora Associada com Agregação da Faculdade de Farmácia da Universidade do Porto

Doutor João Paulo Fernandes Teixeira
Investigador Auxiliar do Instituto Nacional de Saúde do Porto

Doutora Iola Melissa Fernandes Duarte
Equiparada a Investigadora Principal da Universidade de Aveiro

Professor Doutor Mário Guilherme Garcês Pacheco
Professor Auxiliar com Agregação da Universidade de Aveiro

Orientadora

Professora Doutora Maria da Conceição Lopes Vieira dos Santos
Professora Catedrática da Faculdade de Ciências da Universidade do Porto

agradecimentos

Gostaria de agradecer, em primeiro lugar, às minha orientadoras. À professora Doutora Conceição Santos por ter acreditado em mim e me ter proposto o concurso à bolsa de Doutoramento. Por todo apoio, motivação e oportunidades. À Doutora Helena Oliveira agradeço todo o apoio técnico e teórico, a disponibilidade e dedicação.

Ao Doutor Miguel Oliveira pelo apoio técnico e teórico na análise da expressão génica, bem como pela sua positiva intervenção no acompanhamento do trabalho.

À Doutora Iola Duarte pela sua participação activa no desenho do estudo bem como pelo envolvimento do seu projecto neste trabalho.

À FCT e ao departamento de Biologia por me terem acolhido e por me terem dado esta oportunidade.

To Dr Helionor Jonhston and Dr David Brown for having received me so well in Heriot-watt University in Edimburgh, giving me the opportunity to experience other reality and develop laboratory work with their group.

À Bárbara Correia, Cláudia Jesus, Joana Amaral, Fernanda Rosário, Diana Sousa, Sandra Nunes e Sónia Pinho pela partilha, pelo apoio, companhia e amizade nestes 4 anos de trabalho.

A todo(a)s o(a)s colegas de laboratório que de certa forma foram acompanhando o meu trabalho.

A todos os meus amigos e família que me apoiaram e com o seu amor e amizade me ajudaram a ultrapassar os momentos menos bons e a festejar os momentos bons.

Aos meus queridos pais que sempre acreditaram em mim e me incentivaram na realização do doutoramento. São pais maravilhosos, apoiam-me e amam-me incondicionalmente.

Ao meu marido por se ter casado comigo e partilhar todos os bons e maus momentos. “You fill my heart with gladness, take away all my sadness; Ease my troubles that’s what you do!”.

palavras-chave

Nanotoxicologia, nanopartículas de prata revestidas a citrato, nanopartículas de prata revestidas a PEG, células da pele, células do fígado, células do sangue, citotoxicidade, genotoxicidade.

resumo

As nanopartículas de prata (AgNPs) estão entre as nanopartículas mais utilizadas devido às suas propriedades fisico-químicas e biológicas (como por exemplo a sua eficiente actividade antimicrobiana). Contudo, existe uma crescente preocupação relativamente ao seu potencial impacto no ambiente e na saúde humana. Mais especificamente, ainda não está explicada a influência dos revestimentos das nanopartículas na citotoxicidade, inflamação e potencial genotóxico em células humanas. Neste estudo, as AgNPs revestidas com citrato ou poli(etilenoglicol) (PEG) foram utilizadas para determinar *in vitro* a influência do revestimento nos perfis de toxicidade das AgNPs em células da pele, fígado e sangue.

A linha celular de queratinócitos humanos (HaCaT) foi exposta a AgNPs de 30 nm revestidas com citrato ou PEG (Cit30 ou PEG30) onde foram determinados a viabilidade, stress oxidativo, produção de citoquinas, apoptose e efeito citostático. No geral, as Cit30 foram mais citotóxicas do que as PEG30 demonstrando a influência do revestimento relativamente ao modo da morte celular e à progressão do ciclo celular para as concentrações testadas (IC50 e IC20 para as Cit30, correspondendo a 40 µg/mL e 10 µg/mL, respectivamente). Enquanto que as Cit30 induzem morte por apoptose, as células expostas a PEG30 aparentemente estão numa fase precoce dos mecanismos de apoptose, tal como sugere a análise da expressão génica. As Cit30 foram posteriormente utilizadas para determinar o potencial genotóxico na mesma linha celular, através da determinação do dano no DNA e a indução de micronúcleos (MNi). Foi demonstrado que Cit30 induzem dano no DNA e provocam a ocorrência de MNi, bem como, a redução do Índice de Divisão Nuclear (NDI). Finalmente, e considerando que nesta linha de células a modulação do processo inflamatório é particularmente importante, as células foram expostas a AgNPs de 10 nm com revestimento de citrato ou PEG (Cit10 e PEG10). Os resultados mostraram que Cit10 e PEG10 modularam a resposta inflamatória de forma diferente, onde apenas PEG10 estimulou a indução do Factor Nuclear (NF)- κB. Contudo, ambas as AgNPs não estimularam a produção de citoquinas, mas antes, diminuiram a proteina quimio-atrativa de monócitos -1 (MCP1).

A linha celular humana de hepatoma (HepG2) também foi exposta a Cit30 e PEG30 para determinar a influência dos revestimento nos efeitos das AgNPs na viabilidade, apoptose, genes relacionados com a apoptose, ciclo celular e expressão génica de ciclinas. Estas células apresentaram uma sensibilidade similar às AgNPs com ambos os revestimentos, ocorrendo redução de viabilidade e comprometimento do ciclo celular para as concentrações testadas (IC50 e IC20 para as Cit30 que corresponde a 11 µg/mL e 5 µg/mL, respectivamente).

resumo (cont.)

A linha celular de macrofágos de ratinho (murganho) (RAW 264.7) foi utilizada para avaliar a citotoxicidade das Cit30, onde a viabilidade, stress oxidativo e as dinamicas do ciclo celular foram determinados. A proliferação e viabilidade das RAW 264.7 apenas decresceu após exposição a concentrações superiores a 75 µg/mL de Cit30, sugerindo uma baixa sensibilidade destas células a baixas concentrações de Cit30. Após exposição de 24 h o conteúdo de ROS (espécies reactivas de oxigénio) diminuiu nas células expostas a 60 µg/mL de Cit30 (IC20) o que pode ter contribuído para a tolerância destas células às AgNPs revestidas de citrato. Contudo, estas células apresentaram o ciclo celular comprometido e foi ainda observado um aumento de células na fase Sub-G1. Este aumento da população Sub-G1 está correlacionado com um aumento da fragmentação do DNA o que sugere um aumento de apoptose nestas células.

Assim, e comparando a resposta dos diferentes tipos celulares às AgNPs em termos de viabilidade celular, podemos concluir que os hepatócitos são os mais sensiveis às AgNPs e que os macrófagos parecem ser os mais tolerantes (das mais sensíveis para as mais tolerentes: HepG2>HaCaT>RAW 264.7). Este estudo sugere que o revestimento com PEG pode ser considerado como uma boa alternativa à estabilização das AgNPs com o citrato para a utilização ao nível da indústria e nas aplicações médicas em relação às células da pele humana. Contudo, para os hepatócitos, o potencial citotóxico das AgNPs foi independente dos revestimentos. Para além disso, e considerando que as AgNPs estão presentes num vasto número de produtos de consumo e a sua utilização tem sido provada como útil ao nível industrial e da engenharia biomédica, embora os nossos dados sugiram que no geral PEG-AgNP são menos tóxicas, mais investigação é necessária para determinar as propriedades que conferem menor toxicidade das AgNPs para as diferentes linhas celulares.

keywords

Nanotoxicology, citrate-coated silver nanoparticles, PEG-coated silver nanoparticles, skin cells, liver cells, blood cells, cytotoxicity, genotoxicity.

abstract

Silver nanoparticles (AgNPs) are among the most commonly used engineered NPs due to their physicochemical and biological properties (e.g. efficient antimicrobial activity). There is, however, a growing concern about their putative impact on the environment and on human health. In particular, there is no complete understanding of the influence of the coating on the cytotoxic, inflammatory and genotoxic potential of AgNPs to human cells. In this study, AgNPs coated with citrate or poly(ethylene glycol) (PEG) were used to assess in vitro the influence of coating on the AgNPs toxicity profiles on skin, liver and blood cells.

Human Keratinocyte cell line (HaCaT) was exposed to 30 nm AgNPs coated with citrate or PEG (Cit30 or PEG30) and assessed for viability, oxidative stress, cytokine production, apoptosis and cytostaticity. Overall Cit30 was more toxic than PEG30 demonstrating the influence of coating regarding the mode of cell death and cell cycle progression for the concentrations tested (IC50 and IC20 for citrate- AgNPs corresponding to 40 µg/mL and 10 µg/mL, respectively). While Cit30 AgNPs clearly induced apoptotic death, cells exposed to PEG30 AgNPs appeared to be at an earlier phase of apoptosis mechanisms, as supported by gene expression analysis. Later these Cit30 were used to assess genotoxic potential on the same cell line, by measuring DNA damage and micronuclei (MNi) induction. It was demonstrated that Cit30 induced DNA damage, and MNi occurrence as well as a reduction of NDI (Nuclear division index). Finally, and considering that in these cell lines the inflammatory modulation is particularly important, cells were exposed to 10 nm (citrate vs. PEG) AgNPs. Data showed that Cit10 and PEG10 differently modulate the inflammatory response, with only PEG10 stimulating the Nuclear factor (NF)-κB induction. However, both AgNPs did not stimulate the release of cytokines but decreased MCP1 (Monocyte chemoattractant protein-1).

Human Hepatoma cell line (HepG2) was also exposed to Cit30 and PEG30 to assess the influence of coating on the AgNPs effects on viability, apoptosis, apoptotic related genes, cell cycle and cyclins gene expression. These cells had similar sensitivity to both coatings, and suffered a decrease of viability as well as an impairment of the cells cycle for the concentrations tested (IC50 and IC20 for citrate- AgNPs corresponding to 11 µg/mL and 5 µg/mL, respectively).

Mouse macrophage cell line (RAW 264.7) was used to evaluate the cytotoxicity of Cit30, where viability, oxidative stress and cell cycle dynamics were assessed. The proliferation and viability of RAW 264.7 cells only decreased upon exposure to Cit30 at concentrations above 75 µg/mL, suggesting a low sensitivity of RAW cells to lower doses of these AgNPs.

abstract (cont.)

After 24 h exposure, ROS content decreased in cells exposed to 60 µg/mL AgNPs (IC20 value) which can have contributed to the high tolerance of these cells to citrate-AgNPs. However, these cells suffered an impairment of the cell cycle and an increase of cells at Sub-G1 phase was observed. This increase of the subG1 population is correlated with an increase of DNA fragmentation which suggests an increase of apoptosis in these cells.
Therefore, and taking together the different decreases on cells viability, we conclude that hepatocytes are more sensitive to AgNPs than keratinocytes and that macrophages seem the more tolerant (from the most sensitive for more tolerant: HepG2>HaCaT>RAW 264.7). This study suggests that PEG-coating can be regarded as a good alternative to citrate stabilization of AgNPs used in industrial and medical applications towards human skin cells. However, for hepatocyte cells, AgNPs cytotoxic potential was coating independent
Ultimately, and considering that AgNPs are present in a vast number of consumer products and their use has been proved to be helpful in industrial and biomedical engineering, despite our data suggest that overall PEG-AgNP are less toxic, more research is needed to determine the properties that confer less toxicity of AgNPs to different cell lines.

Most results presented in this thesis are part (integrated the main work) of the following papers of which V. Bastos is the first author:

→ Bastos V., Oliveira H., Rosário F., Remédios C., Ferreira de Oliveira J. M. P., Santos C. (2015). "Potential hazard effects of silver nanoparticles to the environment and human health" Chapter 77, In CRC Concise Encyclopedia of Nanotechnology, pp 984-995. ISBN: 1466580348.

→ Bastos V., Ferreira de Oliveira J. M. P., Brown D., Johnston H., Malheiro E., Silva A.L., Duarte I.F., Santos C., and Oliveira H. (2016). "The influence of citrate or PEG coating on silver nanoparticle toxicity to a human keratinocyte cell line". Toxicology Letters, 13;249:29-41. doi: 10.1016/j.toxlet.2016.03.005.

→ Bastos V., Brown D., Johnston H., Duarte I., Santos C. and Oliveira H. "Inflammatory responses of a human keratinocyte cell line to 10 nm citrate- and PEG-coated silver nanoparticles". *Submitted to* Journal of Nanoparticle Research, 2016. *Revisions Required*

→ Bastos V., Duarte I., Santos C. and Oliveira H. "Genotoxicity of citrate-coated silver nanoparticles to human keratinocytes assessed by the comet assay and cytokinesis blocked micronucleus assay".

→ Bastos V., Ferreira de Oliveira J. M. P., Duarte I.F., Santos C. and Oliveira H. (2016). "Coating independent cytotoxicity of Citrate- and PEG-coated silver nanoparticles to human hepatoma cell line". Journal of Environmental Sciences. *Accepted*

→ Bastos V., Duarte I., Santos C. and Oliveira H. "Effects of citrate- silver nanoparticles on RAW 264.7 cell line using a toolbox of cytotoxic endpoints".

The author also collaborated in research (marginaly related with this thesis) of the following paper:

→ Carrola J., Bastos V., Ferreira de Oliveira J. M. P., Oliveira H., Santos C., Gil A. M. and Duarte, I. F. (2015) "Insights into the impact of silver nanoparticles on human keratinocytes metabolism through NMR metabolomics". Arch Biochem Biophys, 589:53-61. doi: 10.1016/j.abb.2015.08.022.

→ Carrola J., Bastos V., Jarak I., Silva R., Malheiro E., Silva A.L., Oliveira H., Santos C., Gil A.M. and Duarte I.F. (2016). "Metabolomics of silver nanoparticles toxicity in HaCaT cells: structure-activity relationships and role of ionic silver and oxidative stress". Nanotoxicology. 4:1-13. doi: 10.1080/17435390.2016.1177744.

Index

List of abbreviations and symbols

Abs	Absorbance
AgNPs	Silver nanoparticles
CBMN	Cytokinesis-bock micronucleus assay
CCNB1	Cyclin B1 gene
CCNE1	Cyclin E1
CDK1	Cyclin-dependent kinase 1
CDK2	Cyclin-dependent kinase 2
cDNA	complementary deoxyribonucleic acid
Cit10	citrate- AgNPs 10 nm
Cit30	citrate- AgNPs 30 nm
DMSO	Dimethyl sulfoxide
FBS	Fetal bovine serum
IC50	Half maximal inhibitory concentration
IL-1β	Interleukin 1 beta
IL-6	Interleukin 6
IL-10	Interleukin 10
INF-γ	Interferon gamma
MA	Metabolic activity
MCP-1	Macrophage chemoattractant protein 1
MDI	Mitotic division index
MNi	Micronuclei
MTT	3-(4,5- dimethyl-2-thiazolyl)-2,5-diphenyl tetrazolium bromide
NAC	N-acetylcysteine
Mw	Molecular weight
NBUDs	Nuclear Buds
NPBs	Nucleoplasmic bridges
PBS	Phosphate buffered saline
PDI	Polydispersity index
PEG	poly(ethylene glycol)
PEG10	PEG- AgNPs 10 nm
PEG30	PEG- AgNPs 30 nm
PI	Propidium iodide
qPCR	quantitative real-time polymerase chain reaction

RNA	Ribonucleic acid
RNase	Ribonuclease
RT	Reverse transcriptase
ROS	Reactive oxygen species
STEM	Scanning transmission electron microscopy
TNF-α	Tumor necrosis factor alpha

Chapter 1

Introduction

Part of this chapter was already published as

V. Bastos, H. Oliveira, F. Rosário, C. Remédios, J.M.P Oliveira, and C. Santos (2015) Silver Nanoparticles: Potential Hazards of Silver Nanoparticles to the Environment and Human Health. Chapter 77, In CRC Concise Encyclopedia of Nanotechnology (Eds Boris Ildusovich Kharisov, Oxana Vasilievna Kharissova, Ubaldo Ortiz-Mendez). CRC Press ISBN: 1466580348, 1288 pages, pp 984-995

1. Introduction

The concept of nanotechnology was introduced by the American physicist and Nobel laureate, Richard Feynman, in 1959. In his lecture "*There's plenty room at the bottom*", Feynman draw the attention to the potential of small matter (near atomic scales) at the production of enhanced materials, products and devices (Feynman, 1960). However, the term Nanotechnology was first coined only several years later by the Japanese researcher Prof. Norio Taniguchi, in 1974. Nowadays, nanotechnology is an emerging science, with wide-ranging applications. In fact, the potential of nanomaterials (NMs) and their beneficial features are so vast that we are constantly witnessing the rise of applications/consumer products relaying on nanotechnology.

Nanoparticles (NPs), the building blocks of nanotechnology (Stern and McNeil, 2008), are particles with at least one dimension at 100 nm or less, with a high surface/volume ratio (Aitken et al., 2006; Buzea et al., 2007; Farre et al., 2011; Handy et al., 2008a; Handy et al., 2008b; Nowack and Bucheli, 2007; Stern and McNeil, 2008; Walker and Bucher, 2009), which confers specific physico-chemical properties as strength, electrical and optical features. In figure 1.1 it is represented the size of NPs and their location between particles only seen by electron microscopy to objects seen at unaided eye.

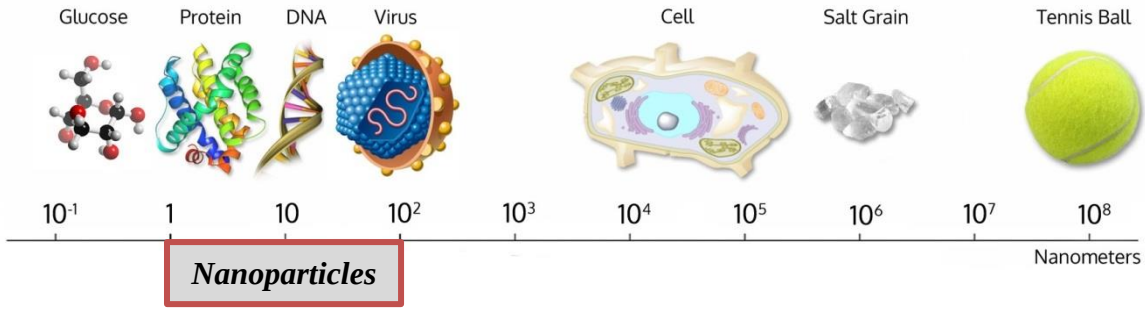

Figure 1.1: Size comparison from electron microscope to unaided eye (adapted form © *http://wichlab.com/research/*)

NPs can derive from natural and anthropic sources, particularly as engineered and/or as unwanted/incidental release (Biswas and Wu, 2005; Liden, 2011; Nowack and Bucheli, 2007; Tervonen et al., 2009). The natural sources of NPs are photochemical reactions, volcanic eruptions, forest fires, simple erosion, and plants and animals (shedding of skin and hair) (Buzea et al., 2007). Anthropic generation of NPs may be both engineered or incidental. Engineered NPs are classified as carbon NPs, metal oxide NPs, zero-valence metal NPs, quantum dots

(QDs) and dendrimers (Farre et al., 2011). Incidental generation of NPs may occur by the by-products of simple combustion, food cooking, and chemical manufacturing; welding or refining and smelting; combustion in vehicles and airplane engines; combustion of treated pulverized sewage sludge and combustion of coal and fuel oil for power generation.

With respect to NPs classification, they can be classified regarding their dimension, morphology, composition, uniformity and agglomeration (Buzea et al., 2007). From their multiple conformation, composition and nature, NPs present multiple functions and almost infinite applications. Indeed, what distinguishes them from the other particles is their small size and high surface/volume ratio, which confers specific properties to the NPs.

Silver-based nano-products show a wide range of applications, which justifies the increasing interest demonstrated by industry on these products. In particular, silver nanoparticles (AgNPs) present unusually enhanced physicochemical and biological properties and activities (including antimicrobial properties), which support the exponential use of these NPs (Behra et al., 2013; Eckhardt et al., 2013). The antimicrobial activity attributed to AgNPs is due to the release of Ag ions from these NPs (Chook et al., 2012) and despite Ag ions are known for long to be cytotoxic to a broad range of microorganisms, the conventional sources of Ag - as salt or metal, which may release the Ag ions respectively too rapidly or too inefficiently - have not been applied with success in e.g., biomedical applications. On other hand, Ag has already been considered by the U.S. Environmental Protection Agency (USEPA) as an environmental hazard and pollutant in natural waters and an environmental hazard, partly due to its persistence in the environment, bioaccumulative features and its high toxicity to life forms (Luoma, 2008). This author claims that nearly one-third of Ag-nanoproducts on the market in september 2007 might have the potential to disperse Ag or AgNP into the environment (Luoma, 2008). Therefore, risk assessments for some of those Ag-based nanoproducts, as well as estimations of mass discharges urge.

1.1.Characteristics and properties of AgNPs

The most fundamental entity of silver is the Ag cation (Ag^{+}), which makes it highly reactive. Indeed, Ag ion (~0.1 nm of ionic radius) is persistent, cannot be destroyed and can associate with other ions. In contrast, a AgNP is made of metallic silver ions in clusters (size 1-100 nm) and/or of silver compounds engineered into a particle of nanoscale size (Balogh et al., 2001) which is not necessarily persistent, since particles can dissolve or disaggregate. It is important to note that silver nanoparticles are usually engineered to release silver ions (the source of antibacterial activity as referred before) (Luoma, 2008).

AgNPs, once released into the environment, start to transform chemically and biochemically, modifying their properties, influencing their bioavailability, uptake and potential toxicity. Depending on their characteristics (figure 1.2) as the size, shape, coating, charge and structure and on the environmental conditions, AgNPs can aggregate or oxidize, releasing Ag^+ (Behra et al., 2013).

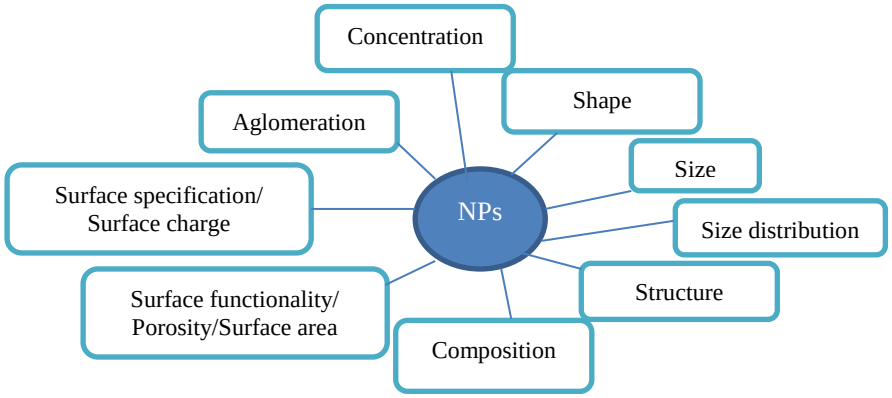

Figure 1.2: The variety of nanoparticles properties. (adapted from *Nanocomposix®* - *"Nanotoxicology: Particle Section"*)

The dissolution of AgNPs depends on the presence of oxygen or ligands, which increase the dissolution rate, forming Ag^+ or Ag^+ complexes (Xiu et al., 2011). Therefore, in order to control the colloidal stability, capping agents are usually used, since it influences the size, morphologies and interactions of AgNPs. The most frequently used capping agents are: citrate (Lee and Meisel, 1982); 3-(aminopropyl)trimethoxysilane (APS) (Pastoriza-Santos and Liz-Marzán, 1999); poly(vinylpyrrolidone) (PVP) (Nair and Laurencin, 2007); and polyethylene glycol (PEG). Beyond these, other polymers may be used as capping agents including polyacrylates, poly(vinyl)alcohol (PVA), polyacrylamide, poly(oxyethylene)-segmented imide (POEM), poly(styrene-co-maleic anhydride)-grafting poly(oxyalkylene) (SMA), silica, among others (Asharani et al., 2009a; Haase et al., 2011; Kim and Choi, 2012; Love and Haynes, 2010; Monteiro-Riviere et al., 2013; Nair and Laurencin, 2007; Wang et al., 2012).

Considering that AgNPs are present in a vast number of consumer products from industrial to biomedical contexts, it is important to determine if or which NPs are more cytotoxic, identifying the properties that confer AgNPs a lower toxicity. On other hand, while citrate is the most commonly reducing agent used to stabilize AgNPs (Gutierrez et al., 2015; Pillai and Kamat, 2004; Sharma et al., 2009), PEG coating has been increasingly used in nanomedical applications (Ginn et al., 2014; Jain and Jain, 2008; Ryan et al., 2008). Therefore, and as comparative studies on these coating formulations' cytotoxicity are scarce, in this work, citrate and PEG coated-

AgNPs were used to further characterize their cytotoxic and genotoxic potential.

Citrate

Citrate is a derivate of citric acid. The formula of the citrate ion is $C_6H_5O_7^{3-}$ or $C_3H_5O(COO)_3^{3-}$ and the figure 1.3 represents their structure form.

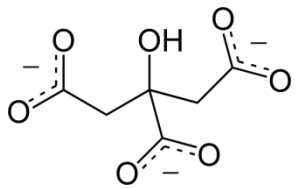

Figure 1.3: Structure form of citrate.

Citrate- coating is one of the most popular silver colloids (Pillai and Kamat, 2004; Tolaymat et al., 2010; Zhang et al., 2011). It is used as both reducing agent and stabilizer of the particles by decorating them with negative charges (Henglein and Giersig, 1999; Wiley et al., 2005; Wiley et al., 2007). The citrate- AgNPs structure is exemplified in figure 1.4.

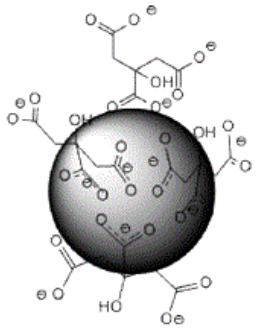

Figure 1.4: Example of Citrate-coated AgNPs structure. © *http://cnsi.ctrl.ucla.edu/nanoscience/pages/biotoxicity*

Polyethylene glycol (PEG)

PEG is a polyether compound, a synthetic biodegradable polymer and it has been applied to numerous biomedical applications (Jegatheeswaran and Sundrarajan, 2015). The structure of PEG is represented in figure 1.5.

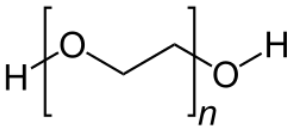

Figure 1.5: Structure form of poly(ethylene) glicol (PEG).

PEG- coating is also used as a reducing agent and stabilizer (Luo et al., 2005; Popa et al., 2007), with many applications from industrial manufacturing to medicine (Thorley et al 2013). Coating particles with low molecular weight PEG renders particles with a neutral charge, significantly improving transport of particles across the mucus layer (Lai et al., 2009; Suk et al., 2011). The PEG- AgNPs structure is exemplified in figure 1.6.

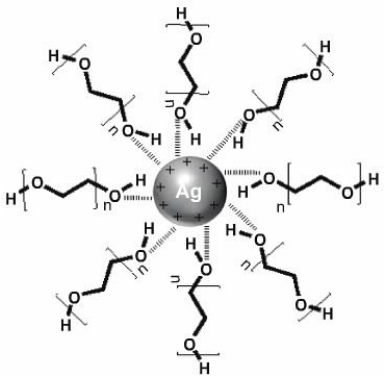

Figure 1.6: Chemical structure of AgNPs coated with PEG (from Jazayeri et al., (2013))

The advent of nanotechnology has prompted the characterization of many NMs and the development of new nanotechnology-based products, but nanoscale silver is not a new finding and it has been known and used over the last 100 years (Nowack et al., 2011).

Currently, AgNPs are explored in a wide range of applications, from medicine and industry to the most common consumer products. As mentioned before this nanomaterial exhibits a broad spectrum of antibacterial activity, against both Gram-negative and Gram-positive bacteria (Panacek et al., 2006). Furthermore, AgNPs are reported to exert an efficient bactericidal activity on drug-resistant strains (Prakash et al., 2013) and to enhance the activity of several antibiotics (Shahverdi et al., 2007). Although the mechanisms of action of AgNPs against fungi are not so clear, its antifungal activity has been confirmed in various genera (Kim et al., 2009a; Qian et al., 2013; Xu et al., 2013). Similarly, it was suggested that AgNPs should be considered as a potential antiviral agent (Galdiero et al., 2011), as studies have demonstrated AgNPs activity against HIV-1 (Elechiguerra et al., 2005), Monkeypox virus (Rogers et al., 2008), and

herpes simplex virus (Baram-Pinto et al., 2009), among others. The ability to destroy an extensive variety of microorganisms gave rise to the widespread use of nanosilver in disinfectant products for virtually all situations, such as groundwater (Mpenyana-Monyatsi et al., 2012), wastewater treatment (Sheng and Liu, 2011) and air filters improvement (Miaśkiewicz-Peska and Łebkowska, 2011). AgNPs are vastly used in medical applications that include antibacterial coatings, diagnosis, cancer therapy and/or drug delivery. To reduce nosocomial infections, AgNPs has been incorporated in antibacterial coatings on medical devices and tools and it can be found in catheters (Bayston et al., 2007), face masks (Li et al., 2006), wound dressings (Li et al., 2013a) and gel formulations for topical use (Jain et al., 2009). Materials used in orthopedics including bone cements (Alt et al., 2004), dentistry (García-Contreras et al., 2011) and ophthalmic (Weisbarth et al., 2007) can contain nanosilver, as well.

Moreover, nanosilver is a potential candidate for cancer treatment. Gurunathan and colleagues (2009) have reported that AgNPs (40 nm) inhibited in vitro cell proliferation and migration in vascular endothelial growth factor (VEGF)-induced angiogenesis in bovine retinal epithelial cells (BREC) and formation of new blood vessels, demonstrating its anti-angiogenic effects. Furthermore, the surface size of AgNPs was found to enhance the thermal sensitivity of glioma cells (Liu et al., 2011a). The possibility of using AgNPs to achieve scar-less wound healing has been also suggested, as several studies highlight the anti-inflammatory properties of these NPs (Bhol and Schechter, 2005; Nadworny et al., 2010).

The unique physico-chemical properties of AgNPs confer them great interest for scientific applications. Upon irradiation with light, metallic NPs exhibit surface plasmon resonance (SPR) – electron charge density waves proportional to their mass - and, as result, SPR peaks in the UV-Vis wavelength range are produced. The characteristics of the SPR peaks depend on various properties of NMs (Ju-Nam and Lead, 2008). Such features make AgNMs valuable tools for enhanced infrared (IR) absorption spectroscopy (Huo et al., 2006), colorimetric sensors (Dubas and Pimpan, 2008; Xiong et al., 2008), among others. The association of nanosilver and surface enhanced Raman scattering (SERS) shows potential in genetic analysis, biomedical diagnostics, and cellular imaging (Vo-Dinh et al., 2010). Another characteristic of metallic nanoparticles, including AgNPs, is the alteration of the intrinsic spectral properties of fluorophores, which enables its use for metal enhanced fluorescence applications (Yang et al., 2013).

The industrial sector has profited with the advances in nanotechnology, too. Silver nanocomposites have been used to catalyse many reactions in industrial processes (Yan et al., 2006). The high electrical conductivity associated with other properties of nanosilver makes this a versatile material to explore in electronics (Roldán et al., 2007).

According to the "living" inventory of nanotechnology-based consumer products compiled by the Project on Emerging Nanotechnologies (http://www.nanotechproject.org/cpi), from the

estimated 1,814 “nano” products that were introduced in the market (revised inventory released in October 2013), 24% are nanosilver-containing products. A wide range of AgNPs applications has emerged in consumer products ranging from household products and electronics to personal care products, including sanitation products (air sanitizer sprays, water filters, swimming pool disinfectants), paints, household appliances (refrigerators, vacuum cleaners, washing machines), consumer electronics (cellular phones, hair straighteners), detergents and fabric softeners, surface cleaners, food supplements, and food contact materials (food storage containers, food packaging materials, water taps, tableware) (EPA, 2010). This AgNPs property has also been explored in textiles, with the production of fabrics (cotton, wool, etc.) that contain AgNPs. These fabrics are widely used in socks to destroy bacteria associated with foot odour (Benn and Westerhoff, 2008), but can also be found in clothing and textiles as shoe insoles, sportswear, underwear, towels, sheets, pillows, and mattress covers. Other examples of consumer products that contain nanosilver include toys, baby carriages, pacifiers, watch chains, cosmetics and personal care products (lotions, soap, shampoo, toothpaste, toothbrush, mouthwash, female-hygiene products, sunscreen), and even spermicidal foam (EPA, 2010).

As the applications of NPs (in particular of AgNPs) and consequent release into the environment have exponentially increased in the last years, their putative risks associated to human exposure have also raised up. It is therefore urgent to know whether the presence of nanosilver in these products is essential or not, as well as to fully investigate all the aspects concerning the impact on human health and environment prior an extensive use (Nowack and Bucheli, 2007).

1.2.Fate, distribution and bioaccumulation of AgNPs

Once metal NPs are released into the environment, it is almost impossible to predict their fate and distribution in soil and water ecosystems, since they can change according to local environmental conditions depending on multiple variables (El Badawy et al., 2010; Simonet and Valcárcel, 2009). The fate and distribution of metal NPs also depend on their transport ability through the ecosystem. This is conditioned by the physico-chemical properties of these metal NPs that may change as result of their interaction with medium and by their retention in smaller pore spaces (Lecoanet and Wiesner, 2004; McDowell-Boyer et al., 1986; Sagee et al., 2012; Sirivithayapakorn and Keller, 2003). Regarding AgNPs, its bioavailability is influenced by their interaction with soil components and transportation through soil and also by the activity of soil organisms (Liang et al., 2013). Sagee, Dror et al., (2012) demonstrated that AgNP transport is

sensitive to the NP surface, porous material and also to the chemical composition of the solution. Soils with small aggregates present a large surface area, thus decreasing the transport of AgNPs as there is a higher surface available for AgNP interaction. Other studies showed that the transport, aging and transformation of AgNPs depend on the presence of organic matter (OM) such as surfactants or humic acids. OM tends to enhance the mobility of AgNPs, while higher ionic strength and divalent cations promote aggregation and retention (Benn and Westerhoff, 2008; Cornelis et al., 2013; Coutris et al., 2012; Geranio et al., 2009; Levard et al., 2012; Lin et al., 2012; Nowack and Bucheli, 2007; Tourinho et al., 2012). Regarding soil organisms, Shoults-Wilson et al (2011a) studied AgNPs effects on earthworms demonstrating significant decrease in *Eisenia fetida* reproduction. Other study determined the role of particle size and soil type on the toxicity of AgNPs to the earthworm *Eisenia fetida*, suggesting that soil type is a more important determinant of Ag accumulation from AgNPs than particle size (Shoults-Wilson et al., 2011b). Also Coleman and collaborators (Coleman, Kennedy et al 2013) used the sediment-dwelling invertebrate, *Lumbriculus variegatus* to assess the impact, bioaccumulation, tissue distribution, uptake, and depuration of AgNPs on ecosystem.

In respect to plants, Stampoulis et al (2009) studied the effects of AgNPs on *Cucurbita pepo* (zucchini). The researchers, during a 15-day hydroponic trial growing the plants in hydroponic solutions amended with 1000mg/L of AgNPs, demonstrate a reduction by 75% of plants biomass. These studies on earthworms and plants help to elucidate the possible fate and bioavailability of these particles, but more information on higher-level organisms and possible bioaccumulation is also needed (Remédios et al., 2012).

AgNPs in the soil appear to end up in ground and surface water and watercourses. Water natural colloids interact with AgNPs affecting their behavior, bioavailability and toxicity. Previous studies on the environmental and physiological implications of Ag ions and AgNPs exposure in seawater and freshwater organisms support the need for further assessment studies and support the increasing concern on the impacts of AgNPs on ecosystems (Fabrega et al., 2011; Matranga and Corsi, 2012; Joo et al., 2013; Zuykov et al., 2011).

NPs interaction with natural colloids present on aquatic system, will be dependent on their surface coating. Studies on coated AgNPs showed that usually they present more threat to water column organisms, opposite to uncoated AgNPs that present higher toxicity to sediment and filter organisms (Navarro et al., 2008). NPs coating disfavor their medium removal, but prevents NPs aggregation, increasing their bioavailability, mobility and their contact with organisms. In contrast, uncoated NPs tend to aggregate and to be removed from water columns by sedimentation, which make sediment organisms more exposed, specially via ingestion and filtration (Fabrega et al., 2009; Fabrega et al., 2011; Navarro et al., 2008; Ward and Kach, 2009). In water systems the most threatening toxicity may be provided by AgNP itself and not

from the Ag^+ ion dissolution, since in oxidative conditions it may take from 6 days to several months for complete dissolution of a 5 nm AgNP (Fabrega et al., 2011). Temperature, pH and salinity may also influence the aggregation behavior. For instance high concentrations of NaCl in seawater, decrease electrostatic colloidal stabilization due to charge screening, increasing the probability to sedimentation (Chinnapongse et al., 2011). It was demonstrated that uncoated AgNPs can be more bioaccessible than other particles and even, than $AgNO_3$, since uncoated AgNPs can act as constant source of relatively stable and bioaccessible Ag, while $AgNO_3$ is rapidly immobilized in soil (Coutris et al., 2012). However, in another study Bastos et al (2012) demonstrated that Ag and Ti uncoated NPs showed high heterogeneous effects on cells behavior, and suggested that uncoated NPs may present different agglomeration states which could have considerable impact on final effect on the cell.

The degree of bioaccumulation is also an important aspect to consider when evaluating hazards and risks of AgNPs. It is determined by a balance between the rate of uptake of AgNPs and the rate of loss and dilution by growth; which varies with time exposure, concentration, nature of the environment, route of exposure and biology and ecology of the organism (Fabrega, Luoma, Tyler, Galloway, & Lead, 2011).

1.3.Effects of AgNPs in tissue/organs

There are three principal routes of xenobiotic entrance from environment into human body: percutaneous, respiratory and oral. After a compound enters the body penetrating the initial cellular barrier (such as skin, intestinal mucosa or the lining of the respiratory tract), it enters interstitial fluid, penetrates the capillaries and enters the bloodstream, which distributes it throughout the body (Zakrzewski, 2002). For NPs, several uptake and translocation pathways have already been deciphered while other routes remain hypothetical (Fig 1.7., see Oberdörster et al., (2005) for review). According to these authors, investigation mostly focuses routes involving translocation, accumulation and retention in critical target sites. However, potential toxicity and its relation with NPs physicochemical characteristics remains little explored.

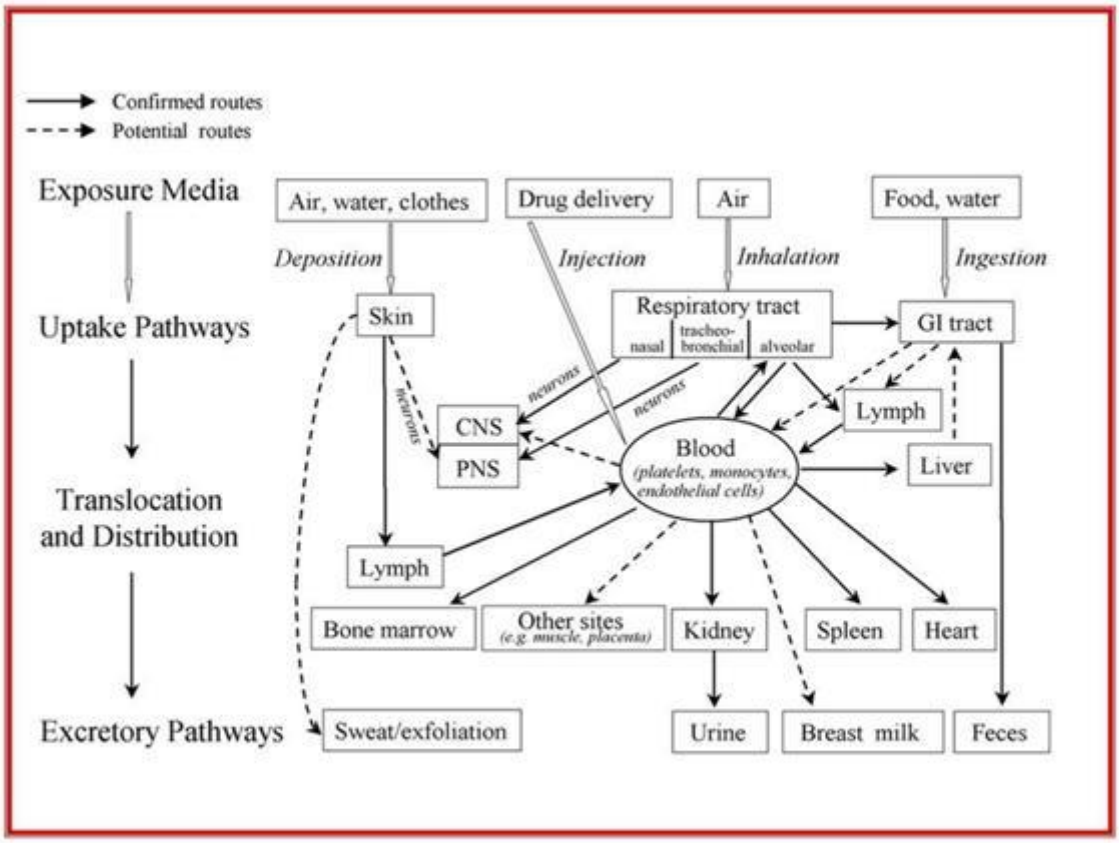

Figure 1.7: Biokinetics of Nano-sized Particles. While many uptake and translocation routes have been demonstrated, others still are hypothetical and need to be investigated (From Oberdorster et al (2005)).

AgNPs may enter in human and animal bodies by several routes of exposure, such as, ingestion, inhalation, dermal contact, or by injection. The main target organs are the skin, lungs, liver, spleen, brain, kidneys, adrenals and testes. AgNPs could also pass through blood vessels walls and lymphatic system which allows them to be transported all over the body (Kruszewski et al., 2011). Loeschner and coworkers (2011) studied an oral exposure of AgNPs to rats, during 28 days, and found that the largest silver concentrations were detected in intestinal system, liver and kidneys, although was also found in lungs and brain.

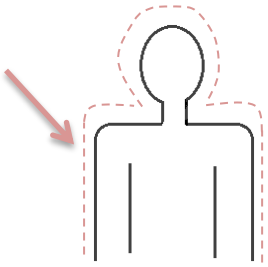

Skin

The skin forms a protective barrier, separating the body from the environment. However, three routes of percutaneous absorption are possible: diffusion through the epidermis into the dermis, entry through the sweat adducts and entry along the hair-follicle orifices. Due to their large surface area, it is believed that absorption through the epidermal cells is the major route of entry of toxins. The main obstacle to

percutaneous penetration of water and xenobiotics is the *stratum corneum* (outermost membrane). The entry of substances through the *stratum corneum* occurs by passive diffusion across several cell layers, depending on the chemical properties of the xenobiotic. Polar substances are believed to penetrate cell membranes trough the protein filaments, while nonpolar substances enter through the lipid matrix. In general, gases penetrate skin more readily than liquids and solutes, while solids do not penetrate much, but they may be dissolved into the skin's secretions and subsequently absorbed as solutes (Zakrzewski, 2002).

Skin can be exposed to AgNPs present in the air and sprays, clothing and wound dressings. Dermal penetration by AgNPs is controversial, since some studies show that NPs are able to penetrate the *stratum corneum* (strongly keratinized – 10µm) (Borm et al., 2006; Monteiro-Riviere et al., 2005), while others show that NPs enter the skin through hair follicles, sweat glands, broken and flexed skin (Buzea et al., 2007; Oberdörster et al., 2005; Teow et al., 2011; Tinkle et al., 2003; Toll et al., 2004). Dermal application of AgNP-coated wound dressing in human burns patient showed reversible silver toxicity and transient discoloration of skin (argyria-like) (Trop et al., 2006; Vlachou et al., 2007). In the Trop et al., (2006) study, one week after treatments, high levels of silver were found in urine and plasma in a young patient. Additionally, inhalation and dermal absorption of AgNPs could lead to the uptake of these particles via nervous system (brain, spinal cord and nerves). Tang et al., (2009; 2010) showed blood brain barrier (BBB) destruction and neuronal degeneration in rats after AgNP exposure with subcutaneous injection.

Ahlberg et al (2014) highlighted that PVP-coated AgNPs when topically applied mostly remained in the superficial horny layers of skin. However, in skin regions with eg, hair follicles, inflamed skin and wounds, contact to viable epidermis and cellular uptake inevitably occur leading to putative cytotoxic effects and free radical production by AgNPs per se and/or due to secondary Ag^{+} ion release (Fig 1.8).

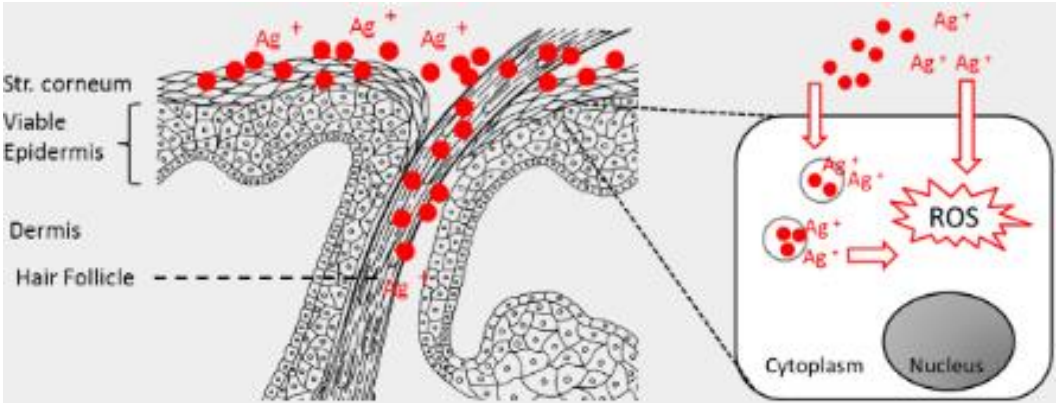

Figure 1.8: Proposed mechanism of cytotoxic effects and free radical production by AgNPs *per se versus* the effects due to secondary Ag^{+} ion release (from Ahlberg et al 2014).

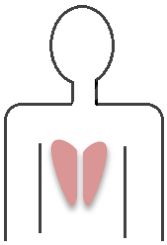

Respiratory system

Respiratory system consists of: nasopharyngeal, tracheobronchial and pulmonary. Nasopharyngeal remove large inhaled particles and increase humidity and temperature of inhaled air. Tracheobronchial region propels foreign particles from the deep parts of the lungs to the oral cavity, where they can be expelled or swallowed. Pulmonary region consists of bronchioles, alveolar ducts and clusters of alveoli. Inhaled xenobiotics can exert their harmful action either by damaging respiratory tissue or by entering the circulation through diffusion across the alveolar membranes. The size of particles influences the absorption rate through the alveolar epithelium: particles between 1 to 5 µm sediment within the bronchiolar region of lung; and those less than 1 µm can diffuse within the alveoli. Smaller sized particles are absorbed in the circulation causing systemic toxicity (Zakrzewski, 2002).

The lungs have a large surface area and are the primary entry for inhaled AgNPs and other nanoparticles. After their entrance, they could deposit into the entire respiratory tract, first at the nose then the pharynx, and finally at the lungs (Buzea et al., 2007; Teow et al., 2011). Particle size and shape will influence the particle deposition and distribution. Smaller particles (< 10 nm), may reach gas exchange surfaces but reliable prediction it is not possible. Larger particles (<100nm) seem to deposit further in the respiratory tract, before transportation into the deep lungs (Wijnhoven and Peijnenburg, 2009). The adverse effect of the inhaled particles depends on the residence time and on the lung burden (rate of particle deposition and clearance by macrophages). Takenaka et al., (2001) observed AgNPs in lung and blood immediately after mice exposure of 10 nm AgNP by inhalation, indicating absorption through systemic

circulation. In Ji, Jung et al. (2007) study, after rat inhalation of AgNPs of different sizes, these nanoparticles were found in liver, kidney and brain, despite no alterations in body weight nor hematological changes were detected.

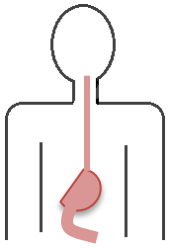

Gastrointestinal Tract

The absorption of compounds taken orally begins in the mouth and esophagus. Most of the ingested compounds move to the stomach, where other parameters influence the rate of absorption, such as the degree of ionization of an ionizable compound upon the acid pH present there. When an acid encounters an acidic environment, readily diffuse out of the stomach through the lipid bilayer of the cell membrane. However, when these compound encounter the blood (pH 7.4), the degree of ionization increases, and in ionized form, very little will diffuse back across the membrane. Thus, the rate at which a xenobiotic is absorbed by the stomach is affected by the pH. Xenobiotic not absorbed from the stomach lumen, passes into the intestine where secretions raises the pH (Roberts et al., 2014). Thus, a percentage of xenobiotics absorbed in the gastrointestinal cells may be biotransformed before entering the circulatory system. Absorbed compounds may enter circulation either via the lymphatic system, which eventually drains into the bloodstream, or via the portal circulation, which carries them to the liver (Zakrzewski, 2002).

Concerning the gastro-intestinal (GI) tract, many food supplements/products and drugs containing AgNPs are available in the market. In addition, inhaled particles cleared by mucociliary escalator can be ingested into the GI tract (Buzea et al., 2007; Teow et al., 2011). Size, surface charge or coating and attachments to ligands are some of the characteristics that control the site-specific target of different regions of the GI tract (Hillyer and Albrecht, 2001). Once in the GI, AgNPs could undergo chemical changes (e.g. pH) which may trigger agglomeration. Agglomeration may lead to fast transit, followed by excretion through feces and urine, however the bigger agglomerates may obstruct GI tract, which could lead to death (Buzea et al., 2007; Teow et al., 2011). Mwilu et al., (2013) showed changes in stomach fluid of human exposed to synthetic silver nanoparticles. Also in their review Buzea et al., (2007) identified some diseases such as Crohn´s disease and colon cancer as putatively related with NPs toxicity in the gastrointestinal system.

Blood

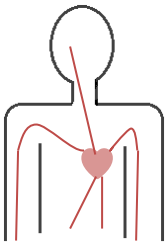

Once the first barrier is passed (skin, lung epithelia or intestinal lining) nanoparticles may then enter the systemic circulation. Indeed, in Pang et al (2015) study, PEG-AgNPs showed a long blood circulation in mice. As reaching the blood, AgNPs could affect blood cells. Chen and coworkers (2015) found that AgNPs induced oxidative stress, membrane injury and subsequently hemolysis in red blood cells, in a dose dependent manner. Otherwise, AgNPs could increase neutrophil cell size, interact with the cell membrane, penetrate neutrophils, localize in vacuole-like structures, and be randomly distributed in the cytosol after 24 h of exposure. In addition treatment with 100 µg/ml of AgNPs for 24 h increased the neutrophil apoptotic rate (Poirier et al., 2014). Other study, using human monocytic cell line THP-1, obtained an apoptosis and necrosis induction after AgNPs exposure, depending on dose and exposure time (Foldbjerg et al., 2009b). Orlowski et al (2013) obtained dose-dependent toxicity and a decreased proliferation of RAW 264.7 monocyte cells after 24h exposure to AgNPs.

After reaching the systemic circulation, distribution through the entire body followed by uptake by the organs could be expected.

Liver

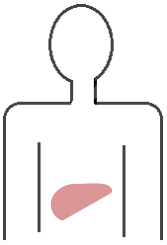

Together with the systemic circulation that translocate NPs to the whole body, the liver also plays a crucial role as it is able to remove compounds from the blood and transform them into chemicals easier excreted. The liver is, quantitatively, the most important organ for xenobiotic metabolism especially because of its high expression levels of many xenobiotic-metabolizing enzymes (Williams et al., 2015). Biotransformation of a xenobiotic (generating a more water-soluble product) can decrease the body burden, time of exposure and consequent toxic manifestations, although similar enzymes can bioactivate some of them to reactive intermediates that bind with the cellular macromolecules inducing cytotoxicity and/or carcinogenicity (Rana and Taketa, 1997). Biotransformation reactions can be classified in Phase I and Phase II. Phase I involves oxidative, reductive, and/or hydrolytic react reactions, which cleaves substract molecules to produce a more polar ones. The reaction products generated at Phase I could produce toxic manifestations before entering Phase II reactions. Phase II involve conjugation or addition of endogenous molecules to the Phase I transformed xenobiotic to make them more polar and highly water soluble (Rana and Taketa, 1997). Among the most important xenobiotic metabolizing enzymes are cytochrome P450s and Flavin monooxygenases (FMOs),

carboxylesterases, and glucoronosyltransferases (Williams et al., 2015).
Many studies showed deposition of AgNP in liver, kidneys, blood, brain and tests after whether oral, inhaled or intravenous exposure (Cha et al., 2008; Ebabe Elle et al., 2013; Ji et al., 2007; Kim et al., 2011a; Kim et al., 2008; Park et al., 2011c; Takenaka et al., 2001). Moreover, more research is required in order to determine the effects of long-term deposition of AgNPs in various organs.

1.4.In vitro assays and cell lines

As the exposure route to AgNPs may occur through the dermatologic, inhalation or ingestion pathway (reaching blood stream), as such the use of medical devices (Oberdörster et al., 2005), it is crucial to study the toxicity of AgNPs in cells/tissues with those pathways.
In vitro methods are increasingly replacing *in vivo* assays in assessing the toxicity of environmental and occupational health risks (eg, Dechsakulthorn et al., 2007). These *in vitro* methods have shown a significant robustness and fiability, while easier and ethically more adequate. As stated by Cho et al., (2013) "*The rapidly increasing number and functionalizations of NPs makes in vivo toxicity tests undesirable on both ethical and financial grounds, creating an urgent need for development of in vitro cell-based assays that accurately predict in vivo toxicity and facilitate safe nanotechnology*". Thus, and knowing that liver is the primary site for NPs accumulation (Sonavane et al., 2008), our study intends to determine the cytotoxic potential of AgNPs on a skin cell line (HaCaT), a liver cell line (HepG2) and a macrophage cell line (RAW 264.7).

Human Keratinocyte cell line – HaCaT

The human skin keratinocyte HaCaT cell line (Fig. 1.9) was obtained from a histologically normal male skin specimen, from distant periphery of a melanoma (second excision). The cells were plated in low Ca^{2+} medium since makes it favorable to long-term growth in primary culture probably due to a marked reduction in terminal differentiation; and were propagated with elevation of culture temperature (38,5ºC) as this increase proliferative activity and prolong the average life span. Thus, "*The resulting cell line was designated HaCaT to denote its origin from human adult skin keratinocytes propagated under low* Ca^{2+} *conditions and elevated temperature*." (Boukamp et al., 1988b).

The spontaneously immortalized HaCaT cell line is closely approximated to normal keratinocytes, and can be considered immortal (>140 passages), highly differentiated and not tumorigenic. HaCaT cells, even after multiple passages have remarkable capacity for normal differentiation offering a suitable model to study regulatory mechanisms in the process of differentiation of human epidermal cells. Despite the alterations related to long-term propagation as *in vitro* growth parameters, differentiation and karyotypic constitution; HaCaT chromosomal content is largely maintained sustaining their nontumorigenic phenotype (Boukamp et al., 1997).

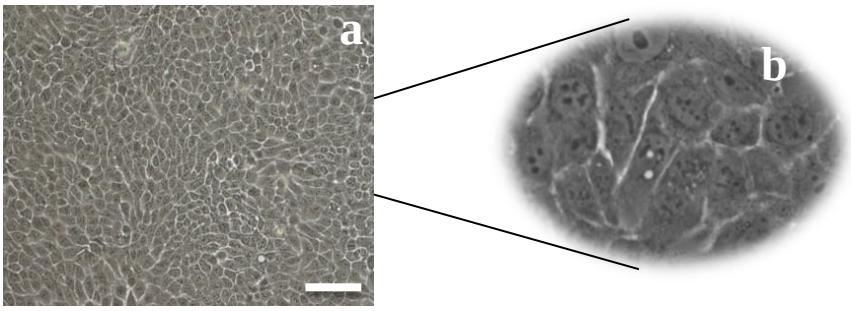

Figure 1.9: Light microscopy image of HaCaT cells: a) 100x; b) 400x. Bar corresponds to 100 μm.

HaCaT cell line has been widely used in *in vitro* studies: to define the protective effects against UVB of non-calcemic secosteroids on human keratinocytes (Slominski et al., 2015); providing evidence for the human relevance of gene signature, where molecular processes of these genes are similar between the HaCaT cell line and freshly isolated skin (Veen et al., 2015); on tests of topical corticosteroids on cell proliferation, cell cycle progression and apoptosis (Alexandre et al., 2015); studying the cytotoxicity potential of bismuth oxychloride nanosheets (Gao et al., 2015), among others.

HaCaT cells have also been used in AgNPs cytotoxic studies. Ahlberg and co-workers (2014a) compared the cytotoxicity of AgNPs after different storage conditions; 70nm AgNPs stored in argon induced a much smaller intracellular ROS production than AgNPs stored in air, suggesting the possibility of reduction of AgNPs toxic effects by storing them under an inert gas atmosphere.

Comfort and colleagues (2014a), evaluated the impact, mechanism of action and continual effects of 50 nm AgNPs on epidermal growth factor (EGF) signal transduction on HaCaT cells, and found that EGF signaling was initially obstructed due to the dissolution of particles into silver ions and at longer durations, the internalized AgNPs increased EGF signaling activity

correlating to sustained HaCaT stress. The researchers hypothesized that retained nanomaterials are capable of acting as a slow-release mechanism for metallic ions, continually stressing and modifying normal cellular functionality. Braroo and co-workers (2014), synthesized colloidal AgNPs from leaf extracts of medicinal herb *Ocimum sanctum (Tulsi)* which also showed *in vitro* cytotoxic effect on human keratinocyte (HaCaT) cell line.

However there are studies reporting advantages of the AgNPs on HaCaT cells. Arora and coworkers (2015), suggested a potential utility of AgNPs as chemopreventive agents against UVB-induced DNA damage and apoptosis in immortalized human epidermal keratinocytes (HaCaT). In David and colleagues (2014) study, AgNPs biosynthesized fast and eco-friendly using European black elderberry (*Sambucus nigra – SN*, Adoxaceae family) fruit extracts, showed anti-inflammatory properties on HaCaT cells exposed to UVB radiation by the decrease of cytokines production. Taken together all these data support the need to evaluate altogether the putative positive *vs* negative effects of AgNPs on cells metabolic pathways, and ultimately on animals and human health.

Human hepatocellular carcinoma cell line - HepG2

Human hepatoma cell line, HepG2 (Fig. 1.10), was primarily isolated by Aden et al (1980) from primary hepatoblastoma of a 15-year-old Argentine boy. Hepatoblastoma (HB) is an embryonal malignancy of hepatocellular origin and the most common type of liver primary malignant tumors of childhood, although accounting 1% of all childhood cancer (Finegold, 2004).

HepG2 cells have an epithelial like morphology, synthesizing and secreting many of the plasma proteins characteristic of normal human liver cells (Faedmaleki et al., 2014; Knowles et al., 1980). Additionally, HepG2 cells express wide range of phase I and phase II drug metabolizing enzymes (Knasmüller et al., 1998). Therefore, liver cell lines are commonly used in biomedical research involving xenobiotic metabolism.

HepG2 cells have been used in liver disease studies (Cederbaum et al., 2001), mechanism of action of drugs (Kim et al., 2003), gene expression and transcription (Carruba et al., 1999; Iyoda et al., 2003), genotoxicity studies (Knasmüller et al., 1998).

There are already some studies determining the potential cytotoxicity of AgNPs on HepG2 cell line. Faedmaleki and co-workers (2014), reported that AgNPs had cytotoxic effects on HepG2 cell line, decreasing cell viability, IC50 value of 2.764 µg/mL. Xin and colleagues (2015), studied the potential cytotoxic of AgNPs on HepG2 cells and found dose-dependent cytotoxicity (significantly decreasing viability from 25 to 200 µg/mL) resulted from an interaction of oxidative stress, DNA damage and mitochondrial injury. Ávalos and co-workers (2015),

assessed the genotoxic potential of AgNPs in cell lines and observed DNA damage in HepG2 in a dose- and size-dependent manner following 24h treatment, which damage could be related to oxidative stress.

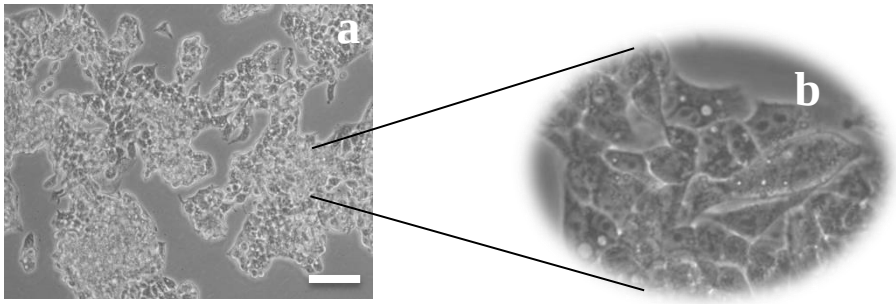

Figure 1.10: Light microscopy image of HepG2 cells: a) 100x; b) 400x. Bar corresponds to 100 µm.

Murine macrophage-like cell line – RAW 264.7

RAW 264.7 cells (Fig. 1.11) are adherent macrophage-like cells derived from a tumor, inoculated with Abelson murine leukemia virus (MuLV) (Raschke et al., 1978). These cells are immortalized, relatively stable and mature and have been used for models of macrophage activation in numerous studies (Bailey et al., 2005; Bailey et al., 2004; Naureckiene et al., 2007; Wu et al., 2006).

Furthermore, there are many studies using murine cell as putative analogs to human macrophages (Gutting et al., 2005; Naureckiene et al., 2007; Vigo et al., 2005).

Macrophage is a highly differentiated phagocyte and a part of the innate protective immune response, which an exposure to a xenobiotic could trigger a chain reaction of inflammatory responses (Giovanni et al., 2015). Thus, on Giovanni and co-workers study (2015), concentrations of AgNPs (considered non-cytotoxic) could induce mild pro-inflammatory responses by RAW 246.7 starting from 10^{-7} µg/mL (lower that the levels found in the environment and in consumer products), while a reduction on macrophages viability was only observed for the highest concentration tested, 10 µg/mL. Also, Munusamy and colleagues (2015) observed cytotoxicity effects on RAW 264.7 cells following 24h exposure of AgNPs at 50 µg/ml.

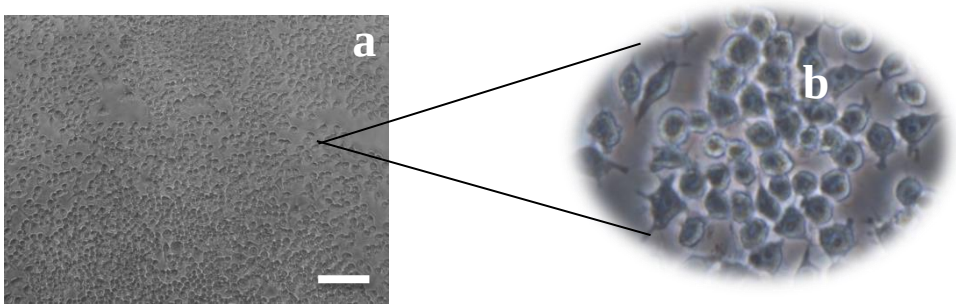

Figure 1.11: Light microscopy image of RAW 246.7 cells: a) 100x; b) 400x. Bar corresponds to 100 μm.

1.5.Cellular uptake of AgNPs

An important issue related to AgNPs toxicity is their capacity to enter cells, since they are able to cross cell membranes and reach organelles. The effects of AgNPs in cells are highly dependent on the effective amount of NP internalized and their location. The uptake and intracellular trafficking of AgNPs is mostly determined by NP physico-chemical properties, concentration, exposure period and specific transport mechanisms. The main physico-chemical properties of AgNPs affecting NP cellular uptake include NP surface charge and chemistry, shape, size and aggregation state.

In *in vitro* studies, AgNP uptake and transport has been analyzed in systems that rely on exposure to uncoated AgNPs (Yen et al., 2009a) or NPs stabilized by coating (exemplified before). Furthermore, cell exposure to AgNPs *in vitro* represents a very complex system, since the culture media have high protein content, ligands and chelators for Ag^+ in the solution. Indeed, the chemical composition of cell culture media is a complex mixture (consisting of inorganic salts, carbohydrates, amino acids, various supplements (i.e. vitamins, fatty acids, lipids) and fetal bovine serum (FBS), which may result in transformations of AgNPs and, consequently, the complexation of Ag^+ (Behra et al., 2013). Thus, the conjugation of charged AgNPs with different types of ligand molecules available in the extracellular milieu can coat NPs with proteins and other biomolecules (protein corona), resulting in different outcomes for cellular uptake rates and transport routes (Fig. 1.12).

In Human Embryonic Kidney, HEK cells, incubation of citrate- or silica-coated AgNPs pre-treated with albumin or IgG showed different uptake rates as measured by ICP-OES quantification of Ag, as well as different dispersion degree in the cell, observed by TEM (Monteiro-Riviere et al., 2013). Such differences according to charge and protein coating may

be explained by different interactions between the surface coating and surrounding proteins, e.g. as observed in studies by Treuel and colleagues (Treuel et al., 2010). The shape of NPs may also influence their internalization, although the effect has not been dissected yet. In a study by Zhang and coworkers (Zhang et al., 2012) polystyrene nanospheres were readily taken up by Human epithelioid cervix carcinoma, HeLa cells, whereas nanodisks of approximately identical diameter were not internalized. However, in another study, when keratinocytes were exposed to 30 nm PVP- coated silver nanomaterials in the form of nanospheres or nanoprisms, the uptake rates were found similar as determined by high-resolution ICP-OES and ICP-MS (Lu et al., 2010a). Moreover, both Ag nanospheres and nanoprisms reached the cell nucleus as assessed by TEM.

Cellular uptake may also be affected by NP size. In murine adrenal medullary chromaffin cells, cellular uptake of citrate-coated AgNPs as determined by ICP-OES showed that exposure to smallest NPs resulted in the highest number of internalized NPs (Love et al., 2012). Direct penetration of AgNP has also been reported in THP-1 monocytic leukemia cells exposed to 20 nm citrate-coated AgNPs, as observed by TEM (Haase et al., 2011).

Multiple internalization mechanisms have been proposed to mediate AgNP cellular uptake. Various complementing techniques can be used to characterize the mechanisms of AgNP internalization and intracellular transport, e.g. incubation with transport inhibitors followed by ICP-OES, plasmon coupling microscopy, Laser-SNMS/TOF-SIMS, confocal Raman microscopy or surface-enhanced Raman scattering (SERS) spectroscopy. Apart from direct penetration (passive uptake), AgNPs can be internalized by active uptake (endocytosis): macropinocytosis, pinocytosis, phagocytosis clathrin-dependent endocytosis, and clathrin-independent endocytosis, which includes caveolae/lipid raft-mediated endocytosis (Fig. 1.12). In macropinocytosis, actin-dependent membrane protrusions also called ruffles are developed, which upon fusion with each other or with the cell membrane engulf large suspended particles, typically up to 1 μm or in the specific case of phagocytosis up to 5 μm. Past studies suggest that in some systems, macropinocytosis is the dominant mechanism of AgNP internalization. Unlike other endocytic processes, macropinocytosis is largely inhibited by the presence of inhibitors of Na^+/H^+ exchange, such as amiloride. Luther et al. reported in astrocytes exposed to PVP-coated AgNPs a 30% uptake decrease after incubation with amiloride (Luther et al., 2011). In human mesenchymal stem cells, Greulich and coworkers observed that internalization of PVP-coated AgNPs was significantly inhibited by wortmannin, an inhibitor of phosphoinositide 3-phosphate kinases (Greulich et al., 2011b). Moreover, in different cell lines exposed to citrate-coated AgNPs, the two non-specific inhibitors of phagocytic/macropinocytic pathways sodium azide and staurosporine significantly reduced cellular uptake (Singh and Ramarao, 2012).

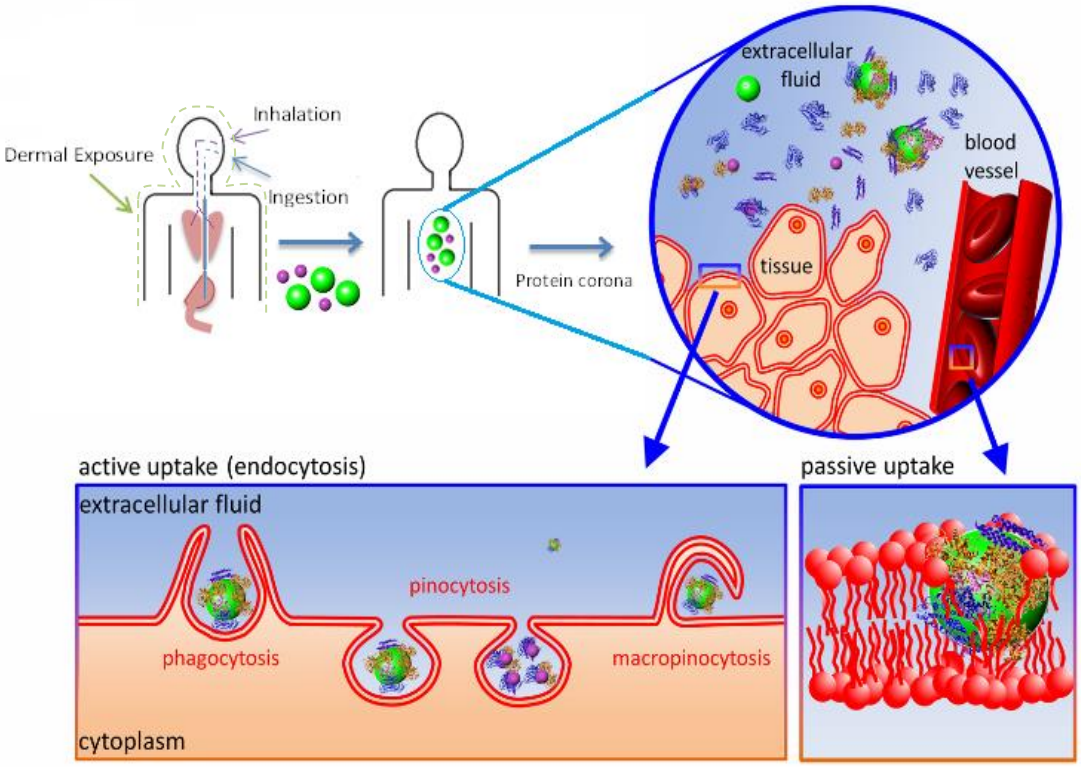

Figure 1.12: Nanoparticle uptake – in the extracellular fluid NPs are coated by proteins and other biomolecules determining how NPs interacts with cells; cellular internalization may involve active (receptor mediated) or passive transport across the membrane (adapted from Shang et al. (2014)).

In addition to sensitivity to inhibitors of macropinocytosis, in some systems depending on the AgNP characteristics and cell line, large intracellular clusters of AgNPs have been observed (e.g. Haase et al., 2011; Wang et al., 2012). In macrophages, different types of AgNPs were shown to interact with the cell membrane by binding to scavenger receptors, as AgNP internalization was inhibited by incubation with polyinosinic acid (Wang et al., 2012) or dextran sulfate (Singh and Ramarao, 2012).

Endocytosis mediated by clathrin-coated vesicles is the most well-studied endocytic pathway and shows preference for particles up to ca. 200 nm, whereas larger particles up to 500 nm are more often internalized by clathrin-independent mechanisms (Rejman et al., 2004). Inhibition of clathrin-dependent endocytosis is most commonly achieved by potassium depletion or incubation with chlorpromazine. In human glioblastoma U251 cells exposed to potato starch coated AgNPs, potassium depletion resulted in decreased AgNP uptake, confirming clathrin-dependent endocytosis of the studied AgNPs (Asharani et al., 2009a). Moreover, in human mesenchymal stem cells exposed to PVP-coated AgNPs, a significant inhibition by

chlorpromazine was observed, also suggesting clathrin-dependent endocytosis (Greulich et al., 2011b).

Internalization of AgNPs by clathrin-independent endocytosis compared to macropinocytosis and clathrin-dependent endocytosis has so far been considered a marginal event in AgNP uptake, since it shows preference for the internalization of particles larger than 200 nn and up to 500 nm (Asharani et al., 2009a; Greulich et al., 2011b; Haase et al., 2012b; Wang et al., 2012). Cellular uptake via clathrin-independent endocytosis is commonly investigated by use of polyene antibiotics such as nystatin and filipin, or the use of methyl-β-cyclodextrin, a less specific inhibitor of clathrin-independent endocytosis (Luther et al., 2011).

Different routes of intracellular transport have been suggested for AgNPs, with the final location depending mainly on the properties of AgNPs, concentration, time and cell type. A cytoplasmic location has been observed either in the form of clusters, e.g. up to 800 μm, in J774 A1 murine macrophages (Yen et al., 2009a). In RAW 264.7 macrophages, cytoplasmic location was confirmed by TEM, close to the cell periphery (Singh and Ramarao, 2012). AgNP clusters of variable sizes were also found in endolysosomal compartments (Asharani et al., 2009a; Greulich et al., 2011b; Haase et al., 2012b; Wang et al., 2012) and in the nucleus (Asharani et al., 2009a; Greulich et al., 2011a; Lu et al., 2010a).

In parallel with active internalization, exocytosis of AgNPs was also shown to occur. Through CFMA (Carbon-fiber microelectrode amperometry), Love and Haynes (2010) demonstrated that citrate-coated AgNPs (~60 nm) perturbed exocytosis in murine adrenal medullary chromaffin cells. Moreover, exposure to potato starch-coated AgNPs in human glioblastoma cells (U251 cells) showed that exocytosis rate increased with time but was slower than endocytosis, suggesting AgNP accumulation (Asharani et al., 2009).

1.6.Cytotoxicity

Once AgNPs enter the cell it is important to determine their putative cytotoxicity and genotoxicity. NPs could trigger the production of reactive oxygen species (ROS), leading to activation of cellular stress-dependent signaling pathways, direct damage of subcellular organelles such as mitochondria, and DNA fragmentation in the nucleus, resulting in cell cycle arrest, apoptosis, and inflammatory response (Fig. 1.13).

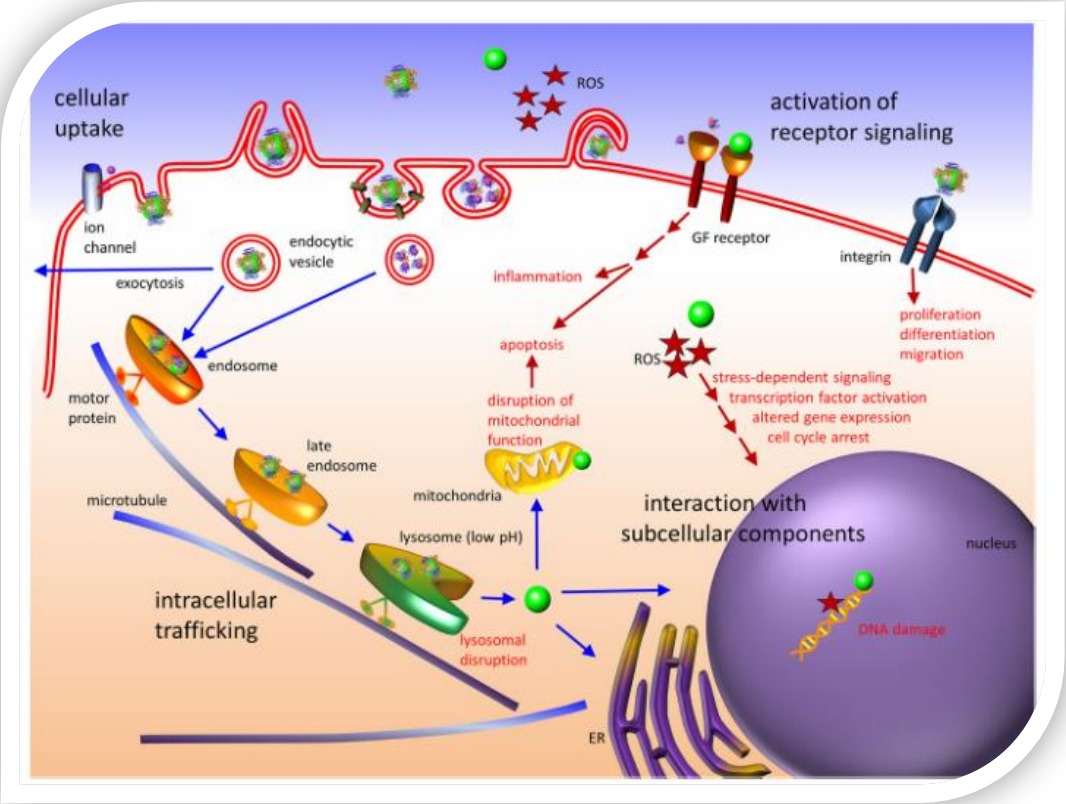

Figure 1.13: Cytotoxic and genotoxic potential effects of NPs (adapted from Shang et al. (2014)).

Most of the *in vitro* studies in the literature report decreases on cell viability upon exposure to AgNPs. For instance, Suliman and co-workers (2013a) found that AgNPs (nanopowder < 100nm) at concentrations higher than 50 µg/ml for 24h, cell viability of human epithelial cells was significantly decreased. Also, Song and co-workers (2012) found a decrease in the viability of normal human liver cell line, HL-7702 cells, after exposure to α-Methoxy-poly (ethylene glycol)-ω-mercapto (mPEG-SH)-coated AgNPs of 40 nm at concentrations of 6.25 µg/ml for 24h. The IC_{50} values were also found to depend on the cell line, the size of the NP and the type of coating. Park and co-workers (2011d) found that the viability of RAW 264.7 cells was significantly reduced by 20% after 24h exposure to 68.9 nm AgNPs dispersed in FBS at 1.6 µg/ml. Foldbjerg et al., (2009a) found an EC_{50} value of 2.4 µg/ml for PVP-coated AgNPs (30-50 nm) compared to 0.6 µg/ml for Ag^{+} in THP-1 cells estimated by the annexin V/PI assay. Also, in A549 lung adenocarcinoma cells, PVP-coated AgNPs induced a decrease in mitochondrial activity and cell viability (Foldbjerg et al., 2011). The degree of contribution of Ag ion to the toxicity of AgNPs has also been discussed in literature. Using human Chang liver cells, Piao et al., (2011a) found an IC_{50} of 4 µg/ml after 24h of exposure, while for the $AgNO_3$ the IC_{50} was 8 µg/ml. Lui and co-workers (2010) compared the cytotoxicity of PVP coated

AgNPs of 5, 20 and 50 nm and ionic silver in four human cell models (A549, SGC-7901, HepG2 and MCF-7) in a series of dilutions and found that the order of toxicity was AgNP 5 nm > Ag^+ > AgNP 20 nm > AgNP 50 nm for all four cell lines, as detected by the MTT assay, while the LDH test revealed the following order of toxicity Ag^+ > AgNP 5nm > AgNP 20nm > AgNP 50 nm. Kim, Choi et al (2009b) compared the toxicity of ionic Ag and AgNPs in human hepatoma cells and found that AgNPs treated cells have limited exposure to ionic Ag, despite the potential release of Ag ion from nanoparticles in the cell culture. For AgNPs these authors found an IC50 of 3.38 µg/ml, while for $AgNO_3$ the IC50 was estimated to be 1.37 µg/ml of Ag.

Oxidative stress is an important mechanism of cytotoxicity related to NPs exposure. Previous studies demonstrated that AgNPs could induce oxidative stress in different cell models. Kim and Ryu (2013) revised the oxidative stress related effects of AgNPs both *in vitro* and *in vivo*. However, in spite of a strong evidence of ROS induction, the mechanisms underlying AgNPs induced oxidative stress are still poorly understood. Evidences for increased ROS generation were shown for AgNP doses as low as 0.2 µg/ml for 1 h in HepG2 cells (Kim et al., 2009b). Studies from Piao et al., (2011a) in human Chang liver cells exposed to 4 µg/ml of AgNP showed increase in ROS levels after 0.5h of exposure and the levels were kept significantly high up to 12h. Foldbjerg et al., (2009a) found that both PVP-coated AgNPs and ionic silver increased the levels of ROS in the human monocytic cell line THP-1. Furthermore, in A549 lung adenocarcinoma cell line the same effect was observed, but when cells were treated with N- acetylcysteine (NAC) the levels of ROS were reduced, suggesting antioxidant scavenging (Foldbjerg et al., 2011). Also, PVP stabilized AgNPs of 5, 20 and 50 nm increased the levels of ROS in HepG2 cells; for the smallest (5 nm) this effect was observed at levels of 1 µg/ml, which was the same as for Ag ion, while for the largest (20 and 50 nm) this effect was observed at doses of 10 µg/ml (Liu et al., 2010). In order to evaluate the contribution of ionic silver present in the nanoparticle suspension to the increase in ROS levels, Beer and co-workers (2012) compared the effect of both AgNP suspension and supernatant and found that AgNP supernatant induces between 2.6- and 6- fold more ROS than AgNP suspension, suggesting that ROS production is mainly due to the presence of silver ions (Beer et al., 2012).

As the oxidative stress is originated by the imbalance between the generation of ROS and the antioxidative capacity of the cell, it is important to evaluate also the effect of AgNPs on the levels and activity of the ROS scavengers. For instance, Piao and co-workers (2011a) found that the increase in ROS levels for 4 µg/ml of AgNP in human Chang liver cells were accompanied by decrease in GSH levels after 0.5h and this profile was kept for the following 24h. A decrease in GSH levels and increase in SOD and catalase activities was also found by Sulliman and co-workers (2013a) in A549 lung adenocarcinoma cells exposed to 25 µg/ml after 48h. Otherwise, the studies of Song and co-workers (2012) with mPEG-SH-coated AgNPs in HL-7702 cells

revealed a decrease in the activities of SOD and GPX. A decrease in both GSH and SOD levels was also detected in fibrosarcoma cells HT-1080 and human skin carcinoma cells A431 treated with 6.25 µg/ml AgNPs for 24h (Arora et al., 2008). Depletion in SOD activity was also observed in HepG2 cells exposed to PVP stabilized AgNps of 5 and 20 nm (Liu et al., 2010). However, in this study a size depend effect was observed for the levels of GSH, a decrease for the lowest sizes (5 nm) and an increase in the largest NP sizes (20 and 50 nm) (Liu et al., 2010). Kang and co-workers (2012) highlighted the protective role of nuclear factor-erythroid 2-related factor-2 (Nrf2) against AgNPs toxicity by demonstrating that in Nrf2 knockdown human renal epithelial cells, AgNPs reduced GSH levels and increased ROS contributing to the increase of DNA damage and cell cycle arrest.

However, it has also been reported, in human liver and colon cells, that AgNPs could cause cytotoxicity without oxidative stress (Sahu et al., 2014). Furthermore, Chairuangkittia et al., (2013) described that the toxicity of AgNPs to A549 lung adenocarcinoma was due both to ROS dependent and independent pathways, the latter related with cell cycle arrest.

The level of lipid peroxidation is an important indicator of oxidative stress in the cell. Several studies show that AgNP induced lipid peroxidation in several cells types, as for instance, studies from Sulliman and co-workers (2013a) in A549 lung adenocarcinoma cells and in HL-7702 liver cells exposed to mPEG-SH-coated AgNps (Song et al., 2012), in human skin carcinoma and fibrosarcoma cells (Arora et al., 2008), as well as in Chang liver cells (Piao et al., 2011a).

1.7.Genotoxicity (clastogenicity, DNA breaks and gene expression)

AgNPs have induced genotoxicity in several cell models. For instance, Piao et al., (2011a), working with human Chang liver cells exposed to AgNPs found an increase in DNA damage, detected by the comet assay. DNA damage detected by ɣ-H2AX phosphorilation was observed in HepG2 cells exposed to AgNPs (Kim et al., 2009b). In another study, Kruszewski et al., (2013) compared the potential of AgNPs of 20 nm and 200 nm to induce DNA damage in HepG2, HT29 colorectal adenocarcinoma and A549 lung adenocarcinoma cells and found that in A549 cell line a shorter exposure (2h) induced the same level of DNA damage as more prolonged exposure (24h), while in HepG2 cells a shorter exposure showed high levels of DNA damage. These different profiles of response may indicate either an effective repair of the damage or the induction of an antioxidant defense (Kruszewski et al., 2013). In human mesenchymal stem cells (hMSCs) AgNPs at 0.1 µg/ml induced DNA damage after 1h assessed by the comet assay and chromosomal aberration test (Hackenberg et al., 2011). The formation

of micronuclei was also detected upon exposure to AgNps in HepG2 cells at relatively low AgNP doses (<1.0 µg/ml) (Kawata et al., 2009) and also in IMR-90 lung fibroblasts and U251 glioblastoma cells exposed to starch coated AgNPs (AshaRani et al., 2009b).

Regarding the role of AgNPs in apoptosis induction, literature still remains conflicting. AshaRani and co-workers (2009b) showed only a small increase in the percentage of IMR-90 fibroblast cells undergoing apoptosis or necrosis after starch coated AgNP exposure, in spite of a significant increase in DNA damage detected by the comet assay. In Jurkat leukaemic T cells, was observed an increase in the apoptotic and necrotic cell populations after exposure to both AgNPs and Ag ions, but more intensely in NP exposed cells. In this cell model AgNPs induced cell death in the following order: late apoptosis > necrosis > early apoptosis (Eom and Choi, 2010a). An increase in apoptosis was also observed in 5 and 20 nm AgNPs after 24h in HepG2 cells (Liu et al., 2010).

AgNP exposure also affects cell cycle dynamics. For instance, a G2 arrest in U251 glioblastoma and IMR-90 lung cell lines was found for AgNP concentrations higher than 25 µg/ml (AshaRani et al. 2009). By other hand, a decrease in relative amounts of cells in G1 and increase in those in S phase was found in HepG2 cells (Liu et al., 2010) and in A549 lung adenocarcinoma cells (Beer et al., 2012). In mPEG-SH-coated AgNPs exposed HL-7702 liver cells, Song and co-workers (2012) found a decrease in the percentage of cells in G0/G1 together with an increase in percentage of cells in G2. In HepG2 cells, DNA microarray analysis showed significant induction of genes associated with cell cycle progression (Kawata et al., 2009).

The presence or persistence of AgNPs has also been reported to induce inflammatory response. Studies reporting the effects of AgNPs on inflammatory response are summarized in table 1.1. Moreover, activation of the transcription factor NF-κB has been shown to play central roles in the enhanced expression and regulation of cytokine genes (Kelso, 1998).

Table 1.1: Resume of the studies found reporting inflammatory response of AgNPs.

Cytokines	NPs	Cell type	Conditions	Reference
↑ IL-8	AgNPs, TiO_2NPs, ZnONPs	Caco-2; SW480	10 and 100 µg/mL; 48h (ELISA kit)	Abbott Chalew and Schwab, 2013
↓ IL-6, ↓ IL1β, ↑ NFKb, ↓ TNFα	AgNPs	RAW 264.7	10 µg/mL, 6h	Giovanni et al., 2015
↑ IL-6, ↓ IL1β, ↑ NFKb, ↓ TNFα	TiO2NPs,			
↑ IL-6, ↑ IL1β, ↑ NFKb, ↑ TNFα	ZnONPs			
↓ TNFα, no dif IL1β, ↓MCP1 (1u) ↑ TNFα, no dif IL1β,	AgNPs (tannic-acid)	RAW 264.7 THP1	1 and 10 µg/mL 12h	Orlowski et al., 2013
↑ MCP1 ↑ MCP1	AgNPs (Unmodified)	RAW264.7 THP1		

Cytokines	NPs	Cell type	Conditions	Reference
No significant production of IL-6, IFN-α, IL-10 and IL-12p70 by monocytes exposed or not to AgNPs was detected.		RAW264.7		
↑Il-1,↑IL-6,↑TNFα	AuNPs	J774 A1 macrophages	1 µg/mL; 3 and 6h 3, 6, 24, 48, 72h	Yen et al., 2009
No significant differences	AgNPs			
↑ IL-6 (1.25 to 10 nM),↑ IL-8 (2.5 to 10 nM)	QD621 (quantum dots)	HEK	24 and 48h	Zhang et al., 2008
↑ IL-6,↑IL-8. Below detectable levels: Il1β, IL-10, TNFα.	Iron oxide NPs	HEK	26 µg/cm2; 24h (BD cytometric bead array)	Murray et al., 2013
↑IL-6, ↑TNFα,↑ MCP1. Below detectable levels: INFγ, IL12.	Iron oxide NPs	JB6 P+ (mouse epidermal)		
↑ IL-1β, IL-6, IL-8, and TNF-α Below detectable level: IL-10	0.34 µg/mL unwashed 20, 50, 80 nm AgNPs	HEK	24h	Samberg et al., 2010
↑ TNF-α and IFN-γ	AgPs	Mice	48h	Xu et al., 2013
↑ IL-1, TNF-α, and IL-6 and Th0 cytokine (IL-2)	AgNPs	Mice	28 days after a single instillation	Park, 2011
↑ IL1β, IL-6	AgNPs	A549	50 µg/mL	Suliman et al., 2013
Progressive release of IL-8	AgNPs	LoVo cells	1 or 10 µg/ml; 24 or 48h	Miethling-Graff et al., 2014
↓ TNFα,↓ INFγ ↓ TNFα on LPS stimulated RAW Evidence of the Anti-inflammatory Effects	AgNPs	abdominal perito-neal tissues (mice)		Wong et al., 2009
↑ IL-6; IL-8; MCP1 Add NAC → ↓ IL6, IL8, MCP-1 (=abnormal expression levels related to oxidative stress)	AgNPs 65nm; sodium citrate	HUVECs	24h; 1, 1.5, 2 µg/ml	Shi et al., 2014
No significant change in gene expression of IL1, IL6, TNFα	AgNPs: 2-4 nm; 5-7nm; 20-40nm	J774 A1 macrophages	1 ppm; 3, 6, 24 and 72h	Yen et al., 2009
↓ TNFα; no alterations on IL2 and IL6	AgNPs sodium citrate+PVP 10-50nm	T-lymphocytic Jurkat	0-7.5ppm; 24h	Parnsamut and Brimson, 2015
no alterations on IL2, IL6 and TNFα		Monocytic U937		
↑ IL1β	AgNPs	Human monocytes		Yang, 2012

The symbol ↑ means increase and ↓ means decrease.

1.8.Effects of AgNPs on cell metabolome

As reported above conventional toxicity assessments show high variability in biological responses to AgNPs, therefore it is important to complement this information with other,

including the cell metabolic profiling. Studies on the effects of AgNPs in the cell metabolome are scarce. Carrola et al (2016) demonstrated by Nuclear Magnetic Resonance (NMR) metabolomics that AgNPs-exposed HaCaT cells displayed upregulated glutathione-based antioxidant protection, increased glutaminolysis, downregulated tricarboxylic acid (TCA) cycle activity, energy depletion and cell membrane modification. In a study by Kim and colleagues (2011b), AgNPs increased intracellular pyruvate, oxidized glutathione (GSSG) and decreased lactate, taurine, glycine, reduced glutathione (GSH). The AgNPs also increased the levels of choline, o-phospho-choline, and sn-glycerol-3-phosphocholine, which are involved in phospholipid pathways. In another study, Szmyd and colleagues reported that in NHEK keratinocytes ATP content decreased (Szmyd et al., 2013). Cells exposed to 6.25 μg/ml AgNPs showed a 40 % decrease in ATP content, whereas cells exposed to 50 μg/ml AgNPs, the ATP content decreased by almost 80 %. The changes were even more pronounced after 48h exposure (Szmyd et al., 2013).

1.9.Aims and outline of this work

The general aim of this thesis was to evaluate AgNPs cytotoxic and genotoxic potential in skin, liver and blood, using cell lines: human keratinocyte (HaCaT), human hepatocellular carcinoma (HepG2) and mouse leukemic monocyte/macrophage (RAW 264.7), respectively.

In this line, the specific aims were:

- To evaluate the effects of AgNPs on cell morphology, cell viability, cell cycle unbalances and clastogenicity;
- To characterize if and how AgNPs induce oxidative stress, apoptosis/necrosis and inflammatory responses;
- To evaluate genotoxic potential of AgNPs measuring DNA damage, chromosome breakage, cytostasis and cytotoxicity;
- To determine the potential effects of AgNPs on gene expression (cell-cycle and apoptosis related genes);
- To compare the toxicity of AgNPs with different surface coatings: citrate- and PEG- AgNPs.

References

Abbott Chalew, T.E. and Schwab, K.J. (2013). Toxicity of commercially available engineered nanoparticles to Caco-2 and SW480 human intestinal epithelial cells. Cell Biol Toxicol, 29, 101-116.

Aden, D.P., Fogel, A., Plotkin, S., Damjanov, I. and Knowles, B.B. (1980). Controlled synthesis of HBsAg in a differentiated human liver carcinoma-derived cell line. Nature, 282(5739):615-6.

Ahlberg, S., Meinke, M. C., Werner, L., Epple, M., Diendorf, J., Blume-Peytavi, U., Lademann, J., Vogt, A. and Rancan, F. (2014). Comparison of silver nanoparticles stored under air or argon with respect to the induction of intracellular free radicals and toxic effects toward keratinocytes. Eur J Pharm Biopharm, 88(3), 651-657.

Ahlberg, S., Antonopulos, A., Diendorf, J., Dringen, R., Epple, M., Flöck, R., Goedecke, W., Graf, C., Haberl, N., Helmlinger, J., et al. (2014). PVP-coated, negatively charged silver nanoparticles: A multi-center study of their physicochemical characteristics, cell culture and in vivo experiments. Beilstein J Nanotechnology, 5(1), 1944–1965.

Aitken, R.J., Chaudhry, M.Q., Boxall, A.B.A. and Hull, M. (2006). Manufacture and use of nanomaterials: current status in the UK and global trends. Occup Med (Lond), 56(5), 300-306.

Alexandre, G., Philippe, H., Marion, T. and Patrice, M. (2015). Effects of topical corticosteroids on cell proliferation, cell cycle progression and apoptosis: In vitro comparison on HaCaT. Int J Pharm, 479(2),422-9.

Alt, V., Bechert, T., Steinrücke, P., Wagener, M., Seidel, P., Dingeldein, E., Domann, E. and Schnettler, R. (2004). An in vitro assessment of the antibacterial properties and cytotoxicity of nanoparticulate silver bone cement. Biomaterials, 25(18), 4383-4391.

Arora, S., Jain, J., Rajwade, J. and Paknikar, K. (2008). Cellular responses induced by silver nanoparticles: In vitro studies. Toxicol Lett, 179(2), 93-100.

Arora, S., Tyagi, N., Bhardwaj, A., Rusu, L. and Palanki, R. (2015). Silver nanoparticles protect human keratinocytes from deleterious effects of ultraviolet radiation: Implications for skin cancer chemoprevention. Cancer Res, 75; 2811.

Asharani, P., Hande, M. and Valiyaveettil, S. (2009). Anti-proliferative activity of silver nanoparticles. BMC cell biology, 10(1), 1.

AshaRani, P. V., Low Kah Mun, G., Hande, M. P., & Valiyaveettil, S. (2008). Cytotoxicity and genotoxicity of silver nanoparticles in human cells. Acs Nano, 3(2), 279-290.

Ávalos, A., Haza, A.I. and Morales, P. (2015). Manufactured silver nanoparticles of different sizes induced DNA strand breaks and oxidative DNA damage in hepatoma and leukaemia cells and in dermal and pulmonary fibroblasts. Folia Biol, 61(1):33-42.

Bailey, L. A. O., S. Lippiatt, F. S. Biancanello, and S. D. Ridder. 2005. The quantification of cellular viability and inflammatory response to stainless steel alloys. Biomaterials, 26(26), 5296-302.

Bailey, L.O., Washburn, N.R., Simon, C.G., Chan, E.S. and Wang, F.W. (2004). Quantification of inflammatory cellular responses using real-time polymerase chain reaction. J Biomed Mater Res A, 69(2), 305-313.

Balogh, L., Swanson, D. R., Tomalia, D. A., Hagnauer, G. L., & McManus, A. T. (2001). Dendrimer−Silver Complexes and Nanocomposites as Antimicrobial Agents. Nano Lett, 1(1), 18-21.

Baram-Pinto, D., Shukla, S., Perkas, N., Gedanken, A. and Sarid, R. (2009). Inhibition of herpes simplex virus type 1 infection by silver nanoparticles capped with mercaptoethane sulfonate. Bioconjug Chem , 20(8), 1497-1502.

Bastos, V., Rosário, F., Oliveira, H., Oliveira, J.M. and Santos, C. (2012). Toxicity assessment of uncoated Ag and TiO2 nanoparticles on human osteosarcoma cell lines. Presentation at the European Society of Toxicology In Vitro. Poster

Bayston, R., Ashraf, W., & Fisher, L. (2007). Prevention of infection in neurosurgery: role of

"antimicrobial" catheters. J Hosp Infect, 65, 39-42.
Beer, C., Foldbjerg, R., Hayashi, Y., Sutherland, D. S., & Autrup, H. (2012). Toxicity of silver nanoparticles - nanoparticle or silver ion? Toxicol Lett, 208(3), 286-292.
Behra, R., Sigg, L., Clift, M. J., Herzog, F., Minghetti, M., Johnston, B., Petri-Fink, A. and Rothen-Rutishauser, B. (2013). Bioavailability of silver nanoparticles and ions: from a chemical and biochemical perspective. J R Soc Interface, 10(87), 20130396.
Benn, T.M. and Westerhoff, P. (2008). Nanoparticle silver released into water from commercially available sock fabrics. Environ Sci Technol, 42(11), 4133-4139.
Bhol, K. and Schechter, P. (2005). Topical nanocrystalline silver cream suppresses inflammatory cytokines and induces apoptosis of inflammatory cells in a murine model of allergic contact dermatitis. Br J Dermatol , 152(6), 1235-1242.
Biswas, P., and Wu, C.Y. (2005). 2005 Critical Review: Nanoparticles and the environment. J Air Waste Manag Assoc , 55(6), 708-746.
Borm, P.J., Robbins, D., Haubold, S., Kuhlbusch, T., Fissan, H., Donaldson, K., Schins, R., Stone, V., Kreyling, W., Lademann, J., Krutmann, J., Warheit, D. and Oberdorster, E. (2006). The potential risks of nanomaterials: a review carried out for ECETOC. Part Fibre Toxicol, 3:11.
Boukamp, P., Petrussevska, R.T., Breitkreutz, D., Hornung, J., Markham, A. and Fusenig, N.E. (1988). Normal keratinization in a spontaneously immortalized aneuploid human keratinocyte cell line. J Cell Biol, 106(3), 761-771.
Boukamp, P., Popp, S., Altmeyer, S., Hülsen, A., Fasching, C., Cremer, T. and Fusenig, N.E. (1997). Sustained nontumorigenic phenotype correlates with a largely stable chromosome content during long-term culture of the human keratinocyte line HaCaT Genes Chromosomes Cancer, 19(4), 201-214.
Braroo, K., Sharma, A.K. and Thakur, M. (2014). Colloidal Silver Nanoparticles from Ocimum sanctum: Synthesis, Separation and Their Implications on Pathogenic Microorganisms, Human Keratinocyte Cells, and Allium cepa Root Tips. J Colloid Sci Biotechnol, 3(3), 245-52.
Buzea, C., Pacheco, I. I., & Robbie, K. (2007). Nanomaterials and nanoparticles: sources and toxicity. Biointerphases, 2(4), 71.
Carruba, G., Cervello, M., Miceli, M. D., Farruggio, R., Notarbartolo, M., Virruso, L. Giannitrapani, R., Gambino, G., Montalto, and Castagnetta, L. (1999). Truncated form of beta-catenin and reduced expression of wild-type catenins feature HepG2 human liver cancer cells. Ann N Y Acad Sci, 886(1), 212-216.
Cederbaum, A. I., Wu, D., Mari, M., & Bai, J. (2001). CYP2E1-dependent toxicity and oxidative stress in HepG2 cells. Free Radic Biol Med, 31(12), 1539-1543.
Cha, K., Hong, H.W., Choi, Y.G., Lee, M.J., Park, J.H., Chae, H.K., Ryu, G., and Myung, H. (2008). Comparison of acute responses of mice livers to short-term exposure to nano-sized or micro-sized silver particles. Biotechnol Lett, 30(11), 1893-1899.
Chairuangkitti, P., Lawanprasert, S., Roytrakul, S., Aueviriyavit, S., Phummiratch, D., Kulthong, K., Chanvorachote, P. and Maniratanachote, R. (2013). Silver nanoparticles induce toxicity in A549 cells via ROS-dependent and ROS-independent pathways. Toxicol In Vitro, 27.1: 330-338.
Chen, L.Q., Fang, L., Ling, J., Ding, C.Z., Kang, B. and Huang, C.Z. (2015). Nanotoxicity of silver nanoparticles to red blood cells: size dependent adsorption, uptake, and hemolytic activity. Chem Res Toxicol, 28(3), 501-509.
Chinnapongse, S.L., MacCuspie, R.I. and Hackley, V.A. (2011). Persistence of singly dispersed silver nanoparticles in natural freshwaters, synthetic seawater, and simulated estuarine waters." Sci Total Environ, 409(12), 2443-2450.
Chook, S. W., Chia, C. H., Zakaria, S., Ayob, M. K., Chee, K. L., Huang, N., Neoh, H., Lim, H., Jamal, R. and Rahman, R. (2012). Antibacterial performance of Ag nanoparticles and AgGO nanocomposites prepared via rapid microwave-assisted synthesis method. Nanoscale Res Lett , 7(1), 541.

Coleman J.G., Kennedy A.J., Bednar A.J., Ranville J.F., Laird J.G., Harmon A.R., Hayes C.A., Gray E.P., Higgins C.P., Lotufo G., Steevens J.A. (2013). Comparing the effects of nanosilver size and coating variations on bioavailability, internalization, and elimination, using Lumbriculus variegatus. Environ Toxicol Chem, 32(9), 2069-77.

Collins, A.R. (2004). The comet assay for DNA damage and repair: principles, applications, and limitations. Mol Biotechnol, 26 (3):249-261.

Comfort, K.K., Maurer, E.I., and Hussain, S.M. (2014). Slow release of ions from internalized silver nanoparticles modifies the epidermal growth factor signaling response. Colloids Surf B Biointerfaces, 1(123), 136-42.

Cornelis, Geert, Liping Pang, Casey Doolette, Jason Kirby, and Mike McLaughlin. (2013). Transport of silver nanoparticles in saturated columns of natural soils. Sci Total Environ, 463-464, 120-130.

Coutris, Claire, Erik Joner, and Deborah Oughton. (2012). Aging and soil organic matter content affect the fate of silver nanoparticles in soil. Sci Total Environ, 420, 327-333.

David, L., Moldovan, B., Vulcu, A., Olenic, L., Perde-Schrepler, M., Fischer-Fodor, E., Florea, A., Crisan, M., Chiorean, I., Clichici, S. and Filip, G.A. (2014). Green synthesis, characterization and anti-inflammatory activity of silver nanoparticles using European black elderberry fruits extract. Colloids Surf B Biointerfaces 122, 767-777.

Dechsakulthorn, F., Hayes, A., Bakand, S., Joeng, L. and Winder, C. (2007). In vitro cytotoxicity assessment of selected nanoparticles using human skin fibroblasts. AATEX, 14(Special Issue), 397-400.

Dubas, S. and Pimpan, V. (2008). "Green synthesis of silver nanoparticles for ammonia sensing." Talanta 76(1), 29-33.

Elle, R. E., Gaillet, S., Vidé, J., Romain, C., Lauret, C., Rugani, N., Cristol, J., and Rouanet, J. (2013). Dietary exposure to silver nanoparticles in Sprague-Dawley rats: effects on oxidative stress and inflammation." Food Chem Toxicol 60, 297-301.

Eckhardt, S., Brunetto, P. S., Gagnon, J., Priebe, M., Giese, B., and Fromm, K. M. (2013). Nanobio silver: its interactions with peptides and bacteria, and its uses in medicine. Chem Rev, 113(7), 4708-4754.

El Badawy , A. M., Luxton, T. P., Silva, R. G., Scheckel, K. G., Suidan, M. T., and Tolaymat, T. M. (2010). Impact of environmental conditions (pH, ionic strength, and electrolyte type) on the surface charge and aggregation of silver nanoparticles suspensions. Environ Sci Technol, 44(4), 1260-1266.

Elechiguerra, J. L., Burt, J. L., Morones, J. R., Camacho-Bragado, A., Gao, X., Lara, H. H., and Yacaman, M. J. (2005). Interaction of silver nanoparticles with HIV-1. J nanobiotechnol, 3(6), 1-10.

Eom, H. J., and Choi, J. (2010). p38 MAPK activation, DNA damage, cell cycle arrest and apoptosis as mechanisms of toxicity of silver nanoparticles in Jurkat T cells. Environ Sci Technol, 44(21), 8337-8342.

EPA, E.P.A. (2010). State of the Science Literature Review: Everything Nanosilver and More. Scientific, Technical, Research, Engineering and Modeling Support Final Report.

Fabrega, J., Fawcett, S. R., Renshaw, J. C., & Lead, J. R. (2009). Silver nanoparticle impact on bacterial growth: effect of pH, concentration, and organic matter. Environ Sci Technol, 43(19), 7285-7290.

Fabrega, J., Luoma, S. N., Tyler, C. R., Galloway, T. S., & Lead, J. R. (2011). Silver nanoparticles: behaviour and effects in the aquatic environment. Environ Int, 37(2), 517-531.

Faedmaleki, F., Shirazi, F., Salarian, A.A., Ahmadi Ashtiani H., and Rastegar, H. 2014. Toxicity Effect of Silver Nanoparticles on Mice Liver Primary Cell Culture and HepG2 Cell Line. Iran J Pharm Res 13 (1), 235-242.

Farré, M., Sanchís, J., & Barceló, D. (2011). Analysis and assessment of the occurrence, the fate and the behavior of nanomaterials in the environment. Trends Analyt Chem, 30(3), 517-527.

Fenech, M. (2007). Cytokinesis-block micronucleus cytome assay. Nature protocols, 2(5), 1084-1104.
Feynman, R.P. (1961). There's plenty of room at the bottom. Eng Sci, 23 (5), 22-36.
Finegold, M.J. (2004). "Hepatic tumors in childhood." Pathology of Pediatric Gastrointestinal and Liver Disease (pp. 300-346). Springer New York.
Foldbjerg, R., Dang, D. A., and Autrup, H. (2011). Cytotoxicity and genotoxicity of silver nanoparticles in the human lung cancer cell line, A549. Arch Toxicol, 85(7), 743-750.
Foldbjerg, R., Olesen, P., Hougaard, M., Dang, D. A., Hoffmann, H. J., & Autrup, H. (2009). PVP-coated silver nanoparticles and silver ions induce reactive oxygen species, apoptosis and necrosis in THP-1 monocytes. Toxicol Lett, 190(2), 156-162.
Galdiero, S., Falanga, A., Vitiello, M., Cantisani, M., Marra, V., & Galdiero, M. (2011). Silver nanoparticles as potential antiviral agents. Molecules, 16(10), 8894-8918.
Gao, X., X. Zhang, Y. Wang, and S. Peng. (2015). An in vitro study on the cytotoxicity of bismuth oxychloride nanosheets in human HaCaT keratinocytes. Food Chem Toxicol, 80, 52-61.
García-Contreras, R., Argueta-Figueroa, L., Mejía-Rubalcava, C., Jiménez-Martínez, R., Cuevas-Guajardo, S., Sánchez-Reyna, P.A. and Mendieta-Zeron, H. (2011). Perspectives for the use of silver nanoparticles in dental practice. Int Dent J, 61(6), 297-301.
Geranio, L., Heuberger, M. and Nowack, B. (2009). The behavior of silver nanotextiles during washing." Environ Sci Technol, 3(21), 8113-8118.
Ginn, C., Khalili, H., Lever, R., and Brocchini, S. (2014). PEGylation and its impact on the design of new protein-based medicines. Future Med Chem, 6(16), 1829-1846.
Giovanni, M., Yue, J., Zhang, L., Xie, J., Ong, C. N. and Leong, D. T. (2015). Pro-Inflammatory Responses of RAW264. 7 Macrophages when Treated with Ultralow Concentrations of Silver, Titanium Dioxide, and Zinc Oxide Nanoparticles. J Hazard Mater, 297, 146-152.
Greulich, C., Diendorf, J., Gessmann, J., Simon, T., Habijan, T., Eggeler, G., Schildhauer, T., Epple, M. and Köller, M. (2011). Cell type-specific responses of peripheral blood mononuclear cells to silver nanoparticles. Acta Biomater, 7(9), 3505-3514.
Greulich, C., Diendorf, J., Simon, T., Eggeler, G., Epple, M., & Köller, M. (2011). Uptake and intracellular distribution of silver nanoparticles in human mesenchymal stem cells. Acta Biomater, 7(1), 347-354.
Gurunathan, S., Lee, K. J., Kalishwaralal, K., Sheikpranbabu, S., Vaidyanathan, R., and Eom, S. H. (2009). Antiangiogenic properties of silver nanoparticles. Biomaterials, 30(31), 6341-6350.
Gutierrez, L., Aubry, C., Cornejo, M., and Croue, J.P. (2015). Citrate-coated silver nanoparticles interactions with effluent organic matter: influence of capping agent and solution conditions. Langmuir, 31(32), 8865-8872.
Gutting, B.W., Gaske, K.S., Schilling, A.S., Slaterbeck, A.F., Sobota, L., Mackie, R.S. and Buhr, T.L. (2005). Differential susceptibility of macrophage cell lines to Bacillus anthracis-Vollum 1B. Toxicol In Vitro, 19(2), 221-229.
Haase, A., Arlinghaus, H. F., Tentschert, J., Jungnickel, H., Graf, P., Mantion, A., Draude, F., Galla, S., Plendl, J., Goetz, M., Masic, A., Meier, W., Thünemann, A., Taubert, A. and Luch, A. (2011). Application of laser postionization secondary neutral mass spectrometry/time-of-flight secondary ion mass spectrometry in nanotoxicology: visualization of nanosilver in human macrophages and cellular responses. Acs Nano, 5(4), 3059-3068.
Haase, A., Rott, S., Mantion, A., Graf, P., Plendl, J., Thünemann, A. F., Meier, W., Taubert, A., Luch, A. and Reiser, G. (2012). Effects of silver nanoparticles on primary mixed neural cell cultures: uptake, oxidative stress and acute calcium responses. Toxicol Sci, 126(2), 457-468.
Hackenberg, S., Scherzed, A., Kessler, M., Hummel, S., Technau, A., Froelich, K, Ginzkey, C., Koehler, C., Hagen, R. and Kleinsasser, N. (2011). Silver nanoparticles: evaluation of

DNA damage, toxicity and functional impairment in human mesenchymal stem cells. Toxicol Lett, 201(1), 27-33.
Handy, R. D., Owen, R., and Valsami-Jones, E. (2008). The ecotoxicology of nanoparticles and nanomaterials: current status, knowledge gaps, challenges, and future needs. Ecotoxicology, 17(5), 315-325.
Handy, R.D., Von der Kammer, F., Lead, J.R., Hassellöv, M., Owen, R. and Crane, M. (2008). The ecotoxicology and chemistry of manufactured nanoparticles. Ecotoxicology, 17(4), 287-314.
Henglein, A., and Giersig, M. (1999). Formation of colloidal silver nanoparticles: capping action of citrate. J Phys Chem B, 103, 9533-9539.
Hillyer, J., and Albrecht, R. (2001). Gastrointestinal persorption and tissue distribution of differently sized colloidal gold nanoparticles. J Pharm Sci, 90(12), 1927-1936.
Huo, S.J., Xue, X.K., Li, Q.X., Xu, S.F., and Cai, W.B. (2006). Seeded-growth approach to fabrication of silver nanoparticle films on silicon for electrochemical ATR surface-enhanced IR absorption spectroscopy. J Phys Chem B, 110(51), 25721-25728.
Iyoda, K., Sasaki, Y., Horimoto, M., Toyama, T., Yakushijin, T., Sakakibara, M., Takehara, T., Fujimoto, J., Hori, M., Wands, J.R. and Hayashi, N. (2003). Involvement of the p38 mitogen- activated protein kinase cascade in hepatocellular carcinoma. Cancer, 97(12), 3017-26.
Jain, J., Arora, S., Rajwade, J.M., Omray, P., Khandelwal, S. and Paknikar, K.M. (2009). Silver nanoparticles in therapeutics: development of an antimicrobial gel formulation for topical use. Mol Pharm, 6(5), 1388-1401.
Jain, A., and Jain, S.K. (2008). PEGylation: an approach for drug delivery. A review. Crit Rev Ther Drug Carrier Syst, 25(5), 403-447.
Jazayeri, S.D., Ideris, A., Shameli, K., Moeini, H., and Omar, A.R. (2013). Gene expression profiles in primary duodenal chick cells following transfection with avian influenza virus H5 DNA plasmid encapsulated in silver nanoparticles. Int J Nanomedicine, 8, 781.
Jegatheeswaran, S., and Sundrarajan, M. (2015). PEGylation of novel hydroxyapatite/PEG/Ag nanocomposite particles to improve its antibacterial efficacy. Mater Sci Eng C, 51, 174-181.
Ji, J. H., Jung, J. H., Kim, S. S., Yoon, J. U., Park, J. D., Choi, B. S, Chung, Y., Kwon, I., Jeong, J., Han, B., Shin, J., Sung, J.,Song, K. and Yu, I. (2007). Twenty-eight-day inhalation toxicity study of silver nanoparticles in Sprague-Dawley rats. Inhal Toxicol, 19(10), 857-871.
Joo, H. S., Kalbassi, M. R., Yu, I. J., Lee, J. H. and Johari, S. A. (2013). Bioaccumulation of silver nanoparticles in rainbow trout (Oncorhynchus mykiss): Influence of concentration and salinity. Aquat Toxicol, 140, 398-406.
Ju-Nam, Y. and Lead, J. (2008). Manufactured nanoparticles: an overview of their chemistry, interactions and potential environmental implications. Sci Total Environ, 400(1-3), 396-414.
Kang, S., Lee, Y., Lee, E.K. and Kwak, M.K. (2012). Silver nanoparticles-mediated G2/M cycle arrest of renal epithelial cells is associated with NRF2-GSH signaling. Toxicol Lett, 211(3), 334-341.
Kawata, K., Osawa, M. and Okabe, S. (2009). In vitro toxicity of silver nanoparticles at noncytotoxic doses to HepG2 human hepatoma cells. Environ Sci Technol, 43(15), 6046-6051.
Kelso, A. (1998). Cytokines: principles and prospects. Immunol Cell Biol 76, 300-317.
Lai, S.K., Wang, Y.-Y.Y., and Hanes, J. (2009). Mucus-penetrating nanoparticles for drug and gene delivery to mucosal tissues. Adv Drug Deliv Rev 61, 158-171.
Kim, H.R., Kim, M.J., Lee, S., Oh, S. and Chung, K. (2011). Genotoxic effects of silver nanoparticles stimulated by oxidative stress in human normal bronchial epithelial (BEAS-2B) cells. Mutat Res, 726(2),129-135.
Kim, J. A., Y. S. Kang, and Y. S. Lee. (2003). Role of Ca 2+-activated Cl− channels in the

mechanism of apoptosis induced by cyclosporin A in a human hepatoma cell line. Biochem Biophys Res Commun,. 309(2), 291-7.
Kim, K.J., Sung, W.S., Suh, B.K., Moon, S.K., Choi, J.S., Kim, J.G. and Lee, D.G. (2009). Antifungal activity and mode of action of silver nano-particles on Candida albicans. Biometals, 22(2), 235-242.
Kim, S. and Choi, I.H. (2012). Phagocytosis and endocytosis of silver nanoparticles induce interleukin-8 production in human macrophages. Yonsei Med J, 53(3), 654-657.
Kim, S., Kim, S., Lee, S., Kwon, B., Choi, J., Hyun, J.W., & Kim, S. (2011). Characterization of the effects of silver nanoparticles on liver cell using HR-MAS NMR spectroscopy. Bull Korean Chem Soc, 32(6), 2021-2026.
Kim, S., Choi, J.E., Choi, J., Chung, K.H., Park, K., Yi, J. and Ryu, D.Y. 2009. Oxidative stress-dependent toxicity of silver nanoparticles in human hepatoma cells. Toxicol In Vitro, 23(6), 1076-1084.
Kim, Soohee, and Doug-Young Ryu. (2013). Silver nanoparticle-induced oxidative stress, genotoxicity and apoptosis in cultured cells and animal tissues. J Appl Toxicol, 33(2), 78-89.
Kim, Y. S., Kim, J. S., Cho, H. S., Rha, D. S., Kim, J. M., Park, J. D, Choi, B., Lim, R., Chang, H., Chung, Y., Kwon, I., Jeong, J., Han, B. and Yu, I. (2008). Twenty-eight-day oral toxicity, genotoxicity, and gender-related tissue distribution of silver nanoparticles in Sprague-Dawley rats. Inhal Toxicol, 20(6), 575-583.
Knasmüller, S., Parzefall, W., Sanyal, R., Ecker, S., Schwab, C., Uhl, M., Mersch-Sundermann, V., Williamson, G., Hietsch, G., Langer, T., Darroudi, F. and Natarajan, A.T. (1998). Use of metabolically competent human hepatoma cells for the detection of mutagens and antimutagens. Mutat Res, 402(1-2), 185-202.
Knowles, B.B., Howe, C.C. and Aden, D.P. (1980). Human hepatocellular carcinoma cell lines secrete the major plasma proteins and hepatitis B surface antigen. Science, 209 (4455), 497-499.
Kruszewski, M., Grądzka, I., Bartłomiejczyk, T., Chwastowska, J., Sommer, S., Grzelak, A., Zuberek, M., Lankoff, A., Dusinska, M. and Wojewódzka, M. (2013). Oxidative DNA damage corresponds to the long term survival of human cells treated with silver nanoparticles. Toxicol Lett, 219(2), 151-159.
Lai, S.K., Wang, Y.-Y.Y., and Hanes, J. (2009). Mucus-penetrating nanoparticles for drug and gene delivery to mucosal tissues. Adv Drug Deliv Rev, 61, 158-171.
Lecoanet, H.F., and Wiesner, M.R. (2004). Velocity effects on fullerene and oxide nanoparticle deposition in porous media. Environ Sci Technol, 38(16), 4377-4382.
Lee, P.C. and Meisel, D. (1982). Adsorption and surface-enhanced Raman of dyes on silver and gold sols. J Phys Chem, 86(17), 3391-3395.
Levard, C., Hotze, E.M., Lowry, G.V., Brown Jr, G.E. (2012). Environmental transformations of silver nanoparticles: impact on stability and toxicity. Environ Sci Technol, 46(13), 6900-6914.
Li, C., Fu, R., Yu, C., Li, Z., Guan, H., Hu, D., Zhao, D. and Lu, L. (2013). Silver nanoparticle/chitosan oligosaccharide/poly(vinyl alcohol) nanofibers as wound dressings: a preclinical study. Int J Nanomedicine, 8, 4131-4145.
Li, Y., Leung, P., Yao, L., Song, Q. and Newton, E. (2006). Antimicrobial effect of surgical masks coated with nanoparticles. J Hosp Infect, 62(1), 58-63.
Liang, Y., Bradford, S. A., Simunek, J., Vereecken, H., and Klumpp, E. (2013). Sensitivity of the transport and retention of stabilized silver nanoparticles to physicochemical factors. Water Res, 47(7), 2572-2582.
Liden, G. (2011). The European Commission Tries to Define Nanomaterials." Ann Occup Hyg, 55(1):1-5.
Lin, S., Cheng, Y., Liu, J. and Wiesner, M.R. (2012). Polymeric coatings on silver nanoparticles hinder autoaggregation but enhance attachment to uncoated surfaces. Langmui, 28(9), 4178-4186.

Liu, L., Ni, F., Zhang, J., Jiang, X., Lu, X., Guo, Z., & Xu, R. (2011). Silver nanocrystals sensitize magnetic-nanoparticle-mediated thermo-induced killing of cancer cells. Acta Biochim Biophys Sin (Shanghai), 43(4), 316-323.

Liu, W., Wu, Y., Wang, C., Li, H.C., Wang, T., Liao, C.Y., and Jiang, G.B. (2010). Impact of silver nanoparticles on human cells: effect of particle size. Nanotoxicology, 4(3), 319-330.

Loeschner, K., Hadrup, N., Qvortrup, K., Larsen, A., Gao, X., Vogel, U., Mortensen, A., Lam, H.R. and Larsen, E.H. (2011). Distribution of silver in rats following 28 days of repeated oral exposure to silver nanoparticles or silver acetate. Part Fibre Toxicol, 8(1), 1.

Love, S.A. and Haynes, C.L. (2010). Assessment of functional changes in nanoparticle-exposed neuroendocrine cells with amperometry: exploring the generalizability of nanoparticle-vesicle matrix interactions. Anal Bioanal Chem, 398(2), 677-688.

Love, S.A., Liu, Z. and Haynes, C.L. (2012). Examining changes in cellular communication in neuroendocrine cells after noble metal nanoparticle exposure. Analyst, 137(13), 3004-3010.

Lu, W., Senapati, D., Wang, S., Tovmachenko, O., Singh, A.K., Yu, H. and Ray, P.C. (2010). Effect of surface coating on the toxicity of silver nanomaterials on human skin keratinocytes. Chem Phys Lett, 487(1), 92-96.

Luo, C., Zhang, Y., Zeng, X., Zeng, Y. and Wang, Y. (2005). The role of poly (ethylene glycol) in the formation of silver nanoparticles. J Colloid Interface Sci, 288(2), 444-448.

Luoma, S. N. (2008). Silver nanotechnologies and the environment: old problems or new challenges? Project on Emerging Nanotechnologies, Wilson Center and The Pew Charitable Trusts, Washington DC USA, September 2008, p72.

Luther, E. M., Koehler, Y., Diendorf, J., Epple, M. and Dringen, R. (2011). Accumulation of silver nanoparticles by cultured primary brain astrocytes. Nanotechnology, 22(37), 375101.

Matranga, V. and Corsi, I. (2012). Toxic effects of engineered nanoparticles in the marine environment: model organisms and molecular approaches. Mar Environ Res, 76, 32-40.

Maynard, A. D., Aitken, R. J., Butz, T., Colvin, V., Donaldson, K., Oberdörster, G., Philbert, M.A., Ryan, J., Seaton, A., Stone, V., Tinkle, S.S., Tran, L., Walker, N.J. and Warheit. D. B. (2006). Safe handling of nanotechnology. Nature, 444(7117), 267-269.

McDowell- Boyer, L. M., Hunt, J. R., and Sitar, N. (1986). Particle transport through porous media. Water Resour Res, 22(13), 1901-1921.

Miaśkiewicz-Peska, E. and Łebkowska, M. (2011). Effect of antimicrobial air filter treatment on bacterial survival." Fibres Text East Eur, 19(84), 73-77.

Miethling-Graff, R., Rumpker, R., Richter, M., Verano-Braga, T., Kjeldsen, F., Brewer, J., Hoyland, J., Rubahn, H.-G.G., and Erdmann, H. (2014). Exposure to silver nanoparticles induces size-and dose-dependent oxidative stress and cytotoxicity in human colon carcinoma cells. Toxicol In Vitro, 28(7), 1280-1289.

Monteiro-Riviere, N A., Nemanich, R.J., Inman, A.O., Wang, Y.Y. and Riviere, J.E. (2005). Multi-walled carbon nanotube interactions with human epidermal keratinocytes. Toxicol Lett, 155(3), 377-384.

Monteiro-Riviere, N.A., Samberg, M.E., Oldenburg, S.J., and Riviere, J.E. (2013). Protein binding modulates the cellular uptake of silver nanoparticles into human cells: implications for in vitro to in vivo extrapolations?. Toxicol Letters, 220(3), 286-293.

Mpenyana-Monyatsi, L., Mthombeni, N.H., Onyango, M.S. and Momba, M.N. (2012). Cost-effective filter materials coated with silver nanoparticles for the removal of pathogenic bacteria in groundwater. Int J Environ Res Public Health, 9(1), 244-271.

Munusamy, P., Wang, C., Engelhard, M. H., Baer, D. R., Smith, J. N., Liu, C. and Ryan, M. P. (2015). Comparison of 20 nm silver nanoparticles synthesized with and without a gold core: Structure, dissolution in cell culture media, and biological impact on macrophages. Biointerphases, 10(3), 031003.

Murray, A.R., Kisin, E., Inman, A., Young, S.-H., Muhammed, M., Burks, T., Uheida, A.,

Tkach, A., Waltz, M., and Castranova, V. (2013). Oxidative stress and dermal toxicity of iron oxide nanoparticles in vitro. Cell Biochem Biophys, 67(2), 461-476.
Mwilu, S.K., El Badawy, A.M., Bradham, K., Nelson, C., Thomas, D., Scheckel, K.G., Tolaymat, T., Ma, L. and Rogers, K. (2013). Changes in silver nanoparticles exposed to human synthetic stomach fluid: effects of particle size and surface chemistry. Sci Total Environ, 447, 90-98.
Nadworny, P. L., Wang, J., Tredget, E. E., and Burrell, R. E. (2010). Anti-inflammatory activity of nanocrystalline silver-derived solutions in porcine contact dermatitis. J Inflamm, 7(1), 13.
Nair, L.S. and Laurencin, C.T. (2007). Silver nanoparticles: synthesis and therapeutic applications. J Biomed Nanotechnol, 3(4), 301-316.
Naureckiene, S., Edris, W., Ajit, S.K., Katz, A.H., Sreekumar, K., Rogers, K.E., and Jones, P.G. (2007). Use of a murine cell line for identification of human nitric oxide synthase inhibitors. J Pharmacol Toxicol Methods, 55(3), 303-13.
Navarro, E., Baun, A., Behra, R., Hartmann, N. B., Filser, J., Miao, A. J., Quigg, A., Santschi, P. and Sigg, L. (2008). Environmental behavior and ecotoxicity of engineered nanoparticles to algae, plants, and fungi. Ecotoxicology, 17(5), 372-386.
Nowack, B., and Bucheli, T. D. (2007). Occurrence, behavior and effects of nanoparticles in the environment. Environ Pollut, 150(1), 5-22.
Nowack, B., Krug, H. F., & Height, M. (2011). 120 years of nanosilver history: implications for policy makers. Environ Sci Technol, 45(4), 1177-1183.
Oberdörster, G., Oberdörster, E., and Oberdörster, J. (2005). Nanotoxicology: an emerging discipline evolving from studies of ultrafine particles. Environ Health Perspect, 823-839.
Orlowski, P., Krzyzowska, M., Zdanowski, R., Winnicka, A., Nowakowska, J., Stankiewicz, Tomaszewska, E., Celichowski, G. and Grobelny, J. (2013). Assessment of in vitro cellular responses of monocytes and keratinocytes to tannic acid modified silver nanoparticles. Toxicol In Vitro, 27(6), 1798-1808.
Panáček, A., Kvitek, L., Prucek, R., Kolar, M., Vecerova, R., Pizurova, N., Sharma, V., Nevecna, T. and Zboril, R. (2006). Silver colloid nanoparticles: synthesis, characterization, and their antibacterial activity. J Phys Chem B, 110(33), 16248-16253.
Pang, C., Brunelli, A., Zhu, C., Hristozov, D., Liu, Y., Semenzin, E., Wang, W., Tao, W., Liang, J., Marcomini, A., Chen, C. and Bin Zhao. (2015). Demonstrating approaches to chemically modify the surface of Ag nanoparticles in order to influence their cytotoxicity and biodistribution after single dose acute intravenous administration. Nanotoxicology, 1-11.
Parnsamut, C., and Brimson, S. (2015). Effects of silver nanoparticles and gold nanoparticles on IL-2, IL-6, and TNF-α production via MAPK pathway in leukemic cell lines. Genet Mol Res, 14(2), 3650.
Park, E.J.J., Choi, K., and Park, K. (2011). Induction of inflammatory responses and gene expression by intratracheal instillation of silver nanoparticles in mice. Arch Pharm Res 34, 299-307.
Park, K., Park, E. J., Chun, I. K., Choi, K., Lee, S. H., Yoon, J. and Lee, B. C. (2011). Bioavailability and toxicokinetics of citrate-coated silver nanoparticles in rats. Arch Pharm Res, 34(1), 153-158.
Park, M.V., Neigh, A.M., Vermeulen, J.P., de la Fonteyne, L.J., Verharen, H.W., Briedé, J.J., Loveren, H. and Jong, W. (2011). The effect of particle size on the cytotoxicity, inflammation, developmental toxicity and genotoxicity of silver nanoparticles. Biomaterials, 32(36), 9810-9817.
Pastoriza-Santos, I. and Liz-Marzán, L. M. (1999). Formation and stabilization of silver nanoparticles through reduction by N, N-dimethylformamide. Langmuir, 15(4), 948-951.
Piao, M.J., Kang, K.A., Lee, I.K., Kim, H.S., Kim, S., Choi, J.Y., Choi, J. and Hyun, J. (2011). Silver nanoparticles induce oxidative cell damage in human liver cells through inhibition of reduced glutathione and induction of mitochondria-involved apoptosis. Toxicol Lett,

201(1), 92-100.
Pillai, Z.S. and Kamat, P.V. (2004). What factors control the size and shape of silver nanoparticles in the citrate ion reduction method?. J Phys Chem B, 108(3), 945-951.
Poirier, M., Simard, J. C., Antoine, F., and Girard, D. (2014). Interaction between silver nanoparticles of 20 nm (AgNP20) and human neutrophils: induction of apoptosis and inhibition of de novo protein synthesis by AgNP20 aggregates. J Appl Toxicol, 34(4), 404-412.
Popa, M., Pradell, T., Crespo, D., & Calderón-Moreno, J. M. (2007). Stable silver colloidal dispersions using short chain polyethylene glycol. Colloids Surf A Physicochem Eng Asp, 303(3), 184-190.
Prakash, P., Gnanaprakasam, P., Emmanuel, R., Arokiyaraj, S., and Saravanan, M. (2013). Green synthesis of silver nanoparticles from leaf extract of Mimusops elengi, Linn. for enhanced antibacterial activity against multi drug resistant clinical isolates. Colloids Surf B Biointerfaces, 108, 255-259.
Prakash, Y.S. and Matalon, S. (2014). Nanoparticles in the lung: friend or foe?. Am J Physiol Lung Cell Mol Physiol, 306 (4), L393-L396.
Qian, Y., Yu, H., He, D., Yang, H., Wang, W., Wan, X., & Wang, L. (2013). Biosynthesis of silver nanoparticles by the endophytic fungus Epicoccum nigrum and their activity against pathogenic fungi. Bioprocess Biosyst Eng, 36(11), 1613-1619.
Rana, S.V.S. and Taketa, K. (1997). Liver and Environmental Xenobiotics. Berlin Heidelberg New York: Springer-Verlag.
Raschke, W.C., Baird, S., Ralph, P. and Nakoinz, I. (1978). Functional macrophage cell lines transformed by Abelson leukemia virus. Cell, 15(1), 261-267.
Rejman, J., Oberle, V., Zuhorn, I. S., & Hoekstra, D. (2004). Size-dependent internalization of particles via the pathways of clathrin-and caveolae-mediated endocytosis. Biochem J, 377(1), 159-169.
Remédios, C., Rosário, F. and Bastos, V. (2012). Environmental Nanoparticles Interactions with Plants: Morphological, Physiological, and Genotoxic Aspects. J Botany, 2012.
Roberts, S. M., James, R. C., & Williams, P. L. (2014). Principles of toxicology: environmental and industrial applications. John Wiley & Sons
Rogers, J.V., Parkinson, C.V., Choi, Y.W., Speshock, J.L. and Hussain, S.M. (2008). A preliminary assessment of silver nanoparticle inhibition of monkeypox virus plaque formation. Nanoscale Res Lett, 3(4), 129-133.
Roldan, M.V., Frattini, A., de Sanctis, O., Troiani, H. and Pellegri, N. (2007). Characterization and applications of Ag nanoparticles in waveguides. Appl Surf Sci, 254(1), 281-285.
Ryan, S.M.M., Mantovani, G., Wang, X., Haddleton, D.M., and Brayden, D.J. (2008). Advances in PEGylation of important biotech molecules: delivery aspects. Expert Opin Drug Deliv 5(4), 371-383.
Sagee, O., Dror, I., and Berkowitz, B. (2012). Transport of silver nanoparticles (AgNPs) in soil. Chemosphere, 88(5), 670-675.
Sahu, S.C., Zheng, J., Graham, L., Chen, L., Ihrie, J., Yourick, J.J. and Sprando, R.L. (2014). Comparative cytotoxicity of nanosilver in human liver HepG2 and colon Caco2 cells in culture. J Appl Toxicol, 34:1155-1166.
Samberg, M.E., Oldenburg, S.J., and Monteiro-Riviere, N.A. (2010). Evaluation of Silver Nanoparticle Toxicity in Skin in Vivo and Keratinocytes in Vitro. Environ Health Perspect, 118, 407-413.
Shahverdi, A. R., Fakhimi, A., Shahverdi, H. R., & Minaian, S. (2007). Synthesis and effect of silver nanoparticles on the antibacterial activity of different antibiotics against Staphylococcus aureus and Escherichia coli. Nanomedicine, 3(2), 168-171.
Shang, L., Nienhaus, K. and Nienhaus, G.U. (2014). Engineered nanoparticles interacting with cells: size matters. J Nanobiotechnol, 12(5), b67.
Sharma, V., Yngard, R., and Lin, Y. (2009). Silver nanoparticles: green synthesis and their antimicrobial activities. Adv Colloid Interface Sci 145(1), 83-96.

Sheng, Z. and Liu, Y. (2011). Effects of silver nanoparticles on wastewater biofilms. Water Res, 45(18), 6039-6050.
Shi, J., Sun, X., Lin, Y., Zou, X., Li, Z., Liao, Y., Du, M., and Zhang, H. (2014). Endothelial cell injury and dysfunction induced by silver nanoparticles through oxidative stress via IKK/NF-κB pathways. Biomaterials, 35(24), 6657-6666.
Shoults-Wilson, W. A., Reinsch, B.C., Tsyusko, O. V., Bertsch, P. M., Lowry, G. V., and Unrine, J. M. (2011). Role of particle size and soil type in toxicity of silver nanoparticles to earthworms. Soil Sci Soc Am J, 75(2), 365-377.
Shoults-Wilson, W. A., Reinsch, B. C., Tsyusko, O. V., Bertsch, P. M., Lowry, G. V. and Unrine, J. M. (2011). Effect of silver nanoparticle surface coating on bioaccumulation and reproductive toxicity in earthworms (Eisenia fetida). Nanotoxicology, 5(3), 432-444.
Simonet, B., and Valcárcel, M. (2009). Monitoring nanoparticles in the environment. Anal Bioanal Chem, 393(1), 17-21.
Singh, N.P. 1998. "A rapid method for the preparation of single-cell suspensions from solid tissues." Cytometry, 31(3), 229-232.
Singh, R.P. and Ramarao, P. (2012). Cellular uptake, intracellular trafficking and cytotoxicity of silver nanoparticles. Toxicol Lett, 213(2), 249-259.
Sirivithayapakorn, S. and Keller, A. (2003). Transport of colloids in saturated porous media: A pore- scale observation of the size exclusion effect and colloid acceleration. Water Resour Res, 39(4).
Slominski, A. T., Janjetovic, Z., Kim, T. K., Wasilewski, P., Rosas, S., Hanna, S., Sayre, R., Dowdy, J.C., Li, W. and Tuckey, R.C. (2015). Novel non-calcemic secosteroids that are produced by human epidermal keratinocytes protect against solar radiation. J Steroid Biochem Mol Biol, 148, 52-63.
Sonavane, G., Tomoda, K. and Makino, K. (2008). Biodistribution of colloidal gold nanoparticles after intravenous administration: effect of particle size. Colloids Surf B Biointerfaces, 66(2), 274-280.
Song, X.L., Li, B., Xu, K., Liu, J., Ju, W., Wang, J., Liu, X., Li, J. and Qi, Y. (2012). Cytotoxicity of water-soluble mPEG-SH-coated silver nanoparticles in HL-7702 cells. Cell Biol Toxicol, 28(4), 225-237.
Stampoulis, D., Sinha, S.K. and White, J.C. (2009). Assay-dependent phytotoxicity of nanoparticles to plants. Environ Sci Technol, 43(24), 9473-9479.
Stern, S.T. and McNeil, S.E. (2008). Nanotechnology safety concerns revisited. Toxicol Sci, 101 (1), 4-21.
Suliman, Y., Omar, A., Ali, D., Alarifi, S., Harrath, A. H., Mansour, L. and Alwasel, S.H. (2015). Evaluation of cytotoxic, oxidative stress, proinflammatory and genotoxic effect of silver nanoparticles in human lung epithelial cells. Environ Toxicol, 30(2), 149-160.
Suk, J.S., Lai, S.K., Boylan, N.J., Dawson, M.R., Boyle, M.P. and Hanes, J. (2011). Rapid transport of muco-inert nanoparticles in cystic fibrosis sputum treated with N-acetyl cysteine. Nanomedicine, 6(2), 365-375.
Szmyd, R., Goralczyk, A. G., Skalniak, L., Cierniak, A., Lipert, B., Filon, F. L., Crosera, M., Borowczyk, J., Laczna, E., Drukala, J., Klein, A. and Jura, J. (2013). Effect of silver nanoparticles on human primary keratinocytes. Biol Chem, 394 (1):113-123.
Takenaka, S., Karg, E., Roth, C., Schulz, H., Ziesenis, A., Heinzmann, U., Schramel, P. and Heyder, J. (2001). Pulmonary and systemic distribution of inhaled ultrafine silver particles in rats. Environ Health Perspect, 109 Suppl 4:547-551.
Tang, J., Xiong, L., Wang, S., Wang, J., Liu, L., Li, J., Yuan, F. and Xi, T. (2009). Distribution, translocation and accumulation of silver nanoparticles in rats. J Nanosci Nanotechnol, 9 (8):4924-4932.
Tang, J., Xiong, L., Zhou, G., Wang, S., Wang, J., Liu, L, Li, J., Yuan, F., Lu, S., Wan, Z., Chou, L. and Xi, T. (2010). Silver nanoparticles crossing through and distribution in the blood-brain barrier in vitro. J Nanosci Nanotechnol no. 10 (10):6313-6317.
Teow, Y., Asharani, P.V., Hande, M.P. and Valiyaveettil, S. (2011). Health impact and safety of

engineered nanomaterials. Chem Commun, 47(25), 7025-7038.
Tervonen, T., Linkov, I., Figueira, J.R., Steevens, J., Chappell, M. and Merad, M. (2009). Risk-based classification system of nanomaterials. J Nanopart Res, 11(4), 757-766.
Tice, R. R., Agurell, E., Anderson, D., Burlinson, B., Hartmann, A., Kobayashi, H., Miyamae, Y., Rojas, E., Ryu, J.C. and Sasaki Y.F. (2000). Single cell gel/comet assay: Guidelines for in vitro and in vivo genetic toxicology testing. Environ Mol Mutagen, 35(3), 206-221.
Tinkle, S.S., Antonini, J.M., Rich, B.A., Roberts, J.R., Salmen, R., DePree, K. and Adkins, E.J. (2003). Skin as a route of exposure and sensitization in chronic beryllium disease. Environ Health Perspect, 111(9), 1202.
Toll, R., Jacobi, U., Richter, H., Lademann, J., Schaefer, H. and Blume-Peytavi, U. (2004). Penetration profile of microspheres in follicular targeting of terminal hair follicles. J Investig Dermatol, 123(1), 168-176.
Tolaymat, T.M., El Badawy, A.M., Genaidy, A., Scheckel, K.G., Luxton, T.P. and Suidan, M. (2010). An evidence-based environmental perspective of manufactured silver nanoparticle in syntheses and applications: a systematic review and critical appraisal of peer-reviewed scientific papers. Sci Total Environ, 408(5), 999-1006.
Tomankova, K., Horakova, J., Harvanova, M., Malina, L., Soukupova, J., Hradilova, S, Kejlova, K., Malohlava, J., Licman, L., Dvorakova, M., Jirova, D. and Kolarova, H. (2015). Cytotoxicity, cell uptake and microscopic analysis of titanium dioxide and silver nanoparticles in vitro. Food Chem Toxicol, 82, 106-115.
Tourinho, P. S., Van Gestel, C. A., Lofts, S., Svendsen, C., Soares, A. M. and Loureiro, S. (2012). Metal-based nanoparticles in soil: fate, behavior, and effects on soil invertebrates." Environ Toxicol Chem 31(8), 1679-1692.
Treuel, L., Malissek, M., Gebauer, J. S. and Zellner, R. (2010). The influence of surface composition of nanoparticles on their interactions with serum albumin.ChemPhysChem, 11(14), 3093-3099.
Trop, M., Novak, M., Rodl, S., Hellbom, B., Kroell, W. and Goessler, W. (2006). Silver-coated dressing acticoat caused raised liver enzymes and argyria-like symptoms in burn patient. J Trauma Acute Care Surg, 60(3), 648-652.
Van der Veen, J.W., Hodemaekers, H., Reus, A.A., Maas, W.J., van Loveren, H. and Ezendam, J. (2015). Human relevance of an in vitro gene signature in HaCaT for skin sensitization. Toxicol In Vitro, 29(1), 81-84.
Vigo, E., Cepeda, A. and Gualillo, O. (2005). In-vitro anti-inflammatory activity of Pinus sylvestris and Plantago lanceolata extracts: effect on inducible NOS, COX-1, COX-2 and their products in J774A.1 murine macrophages. J Pharm Pharmacol, 57(3), 383-391.
Vlachou, E., Chipp, E., Shale, E., Wilson, Y. T., Papini, R. and Moiemen, N. S. (2007). The safety of nanocrystalline silver dressings on burns: a study of systemic silver absorption. Burns, 33(8), 979-985.
Vo-Dinh, T., Wang, H.N. and Scaffidi, J. (2010). Plasmonic nanoprobes for SERS biosensing and bioimaging. J Biophotonics, 3(1-2), 89-102.
Walker, N.J. and Bucher, J.R. (2009). A 21st century paradigm for evaluating the health hazards of nanoscale materials?. Toxicol Sci, 110(2), 251-254.
Wang, H., Wu, L. and Reinhard, B. M. (2012). Scavenger receptor mediated endocytosis of silver nanoparticles into J774A. 1 macrophages is heterogeneous. Acs Nano, 6(8), 7122-7132.
Ward, J., and Kach, D.J. (2009). Marine aggregates facilitate ingestion of nanoparticles by suspension-feeding bivalves. Mar Environ Res, 68 (3):137-142.
Weisbarth, R.E., Gabriel, M.M., George, M., Rappon, J., Miller, M., Chalmers, R. and Winterton, L. (2007). Creating antimicrobial surfaces and materials for contact lenses and lens cases. Eye Contact Lens, 33(6, Part 2 of 2), 426-429.
Wiley, B., Sun, Y., Mayers, B. and Xia, Y. (2005). Shape-controlled synthesis of metal nanostructures: the case of silver. Chem A Eur J, 11(2), 454-463.

Wiley, B., Sun, Y. and Xia, Y. (2007). Synthesis of silver nanostructures with controlled shapes and properties. Acc Chem Res, 40(10), 1067-1076.

Wijnhoven, S. W., Peijnenburg, W. J., Herberts, C. A., Hagens, W. I., Oomen, A. G., Heugens, E. H., Roszek, B., Bisschops, J., Gosens, I., Van De Meent, D., Dekkers, S., De Jong, W., Van Zijverden, M. and Geertsma, R. (2009). Nano-silver–a review of available data and knowledge gaps in human and environmental risk assessment. Nanotoxicology, 3(2), 109-138.

Wong, K. K., Cheung, S. O., Huang, L., Niu, J., Tao, C., Ho, C. M., Che, C.M.M. and Tam, P.K. (2009). "Further evidence of the anti-inflammatory effects of silver nanoparticles." ChemMedChem 4(7), 1129-1135.

Wu, A.C., Grøndahl, L., Jack, K.S., Foo, M.X., Trau, M., Hume, D.A. and Cassady, A. I. (2006). Reduction of the in vitro pro-inflammatory response by macrophages to poly (3-hydroxybutyrate-co-3-hydroxyvalerate). Biomaterials,27(27), 4715-4725.

Xin, L., Wang, J., Fan, G., Che, B., Wu, Y., Guo, S. and Tong, J. (2015). Oxidative stress and mitochondrial injury- mediated cytotoxicity induced by silver nanoparticles in human A549 and HepG2 cells. Environ Toxicol.

Xiong, D., Chen, M. and Li, H. (2008). Synthesis of para-sulfonatocalix [4] arene-modified silver nanoparticles as colorimetric histidine probes. Chem Commun, (7), 880-882.

Xiu, Z. M., Ma, J. and Alvarez, P. J. (2011). Differential effect of common ligands and molecular oxygen on antimicrobial activity of silver nanoparticles versus silver ions. Environ Sci Technol, 45(20), 9003-9008.

Xu, Y., Tang, H., Liu, J.H., Wang, H. and Liu, Y. (2013). Evaluation of the adjuvant effect of silver nanoparticles both in vitro and in vivo. Toxicol Lett,219(1), 42-48.

Xu, Y., Gao, C., Li, X., He, Y., Zhou, L., Pang, G. and Sun, S. (2013). In vitro antifungal activity of silver nanoparticles against ocular pathogenic filamentous fungi. J Ocul Pharmacol Ther, 29(2), 270-274.

Yan, W., Wang, R., Xu, Z., Xu, J., Lin, L., Shen, Z. and Zhou, Y. (2006). A novel, practical and green synthesis of Ag nanoparticles catalyst and its application in three-component coupling of aldehyde, alkyne, and amine. J Mol Catal A Chem, 255(1), 81-85.

Yang, E. J., Jang, J., Lim, D. H. and Choi, I. H. (2012). Enzyme-linked immunosorbent assay of IL-8 production in response to silver nanoparticles. Nanotoxicity: Methods and Protocols, 131-139.

Yang, X., Dou, Y., & Zhu, S. (2013). Highly sensitive detection of superoxide dismutase based on an immunoassay with surface-enhanced fluorescence. Analyst, 138(11), 3246-3252.

Yen, H. J., Hsu, S. H., & Tsai, C. L. (2009). Cytotoxicity and immunological response of gold and silver nanoparticles of different sizes. Small, 5(13), 1553-1561.

Zakrzewski, S.F. 2002. Environmental Toxicology. New York: Oxford University Press, Inc.

Zhang, L. W., William, W. Y., Colvin, V. L. and Monteiro-Riviere, N. A. (2008). Biological interactions of quantum dot nanoparticles in skin and in human epidermal keratinocytes. Toxicol and App Pharm, 228(2), 200-211.

Zhang, Y., Tekobo, S., Tu, Y., Zhou, Q., Jin, X., Dergunov, S. A., Pinkhassik, E. and Yan, B. (2012). Permission to enter cell by shape: nanodisk vs nanosphere. ACS Appl Mater Interfaces, 4(8), 4099-4105.

Zhang, W., Yao, Y., Sullivan, N. and Chen, Y. (2011). Modeling the primary size effects of citrate-coated silver nanoparticles on their ion release kinetics. Environ Science Technol, 45(10), 4422-4428.

Zuykov, M., Pelletier, E. and Demers, S. (2011). Colloidal complexed silver and silver nanoparticles in extrapallial fluid of Mytilus edulis. Mar Environ Res, 71(1), 17-21.

Chapter 2

The influence of Citrate or PEG coating on silver nanoparticle toxicity to a human keratinocyte cell line

Part of this chapter was submitted as:

Bastos V.[1], Ferreira de Oliveira J. M. P.[1], Brown D.[2], Johnston H.[2], Malheiro E.[2], Silva A.L.[2], Duarte I.F.[2], Oliveira H[1], Santos C.[1,4] (2016) The influence of Citrate or PEG coating on silver nanoparticle toxicity to a human keratinocyte cell line. Toxicology Letters, 13;249:29-41. doi: 10.1016/j.toxlet.2016.03.005.

The influence of Citrate or PEG coating on silver nanoparticle toxicity to a human keratinocyte cell line

Bastos V.[1], Ferreira de Oliveira J. M. P.[1], Brown D.[2], Johnston H.[2], Malheiro E. [3], Daniel-da-Silva A.L.[3], Duarte I.F.[3], Santos C.[1,4*] and Oliveira H.[1]

[1]*CESAM & Laboratory of Biotechnology and Cytomics, Department of Biology, University of Aveiro, 3810-193 Aveiro, Portugal*
[2]*School of Life sciences, Heriot-Watt University, Riccarton, Edinburgh EH14 4AS, UK*
[3]*CICECO – Aveiro Institute of Materials, Department of Chemistry, University of Aveiro, Aveiro, Portugal*
[4]*Department of Biology, Faculty of Sciences, University of Porto, Rua do Campo Alegre, Porto,*

*corresponding author: csantos@fc.up.pt

Abstract

Surface coating of silver nanoparticles may influence their toxicity, in a way yet to decipher. In this study, human keratinocytes (HaCaT cells) were exposed for 24 and 48h to well-characterized 30 nm AgNPs coated either with citrate (Cit30 AgNPs) or with poly(ethylene glycol) (PEG30 AgNPs), and assessed for cell viability, reactive oxygen species (ROS), cytokine release, apoptosis and cell cycle dynamics. The results showed that Cit30 AgNPs and PEG30 AgNPs decreased cell proliferation and viability, the former being more cytotoxic. The coating molecules *per se* were not cytotoxic. Moreover, Ag^+ release and ROS production were similar for both AgNP types. Cit30 AgNPs clearly induced apoptotic death, while cells exposed to PEG30 AgNPs appeared to be at an earlier phase of apoptosis, supported by changes in BAX, BCL2 and CASP-3 expressions. Concerning the impact on cell cycle dynamics, both Cit30 and PEG30 AgNPs affected cell cycle regulation of HaCaT cells, but, again, citrate-coating induced more drastic effects, showing earlier downregulation of cyclin B1 gene and cellular arrest at the G2 phase. Overall, this study has shown that the surface coating of AgNPs influences their toxicity by differently regulating cell-cycle and cell death mechanisms.

Keywords: Apoptosis, Cell cycle, Citrate-coating, Cytokines, Nanotoxicology, PEG-coating, ROS, silver nanoparticles.

Introduction

Silver nanoparticles (AgNPs) have very efficient antimicrobial activity, which has encouraged their widespread use in a range of applications, from medicine and industry to household and personal care products or clothing (Abdelhalim and Jarrar 2011; Behra et al. 2013; Benn and Westerhoff 2008; Eckhardt et al. 2013; EPA 2010; Nowack et al. 2011). According to the

inventory of nanotechnology-based consumer products compiled by the Project on Emerging Nanotechnologies (http://www.nanotechproject.org/cpi), ~24% of 1800 "nano" products that were introduced in the market to date are nanosilver-containing products. In face of the rapid increase in AgNP production and use, concerns about their possible impacts on the environment and human health have also grown (Nowack and Bucheli 2007). There are many routes of human exposure to AgNPs, including dermal absorption, ingestion, inhalation and injection (Ahamed et al. 2010; Chen and Schluesener 2008) and several in vitro studies have reported toxic effects of AgNPs towards different types of human cells (Asharani et al. 2012; Chairuangkitti et al. 2013; Foldbjerg et al. 2012; Gliga et al. 2014; Grosse et al. 2013; Hsiao et al. 2015; Jiang et al. 2013; Kang et al. 2012; Kim et al. 2009). However, the mechanisms of AgNPs-induced toxicity are still not completely understood (Browning et al. 2013). In particular, it is crucially important to determine how specific physicochemical properties, such as particle size and surface chemistry, influence AgNPs uptake, cellular fate and toxicity (Ahlberg et al. 2014; Comfort et al. 2014; Lu et al. 2010; Samberg et al. 2010).

Different properties such as NP formulation (Boonkaew et al. 2014) and size (Kim et al. 2012; Park et al. 2011), the storage environment (Ahlberg et al. 2014) and the duration of exposure (Comfort et al. 2014) have all been previously assessed in different cell types with regard to AgNPs toxic potential. However, little attention has been paid so far to the coating-dependent toxicity of AgNPs. AgNPs are frequently coated to promote stability and avoid aggregation, citrate being the most commonly used reducing agent and stabilizer (Sharma et al. 2009). Numerous polymers have also been used to coat AgNPs, such as polyvinyl pyrrolidone (PVP) (Haberl et al. 2013; Nymark et al. 2013; Wang et al. 2014), and poly(ethylene glycol) (PEG) (Fernández-López et al. 2009; Tao et al. 2007). Citrate renders NPs a negative surface charge and provides colloidal stability through electrostatic repulsions, while low molecular weight PEG can neutralize surface charge and stabilize NPs through steric hindrance. PEG coating has been reported to reduce NP reactivity (Povoski et al. 2013) and to improve penetration through the mucus layer, increasing the interest in the use of this polymer for nanomedicine purposes (Suk et al. 2011; Thorley and Tetley 2013).

The few studies which have addressed the influence of coating on AgNPs toxicity provided conflicting information. It has been reported that the charged citrate coating improved the stability of AgNPs and decreased their toxicity (Zhang et al. 2014), while other studies found that citrate-coated AgNPs could be highly cytotoxic to mammalian cells (Grosse et al. 2013; Wang et al. 2014). On the other hand, Gliga et al. (2014) compared the cytoxicity of uncoated, PVP- and citrate-coated AgNPs in bronchial BEAS-2B cells and found no coating-dependent differences in cytotoxicity. Caballero-Díaz et al. (2013) reported that pegylation of AgNPs reduced cellular uptake and reduced the toxicity in NIH/3T3 (mouse embryonic fibroblasts),

compared to AgNPs coated with other polymers. Using an *in vivo* system, England et al. (2013) demonstrated that PEG coating could "mask" the NPs from the immune system, decreasing their toxicity. However, α-methoxy-poly(ethylene glycol)-ω-mercapto (mPEG-SH)-coated AgNPs decreased viability and affected cell cycle dynamics of human liver cells (HL-7702) (Song et al. 2012). The differential effects of citrate and PEG coatings have been assessed for gold nanoparticles (AuNPs) (Brandenberger et al. 2010) in human alveolar epithelial cells (A549) cells. The authors found that the uptake of citrate-coated AuNPs by A549 cells was significantly increased compared to that of the PEG-coated AuNPs, concluding that NP surface coatings can modulate endocytic uptake pathways and cellular NP trafficking.

In this study, we aimed to compare the cytotoxic effects of AgNPs coated with citrate or PEG on human keratinocytes. Given that skin is a major entry route of AgNPs into the body, HaCaT (human keratinocyte) cells have been chosen as an *in vitro* model. Indeed, there has been evidence that AgNPs with diameters in the 20-40 nm range can penetrate skin *in vivo* and be detected in deeper layers (George et al. 2014; Larese et al. 2009). HaCaT cells were exposed to citrate- and PEG-coated AgNPs of 30 nm (Cit30 and PEG30, respectively) and the effects on cell viability, intracellular ROS production, cytokines expression, apoptosis induction and cell cycle profile were assessed after 24 and 48h. Putative toxicity of the coatings alone was also investigated.

Material and methods

Chemicals

Sterile, purified and endotoxin-free silver nanoparticles (Biopure AgNPs 1.0 mg/mL in water), with a diameter of 30 nm and a citrate or polyethyleneglycol (PEG) surface, designated as Cit30 and PEG30, respectively, were purchased from Nanocomposix Europe (Prague, Czech Republic). Citric acid ($C_6H_8O_7.H_2O$) was purchased from Sigma Aldrich (St. Louis, Missouri, USA); Poly(ethylene glycol) PEG (Mw 5 kDa) from Laysan Bio® (Arab, Alabama, USA) . Dulbecco's modified Eagle's medium (DMEM), fetal bovine serum (FBS), antibiotics and phosphate buffer saline (PBS, pH 7.4) were purchased from Life Technologies (Carlsbad, CA, USA). 3-(4,5-dimethylthiazol-2-yl)-2,5-diphenyltetrazolium bromide (MTT), dimethyl sulfoxide (DMSO), dichlorodihydrofluorescein diacetate (DCFH2-DA), propidium iodide (PI), RNase and DNase I were obtained from Sigma-Aldrich (St. Louis, MO, USA). FITC Annexin V Apoptosis Detection Kit (BD Pharmingen, San Diego, CA-USA); RNeasy Mini Kit columns was from Qiagen, Hilden, Germany; Omniscript RT Kit from Qiagen, Hilden, Germany; and iQ SYBR Green Supermix from BioRad, Hercules, CA-USA.

Physicochemical characterization of AgNPs

The morphology and size of AgNPs was assessed by scanning transmission electron microscopy (STEM, Hitachi SU-70 (Hitachi High-Technologies Europe GmbH, Germany) operating at 30 kV. Samples for STEM analysis were prepared by evaporating dilute suspensions (concentration) of the nanoparticles on a copper grid coated with an amorphous carbon film. The hydrodynamic diameter and polydispersity index (PdI) of the nanoparticles were measured by dynamic light scattering (DLS) and the zeta potential was assessed by electrophoretic mobility, both measurements using a Zetasizer Nano ZS (Malvern Instruments, UK).

Silver quantification measurements were performed by inductively coupled plasma optical emission spectrometry (ICP-OES) in an Activa M Radial spectrometer (Horiba Jobin Yvon, France), employing a charge coupled device (CCD) array detector, with a wavelength range of 166–847 nm and radial plasma view. Samples were introduced into the ICP plasma using an HF resistant sample introduction system including a Burgener nebulizer, a cyclonic spray chamber and a quartz torch with aluminium injector. Samples for ICP-OES were prepared by addition of 10 µL AgNPs (1.0 mg/mL) to 990 µL of either ultrapure water or complete culture medium, incubation for variable periods (0, 4, 24 or 48h), followed by centrifugation at 40000 rcf for 120 min at 4ºC (in accordance with the manufacturer's recommendations) to deposit the nanoparticles and separate the supernatant (with dissolved ionic silver). Acid digestion of the supernatant was then performed by mixing 500 µL with 100 µL of acids (HCl:HNO3 2:1 v/v) and 400 µL of ultrapure water. The % dissolution of AgNPs to ionic silver was calculated as 100×F×[Ag]/Ci, where F is the dilution factor, Ci the initial concentration of AgNPs (based on the stock solution concentration, indicated by the manufacturer) and [Ag] the concentration of silver determined by ICP-OES.

Cell Culture

The HaCaT cell line, a nontumorigenic immortalized human keratinocyte cell line (Boukamp et al., 1988), was obtained from Cell Lines Services (Eppelheim, Germany). Cells were grown in complete medium, (Dulbecco's modified Eagle's medium, supplemented with 10% fetal bovine serum (FBS), 2 mM L-glutamine, 100 U/mL penicillin, 100 µg/mL streptomycin and 250 µg/mL fungizone) at 37°C in 5% CO_2 humidified atmosphere. For each experiment, cells were seeded at a concentration 60000 cells/mL in 96 well plates, and allowed to adhere for 24h and then medium was replaced with fresh medium containing citrate- or PEG-coated AgNPs. Depending on the experiment, the silver ion and the coating agent *per se*, dissolved in complete medium, were used as controls. The effects were measured after 24 and 48h.

Exposure and Viability assay

Cell viability was determined by the colorimetric 3-(4,5- dimethyl-2-thiazolyl)-2,5-diphenyl tetrazolium bromide (MTT) assay (Twentyman and Luscombe 1987). Cells were seeded in 96-well plates and cultured as described above. Cell viability was assessed in cells exposed to free citrate and PEG (same Mw as in AgNPs coating) at concentrations below the maximum quantity added at the time of NP synthesis (before wash process), which was 2 mM for citrate (~378 µg/mL) and 200 µg/mL for PEG (information provided by the manufacturer Nanocomposix). Cells were exposed to citrate or PEG dissolved in complete culture medium at 0, 50, 100, 200, 300, 350 and 400 µg citrate/mL, and 0, 6, 12.5, 25, 50, 100 and 200 µg PEG/mL. Silver nitrate was dissolved in complete medium at concentrations of 0, 0.2, 0.5, 1, 2.5, 5, 7.5, 10 and 50 µg Ag^+/mL. Cells were exposed to citrate- or PEG-coated AgNPs at concentrations of 0, 0.5, 5, 10, 25, 50, 75 and 100 µg/mL. Cell viability was measured after 24h, but in the case of Ag^+ and coated AgNPs a 48h exposure was also assayed. Fifty microliters of MTT (1 mg/mL) in phosphate buffered saline (PBS) was then added to each well, and incubated for 4h at 37°C, 5% CO_2. Medium was then removed and 150 µL of DMSO were added to each well to solubilize the formazan crystals.

The optical density of reduced MTT was measured at 570 nm in a microtiter plate reader (Synergy HT Multi-Mode, BioTeK, Winooski, VT), and the relative cell metabolic activity (MA) (calculated as a % with respect to control cells) was calculated as: MA = [(Sample Abs – DMSO Abs) / (Control Abs – DMSO Abs)]*100. Three independent assays were performed with at least 2 technical replicates each and the results compared with the control (no exposure). From the MTT results, the IC50 for citrate coated AgNPs (the most cytotoxic) was 40 µg/mL and 37.4 µg/mL at 24 and 48h respectively. Therefore, the concentrations of coated AgNPs corresponding to IC50 and IC20 (40 µg/mL and 10 µg/mL, respectively) were selected for the following assays, for the silver ion, the IC50 was 1.26 µg/mL and in that case a concentration which didn't cause significant cytotoxicity (0.8 µg/mL) was selected. This concentration was higher than the Ag^+ concentration released from citrate-coated AgNPs at time 0h (3.77% in 10 µg/mL of citrate- AgNPs, which corresponds to 0.377 µg/mL of Ag^+), but was a dose that did not cause significant cytotoxicity through MTT assay.

Uptake potential by flow cytometry

Uptake potential of Cit30 and PEG30 by HaCaT cells was assessed by flow cytometry (FCM) as previously described by Suzuki et al (2007). Briefly, cells were seeded in 6-well plates and after AgNPs exposure they were trypsinized, collected to FCM tubes and analyzed by FCM. Both parameters, forward scatter (FS), which give information on the cell's size, and side scatter (SS), information on complexity of cells, were measured in a Coulter XL Flow Cytometer

(Beckman Coulter, Hialeah, FL-USA) equipped with an argon laser (15 mW, 488 nm). Acquisitions were made using SYSTEM II software v. 3.0 (Beckman Coulter, Hialeah, FL). For each sample, 5000–20000 cells were analyzed at a flow rate of about 1000 cells/s.

Intracellular ROS Formation

Intracellular ROS production was assessed by flow cytometry (FCM) with the use of dichlorodihydrofluorescein diacetate (DCFH2-DA) as a fluorescent probe. This probe enters the cells and is deacetylated by cellular esterases producing non-fluorescent DCFH2 and diacetate. In the cytosol DCFH2 is quickly oxidized to fluorescent DCF by intracellular ROS. Cells were seeded in 6-well plates at a concentration of 60000 cells/mL and after AgNPs exposure for 24h, medium was discarded and cells were incubated for 30 min, at 37ºC, in the dark with serum-free DMEM containing 10 mM DCFH2-DA. Cells were washed with PBS, trypsinised and collected for analysis. Acquisitions were made using a Coulter EPICS XL flow cytometer (Coulter Electronics, Hialeah, Florida, USA) equipped with an argon laser (15 mW, 488 nm). Acquisitions were made using SYSTEM II software v. 3.0 (Beckman Coulter, Hialeah, FL). ROS formation was estimated from the median fluorescence intensity (MFI) of DCF using the FlowJo software (Tree Star Inc., Ashland, OR-USA). For each sample, the number of events reached at least 10000.

Cytokine estimation using cytometric bead array

Cytokine production was assessed using Bioplex kits. Briefly, the cell supernatants (removed, centrifuged and frozen at -80ºC) were used to estimate the release of the following cytokines from treated cells: interleukin-1 beta (IL-1β), IL-6, tumour necrosis factor-alpha (TNF-α), IL-10 and monocyte chemoattractant protein-1 (MCP-1). Lipopolysaccharide (LPS) was used as a positive control. Bead array kits were obtained from Beckton Dickinson (Oxford, UK) and a master mix prepared according to the manufacturer's instructions. The master mix was incubated with each of the test supernatants for 1 h, followed by the addition of detection beads and incubated for a further 2 h at room temperature. The beads were then washed in wash buffer and analyzed using a BD^{TM} FACS array flow cytometer which had previously been set up and calibrated using standard beads for each cytokine under investigation.

Annexin V assay

Apoptosis and cell viability were measured by flow cytometry (FCM) in a Coulter XL Flow Cytometer (Beckman Coulter, Hialeah, FL-USA), through the FITC Annexin V Apoptosis Detection Kit, according to manufacturer. Briefly, cells were detached and washed with PBS, and the cells resuspended in diluted binding buffer provided with the kit (1:10 in distilled water)

at 1×10^6 cells/ml. To stain the cell suspension, 5µL of FITC-Annexin V and 5µL of PI were added for 15 min at room temperature in the dark, after which each sample was diluted in 400µL binding buffer. For each sample, 10000 events were analyzed and the percentages were calculated from the number of cells in each quadrant divided by the total number of cells.

Gene expression of apoptosis related genes

Total RNA of control and exposed cells was extracted using the TRIzol method. Organic phase separation was achieved in Phase-Lock Gel Heavy tubes (5 Prime 3 Prime, Inc., Boulder, CO). The aqueous phase was mixed with 1 vol 70% ethanol and RNA was purified using RNeasy Mini Kit columns. Synthesis of cDNAs was performed by a reverse transcriptase (RT) reaction: 2 µg total RNA were pre-incubated with DNase I and reverse-transcribed with 1 µM Oligo dT18, using the Omniscript RT Kit. The cDNA samples were prediluted in ultrapure MilliQ water (1:20). The final individual qPCR reactions contained iQ SYBR Green Supermix, 150nM each gene-specific primer and 1:4 (v/v) prediluted cDNA (1:20). Primers were designed using the program Primer3 (Rozen and Skaletsky 2000) and confirmed for specificity by the UCSC In-Silico PCR Genome Browser (http://genome.ucsc.edu/cgi-bin/hgPcr). The qPCR program included 1 min denaturation at 95 °C, followed by 40 cycles at 94 °C for 5 s, 58 °C for 15 s, and 72 °C for 15 s. After qPCR, a melting temperature curve was performed. At least two technical replicates per sample of qPCR were used from each of three independent biological replicates. Average PCR and cycle thresholds were determined from the fluorescence data using the algorithm Real-Time PCR Miner (Zhao and Fernald 2005). Gene expression of *BAX*, *BCL2*, *CASP3* were normalized with the *GAPDH* reference gene and expressed relative to control cells, calculated from the average efficiencies and cycle thresholds using the Pfaffl method (Pfaffl 2001).

Cell cycle

Cell cycle was analyzed by flow cytometry according to the method previously described (Oliveira et al. 2014). Briefly, cells were seeded in 6-well plates and after exposure they were washed with PBS, harvested using Trypsin-EDTA and centrifuged twice at 300 x*g* for 5 min. Cells were then fixed with 85% cold ethanol and kept at -20 ºC until analysis. At the time of analysis cells were centrifuged at 300 *g* for 5 min, resuspended in PBS and filtered through a 35-µm nylon mesh to separate aggregates. Then, 50 µL RNase (1mg/mL) and 50 µL propidium iodide (PI) (1mg/mL) were added to each sample which were then incubated for 20 min in darkness at room temperature until analysis. The relative fluorescence intensity of the stained nuclei was measured in a Coulter XL Flow Cytometer. For each sample, the number of nuclei analyzed was approximately 5,000. The percentage of nuclei in each phase of the cell cycle

(G0/G1, S and G2 phases) was analyzed using the FlowJo software **(**Tree Star Inc., Ashland, Oregon, USA).

Gene expression of cell cycle related genes

Total RNA extraction and cDNA synthesis were performed as described above. Gene expression of cyclin B1 (*CCNB1*), cyclin E1 (*CCNE1*), cyclin-dependent kinase 1 (*CDK1*) and cyclin-dependent kinase 2 (*CDK2*) were normalized with the *GAPDH* reference gene and expressed relative to control cells, calculated from the average efficiencies and cycle thresholds using the Pfaffl method (Pfaffl 2001).

Statistical analysis

The results are reported as mean ± standard deviation (SD) of 2 technical replicates in each of the 3 independent experiments. For MTT assay, the statistical significance between control and exposed cells was performed by one-way ANOVA, followed by Dunnet and Dunn's method (as parametric and non-parametric test, respectively), using Sigma Plot 12.5 software (Systat Software Inc.). For the other assays, results were compared using two-way ANOVA, followed by Holm-Sidak test using also Sigma Plot 12.5 software (Systat Software Inc.). The differences were considered statistically significant for $p < 0.05$. Principal Component Analysis (PCA) was used to perform multivariate analysis. All multivariate analyses in this paper were carried out using the Canoco for Windows vs 4.5.

Results

Physicochemical characterization of AgNPs dispersed in water and in cell culture medium

Scanning transmission electron microscopy (STEM) images (Figure 2.1) showed that AgNPs were mainly spherical in shape with a mean diameter of 27.1 ± 3.0 nm and 27.7 ± 3.2 nm, for citrate and PEG coated nanoparticles respectively, and with a narrow size distribution. The hydrodynamic diameter (Z-average size) in water was above the primary particle size (Table 2.1), especially in the case of PEG30 AgNPs, as expected based on the larger volume of PEG molecules compared to citrate. The values of polydispersity indexes (PdI) were below 0.3, thus indicating monodisperse distributions. As to the zeta potential, citrate-stabilized NPs carried a strong negative surface charge (ζ -42.7 ± 2.7 mV), while the surface of the PEG-stabilized NPs was less negative (ζ -12.1 ± 0.5 mV, Table 1). The amount of dissolved ionic silver in ultrapure water suspensions of Cit30 and PEG30 AgNPs was 3.32 ± 0.04% and 0.63 ± 0.01%, respectively.

Table 2.1: Hydrodynamic diameter D_h (with respective polydispersity index PdI) and zeta potential (ζ) of Cit30 and PEG30 AgNPs (30 nm nominal diameter, citrate and polyethyleneglycol coating, respectively) dispersed in ultrapure water or in DMEM culture medium (10 µg/ml). Standard deviations calculated from 3 replicate measurements.

AgNPs		D_h (nm)	PdI	ζ (mV)
Cit30	In water	43.3 ± 0.5	0.25-0.26	-42.7 ± 2.7
	In DMEM	64.8 ± 0.4	0.40-0.41	-8.5 ± 0.4
PEG30	In water	62.1 ± 0.5	0.15-0.16	-12.1 ± 0.5
	In DMEM	57.7± 0.3	0.25-0.27	-6.5 ± 0.4

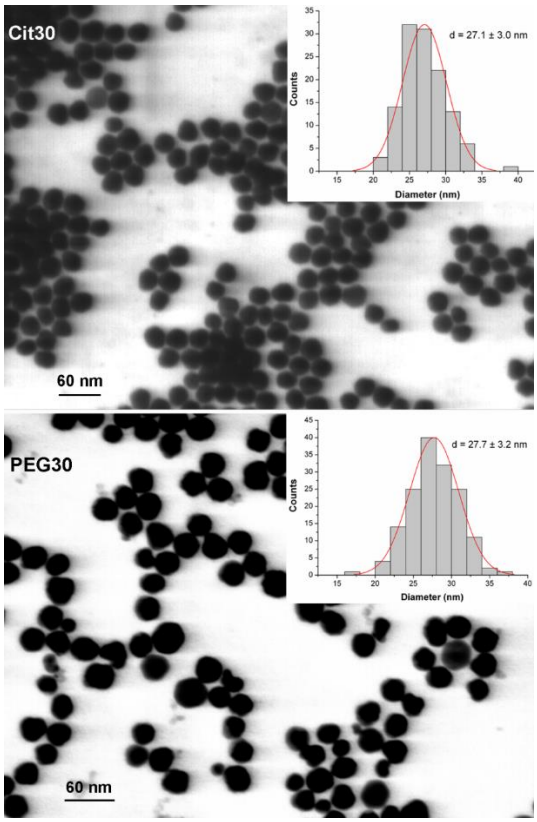

Figure 2.1: STEM micrographs of AgNPs Citrate- and PEG- AgNPs (30 nm nominal diameter, citrate and polyethyleneglycol coating, respectively) dispersed in deionised water (5 µg/ml).

Regarding the behavior of AgNPs in cell culture medium (DMEM with 10% FBS), Cit30 AgNPs increased their hydrodynamic diameter, as soon as they were suspended in the medium and progressively over time up to 93.7 nm after 48h (Figure 2.2a), possibly reflecting the formation of a protein corona. Additionally, the zeta potential (ζ) increased from -42.7 ± 2.7 in

water to -8.5 ± 0.4 mV in the cell culture medium, indicating a less negative surface, hence lower electrostatic repulsions. The release of ionic silver (Ag^+) increased to 7.6 ± 0.1% at 48h, which corresponds to an absolute concentration of 0.77 µg/mL Ag^+ (Figure 2.2b). PEG30 AgNPs showed a more stable hydrodynamic diameter over incubation time, likely because PEG was not as readily displaceable as citrate by the medium proteins. The dissolution behavior of PEG30 AgNPs was very similar to that of Cit30 AgNPs, reaching identical ionic silver concentrations at 48h (Figure 2.2b).

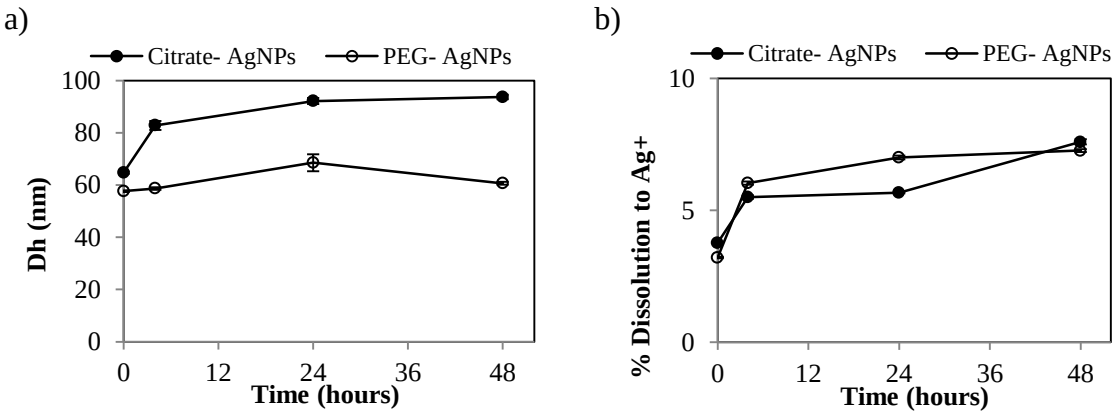

Figure 2.2: a) Z-average size and b) % dissolution to Ag^+ of AgNPs Citrate-and PEG- AgNPs (30 nm nominal diameter, citrate and PEG coating, respectively) incubated in culture medium (10 µg/mL) at 37ºC for 4, 24 and 48h. Error bars correspond to the standard deviations of 3 replicate measurements.

Effects on cell growth and morphology

HaCaT cells in control conditions (exposed to cell culture medium) showed typical morphology (Figure 2.3a, f). When cells were exposed to Cit30 AgNPs for 24 and 48h, their confluence decreased, especially at the highest concentration tested (40 µg/mL) (Fig. 2.3c, h). Compared to Cit30 AgNPs, PEG30 AgNPs induced a lesser decrease in cell confluence, which was only visible after 48h (Fig. 2.3j). No visible morphological alterations were detected at 24h for Cit30 NPs.

Cell Viability

The viability of HaCaT cells was negatively affected by AgNPs coated either with citrate or with PEG, although to different extents (Fig. 2.4a, b). Upon exposure to Cit30 AgNPs at concentrations higher than 25 µg/mL and 50 µg/mL cell viability was significantly reduced after 24h and 48h. Furthermore, Cit30 AgNPs at concentrations higher that 50 µg/mL reduced cell viability to < 20% even after 24h.

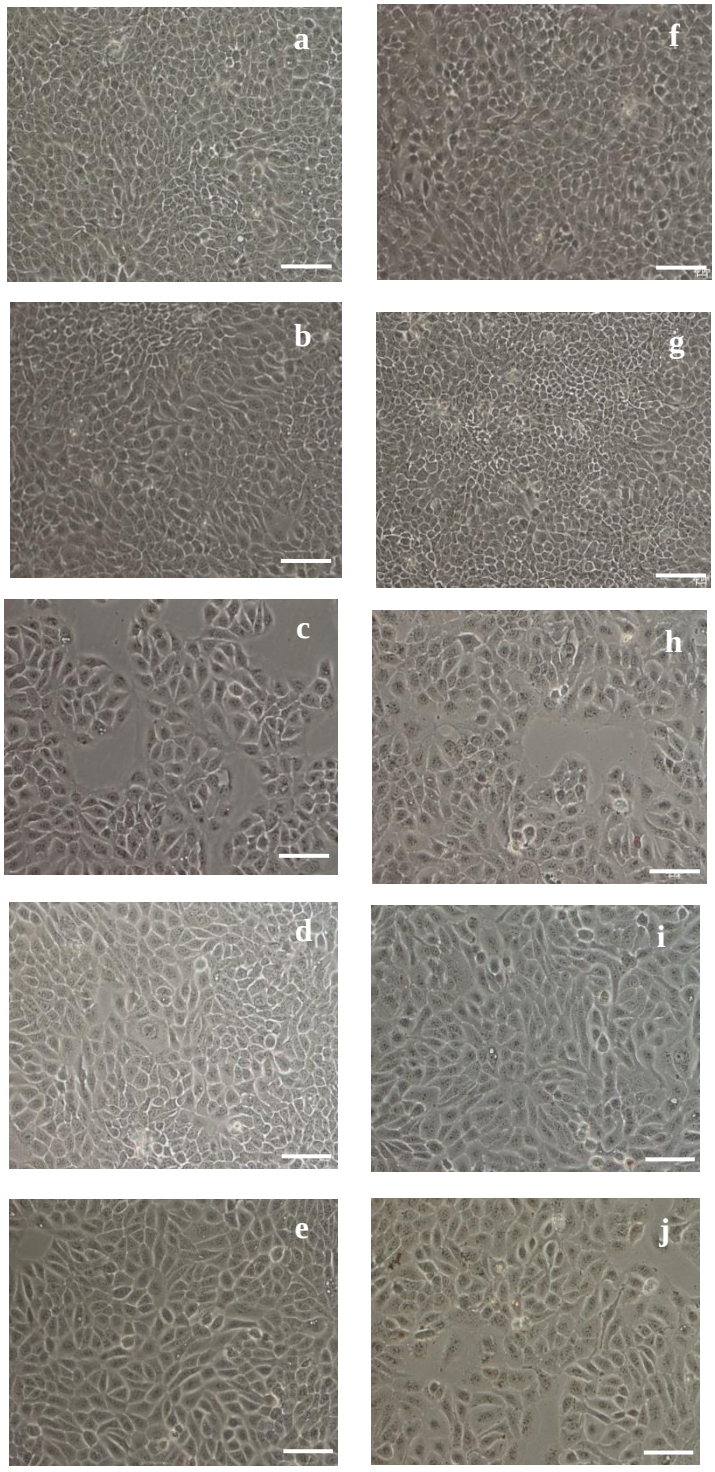

Figure 2.3: Light microscopy images (100X) of HaCaT cells in control conditions at 24h (a) and 48h (f) and exposed to 30 nm citrate-coated AgNPs for 24h - b) 10 µg/mL; c) 40 µg/mL; 48h – g) 10 µg/mL; h) 40 µg/mL and 30 nm PEG-coated AgNPs for 24h - d) 10 µg/mL; e) 40 µg/mL; 48h – i) 10 µg/mL; j) 40 µg/m. Bar corresponds to 100 µm.

In contrast, PEG30 AgNPs, decreased cell viability significantly from concentrations >25 µg/mL, but only after 48h. The viability results were also expressed using surface area as dose metrics, instead of mass concentration. The curves obtained (Fig. 2.5) actually had very similar profiles to those shown in Figure 2.4a-b, indicating that surface area was not determinant for the different toxicity of the two AgNP types.

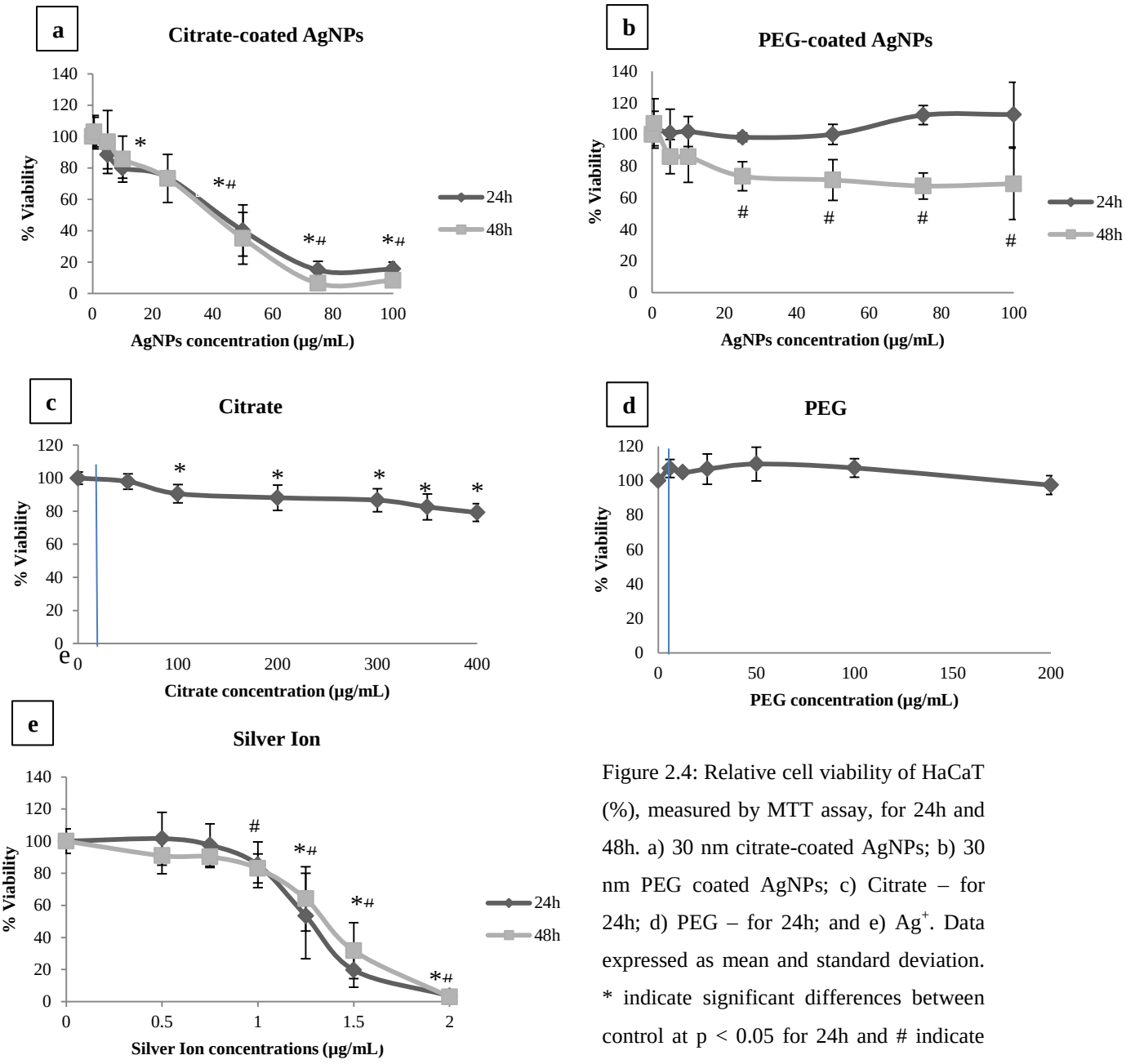

Figure 2.4: Relative cell viability of HaCaT (%), measured by MTT assay, for 24h and 48h. a) 30 nm citrate-coated AgNPs; b) 30 nm PEG coated AgNPs; c) Citrate – for 24h; d) PEG – for 24h; and e) Ag^{+}. Data expressed as mean and standard deviation. * indicate significant differences between control at $p < 0.05$ for 24h and # indicate significant differences between control at $p < 0.05$ for 48h. Vertical line in c) and d) corresponds to the maximum dose of citrate and PEG that exists in the concentrations used of AgNPs.

In order to investigate potential inherent toxicity of the coating substances, the viability of cells upon exposure to citrate and PEG (in the same Mw as in AgNP coating) was assessed (Fig. 2.4c, d). Citrate induced a significant decrease in cell viability at concentrations above 100 µg/mL. However, the concentrations of citrate that corresponded to the administered AgNPs doses were well below this value (at 100 µg/mL of Cit30 AgNPs the maximum citrate concentration is 37.8 µg/mL (*Nanocomposix*® information)), thus not accounting for the observed toxicity of Cit30 AgNPs. In the case of exposure to PEG, the viability did not decrease significantly for any of the concentrations tested. Concerning silver ions (Fig. 2.4e), viability decreased sharply for concentrations higher than 1.25 µg/mL for both 24 and 48h.

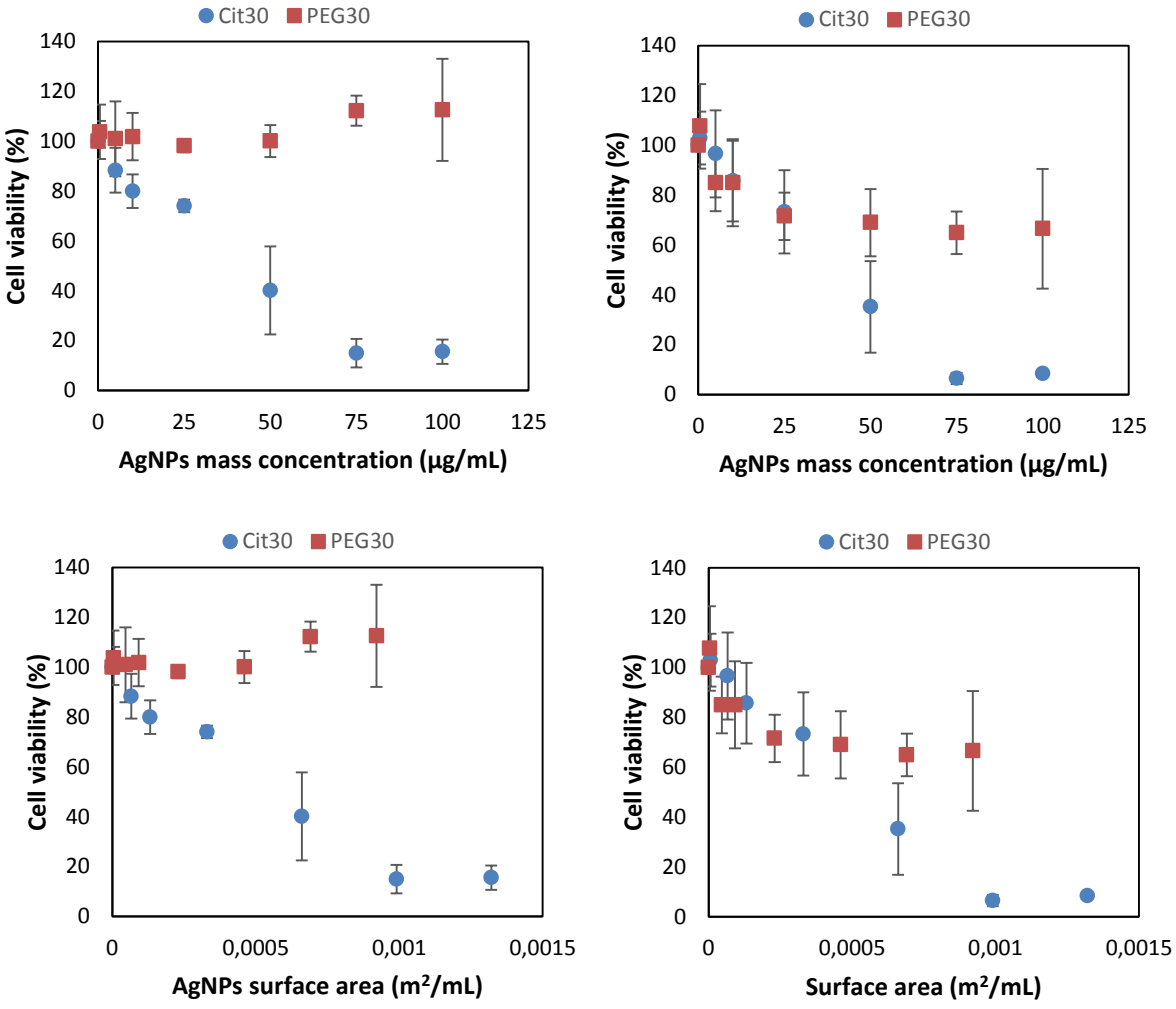

Figure 2.5: Cell viability results expressed as a function of AgNPs mass concentration (top) or of AgNPs total surface area (bottom). Surface area was calculated by: i) considering the TEM diameter to calculate the number of particles present at each silver concentration (assuming a spherical shape for AgNPs), ii) considering the hydrodynamic diameter in water to calculate the area of each particle, iii) multiplying the no. particles by the area of one particle. Data expressed as mean and standard deviation.

Uptake potential by flow cytometry

The uptake of both Cit30 and PEG30 AgNPs at 24h was determined by quantitative analysis of the intracellular side scatter signal by flow cytometry (Figure 2.6). Both concentrations (10 and 40 µg/mL) induced an increase in the uptake potential of Cit30 AgNPs by HaCaT cells, while for PEG30 an increase in the uptake potential was only observed for the highest concentration (40 µg/mL). Overall, the results suggest that PEG30 AgNPs are taken up by HaCaT cells to a lower extent than Cit30 AgNPs.

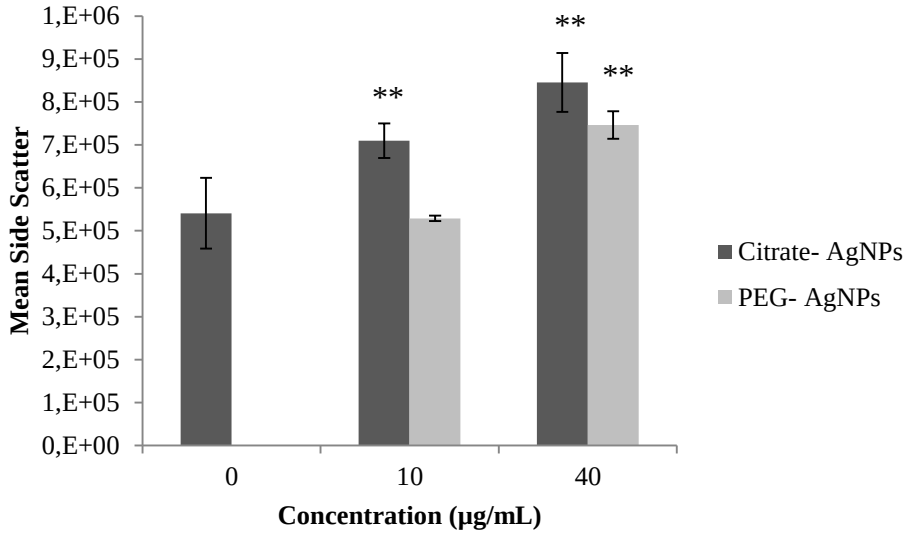

Figure 2.6: Uptake potential of AgNP by HaCaT cells assessed by the side scattered light by flow cytometry. The results were expressed as the mean +/- SD versus control. ** indicate significant differences between control at $p < 0.01$.

Intracellular ROS Formation

The quantification of intracellular ROS in HaCaT cells exposed to AgNPs for 24h is presented in Fig. 2.7. Both Cit30 and PEG30 AgNPs induced the production of ROS reaching a significant 1.2 fold increase at the highest dose tested (40 µg/mL), compared to control cells. The ROS levels were similar for the two NP types.

Inflammatory Cytokine release

Significant differences in cytokine release upon AgNPs exposure were noted only for MCP-1, while there was no effect on the other cytokines studied (IL-1β, IL-6, IL-10 and TNF-α) (data not shown). The results regarding the release of MCP-1 by HaCaT cells treated with Cit30 and PEG30 AgNPs are shown in Fig. 2.8. While LPS, used as positive control, induced a significant

increase in MCP-1 release at 48h, both Cit30 and PEG30 AgNPs induced a significant decrease compared to control cells.

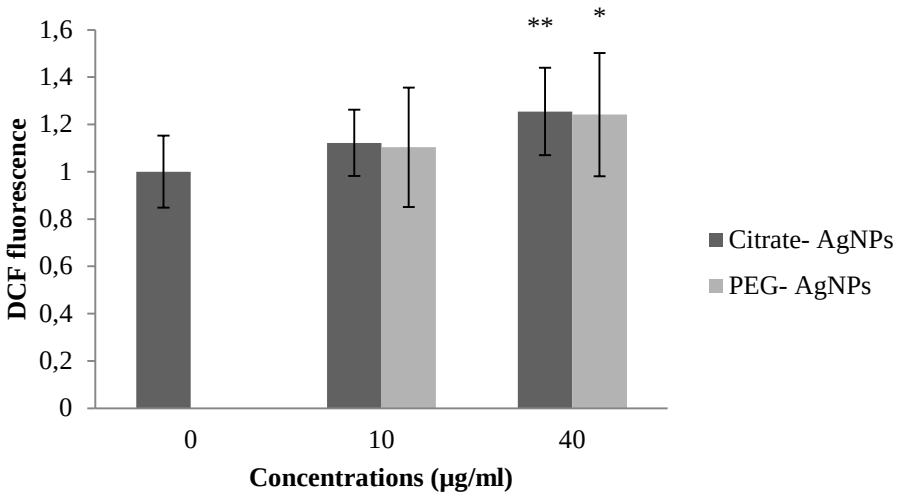

Figure 2.7: Characterization of intracellular ROS production of HaCaT after exposure to citrate- and PEG- AgNPs for 24h, using the DCFDA assay. The results were expressed as the mean +/- SD versus control. ** indicate significant differences between control at $p < 0.01$ and * at $p < 0.05$.

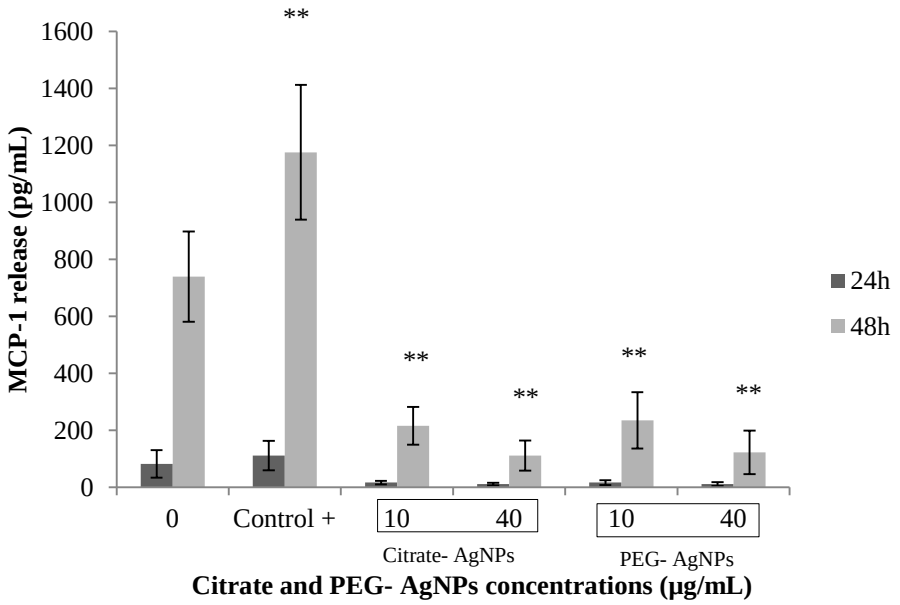

Figure 2.8: MCP-1 release by HaCaT cells after 24 and 48h exposure to Citrate- and PEG- AgNPs. Data represent the mean ± SEM (n = 3) of the concentration (pg /ml) of MCP-1 cytokine released from the cells after NPs treatment. ** indicate significant differences between control at $p < 0.01$.

Annexin V assay

The potential of AgNPs to induce apoptosis in HaCaT cells was assessed by the Annexin V-FITC/PI assay. As shown in Fig. 2.9a-b, Ci30 AgNPs decreased the percentage of intact cells (not significantly for 48h exposure to the lowest concentration) and increased the percentage of dead cells, especially at 24h exposure to the high concentration. Concerning early apoptosis, the results showed a significant increase after 48h exposure to 40 µg/mL Cit30 AgNPs, while the percentage of cells at late apoptosis/necrosis was increased for all conditions (not significantly for 48h exposure to the low concentration) In contrast, the exposure of HaCaT cells to PEG30 AgNPs did not induce any significant changes in the apoptosis profile for neither periods or NP concentrations (Fig. 2.9c-d).

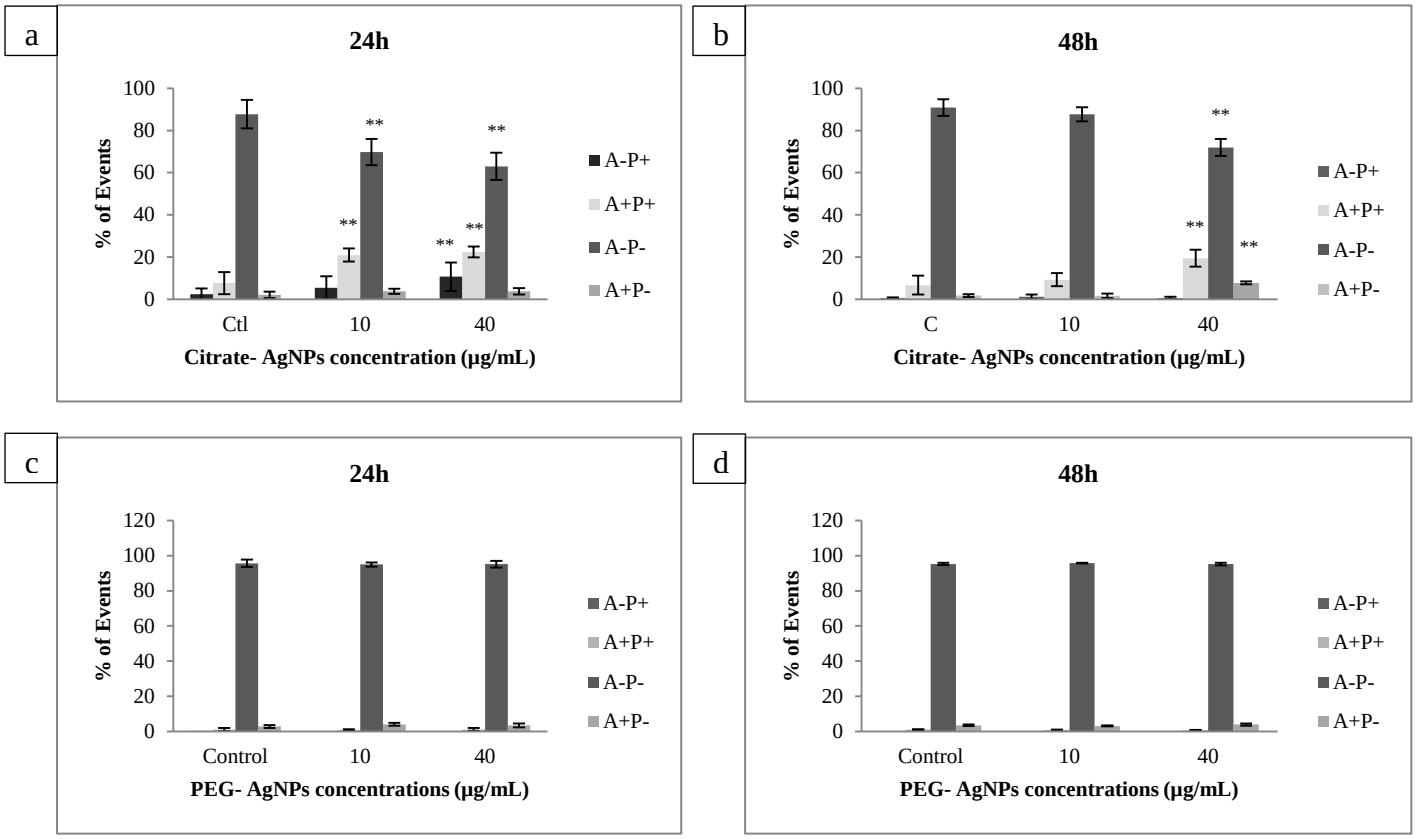

Figure 2.9: Citrate- and PEG- AgNPs effects on HaCaT cells exposed to 10 and 40 µg/mL during 24 and 48h, measured by annexin V assay. Intact cells are represented by "A-P-", dead cells "A-P+", early apoptotic cells "A+P-" and late apoptotic cells "A+P+". The results were expressed as the mean +/- SD versus control. ** indicate significant differences between control at $p < 0.01$.

Gene Expression of apoptosis related genes

Apoptosis was evaluated at transcriptional level by the analysis of the expression of apoptosis related genes BAX, BCL2 and CASP3 (Fig. 2.10). In cells exposed to Cit30 AgNPs, there was a

trend for BAX expression to be upregulated, reaching statistical significance at low concentration (10 µg/mL) 24h exposure and at high concentration (40 µg/mL) 48h exposure. Moreover, BCL2 was found to be upregulated at 48h exposure to high concentration of Cit30 AgNPs. On the other hand, the three genes showed consistent upregulation in cells exposed to PEG30 AgNPs. The statistical comparison between Cit30 and PEG30 AgNPs exposed cells showed that for both times and concentrations the expression level of the three selected genes was significant lower in cells exposed to Cit30 AgNPs.

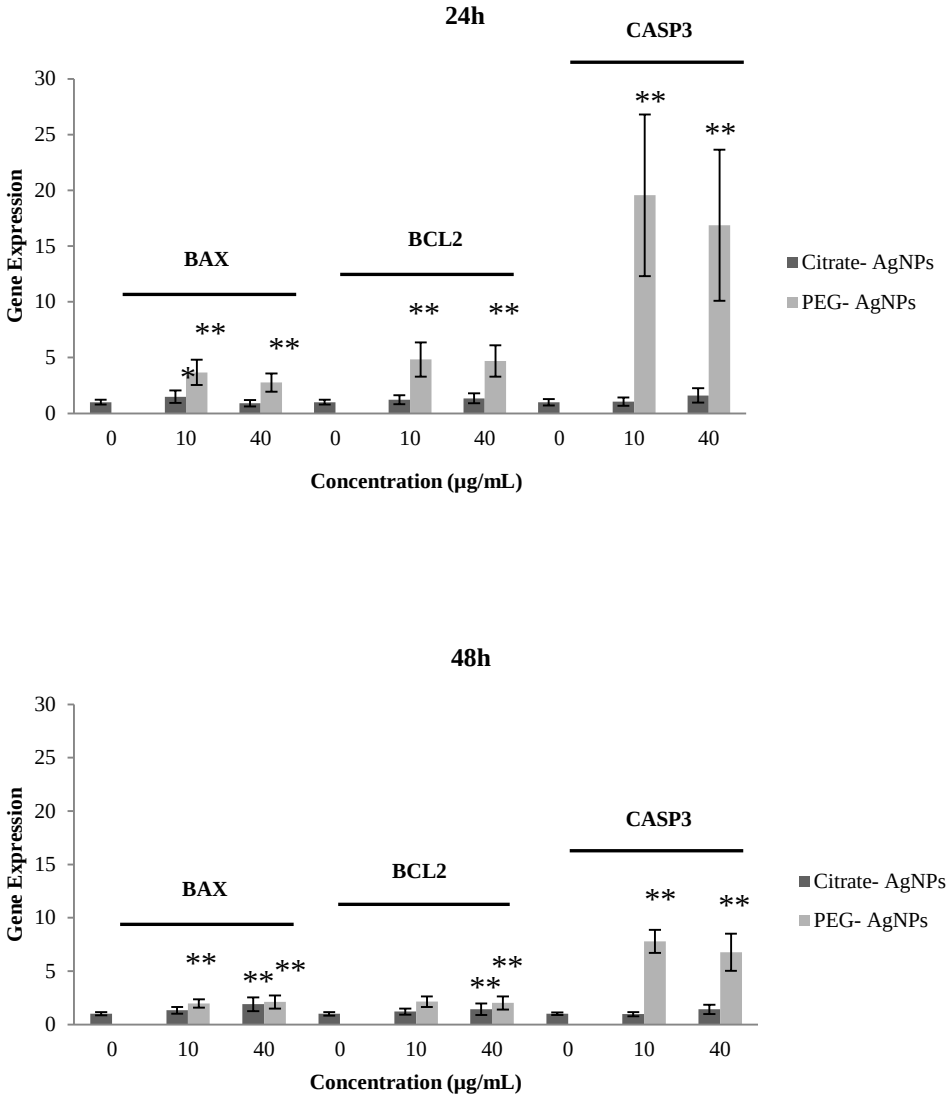

Figure 2.10: HaCaT gene expression of apoptotic genes, after 24h and 48h exposure to Citrate- and PEG-AgNPs. The results were expressed as the mean relative to control cells (normalized with the GAPDH reference gene) +/- SD versus control.

Cell cycle and clastogenicity

Figure 2.11 shows the effect of Cit30 and PEG30 AgNPs on the cell cycle of HaCaT cells. Cit30 AgNPs in both doses induced a decrease in the percentage of cells in G0/G1 and an increase in the percentage of cells in G2, this effect being visible for both periods, but more pronounced at 48h ($p < 0.01$) (Fig. 2.11a).

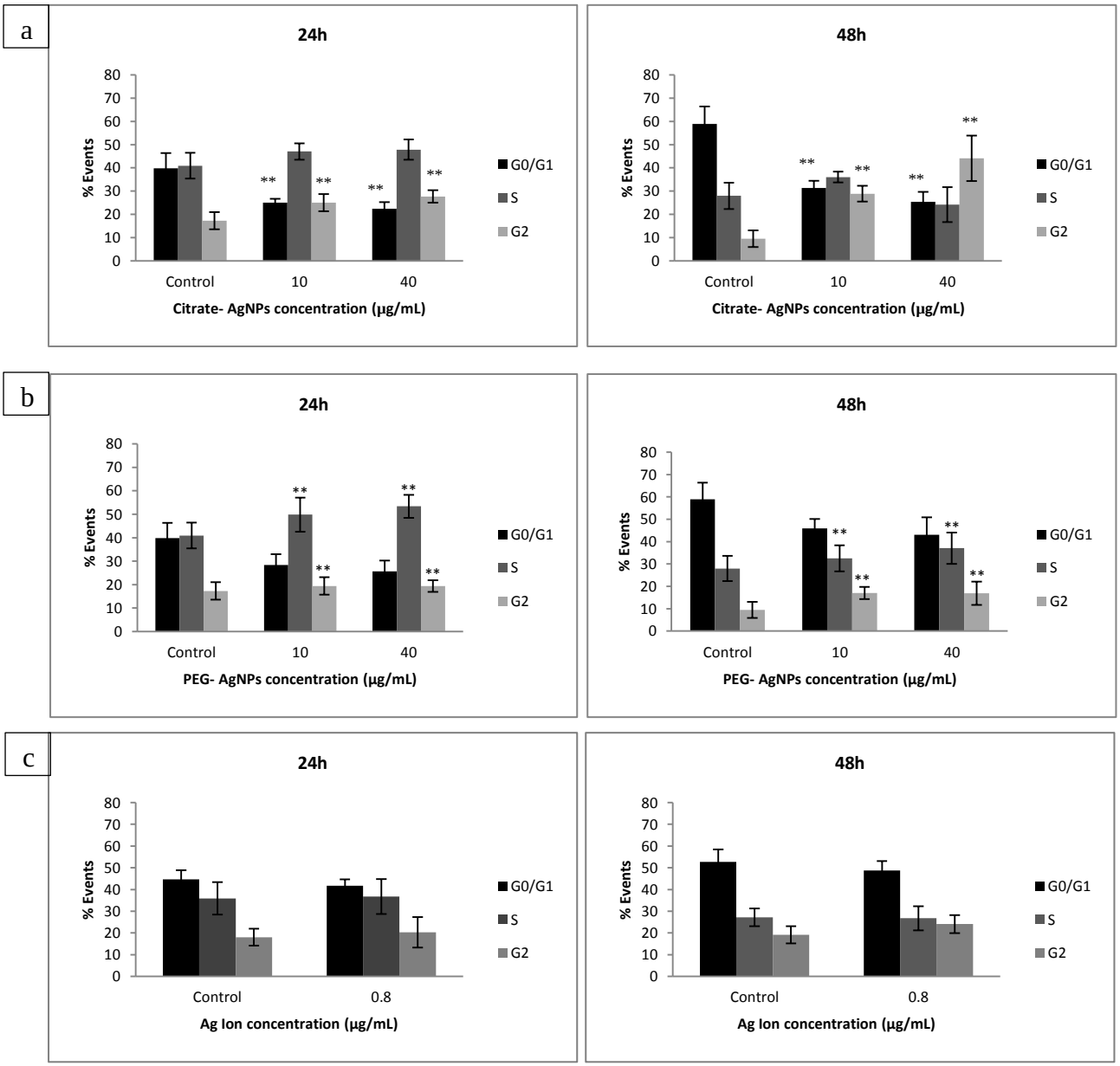

Figure 2.11: Effects of AgNPs on cell cycle dynamics, measured by flow cytometry, exposed for 24h and 48h. a) citrate-coated AgNPs; b) PEG-coated AgNPs; and c) Ag ion. The results were expressed as mean and standard deviation. ** indicate significant differences between control at $p < 0.01$.

As for PEG30 AgNPs, in addition to a decrease in the number of cells in G0/G1 and a slight increase in cells at G2 there was a significant increase in the number of cells in S phase. An example of the histograms obtained after 40 µg/mL Cit30 and PEG30 AgNPs exposure during 48h are shown in Fig. 2.12. HaCaT exposed to Ag^+ for 24h and 48h did not induce significant alterations to the cell cycle dynamics (Fig. 2.11c). The coefficient of variation (CV) corresponding to cells in G0/G1 peak does not change significantly with exposure to Ag^+ or AgNPs, comparatively to the respective controls (Table 2.2).

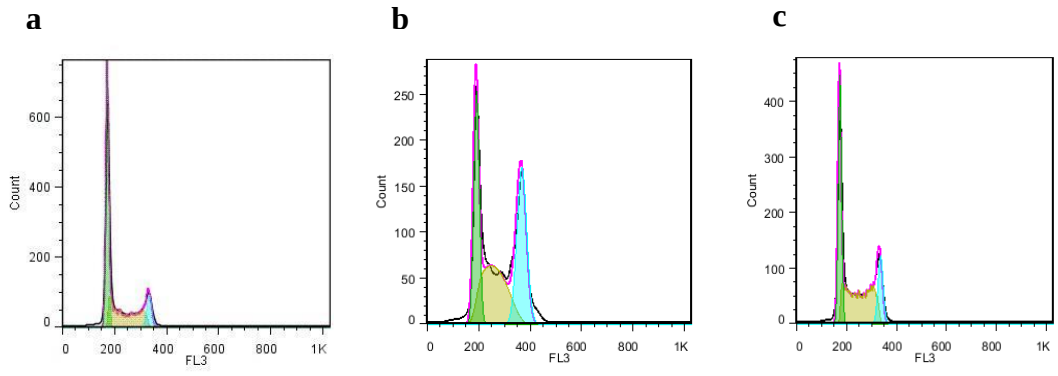

Figure 2.12: Examples of HaCaT cell cycle histograms obtained after AgNPs exposure, measured by flow cytometry. a) Control after 48h; b) 40 µg/mL of citrate- AgNPs after 48h; and c) 40 µg/mL of PEG-AgNPs after 48h.

Table 2.2: Coefficient of variation (CV) values of cells exposed to AgNPs and Silver Ion.

	24h			**48h**		
	Control	**10 µg/mL**	**40 µg/mL**	**Control**	**10 µg/mL**	**40 µg/mL**
Citrate coated AgNPs	5.8±0.82	5.9±0.67	8.3±0.87	5.3±0.84	6.9±1.43	9.3±1.89
PEG coated AgNPs	5.3±0.998	5.6±0.79	5.7±0.77	5.3±1.0	6.4±1.14	6.4±0.62
	Control	**0.8 µg/mL**		**Control**	**0.8 µg/mL**	
Silver ion	6.1±1.24	6.5±1.5		11.9±1.97	10.6±2.22	

Expression of cell cycle related genes

Exposure to AgNPs significantly changed the expression levels of selected genes involved in cell cycle regulation (Fig. 2.13). Exposure to Cit30 AgNPs downregulated the expression of cyclin B1 gene (*CCNB1*) for 40 µg/mL at both time points. For PEG30 AgNPs *CCNB1*, expression was decreased for 40 µg/mL only at 48h exposure. The expression of the *CDK2* gene, for cells exposed to citrate- AgNPs was increased for 40 µg/mL at 24h and decreased at

48h for the same concentration. The expression of the other genes tested was not significantly altered upon exposure to AgNPs.

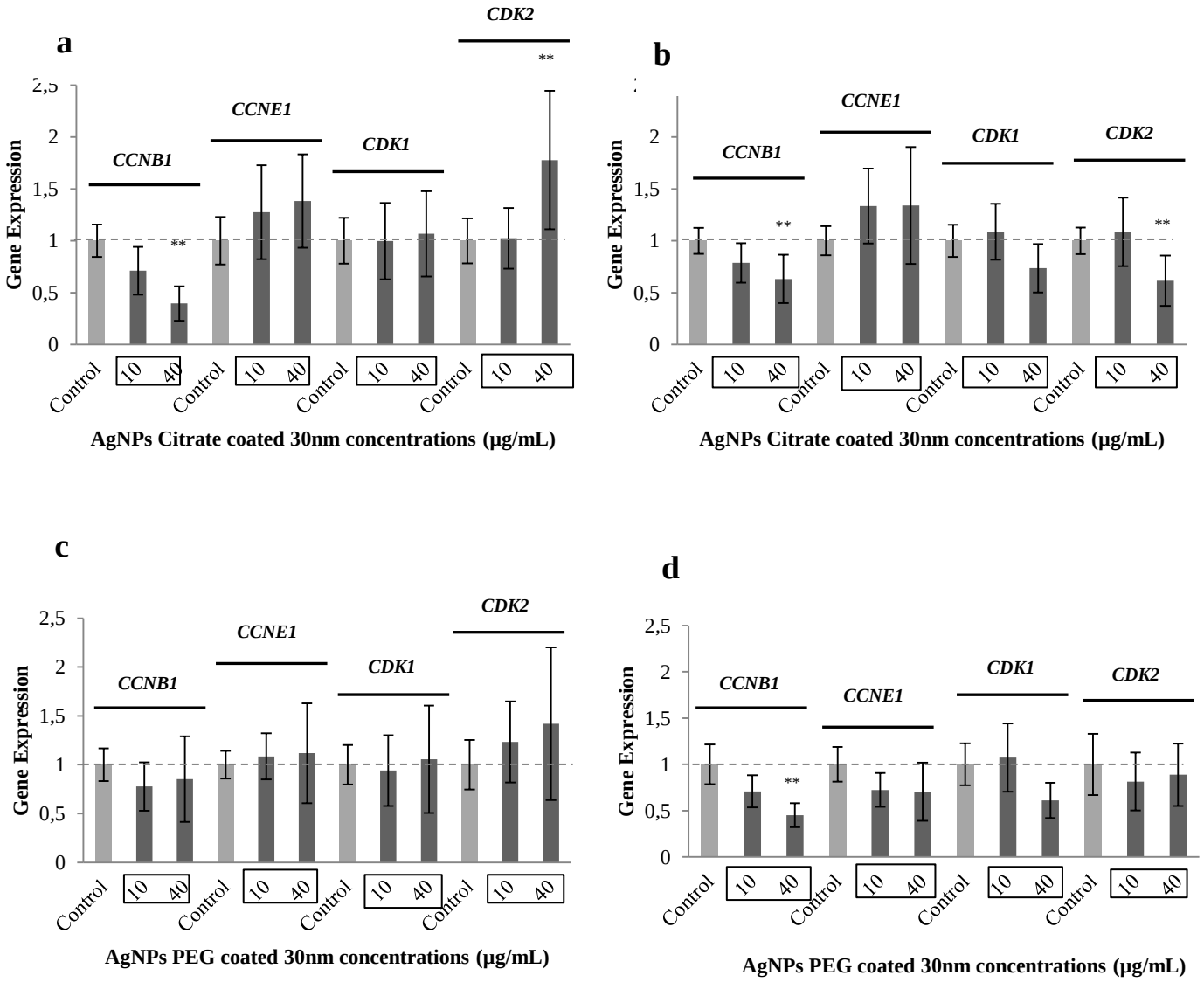

Figure 2.13: HaCaT gene expression of cell cycle genes after exposure to: a) and b) citrate-coated AgNPs 24h and 48h, respectively; c) and d) PEG-coated AgNPs 24h and 48h, respectively. The results were expressed as mean relative to control cells (normalized with the GAPDH reference gene) and standard deviation. ** indicate significant differences between control at $p < 0.01$.

Discussion

In this work, we have investigated the cellular effects of well-characterized AgNPs with different coatings (citrate and PEG) but the same nominal diameter (30 nm), in order to address the influence of NP surface coating on biological outcomes in keratinocytes, assessing, among other endpoints, less commonly reported changes in cell cycle dynamics. Further motivation for testing the toxicity of these NP types arose from the growing interest in using PEG-coated NPs in nanomedicine applications (Jokerst et al. 2011) and the widespread use of citrate coating in AgNPs synthesis (Zhang et al. 2011), thus making it timely and useful to report on the cytotoxic effects of such particles.

The characterization results revealed that AgNPs exhibited different time-course behavior in culture medium, depending on the coating surface. The hydrodynamic diameter of Cit30 AgNPs increased immediately after suspension in culture medium, which is in agreement with previous observations (Wang et al. 2014) and is likely to be due to the formation of a protein corona, as reported for metal nanoparticles (Casals et al. 2010; Maiorano et al. 2010). Moreover, some aggregation induced by the high ionic strength of the culture medium may also have occurred (El Badawy et al. 2012; Li et al. 2012; Robert 2010). Conversely, the hydrodynamic diameter of PEG30 AgNPs did not show significant variation in culture medium indicating high colloidal stability, which is likely to derive from steric repulsions (Caballero-Díaz et al. 2013), and lower propensity for the PEG coating molecules to be displaced by proteins (Michel et al. 2005).

In terms of cell viability, evaluated through the MTT mitochondrial activity assay, Cit30 AgNPs were found to be more cytotoxic than PEG30 AgNPs. Although, to our knowledge, the direct comparison between these two NP types hasn't been previously reported, Wang et al. (2014) found a significant decrease in the viability of bronchial BEAS-2B cells upon 24h exposure to 20 nm citrate-coated AgNPs at 6.25-50 μg/mL, while Song et al. (2012) showed PEG-coated AgNPs to cause significant viability decreases in human liver cells (HL-7702) at concentrations as low as 6.25 μg/mL. Differences in NP properties (e.g. size and surface area) as well as cell type-dependent effects (e.g. uptake) may account for the discrepancy in relation to our results. The coating substances *per se* were not responsible for the larger cytotoxicity hereby found for Cit30 NPs compared to PEG30 NPs, as neither of them decreased cell viability at the concentrations present when AgNPs were administered to cells. Also, Cit30 and PEG30 NPs showed similar dissolution behavior in culture medium, thus extracellular Ag^+ could not justify the difference in the toxicity of the two NP types. Also, the tested doses of Ag^+ (0.8 μg/mL a concentration bellow IC50 value) did not induce changes in the cell cycle dynamics. As observed by Cronholm et al. (2013) after cells exposure to $AgNO_3$, released silver ions outside the cells can act by disrupting the cell membrane, which can explain the fact that lower

concentrations of silver ion induce more cytotoxicity than AgNPs. This could also explain why the concentrations below IC50 for silver ion did not cause cell cycle alterations. Moreover, the results of Kim et al. (2009) indicated that AgNPs treated cells have limited exposure to silver ions, despite their potential release from AgNPs in cell culture; the authors reported also that AgNPs cytotoxicity is primarily the result of oxidative stress and is independent of the toxicity of silver ion. Cronholm and coworkers (2013) also suggest that silver ion toxicity differs from the mechanisms of AgNP cytotoxicity since this last one resulted from a mechanism driven by oxidative stress and released silver ions after cellular uptake of the particles. Accordingly, Gliga and co-workers (Gliga et al. 2014) have shown that AgNPs supernatants, containing ionic silver, did not affect cells. On the other hand, the intracellular release of Ag^+ following cellular uptake (sometimes called the Trojan horse effect) has been proposed by several authors (Hsiao et al. 2015; Park et al. 2010) to be greatly responsible for AgNPs toxicity. Thus, it is possible that the different coatings used in our study influenced cytotoxicity indirectly, by modulating the interaction of NPs with cells, namely the extent of NP uptake and intracellular release of Ag^+.

To quantitatively evaluate the cellular uptake of AgNPs we have used flow cytometry and related the increase in side scatter (SS) intensity with an increase in intracellular AgNPs, as previously described (e.g. Greulich et al. 2011, Zucker et al. 2013). The obtained data suggested that PEG30 AgNPs were taken up by cells to a lower extent than Cit30 AgNPs, which could justify the lower cytotoxic potential of the former particles. Concordantly, Caballero-Díaz et al (2013) showed that pegylation of polymer-coated AgNPs reduced cellular uptake and toxicity to mouse embryonic fibroblasts (NIH/3T3 cells). Furthermore, it can be postulated that thiolated PEG may complex Ag^+ ions and lower their bioavailability and toxicity, as proposed for PVP-coated AgNPs (Wang et al. 2014). Also, when evaluating the uptake rates of gold NPs on human alveolar epithelial cells (A549), Brandenberger et al (2010) observed that significantly more plain NPs (i.e., stabilized with citrate buffer) could enter the cells than PEG-coated gold NPs.

ROS can be generated either by a direct pro-oxidant effect of the NP or endogenously upon interaction with cellular material. In our work, both NP types caused a similar increase in intracellular ROS, supporting ROS-induced cytotoxicity, although not explaining the higher toxicity of Cit30 compared to PEG30 AgNPs. Enhanced ROS production has been often highlighted as a major cause for AgNP toxicity in several cell types (Kim and Ryu 2013), although it has also been reported, in human liver and colon cells, that AgNPs could cause cytotoxicity without oxidative stress (Sahu et al. 2014). Furthermore, Chairuangkittia et al. 2013 described that the toxicity of AgNPs to A549 was due both to ROS dependent and independent pathways, the latter related with cell cycle arrest. Our results show that both AgNPs induce arrest in cell cycle at 24h with more drastic effects for Cit30 at 48h. In fact, in previous studies

from our group (Carrola et al. 2016) the cell metabolic profile of HaCaT cells exposed to the same Cit30 AgNPs was evaluated and an increase in GSH was detected, suggesting the triggering of a protective mechanism against ROS-induced oxidative damage, which is consistent with the strong antioxidant capacity of this cell line (Mukherjee et al 2012). Therefore, from our results we can hypothesize that the induction of ROS is one of several mechanisms of AgNP induced toxicity in HaCaT cells. Further studies are needed to clarify how the different coatings modulate ROS dependent and independent pathways of AgNPs induced toxicity.

Regarding cytokine release, the only significant effect was a decrease in MCP-1 production compared to control cells, caused in similar extent by Cit30 and PEG30 NPs. Other cytokines, namely IL-1β, IL-6, IL-10 and TNF-α did not vary upon AgNPs exposure. These results are comparable to those reported by Orlowski et al. (2013), where AgNPs coated with tannic acid led to a decrease of MCP-1 and non-relevant changes in the IL family in murine monocytes and keratinocytes cells. However, the same study reported an increase of MCP-1 after exposure to unmodified AgNPs, showing that coating can influence the inflammatory response to AgNPs. Oppositely to our results, increases in cytokines release have also been reported by others (Suliman Y et al. 2015; Yang et al. 2012); different cell types as well as different properties of the AgNPs tested may account for the discrepancies observed. Also, adsorption of cytokine proteins onto the NP surface may have occurred contributing to a decrease in protein function (Brown et al. 2010).

Apoptosis and necrosis results showed that Cit30 AgNPs increased the number of necrotic/late apoptotic cells, as well as early apoptotic cells. A slight increase of apoptotic and necrotic A549 cells after exposure to citrate-stabilized AgNPs has also been reported by Foldbjerg et al. (Foldbjerg et al. 2012). On the other hand, PEG30 AgNPs did not significantly influence these populations, although a trend to increase early-apoptotic cells was seen, in agreement with the results reported by Zhang and co-workers (2015) for male somatic Leydig (TM3) and Sertoli (TM4) cells. Interestingly, in the present work, the expression of apoptosis-related genes was also found to differ between Cit30 and PEG30 AgNPs. In particular, PEG30 AgNPs increased the expression of *BAX* (pro-apoptotic), *BCL-2* (anti-apoptotic) and *CASP-3* genes at both concentrations and time points. Piao and co-workers (2011) observed that AgNPs induced a mitochondria-dependent apoptotic pathway via modulation of *BAX* and *BCL-2* expressions, resulting in the disruption of mitochondrial membrane potential, followed by cytochrome c release from the mitochondria and activation of caspases 9 and 3. Furthermore, Jeyaraj and co-workers (2015) found an upregulation of *BAX*, caspases-6 and -9 and downregulation of *BCL-2*. In our study, both *BCL-2* and *BAX* and of the effector *CASP-3* were upregulated, particularly by PEG30 AgNPs, supporting that these NPs were more prone to induce intrinsic apoptosis than

Cit30 NPs. This difference between the two NP types concerning the effects on apoptotic/necrotic cells and on the transcripts of apoptotic-related genes strongly suggests that, when exposed to PEG30 AgNPs, HaCaT cells may cope with the apoptotic cascade at the early stage, promoting apoptotic and antiapoptotic expression and resulting in lower cytotoxicity. The upregulation of *BCL-2* by PEG30 AgNPs was particularly relevant. Belonging to the anti-apoptotic protein family, it performs its anti-death function by sequestering monomeric *BAX* and *BAK*. It is known that certain cancer cells depend upon *BCL-2* and other anti-apoptotic proteins for survival (Brunelle and Letai 2009). In contrast, Cit30 AgNPs seemed to act mainly at a necrotic and/or late apoptotic level and, in the cells undergoing apoptosis, this will lead to cell death. Overall, our data showed that Cit30 and PEG30 AgNPs differed in the way they induced apoptosis, with the former leading to necrotic/late apoptotic processes, and the latter stimulating both apoptotic and anti-apoptotic transcripts, which may modulate cells apoptotic response at the early stage. This influence of NP coating on the apoptotic/necrotic mechanisms was also evidenced by the PCA analyses (Figure 2.14).

Both Cit30 and PEG30 AgNPs were found to induce changes on the cell cycle dynamics of HaCaT cells. In particular, Cit30 AgNPs induced a significant increase in the percentage of cells in G2, indicating an arrest at this phase, visible for both concentrations and time periods, while the PEG30 AgNPs induced an increase in the number of cells in S phase, more visible at 24h, pointing to an S phase delay. The cell cycle arrest in G2/M phase after exposure to NPs was previously related to DNA damage repair (AshaRani et al. 2009). Indeed, 24hin another report, we have presented data showing that Cit30 AgNPs induced DNA damage and micronucleus (MNi) formation, increased mononucleated cells, and decreased binucleated cells and the nuclear division index, thus pointing to clear cytostatic effects even at a low dose (~IC20) and after a short period of exposure (24h) (Chapter 4). Cell cycle arrest at G2 as a result of AgNP exposure was previously observed by others (AshaRani et al. 2009; Kang et al. 2012; Lee et al. 2011; Wei et al. 2010). For instance, Song et al. (2012) found an increase in the percentage of liver cells at the G2/M phase upon 24h exposure to 100 μg/mL mPEG-SH coated AgNPs. Also, Foldbjerg et al. (2012) found that PVP-coated AgNPs significantly increased the percentage of A549 cells in G2/M and S phases. S phase delay was also observed by Liu et al. (2010) in HepG2 cells exposed to PVP-coated AgNPs. Furthermore, an increase in the sub-G1 population of cells (which may indicate apoptosis) was reported by Jiang et al. (2013) in CHO-K1 cells exposed to BSA-coated AgNPs and by Chairuangkitti et al. (2013) in A549 cells exposed to 200 μg/mL AgNPs. Li et al. (2013) reported cell cycle arrest at G0/G1 phase and a shortened S phase after only 8 h of AgNPs exposure, showing that AgNPs may interfere in cell cycle regulation at different checkpoints. In the present work, we have also assessed the expression of selected cell cycle regulator genes. Exposure to Cit30 AgNPs at 40 μg/mL for 24 and 48h

induced downregulation of *CCNB1*, while for PEG30 AgNPs, the expression of *CCNB1* was only significantly decreased after exposure for 48h. Cyclin B1, encoded by the *CCNB1* gene, is a regulatory protein which complexes with *CDK1*, both playing a determinant role in G2/M phase transition of the cell cycle. In general, our results agree with the study of Foldbjerg and co-workers (2012), where they found downregulation of *CCNB1* and *CDK1* for the A549 cell line exposed to AgNPs during 24 and 48h. Furthermore, we found a statistically significant difference between the two NP types for the expression of *CCNE1*. Cyclin E1, encoded by the *CCNE1* gene, forms a complex with *CDK2*, which accumulates at the G1-S phase and is degraded as cells progress through the S phase. *CCNE1* expression was generally lower upon exposure to PEG30 compared to Cit30 exposure, which agrees with the increase in the percentage of cells in S phase observed for PEG30 AgNPs. AshaRani et al. (2012) also reported downregulation of *CCNB1* and *CCNE1* genes in lung and brain cells exposed to AgNPs. In summary, as corroborated by the PCA analysis (Figure 2.14), coating influenced the way that AgNPs interfered with the cell cycle, with Cit30 AgNPs leading to an impairment of the MPF (maturation promoting factor) complex and blocking cells in G2, and PEG30 AgNPs leading to a delay in the S-phase. Impacts on cell cycle are not routinely assessed for NPs, and we suggest that this response is tested for a wider range of NPs and cell types in the future.

Conclusions

In summary, this study demonstrates that the widely used citrate-coated AgNPs decreased the viability of HaCaT cells more severely than PEG-coated AgNPs. This difference was not due to putative effects of the coating molecules *per se* (as they produced no cytotoxicity), neither to the extent of extracellular release of ionic silver or the amount of ROS produced, as they were similar for both NP types. The differently coated AgNPs produced, however, distinct effects regarding the mode of cell death and cell cycle progression. While Cit30 AgNPs clearly induced apoptotic/necrotic death, cells exposed to PEG30 AgNPs appeared to be at an earlier phase of apoptosis mechanisms, as supported by gene expression analysis. With regard to the impact on cell cycle progression, both Cit30 and PEG30 AgNPs affected cell cycle regulation of HaCaT cells, but, again, citrate-coating induced more severe effects, showing earlier downregulation of the cyclin B1 gene and blockage of cells at G2.

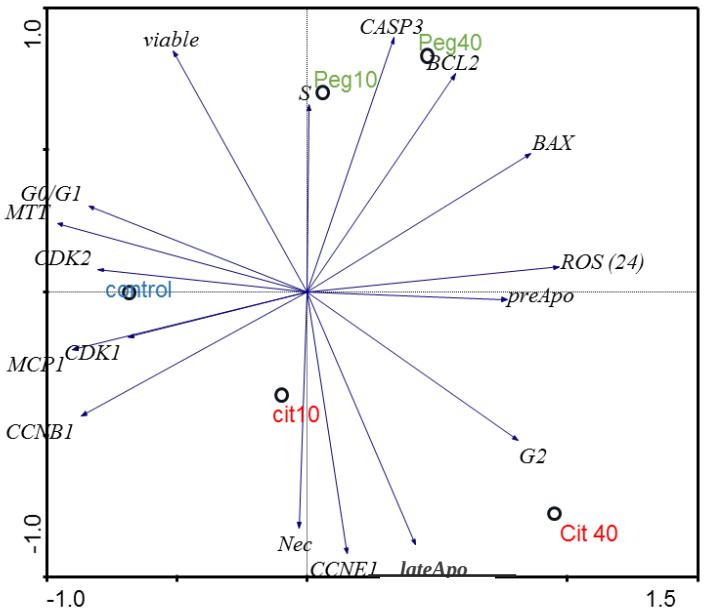

Figure 2.14: Principal Component Analysis (PCA) was used to perform multivariate analysis. All multivariate analyses in this paper were carried out using the Canoco for Windows vs 4.5. The analysis was conducted for the medium values of 48h citrate- and PEG- AgNPs exposure. "Peg10" and "Peg40" represents PEG- AgNPs 10 µg/mL and PEG- AgNPs 40 µg/mL, respectively; and "Cit10" and "Cit40" represents citrate- AgNPs 10 µg/mL and citrate- AgNPs 40 µg/mL, respectively.

Considering that AgNPs are present in a vast number of consumer products, it is important to determine if or which NPs are more cytotoxic. This study suggests that PEG-coating can be regarded as a good alternative to citrate stabilization of AgNPs used in industrial and medical applications, where it is important to reduce the toxicity towards human skin cells. The applicability of these findings to other cell types needs to be investigated in future studies.

Acknowledgments

This work was developed in the scope of the projects CICECO-Aveiro Institute of Materials (Ref. FCT UID/CTM/50011/2013) and CESAM (Ref. FCT UID/AMB/50017/2013), financed by national funds through the FCT/MEC and when applicable co-financed by the European Regional Development Fund (FEDER) under the PT2020 Partnership Agreement. Funding to the project FCOMP-01-0124-FEDER-021456 (Ref. FCT PTDC/SAU-TOX/120953/2010) by FEDER through COMPETE and by national funds through FCT, and the FCT-awarded grants (SFRH/BD/81792/2011; SFRH/BPD/48853/2008; SFRH/BPD/74868/2010) are acknowledged. I.F.D and A.L.D.S. acknowledge FCT/MCTES for the research contracts under the Program

'Investigador FCT' 2014. Authors acknowledge Tiago Pedrosa for the technical assistance in MTT assay and ROS assessment.

Contributions

V.B. participated in the design experiment with the supervisors and did all laboratorial experiments and statistical data analyses. Also had a key role in the data analyses integration, and together with the supervisors wrote and revised the manuscripts. C.S. and H.O. planned the experimental design, contributed to data analyses and integration of all data, and in the manuscript preparation. E.M. performed AgNPs characterization. A.L.D.S. was involved in AgNPs characterization and in writing this section. I.F.D. coordinated NPs analyses and revised the manuscript. J.M.P.O. coordinated gene expression and revised the manuscript. D.B. and H.J. coordinated the inflammatory assays and revised the manuscript.

References

Abdelhalim, M.A.K. and Jarrar, B.M. (2011). Renal tissue alterations were size-dependent with smaller ones induced more effects and related with time exposure of gold nanoparticles. Lipids Health Dis, 10.

Ahamed, M., Alsalhi, M. and Siddiqui, M. (2010). Silver nanoparticle applications and human health. Clin Chim Acta, 411.23: 1841-1848.

Ahlberg, S., Meinke, M.C., Werner, L., Epple, M., Diendorf, J., Blume-Peytavi, U., Lademann, J., Vogt, A., and Rancan, F. (2014). Comparison of silver nanoparticles stored under air or argon with respect to the induction of intracellular free radicals and toxic effects toward keratinocytes. Eur J Pharm Biopharm, 88.3: 651-657

AshaRani. P., Low, Kah., Mun, G., Hande, M. and Valiyaveettil, S. (2009). Cytotoxicity and genotoxicity of silver nanoparticles in human cells. ACS Nano, 3:279-290.

Asharani, P., Sethu, S., Lim, H., Balaji, G., Valiyaveettil, S. and Hande, M. (2012) Differential regulation of intracellular factors mediating cell cycle, DNA repair and inflammation following exposure to silver nanoparticles in human cells. Genome Integr, 3.1: 2.

Behra R, Sigg L, Clift M, Herzog F, Minghetti M, Johnston B, Petri-Fink A, Rothen-Rutishauser B. (2013). Bioavailability of silver nanoparticles and ions: from a chemical and biochemical perspective. J R Soc, Interface, 10:20130396.

Benn T, Westerhoff P. (2008). Nanoparticle silver released into water from commercially available sock fabrics. Environ Sci Technol, 42:4133-4139.

Boonkaew B, Kempf M, Kimble R, Cuttle L. (2014). Cytotoxicity testing of silver-containing burn treatments using primary and immortal skin cells. Burns, 40.8: 1562-1569

Boukamp P, Petrussevska R, Breitkreutz D, Hornung J, Markham A, Fusenig N. (1988). Normal keratinization in a spontaneously immortalized aneuploid human keratinocyte cell line. J Cell Biol, 106:761-771.

Braakhuis HM, Cassee FR, Fokkens PH, de la Fonteyne LJ, Oomen AG, Krystek P, de Jong WH, van Loveren H, Park MV. (2016). Identification of the appropriate dose metric for pulmonary inflammation of silver nanoparticles in an inhalation toxicity study. Nanotoxicology. (in press).Brandenberger C, Mühlfeld C, Ali Z, Lenz A-GG, Schmid O, Parak WJ, Gehr P, Rothen-Rutishauser B. Quantitative evaluation of cellular uptake and trafficking of plain and polyethylene glycol-coated gold nanoparticles. Small. 2010; 6:1669-1678.

Brown DM, Dickson C, Duncan P, Al-Attili F, Stone V. (2010). Interaction between nanoparticles and cytokine proteins: impact on protein and particle functionality. Nanotechnology, 21:215104.

Browning L, Lee K, Nallathamby P, Xu X-HN. (2013). Silver nanoparticles incite size- and dose-dependent developmental phenotypes and nanotoxicity in zebrafish embryos. Chem Res Toxicol, 26:1503-1513.

Brunelle JK, Letai A. (2009). Control of mitochondrial apoptosis by the Bcl-2 family. J Cell Sci, 122:437-441.

Caballero-Díaz E, Pfeiffer C, Kastl L, Gil P, Simonet B, Valcárcel M, Lamana J, Laborda F, Parak WJ. (2013). The toxicity of silver nanoparticles depends on their uptake by cells and thus on their surface chemistry. Part Part Syst Char, 30:1079-1085.

Carrola J, Bastos V, Ferreira de Oliveira JM, Oliveira H, Santos C, Gil AM, Duarte IF. (2016). Insights into the impact of silver nanoparticles on human keratinocytes metabolism through NMR metabolomics. Arch Biochem Biophys, 589:53-61.

Casals E, Pfaller T, Duschl A, Oostingh GJ, Puntes V. (2010). Time evolution of the nanoparticle protein corona. ACS Nano, 4:3623-3632.

Chairuangkitti P, Lawanprasert S, Roytrakul S, Aueviriyavit S, Phummiratch D, Kulthong K, Chanvorachote P, Maniratanachote R. (2013). Silver nanoparticles induce toxicity in A549 cells via ROS-dependent and ROS-independent pathways. Toxicol In Vitro, 27.1: 330-338.

Chen X, Schluesener H. (2008). Nanosilver: a nanoproduct in medical application. Toxicol Lett, 176:1-12.

Comfort KK, Maurer EI, Hussain SM. (2014). Slow release of ions from internalized silver nanoparticles modifies the epidermal growth factor signaling response. Colloid Surface B, 123: 136-142

Cronholm P, Karlsson HL, Hedberg J, Lowe TA, Winnberg L, Elihn K, Wallinder IO, Möller L. (2013). Intracellular uptake and toxicity of Ag and CuO nanoparticles: a comparison between nanoparticles and their corresponding metal ions. Small, 9(7), 970-982.

Eckhardt S, Brunetto P, Gagnon J, Priebe M, Giese B, Fromm K. (2013). Nanobio silver: its interactions with peptides and bacteria, and its uses in medicine. Chem Rev 113:4708-4754.

El Badawy AM, Scheckel KG, Suidan M, Tolaymat T. (2012). The impact of stabilization mechanism on the aggregation kinetics of silver nanoparticles. Sci Total Environ, 429:325-331.

England C, Priest T, Zhang G, Sun X, Patel D, McNally L, van Berkel V, Gobin A, Frieboes H. (2013). Enhanced penetration into 3D cell culture using two and three layered gold nanoparticles. Int J Nanomed, 8:3603-3617.

EPA EPA. (2010). State of the Science Literature Review: Everything Nanosilver and More. Scientific, Technical, Research, Engineering and Modeling Support Final Report.

Fernández-López C, Mateo-Mateo C, Alvarez-Puebla R, Pérez-Juste J, Pastoriza-Santos I, Liz-Marzán L. (2009). Highly controlled silica coating of PEG-capped metal nanoparticles and preparation of SERS-encoded particles. Langmuir, 25:13894-13899.

Foldbjerg R, Irving E, Hayashi Y, Sutherland D, Thorsen K, Autrup H, Beer C. (2012). Global gene expression profiling of human lung epithelial cells after exposure to nanosilver. Toxicol Sci, 130:145-157.

George R, Merten S, Wang TT, Kennedy P, Maitz P. (2014). In vivo analysis of dermal and systemic absorption of silver nanoparticles through healthy human skin. Australas J Dermatol, 55:185-190.

Gliga A, Skoglund S, Odnevall Wallinder I, Fadeel B, Karlsson H. (2014). Size-dependent cytotoxicity of silver nanoparticles in human lung cells: the role of cellular uptake, agglomeration and Ag release. Part Fibre Toxicol, 11.11: 1-17.

Greulich C, Diendorf J, Simon T, Eggeler G, Epple M, Köller M. (2011). Uptake and intracellular distribution of silver nanoparticles in human mesenchymal stem cells. Acta

Biomater,7:347-54.
Grosse S, Evje L, Syversen T. (2013). Silver nanoparticle-induced cytotoxicity in rat brain endothelial cell culture. Toxicol In Vitro, 27.1: 305-313.
Haberl N, Hirn S, Wenk A, Diendorf J, Epple M, Johnston B, Krombach F, Kreyling W, Schleh C. (2013). Cytotoxic and proinflammatory effects of PVP-coated silver nanoparticles after intratracheal instillation in rats. Beilstein J Nanotech, 4.1: 933-940.
Hsiao ILL, Hsieh Y-KK, Wang C-FF, Chen ICC, Huang Y-JJ. (2015). Trojan-horse mechanism in the cellular uptake of silver nanoparticles verified by direct intra- and extracellular silver speciation analysis. Environ Sci Technol, 49:3813-3821.
Jeyaraj M, Renganathan A, Sathishkumar G. (2015). Biogenic metal nanoformulations induce Bax/Bcl2 and caspase mediated mitochondrial dysfunction in human breast cancer cells (MCF 7). RSC Adv, 5.3:2159-2166.
Jiang X, Foldbjerg R, Miclaus T, Wang L, Singh R, Hayashi Y, Sutherland D, Chen C, Autrup H, Beer C. (2013). Multi-platform genotoxicity analysis of silver nanoparticles in the model cell line CHO-K1. Toxicol Lett, 222:55-63.
Jokerst JV, Lobovkina T, Zare RN, Gambhir SS. (2011). Nanoparticle PEGylation for imaging and therapy. Nanomedicine (Lond), 6:715-728.
Kang S, Lee Y, Lee E-K, Kwak M-K. (2012). Silver nanoparticles-mediated G2/M cycle arrest of renal epithelial cells is associated with NRF2-GSH signaling. Toxicol Lett, 211:334-341.
Kennedy AJ, Hull MS, Diamond S, Chappell M, Bednar AJ, Laird JG, Melby NL, Steevens JA. (2015). Gaining a critical mass: a dose metric conversion case study using silver nanoparticles. Environ Sci Technol, 49:12490-12499.
Kim S, Choi J, Choi J, Chung K-H, Park K, Yi J, Ryu D-Y. (2009). Oxidative stress-dependent toxicity of silver nanoparticles in human hepatoma cells. Toxicol In Vitro, 23:1076-1084.
Kim S, Ryu D-Y. (2013). Silver nanoparticle-induced oxidative stress, genotoxicity and apoptosis in cultured cells and animal tissues. J Appl Toxicol, 33:78-89.
Kim TH, Kim M, Park HS, Shin US, Gong MS, Kim HW. (2012). Size-dependent cellular toxicity of silver nanoparticles. J Biomed Mater Res Part A, 100A:1033-1043.
Larese FF, D'Agostin F, Crosera M, Adami G, Renzi N, Bovenzi M, Maina G. (2009). Human skin penetration of silver nanoparticles through intact and damaged skin. Toxicology, 255:33-37.
Lee Y, Kim D, Oh J, Yoon S, Choi M, Lee S, Kim J, Lee K, Song C-W. (2011). Silver nanoparticles induce apoptosis and G2/M arrest via PKCζ-dependent signaling in A549 lung cells. Arch Toxicol, 85:1529-1540.
Li X, Lenhart JJ, Walker HW. (2012). Aggregation kinetics and dissolution of coated silver nanoparticles. Langmuir, 28:1095-1104.
Li X, Xu L, Shao A, Wu G, Hanagata N. (2013). Cytotoxic and genotoxic effects of silver nanoparticles on primary Syrian hamster embryo (SHE) cells. J Nanosci Nanotechnol, 13:161-170.
Liu W, Wu Y, Wang C, Li H, Wang T, Liao C, Cui L, Zhou Q, Yan B, Jiang G. (2010). Impact of silver nanoparticles on human cells: effect of particle size. Nanotoxicology, 4:319-330.
Lu W, Senapati D, Wang S, Tovmachenko O, Singh A, Yu H, Ray P. (2010). Effect of Surface Coating on the Toxicity of Silver Nanomaterials on Human Skin Keratinocytes. Chem Phys Lett, 487.
Maiorano G, Sabella S, Sorce B, Brunetti V, Malvindi MA, Cingolani R, Pompa PP. (2010). Effects of cell culture media on the dynamic formation of protein-nanoparticle complexes and influence on the cellular response. ACS Nano, 4:7481-7491.
Michel R, Pasche S, Textor M, Castner DG. (2005). Influence of PEG architecture on protein adsorption and conformation. Langmuir, 21:12327-12332.
Mukherjee SG, O'Claonadh N, Casey A, Chambers G. (2012). Comparative in vitro cytotoxicity

study of silver nanoparticle on two mammalian cell lines. Toxicol In Vitro, 26:238-51.
Nowack B, Bucheli T. (2007). Occurrence, behavior and effects of nanoparticles in the environment. Environ Pollut, 150:5-22.
Nowack B, Krug H, Height M. (2011). 120 years of nanosilver history: implications for policy makers. Environ Sci Technol, 45:1177-1183.
Nymark P, Catalán J, Suhonen S, Järventaus H, Birkedal R, Clausen P, Jensen K, Vippola M, Savolainen K, Norppa H. (2013). Genotoxicity of polyvinylpyrrolidone-coated silver nanoparticles in BEAS 2B cells. Toxicology, 313:38-48.
Oliveira H, Monteiro C, Pinho F, Pinho S, Ferreira de Oliveira JM, Santos C. (2014). Cadmium-induced genotoxicity in human osteoblast-like cells. Mutat Res Genet Toxicol Environ Mutagen, 775-776:38-47.
Orlowski P, Krzyzowska M, Zdanowski R, Winnicka A, Nowakowska J, Stankiewicz W, Tomaszewska E, Celichowski G, Grobelny J. (2013). Assessment of in vitro cellular responses of monocytes and keratinocytes to tannic acid modified silver nanoparticles. Toxicol In Vitro, 27:1798-1808.
Park E-JJ, Yi J, Kim Y, Choi K, Park K. (2010). Silver nanoparticles induce cytotoxicity by a Trojan-horse type mechanism. Toxicol In Vitro, 24:872-878.
Park J, Lim D-HH, Lim H-JJ, Kwon T, Choi J-sS, Jeong S, Choi I-HH, Cheon J. (2011). Size dependent macrophage responses and toxicological effects of Ag nanoparticles. Chem Commun, 47.15: 4382-4384.
Pfaffl M. (2001). A new mathematical model for relative quantification in real-time RT-PCR. Nucleic Acids Res, 29.9:e45-e45.
Piao MJ, Kang KA, Lee IK, Kim HS, Kim S, Choi JY, Choi J, Hyun JW. (2011). Silver nanoparticles induce oxidative cell damage in human liver cells through inhibition of reduced glutathione and induction of mitochondria-involved apoptosis. Toxicol Lett, 201:92-100.
Povoski SP, Davis PD, Colcher D, Martin EW. (2013). Single molecular weight discrete PEG compounds: emerging roles in molecular diagnostics, imaging and therapeutics. Expert Rev Mol Diagn, 13:315-319.
Robert, I.M. (2010). Colloidal stability of silver nanoparticles in biologically relevant conditions. Journal of Nanoparticle Research.
Rozen S, Skaletsky H. (2000). Primer3 on the WWW for general users and for biologist programmers. Methods Mol Biol, 132:365-386.
Sahu SC, Zheng J, Graham L, Chen L, Ihrie J, Yourick JJ, Sprando RL. (2014). Comparative cytotoxicity of nanosilver in human liver HepG2 and colon Caco2 cells in culture. J Appl Toxicol, 34:1155-1166.
Samberg ME, Oldenburg SJ, Monteiro-Riviere NA. (2010). Evaluation of Silver Nanoparticle Toxicity in Skin in Vivo and Keratinocytes in Vitro. Environ Health Perspect, 118:407-413.
Sharma V, Yngard R, Lin Y. (2009). Silver nanoparticles: green synthesis and their antimicrobial activities. Adv Colloid Interfac, 145.1:83-96.
Song X-l, Li B, Xu K, Liu J, Ju W, Wang J, Liu X-d, Li J, Qi Y-f. (2012). Cytotoxicity of water-soluble mPEG-SH-coated silver nanoparticles in HL-7702 cells. Cell Biol Toxicol, 28:225-237.
Suk JS, Lai SK, Boylan NJ, Dawson MR, Boyle MP, Hanes J. (2011). Rapid transport of muco-inert nanoparticles in cystic fibrosis sputum treated with N-acetyl cysteine. Nanomedicine-UK, 6:365-375.
Suliman Y AO, Ali D, Alarifi S, Harrath AH, Mansour L, Alwasel SH. (2015). Evaluation of cytotoxic, oxidative stress, proinflammatory and genotoxic effect of silver nanoparticles in human lung epithelial cells. Environ Toxicol, 30:149-160.
Suzuki H, Toyooka T, Ibuki Y. (2007). Simple and easy method to evaluate uptake potential of nanoparticles in mammalian cells using a flow cytometric light scatter analysis. Environ Sci Technol, 41: 3018–3024

Tao X, Ning Z, Heather LN, Donglu S, Xuejun W. (2007). Modification of nanostructured materials for biomedical applications. Mater Sci Eng: C, 27.3: 579-594.
Thorley AJ, Tetley TD. (2013). New perspectives in nanomedicine. Pharmacol Therapeut, 140:176-185.
Twentyman P, Luscombe M. (1987). A study of some variables in a tetrazolium dye (MTT) based assay for cell growth and chemosensitivity. Brit J Cancer, 56:279-285.
Wang X, Ji Z, Chang CH, Zhang H, Wang M, Liao Y-PP, Lin S, Meng H, Li R, Sun B, et al. (2014). Use of coated silver nanoparticles to understand the relationship of particle dissolution and bioavailability to cell and lung toxicological potential. Small, 10:385-398.
Wei L, Tang J, Zhang Z, Chen Y, Zhou G, Xi T. (2010). Investigation of the cytotoxicity mechanism of silver nanoparticles in vitro. Biomed Mater, 5:44103.
Yang E-JJ, Jang J, Lim D-HH, Choi I-HH. (2012). Enzyme-linked immunosorbent assay of IL-8 production in response to silver nanoparticles. Methods Mol Biol, 926:131-139.
Zhang T, Wang L, Chen Q, Chen C. (2014). Cytotoxic potential of silver nanoparticles. Yonsei Med J, 55:283-291.
Zhang W, Yao Y, Sullivan N, Chen Y. 2011 (). Modeling the primary size effects of citrate-coated silver nanoparticles on their ion release kinetics. Environ Sci Technol, 45:4422-4428.
Zhang X-FF, Choi Y-JJ, Han JW, Kim E, Park JH, Gurunathan S, Kim J-HH. (2015). Differential nanoreprotoxicity of silver nanoparticles in male somatic cells and spermatogonial stem cells. Int J Nanomed, 10:1335-1357.
Zhao S, Fernald R. (2005). Comprehensive algorithm for quantitative real-time polymerase chain reaction. J Comput Biol, 12:1047-1064.
Zucker RM, Daniel KM, Massaro EJ, Karafas SJ, Degn LL, Boyes WK. (2013). Detection of silver nanoparticles in cells by flow cytometry using light scatter and far-red fluorescence. Cytometry A, 83(10):962-72.

Chapter 3

Inflammatory responses of a human keratinocyte cell line to 10 nm citrate- and PEG-coated silver nanoparticles

Part of this chapter was submitted as:

Bastos V., Brown D., Johnston H., Daniel-da-Silva, A.L., Duarte I.F., Santos C. and Oliveira H. (2016) Inflammatory responses of a human keratinocyte cell line to 10 nm citrate- and PEG-coated silver nanoparticles. *Submitted to* Journal of Nanoparticle Research. *Revisions Requied*

Inflammatory responses of a human keratinocyte cell line to 10 nm citrate- and PEG-coated silver nanoparticles

Bastos V.[1], Brown D.[2], Johnston H. [2], Daniel-da-Silva, A.L.[3], Duarte I.F. [3], Santos C. [1,4] and Oliveira H. [1]

[1]*CESAM & Laboratory of Biotechnology and Cytomics, Department of Biology, University of Aveiro, 3810-193 Aveiro, Portugal*
[2] *School of Life sciences, Heriot-Watt University, Riccarton, Edinburgh EH14 4AS, UK*
[3]*CICECO, Department of Chemistry, University of Aveiro, Aveiro, Portugal*
4 Department of Biology, Faculty of Sciences, University of Porto, Rua do Campo Alegre, Porto, *corresponding author: csantos@fc.up.pt

Abstract

Silver nanoparticles (AgNPs) are among the most commonly used engineered NPs and various commercially available products are designed to come in direct contact with the skin (wound dressings, textiles, creams, among others). Currently, there is limited understanding of the influence of coatings on the toxicity of AgNPs and in particular their ability to impact on AgNP mediated inflammatory responses. As AgNPs are often stabilized by different coatings, including citrate and polyethyleneglycol (PEG), in this study we investigate the influence of citrate (Cit10) or PEG (PEG10) coatings to 10 nm AgNP on skin using human HaCaT keratinocytes. AgNPs cytotoxicity and inflammatory response (nuclear factor (NF)-κB induction and cytokine production) of HaCaT were assessed after in vitro exposure to 10 μg/mL and 40 μg/mL 4, 24 and 48h. Results showed that although both types of coated AgNPs decreased cell proliferation and viability, Cit10 AgNPs were most toxic. NF-κB inhibition was only observed for the highest concentration (40 μg/mL) of PEG10 AgNPs, and the putative link to early apoptotic pathways observed in these cells is discussed. No production of IL-1β, IL-6, IL-10 and TNFα was stimulated by AgNPs. Cit10 and PEG10 AgNPs decreased the release of monocyte chemoattractant protein-1 (MCP-1) by HaCaT cells after 48h of exposure. As cytokines are vital for the immunologic regulation in the human body, and it is demonstrated that they may interfere with NPs, more research is needed to understand how different AgNPs affect the immune system.

Keywords: Silver nanoparticles, Coating, Cytokines, HaCaT, Nanotoxicology, NF-κB, Skin, Viability.

Introduction

Nanotechnology-based consumer products are exponentially increasing and nanosilver-containing products are among the most commonly used (Vance et al., 2015). Silver

nanoparticles (AgNPs) are widely used due to their enhanced physicochemical properties and biological activities such as their antimicrobial activity. Their applications range from medicine and industry to household and personal care products (EPA, 2010) or clothing (Abdelhalim and Jarrar, 2011; Behra et al., 2013; Benn and Westerhoff, 2008; Eckhardt et al., 2013; Nowack et al., 2011). The increased exploitation of AgNPs and consequent release into the environment raises concern about their possible impacts on the environment and on human health (Nowack and Bucheli, 2007). There is an array of AgNPs that are being exploited, which vary with respect to their physico-chemical properties (e.g. size, shape, charge, surface coating, dispersion state) (Ahlberg et al., 2014; Boonkaew et al., 2014; Comfort et al., 2014; Kim et al., 2012; Park et al., 2011b). Existing studies have demonstrated that the physico-chemical properties of AgNPs are able to influence their toxicity for different cell lines [eg., human keratinocytes (HaCaT and primary HEK) and normal fibroblasts (NHF), rat adrenal pheochromocytoma cell line (PC12), and mouse osteoblastic cell line (MC3T3-E1), fibroblasts (L929) and macrophages (RAW 264.7)]. However, little attention has been given to the coating-dependent toxicity of AgNPs. Thus, research on the toxicity of AgNPs of varied physico-chemical properties is critical in order to better predict the risks they pose.

It has been reported that nanoparticle coating, media composition and ionic strength influence the surface chemistry, shape, aggregation state and dissolution of AgNPs, which in turn can differently affect their cellular uptake and biological effects (Tejamaya et al., 2012). Indeed, a few studies addressing the uptake (by embryonic fibroblasts NIH/3T3, keratinocytes HaCaT and hepatoma cells Hepa-1c1c7, respectively) of different coated AgNPs and their influence on cytotoxicity have been reported (Caballero-Díaz et al., 2013; Lu et al., 2010; Pang et al., 2015). Citrate is the most commonly used reducing and stabilizing agent of AgNPs, rendering NPs with a negative surface charge and providing colloidal stability through electrostatic repulsions (Sharma et al., 2009). Among other coating agents of AgNPs, low molecular weight polyethyleneglycol (PEG), which stabilizes AgNPs through steric interactions, has been increasingly used in biomedical applications as it enhances biocompatibility and increases blood circulation time (Ginn et al., 2014; Ryan et al., 2008).

Assessment of the ability of NPs to induce inflammatory responses is commonly used as an indicator of toxicity. For example, Chalew and Schwab (2013) studied the inflammatory effects of AgNPs, titanium dioxide (TiO2NPs), and zinc oxide (ZnONPs) (0, 0.1, 1, 10, and 100 mg/L) on human intestinal Caco-2 and SW480 cells and found that all NPs increased IL-8 cytokine generation in both cell lines. Also, Park et al (2011a) observed that pro-inflammatory cytokines (IL-1, TNF-α, and IL-6) and Th0 cytokine (IL-2) were progressively increased by day 28 after a single intratracheal instillation of AgNPs in mice. Suliman and co-workers (2013b) found that 50 µg/mL AgNPs exposure to human lung epithelial (A549) cells significantly increased the

level of pro-inflammatory cytokines, namely interleukin-1β (IL-1β) and interleukin-6 (IL-6). Yang and collaborators also observed IL-1β release by human blood monocytes in response to AgNPs (Yang et al., 2012). However, Wong et al (2009) found an anti-inflammatory effect of AgNPs to two mouse macrophage cell lines, RAW264.7 and J774.1, where AgNPs blocked TNF-α production. On the other hand, we could not found studies reporting the induction of anti-inflammatory cytokines after exposure to NPs (Murray et al., 2013; Orlowski et al., 2013; Samberg et al., 2009). Cytokines can strongly activate inflammatory responses and cell death in various tissues, including the skin (Fujiwara and Kobayashi, 2005; Graves et al., 2004). Indeed, a study on the effects of UVB radiation using HaCaT cells reported an increase of various pro-inflammatory cytokines - interleukin (IL)-1beta, IL-6, IL-8, interferon (IFN)-gamma, granulocyte-colony stimulating factor (G-CSF), macrophage inflammatory protein (MIP)-1beta, and tumor necrosis factor (TNF)-alpha (Yoshizumi et al., 2008). Murray et al (2013) found increased IL-8 and IL-6 in human epidermal keratinocytes (HEK cells) after exposure to superparamagnetic iron oxide (SPION) NPs (2.6, 5.2, 13, or 26 µg/cm2 for 24h). In other study using HEK cells, quantum dot NPs significantly increase IL-6 at 1.25 nM to 10 nM, while IL-8 increased from 2.5 nM to 10 nM after 24h and 48h (Zhang et al., 2008). Thus, as products containing AgNPs can be applied to the skin (e.g. wound dressing), and as there are experimental evidence for skin penetration of 25 ± 7 nm AgNPs (also in intact skin) (Larese et al., 2009) and 20 – 40 nm AgNPs (George et al., 2014), the human keratinocyte cell line HaCaT was used as an in vitro model in this study. It is well known that cytokines play crucial roles in immunologic regulation in the human body and are involved in the induction of proliferation, differentiation, and cell death in many cell types (Yarilin and Belyakov, 2004). Moreover, activation of the transcription factor nuclear factor kappa B (NF-κB) has been shown to play a central role in the enhanced expression and regulation of cytokine genes (Kelso, 1998). There is also evidence that carbon NPs can activate NFkB in macrophages which stimulates TNFα production (Brown et al., 2004). To our knowledge, the activation of NFkB in keratinocytes has not been studied previously.

In this study, we aimed to compare the inflammatory responses of HaCaT cells exposed to well-characterized 10 nm AgNPs coated with citrate or PEG. In particular, the effects on viability, expression of the pro-inflammatory transcription factor NF-κB and production of cytokines such as interleukin-1 beta (IL-1β), IL-6, tumour necrosis factor-alpha (TNF-α), IL-10 and monocyte chemoattractant protein-1 (MCP-1) were assessed.

Material and methods

Chemicals

Sterile, purified and endotoxin-free silver nanoparticles (Biopure AgNPs 1.0 mg/mL in water), with a diameter of 10 nm and a citrate or polyethyleneglycol (PEG) surface, designated as Cit10 and PEG10, respectively, were purchased from Nanocomposix Europe (Prague, Czech Republic). Dulbecco's modified Eagle's medium (DMEM), fetal bovine serum (FBS), antibiotics and phosphate buffer saline (PBS, pH 7.4) were purchased from Life Technologies (Carlsbad, CA, USA). 3-(4,5-dimethylthiazol-2-yl)-2,5-diphenyltetrazolium bromide (MTT), Mowoil and DAPI were obtained from Sigma-Aldrich (St. Louis, MO, USA).

Physicochemical characterization of AgNPs

The morphology and size of AgNPs were assessed by transmission electron microscopy (TEM) using a transmission electron microscope Hitachi H9000 NAR (Hitachi High-Technologies Europe GmbH, Germany) operating at 300 kV. The hydrodynamic diameter and polydispersity index (PdI) were measured by dynamic light scattering (DLS) and the zeta potential was assessed by electrophoretic mobility, both measurements using a Zetasizer Nano ZS (Malvern Instruments, UK). Silver quantification measurements were performed by inductively coupled plasma optical emission spectrometry (ICP-OES) in an Activa M Radial spectrometer (Horiba Jobin Yvon), employing a charge coupled device (CCD) array detector, with a wavelength range of 166–847 nm and radial plasma view. Samples for ICP-OES were prepared by addition of 10 µL AgNPs (1.0 mg/mL) to 990 µL of either ultrapure water or complete culture medium, incubated for 0, 4, 24 or 48h, then centrifuged at 40000 rcf for 120 min at 4ºC (in accordance with the manufacturer's recommendations) to deposit the nanoparticles and separate the supernatant, which was then digested with acid (HCl:HNO3 2:1 v/v) before ICP-OES analysis.

Cell Culture

The HaCaT cell line, a nontumorigenic immortalized human keratinocyte cell line (Boukamp et al., 1988), was obtained from Cell Lines Services (Eppelheim, Germany). Cells were grown in complete medium, i.e., Dulbecco's modified Eagle's medium, supplemented with 10% fetal bovine serum (FBS), 2 mM L-glutamine, 100 U/mL penicillin, 100 µg/mL streptomycin and 250 µg/mL fungizone at 37°C in 5% CO_2 humidified atmosphere. Cells were observed daily under an inverted phase-contrast Eclipse TS100 microscope (Nikon, Tokyo, Japan). For each experiment, cells were allowed to adhere for 24h and then exposed to Cit10 or PEG10 AgNPs (dispersed through vortex in cell culture medium). The effects were measured after 4, 24 and 48h.

Viability assay

Cell viability was determined by the colorimetric 3-(4,5- dimethyl-2-thiazolyl)-2,5-diphenyl tetrazolium bromide (MTT) assay, measuring intracellular reduction of tetrazolium salts into purple formazan by viable cells (Twentyman and Luscombe, 1987). Cells were seeded in 96-well plates at a concentration of $6x10^4$ cells/mL. Fifty microliters of MTT (1 mg/mL) in phosphate buffered saline (PBS) were then added to each well, and incubated for 4h at 37°C, 5% CO_2. Medium was then removed and 150 µL of DMSO were added to each well for solubilization of formazan crystals. The optical density of reduced MTT was measured at 570 nm in a microtiter plate reader (Synergy HT Multi-Mode, BioTeK, Winooski, VT), and the ratio of cell metabolic activity (MA, a usual marker for cell viability) was calculated as: MA = [(Sample Abs –DMSO Abs) / (Control Abs – DMSO Abs)]*100. Three independent assays were performed with at least 2 technical replicates each and the results compared with the control (no exposure).

Immunofluorescence of p65 subunit of NF-κB in human keratinocytes

After the 4h treatments with 10 and 40 µg/mL of Cit10 or PEG10 AgNPs, coverslips were washed with PBS and permeabilized with 0.2% Triton X-100 for 15 min followed by three washes with PBS. Cells were treated with PBS containing BSA at a concentration of 1 mg/mL as a blocking agent for 1 hour. Cells were then washed three times with PBS and treated with anti-human NF-κB antibody (p65 subunit, Santa Cruz Biotechnology,Inc. Dallas, Texas USA) diluted 1/200 in PBS plus 0.5% BSA for 1 hour at room temperature. After three washes with PBS, coverslips were treated with a second antibody, Alexa fluor 488 anti-rabbit IgG diluted 1:200 in PBS plus 0.5% BSA for 1 hour at room temperature. After three washes with PBS, coverslips were treated with 0.5 µg/ml DAPI in PBS plus 0.5% BSA for 20 seconds, washed in PBS and mounted on glass microscope slides using Mowoil. Cells were imaged using confocal microscopy.

Cytokine estimation using cytometric bead array

Cytokine production was assessed using Bioplex kits. Briefly, the supernatants (collected from cell viability studies, centrifuged and frozen at -80ºC) were used to estimate the release of the following cytokines from treated cells: interleukin-1 beta (IL-1β), IL-6, tumour necrosis factor-alpha (TNF-α), IL-10 and monocyte chemoattractant protein-1 (MCP-1). Bead array kits were obtained from Beckton Dickinson (Oxford, UK) and a master mix prepared according to the manufacturer's instructions. The master mix was incubated with each of the test supernatants for 1 h, followed by the addition of detection beads and incubated for a further 2 h at room temperature. The beads were then washed in wash buffer and analysed using a BD

FACSArray™ flow cytometer which had previously been set up and calibrated using standard beads for each cytokine under investigation.

Statistical analysis

The results are reported as mean ± standard deviation (SD) of 2 technical replicates in each of the 3 independent experiments. For MTT assay, the statistical significance between control and exposed cells was performed by one-way ANOVA, followed by Dunnet and Dunn's method (as parametric and non-parametric test, respectively), using Sigma Plot 12.5 software (Systat Software Inc.). For the other assays, results were compared using two-way ANOVA, followed by Holm-Sidak test using also Sigma Plot 12.5 software (Systat Software Inc.). The differences were considered statistically significant for $p < 0.05$.

Results

Physicochemical characterization of AgNPs

A summary of the physico-chemical properties of the NMs is provided in table 3.1. The spherical shape and diameter of the AgNPs were verified by transmission electron microscopy (TEM) and found to agree with the manufacturer information (Table 3.1). The wavelength of the maximum absorbance peak in the UV-Vis spectra also matched the expected values. Regarding the DLS assessment of hydrodynamic diameters (Dh), polydispersity indexes (PdI > 0.3) indicated large variability in particle size, especially for the Cit10 NPs, hence the Z-average sizes may lack accuracy. PEG10 NPs showed higher Dh than Cit10, as expected based on the larger size of PEG compared to citrate. The zeta-potential values confirmed Cit10 AgNPs to have a negative surface charge (ζ-34 mV), which is expected as citrate is using as a coating to prevent agglomeration/aggregation through electrostatic repulsions, whereas PEG10 NPs, which are also designed to stabilize NPs through steric interactions, showed a less negative surface (ζ -14 mV). We have also assessed the amount of ionic silver (Ag^+) released from AgNPs, which was found to be low in water (< 1%), but significantly increased when the NPs were incubated in culture medium. Dissolved Ag^+ reached 14% in Cit10 suspensions after 4h and 11 % in PEG10 suspensions after 24 and 48h, this lower value likely relating to a more efficient protection of PEG coating against NP surface oxidation.

Effects on cell growth and viability

HaCaT cells in control conditions (exposed to cell culture medium) showed typical morphology (Fig. 3.1a and 3.2a). When cells were exposed to Cit10 and PEG10 AgNPs for 24h (3.1b, 3.1c, 3.1d and 3.1e), their confluence decreased, especially at the highest concentration (40 µg/mL).

The decrease in cell confluence was more visible after 48h (Fig. 3.2b, 3.2c, 3.2d and 3.2e). Morphologically, exposed cells (to both Cit10 and PEG10 NPs) showed large precipitates/aggregates of AgNPs in the medium, and confluence appeared to be, on average, lower for Cit10 exposed cultures.

Table 3.1. Physicochemical properties of AgNPs.

	Cit10	**PEG10**
D (nm)[a]	9.3±1.8	9.8±2.0
D (nm)[b]	11.0±2.4	9.4±2.8
D_h (nm)[c]	25.1±3.6	40.6±3.8
PdI[c]	0.42-0.52	0.26-0.37
ζ (mV)[d]	-34.5±3.3	-14.3±1.0
λ_{max}[e] (nm)	389	396
$\%Ag^+$ in water 0h[f]	0.93±0.02	n.a.
$\%Ag^+$ in DMEM 0h[f]	3.7±0.05	9.1±0.13
$\%Ag^+$ in DMEM 4h[f]	14.3±0.22	6.0±0.12
$\%Ag^+$ in DMEM 24h[f]	13.6±0.35	11.2±0.33
$\%Ag^+$ in DMEM 48h[f]	12.9±0.16	11.2±0.34

[a]Diameter indicated by the manufacturer; [b]Diameter measured by TEM; [c]Hydrodynamic diameter and polydispersity index (PdI) measured by DLS; [d]Zeta pontential assessed by electrophoretic mobility; [e]Wavelength of maximum absorbance peak in the UV-Vis spectrum; [f]Percentage of ionic silver in the AgNPs suspension (10 ug/mL). Standard deviations calculated for Dh, ζ and $\%Ag^+$ correspond to 3 replicate measurements. n.a. Not available.

The viability of HaCaT cells was negatively affected by both types of AgNP investigated in this study (Fig. 3.3). Relative to controls, the viability of exposed cells was significantly reduced ($p < 0.05$) upon exposure to Cit10 AgNPs at 10 µg/mL and 40 µg/mL after 4h, 24h and 48h. Following PEG10 AgNP exposure, the viability of cells following exposure at a concentration of 10 µg/mL was not affected at 4h but a significant reduction in cell viability was observed at 24 and 48h at this concentration. At a concentration of 40µg/ml PEG10 NPs significantly decreased cell viability at all time points (4, 24 and 48h).

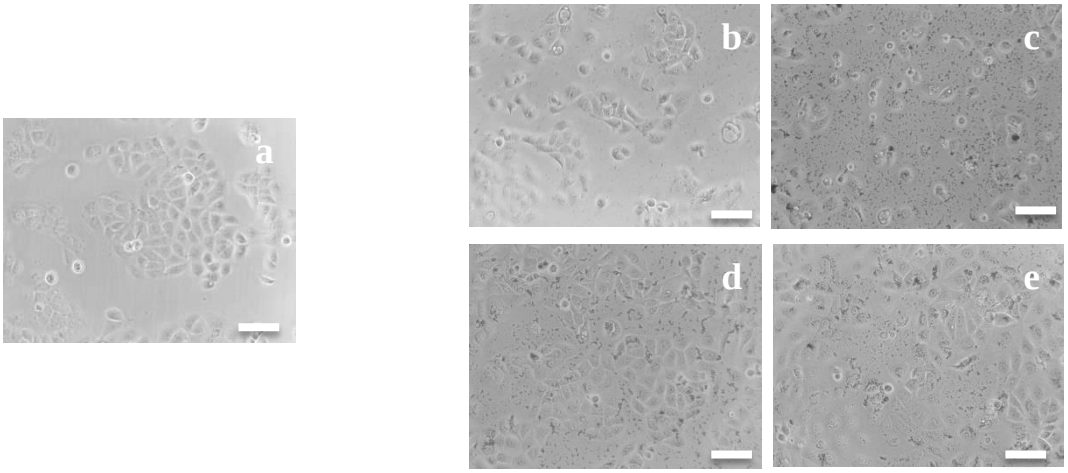

Figure 3.1: Light microscopy images (100X) of HaCaT cells exposed to AgNPs for 24h: a) 0, b) citrate-AgNPs 10 µg/mL, c) citrate- AgNPs 40 µg/mL, d) PEG-AgNPs 10 µg/mL and e) PEG- AgNPs 40 µg/mL. Bar corresponds to 100 µm.

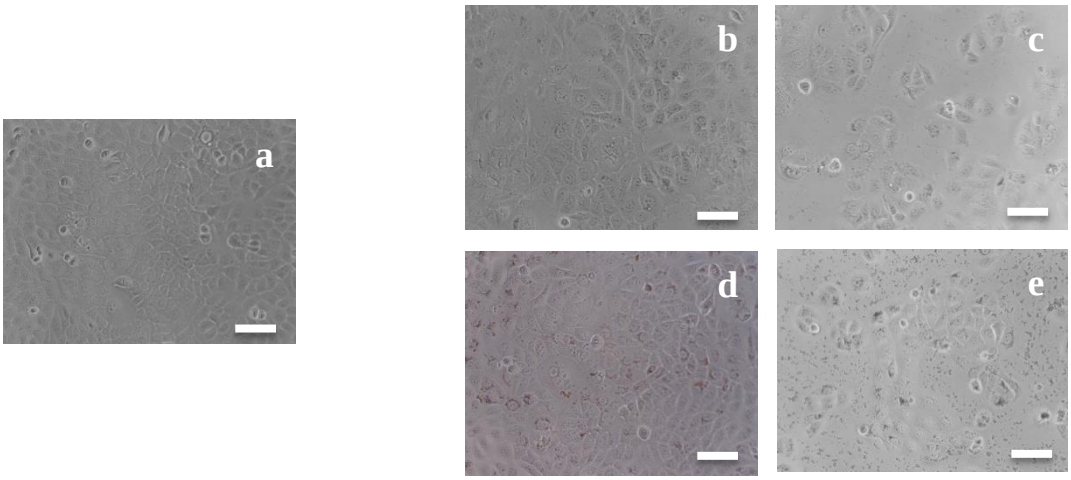

Figure 3.2: Light microscopy images (100X) of HaCaT cells exposed to AgNPs for 48h: a) 0, b) citrate-AgNPs 10 µg/mL, c) citrate- AgNPs 40 µg/mL, d) PEG-AgNPs 10 µg/mL and e) PEG- AgNPs 40 µg/mL. Bar corresponds to 100 µm.

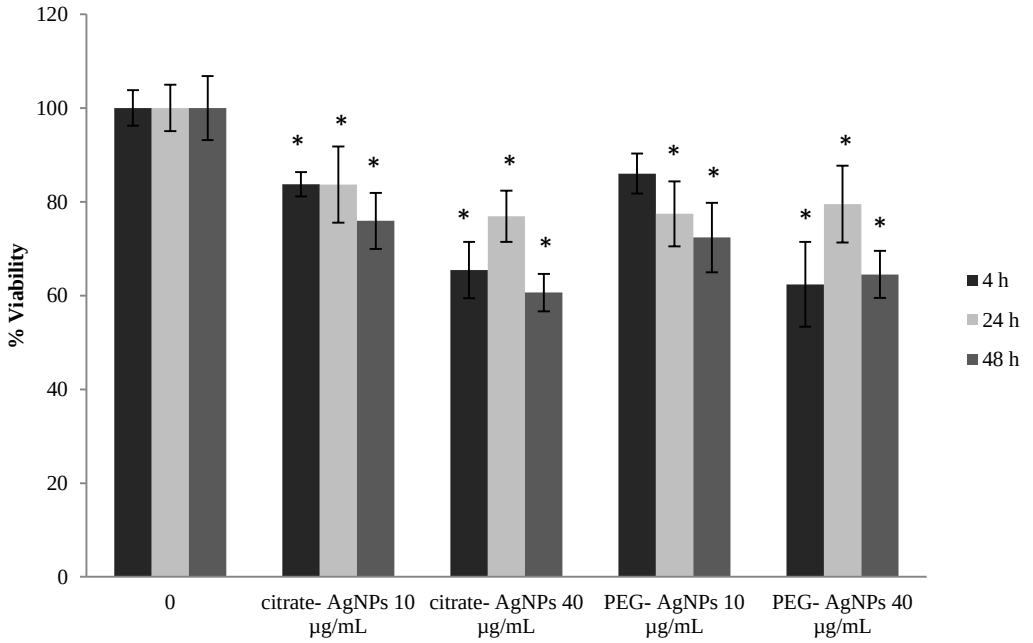

Figure 3.3: Relative cell viability (%) of HaCaT after exposure to 10 and 40 µg/mL citrate- AgNPs or PEG- AgNPs, measured by MTT assay, for 4, 24 and 48h. Data expressed as mean and standard deviation. * indicate significant differences between control at $p < 0.05$.

NF-κB and inflammatory cytokine release

Activation of NF-κB in HaCaT cells by AgNPs was evaluated by immunofluorescence; in its inactive state NFkB is located in the cytoplasm, and in its active state is localized in the nucleus. Figure 3.4a-c shows a positive control with 240 µM of H_2O_2 where there is a great intensity of p65 staining in the nucleus. Also, controls (including: cells only (no staining), cells stained with only the primary antibody and samples stained with the second antibody only) were done to check the autofluorescence in cells (data not shown). In control cells, most NFkB staining was localized in the cell cytoplasm, with occasional occurrence in the nucleus. Regarding AgNP exposed cells, there was no evidence of NFkB activation (i.e. no increase in the intensity of staining in the nucleus) (Fig. 3.4e-g). A decrease in p65 staining in the nucleus after exposure to 40 µg/mL PEG10 AgNPs was observed comparing to control cells (Fig. 3.4h).

The release of cytokines by HaCaT cells treated with AgNPs is shown in Figure 3.5. Lipopolysaccharide (LPS) stimulated a significant increase in MCP-1 release at 48h, when compared to the control. MCP-1 production significantly decreased following exposure of HaCaT cells to both AgNP types and was most pronounced at a concentration of for 40 µg/mL, compared to negative and positive controls ($p < 0.001$). No effects were observed on the other cytokines studied, IL-1β, IL-6, IL-10 and TNF-α, after exposure to both AgNPs at both times (data not shown).

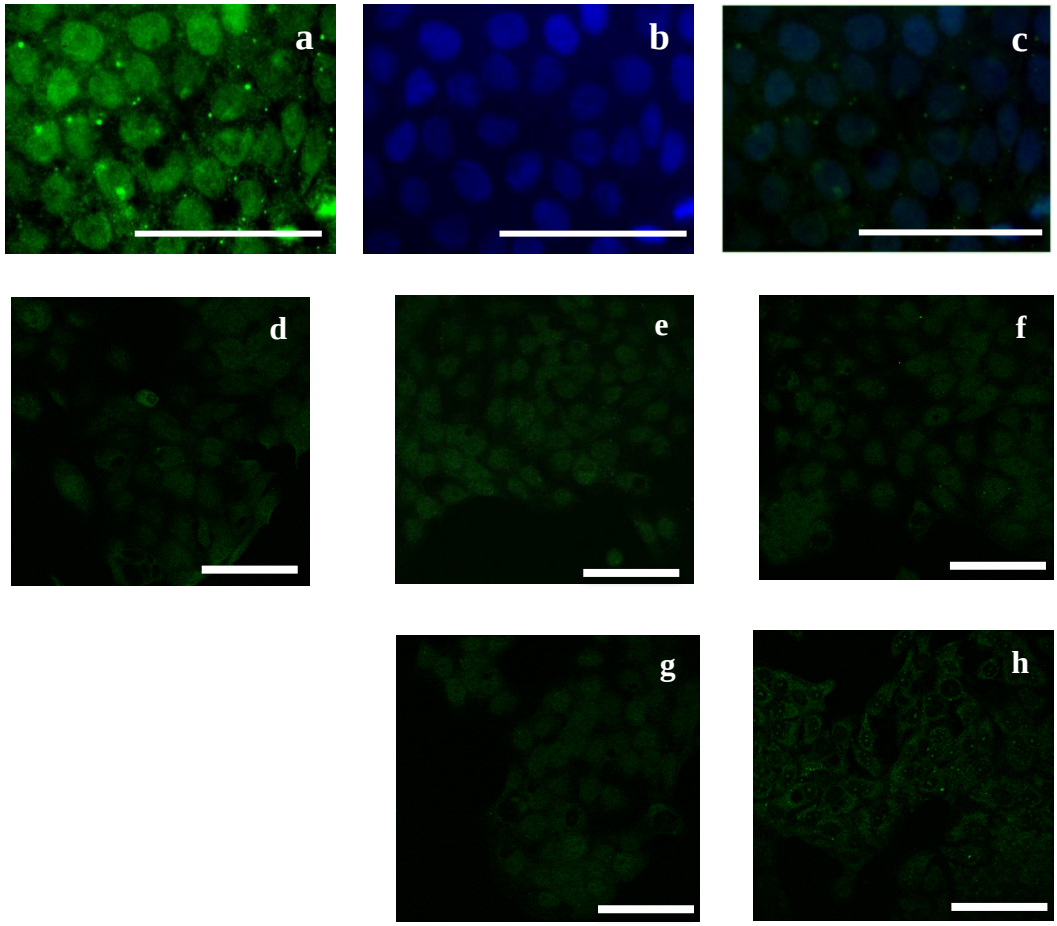

Figure 3.4: a) - c) are fluorescence microscopy images (400X) of immunofluorescence of HaCaT cells treated with anti NF-kB p65 antibody after stimulation with 240 µM H_2O_2 for 10 min prior fixation. a) p65 subunit of NF-kB (alexa fluor 488 anti-rabbit IgG); b) DAPI staining the nucleus; c) Overlap of a and b images. d) - h) are confocal microscopy images of immunofluorescence of p65 subunits of NF-kB in human HaCaT keratinocytes exposed to AgNPs for 4h: d) 0 (control); e) 10 µg/mL of Cit10; f) 40 µg/mL of Cit10; g) 10 µg/mL of PEG10; h) 40 µg/mL of PEG10. Bar corresponds to 100 µm.

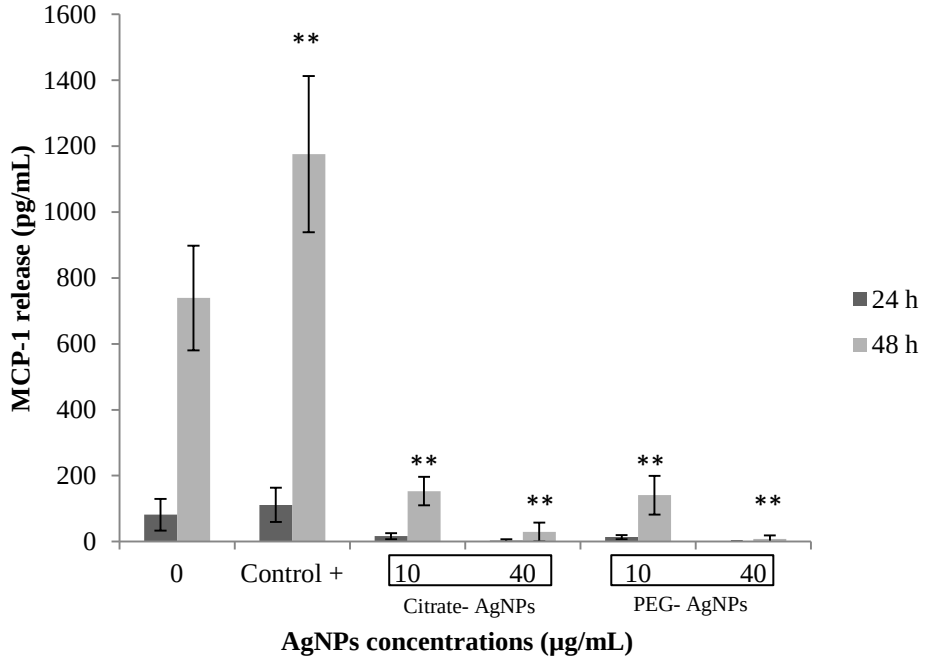

Figure 3.5: Cytokine release by HaCaT cells after 24 and 48h exposure to citrate- or PEG- AgNPs. Control + is a positive control by adding LPS to cells. Data represent the mean ± SEM (n = 3) of the concentration (pg /ml) of MCP-1 cytokine released from the cells after NPs treatment. ** indicate significant differences between control at $p < 0.01$.

Discussion

Citrate-coated AgNPs are among the most widely used AgNPs in multiple industrial applications (Tolaymat et al., 2010), while the less used PEG-coated AgNPs have gained increasing attention over recent years by e.g. biomedical industry due to their high stability and reduced reactivity (Brandenberger et al., 2010; Ginn et al., 2014; Ryan et al., 2008; Thorley and Tetley, 2013). Thus, there is need to better understand the influence of coatings of the biological effects of NPs, and in particular the inflammatory responses. As skin represents one of the major organs in contact with AgNPs, we compared the viability and inflammatory responses induced by citrate or PEG-coated AgNPs with a core diameter of 10 nm (Cit10 and PEG10 AgNPs) in human epidermis keratinocytes (HaCaT cells).

From the cytotoxicity results, Cit10 AgNPs were observed to be more toxic than PEG10 NPs. The greater toxicity of Cit10 AgNPs was particularly relevant for low doses, since a lower concentration (10 µg/mL) of Cit10 NPs induced a statistically significant decrease in cell viability 4h post exposure, that was not evident for PEG AgNPs. At higher doses (40 µg/mL) and exposure periods, PEG10 and Cit10 AgNPs reduced viability in similar ways. These data

suggest that, for these skin cells, the influence of coating is more important at low AgNP concentrations, whereas by increasing concentration, the influence of coating seems to be less relevant. A significant decrease in BEAS-2B (bronchial epithelial) cell viability upon exposure to 20 nm citrate-coated AgNPs at 6.25-50 µg/mL after 24h has been observed previously (Wang et al., 2014). Also, Song et al. (2012) showed a decrease on cell viability in human liver cell line - HL-7702 after exposure to PEG-coated AgNPs in dose- and time-dependent manner at doses from 6.25µg/mL. Future studies could assess the sensitivity of different cell types to the AgNPs used in this study.

A complex interplay between environmental and genetic factors control immune system responses and when a deregulation of immune homeostasis occurs, host defense can be impaired and at the same time cause excessive and potential harmful inflammatory responses, which could be responsible for several immune disorders (Bieber, 2008; Morar et al., 2006). The ability of NPs to elicit pro-inflammatory responses is frequently assessed in *in vitro* and *in vivo* studies as a marker of their toxicity (eg, Schoemaker et al., (2002)). Thus, understanding NP-dependent regulation of cytokine production is essential since this process conditions shifts from acute to chronic phases of allergic inflammation (Rossi and Zlotnik, 2000). NF-κB pathways has been traditionally associated to increases in the production of inflammatory cytokines which could be implicated in the development of a variety of diseases (Driscoll et al., 1997; Mossman and Churg, 1998). AgNPs did not activate NFkB in HaCaT cells in this study. In fact, NF-κB may be inhibited after exposure to the higher concentration (40 µg/mL) of PEG10 AgNPs. It is described in literature that the inhibition or absence of NF-kB activation, induces apoptosis or sensitizes cells to apoptosis (Schoemaker et al., 2002).

Murray et al (2013) found that a co-exposure of human epidermal keratinocytes (HEK cells) to superparamagnetic iron oxide (SPION) nanoparticles and UVB induced NF-κB activation and release of inflammatory mediators such as the cytokines IL-6 and IL-8. Carbon black NPs have also been demonstrated to induce NFkB activation in macrophages and to stimulate TNFα production (Brown et al., 2004). However, it has also been recognized that NF-κB signaling has important functions in the maintenance of physiological immune homeostasis, particularly in epithelial cells (Wullaert et al., 2011). In a previous work (Bastos et al., 2016 manuscript submitted), we have demonstrated, by Annexin-V and gene expression, that Cit30 AgNPs induced preferably necrotic pathways, while cells exposed to PEG30 AgNPs stimulated increases of cells in earlier phase of apoptosis (therefore a more reversible process) and no necrosis, supporting that coating conditions how these AgNPs influence the cell apoptosis/necrosis pathways. A major role of NF-kB pathways involve the regulation of anti-apoptotic genes, by NF-KB directly binding and inhibiting CASP3, -7 and -9 which seems to be happening in citrate- AgNPs exposed cells (Schoemaker et al., 2002). Considering that only

PEG10 AgNPs inhibit NF-κB, we therefore hypothesize that this may be involved in the induction of apoptosis by activating CASP3 found in PEG30-exposed cells versus Cit30-exposed ones. In the future we suggest that NF-kB activation/inhibition may be used to a greater extent when assessing the hazard of coating and AgNPs to better understand the mechanisms (i.e. cellular and molecular events) underlying their toxicity. On the other hand, Brown et al (2004) showed that ultrafine carbon black particles (UfCB)-induced nuclear translocation of NF-kB in human monocytes which occurs through ROS-mediated mechanism. Indeed, in our previous study Cit30 and PEG30 AgNPs induced a significant increase in the production of ROS by HaCaT cells at the highest dose tested (40 μg/mL), compared to control cells. However, the ROS levels were similar for both NP types which do not explain the NF-κB inhibition by PEG10 AgNPs. Thus, for further studies we also suggest the quantification of NF-kB activation (e.g. by western blotting) and determination of ROS production.

Concerning cytokine release, neither Cit10 nor PEG10 AgNPs induced IL-1β, IL-6, IL-10, TNF-α and MCP-1 production by HaCaT cells. Instead, compared to control cells, they decreased MCP-1 production after 48h exposure, this reduction being more pronounced at the higher concentration (40 μg/mL). The information regarding the influence of AgNPs on the stimulation of these cytokines from keratinocytes release is scarce, and sometimes contradictory, as different exposure conditions, concentrations, coating, cell type, NP size and synthesis have been considered in the literature (Abbott Chalew and Schwab, 2013; Giovanni et al., 2015; Miethling-Graff et al., 2014; Orlowski et al., 2013; Samberg et al., 2010; Suliman Y et al., 2013a; Wong et al., 2009; Yen et al., 2009). For instance, Orlowski and co-workers (2013) found an increase of MCP-1 production in murine keratinocytes (murine 291.03C) and by monocytes (RAW 264.7) after exposure to unmodified AgNPs. Also, human umbilical vein endothelial (HUVEC) cells showed a significant increase of IL-6, IL-8 and MCP-1 at doses higher than 1 mg/L AgNPs (Shi et al., 2014). Moreover, confirming the inflammatory potential of AgNPs, several interleukins and TNF-α were reported to increase upon exposure of HEK cells (Samberg et al., 2010) and macrophages (Yen et al., 2010) to AgNPs. On the other hand, several authors reported an undetectable stimulation of cytokines in response to metal NPs, as observed in the present study. For example, Murray et al (2013) demonstrated that HEK cells exposed to superparamagnetic iron oxide nanoparticles maintained the IL-1β, IL-10 and TNF-α below detectable levels (while increasing IL-6); and also that mouse epidermal cells (JB6 P+) maintained INF-γ and IL-12 below the detectable levels after exposure to the same nanoparticles. Similarly, Samberg et al (2010) did not find detectable levels of IL-10 in HEK cells exposed to unwashed AgNPs. In mice peritoneal tissues and in RAW cells, Wong et al (2009) demonstrated that AgNPs have an anti-inflammatory effect decreasing TNF-α, and INF-γ. Also, Parnsamut and Brimson (2015) found that AgNPs inhibited TNF-α expression in

leukemic cell lines. It is known that cytokines can adsorb onto the surface of particles, which may compromise their detection (Brown et al., 2010). Thus, it should not be excluded that AgNPs may induce cytokine production by keratinocytes but that the cytokines bind to the AgNP surface to prevent their detection. How proteins bind to nanoparticles is currently an important topic of debate. For example, Deng et al (2013) showed that human plasma proteins differently bind to positively and negatively charged polymer-coated gold NPs, which elicited different biological responses, and that only the negatively charged nanoparticles induced cytokine release from THP-1 cells. While proteins can bind to different nanoparticles, the biological outcome may not be the same. Selection of cytokines for assessment in this study was prioritized based on the outcome of a literature search which identified cytokines that are commonly produced following exposure of cells to NPs. Future studies could therefore assess a wider panel of cytokines.

In summary, our study demonstrated that while citrate- and PEG-coated AgNPs decreased the viability of HaCaT cells, citrate coated AgNPs were more cytotoxic than PEG coated NPs, particularly at low concentrations and shorter incubation times. At higher AgNPs concentration, the influence of coating became less relevant. Also, we demonstrated that, independent of the coating, AgNPs did not induce cytokine production, and decreased MCP-1 release. Finally, PEG10 AgNPs at high concentrations inactivated the transcription factor NF-κB, and putative correlation with anti-inflammatory and anti-apoptotic homeostasis should be further explored.

Acknowledgments

This work was developed in the scope of the projects CICECO-Aveiro Institute of Materials (Ref. FCT UID/CTM/50011/2013) and CESAM (Ref. FCT UID/AMB/50017/2013), financed by national funds through the FCT/MEC and when applicable co-financed by the European Regional Development Fund (FEDER) under the PT2020 Partnership Agreement. Funding to the project FCOMP-01-0124-FEDER-021456 (Ref. FCT PTDC/SAU-TOX/120953/2010) by FEDER through COMPETE and by national funds through FCT, and the FCT-awarded grants (SFRH/BD/81792/2011; SFRH/BPD/48853/2008) are acknowledged. I.F.D and A.L.D.S. acknowledge FCT/MCTES for the research contracts under the Program 'Investigador FCT' 2014.

Contributions

V.B. participated in the design experiment with the supervisors and did all laboratorial experiments and statistical data analyses. Also had a key role in the data analyses integration,

and together with the supervisors wrote and revised the manuscripts. C.S. and H.O. planned the experimental design, contributed to data analyses and integration of all data, and in the manuscript preparation. A.L.D.S. was involved in AgNPs characterization and in writing this section. I.F.D. coordinated NPs analyses and revised the manuscript. D.B. and H.J. coordinated the inflammatory assays and revised the manuscript.

References

Abbott Chalew, T.E., and Schwab, K.J. (2013). Toxicity of commercially available engineered nanoparticles to Caco-2 and SW480 human intestinal epithelial cells. Cell Biol Toxicol, 29(2), 101-116.

Abdelhalim, M.A.K., and Jarrar, B.M. (2011). Renal tissue alterations were size-dependent with smaller ones induced more effects and related with time exposure of gold nanoparticles. Lipids Health Dis, 10(1), 1.

Ahlberg, S., Meinke, M.C., Werner, L., Epple, M., Diendorf, J., Blume-Peytavi, U., Lademann, J., Vogt, A., and Rancan, F. (2014). Comparison of silver nanoparticles stored under air or argon with respect to the induction of intracellular free radicals and toxic effects toward keratinocytes. Eur J Pharm Biopharm, 88(3), 651-657

Behra, R., Sigg, L., Clift, M., Herzog, F., Minghetti, M., Johnston, B., Petri-Fink, A., and Rothen-Rutishauser, B. (2013). Bioavailability of silver nanoparticles and ions: from a chemical and biochemical perspective. J R Soc Interface, 10(87), 20130396.

Benn, T., and Westerhoff, P. (2008). Nanoparticle silver released into water from commercially available sock fabrics. Environ Sci Technol, 42(11), 4133-4139 .

Bieber, T. (2008). Atopic dermatitis. N Engl J Med, *358* (14), 1483-1494.

Boonkaew, B., Kempf, M., Kimble, R., and Cuttle, L. (2014). Cytotoxicity testing of silver-containing burn treatments using primary and immortal skin cells. Burns, 40(8), 1562-1569.

Brandenberger, C., Mühlfeld, C., Ali, Z., Lenz, A.-G.G., Schmid, O., Parak, W.J., Gehr, P., and Rothen-Rutishauser, B. (2010). Quantitative evaluation of cellular uptake and trafficking of plain and polyethylene glycol-coated gold nanoparticles. Small, 6(15), 1669-1678.

Brown, D.M., Dickson, C., Duncan, P., Al-Attili, F., and Stone, V. (2010). Interaction between nanoparticles and cytokine proteins: impact on protein and particle functionality. Nanotechnology, 21(21), 215104.

Brown, D.M., Donaldson, K., Borm, P.J., Schins, R.P., Dehnhardt, M., Gilmour, P., Jimenez, L.A., and Stone, V. (2004). Calcium and ROS-mediated activation of transcription factors and TNF-alpha cytokine gene expression in macrophages exposed to ultrafine particles. Am J Physiol Lung Cell Mol Physiol, 286(2), L344-L353.

Caballero-Díaz, E., Pfeiffer, C., Kastl, L., Gil, P., Simonet, B., Valcárcel, M., Lamana, J., Laborda, F., and Parak, W.J. (2013). The toxicity of silver nanoparticles depends on their uptake by cells and thus on their surface chemistry. Part Part Syst Charact, 30(12), 1079-1085.

Comfort, K.K., Maurer, E.I., and Hussain, S.M. (2014). Slow release of ions from internalized silver nanoparticles modifies the epidermal growth factor signaling response. Colloids Surf B Biointerfaces, 123, 136-142.

Deng, Z.J., Liang, M., Toth, I., Monteiro, M., and Minchin, R.F. (2013). Plasma protein binding of positively and negatively charged polymer-coated gold nanoparticles elicits different biological responses. Nanotoxicology, 7(3), 314-322.

Driscoll, K.E., Carter, J.M., and Hassenbein, D.G. (1997). Cytokines and particle-induced inflammatory cell recruitment. Environ Health Perspect, 105(Suppl 5), 1159.

Eckhardt, S., Brunetto, P., Gagnon, J., Priebe, M., Giese, B., and Fromm, K. (2013). Nanobio silver: its interactions with peptides and bacteria, and its uses in medicine. Chem Rev, 113(7), 4708-4754.

EPA, E.P.A. (2010). State of the Science Literature Review: Everything Nanosilver and More. Scientific, Technical, Research, Engineering and Modeling Support Final Report.

Fujiwara, N., and Kobayashi, K. (2005). Macrophages in inflammation. Curr Drug Targets Inflamm Allergy, 4(3), 281-286.

George, R., Merten, S., Wang, T.T., Kennedy, P., and Maitz, P. (2014). In vivo analysis of dermal and systemic absorption of silver nanoparticles through healthy human skin. Australas J Dermatol, 55(3), 185-190.

Ginn, C., Khalili, H., Lever, R., and Brocchini, S. (2014). PEGylation and its impact on the design of new protein-based medicines. Future Med Chem, 6(16), 1829-1846.

Giovanni, M., Yue, J., Zhang, L., Xie, J., and Ong, C.N. (2015). Pro-Inflammatory Responses of RAW264. 7 Macrophages when Treated with Ultralow Concentrations of Silver, Titanium Dioxide, and Zinc Oxide Nanoparticles. J Hazard Mater, 297, 146-152.

Graves, J.D., Craxton, A., and Clark, E.A. (2004). Modulation and function of caspase pathways in B lymphocytes. Immunol Rev, 197(1), 129-146.

Kelso, A. (1998). Cytokines: principles and prospects. Immunol Cell Biol, 76(4), 300-317.

Kim, T.H., Kim, M., Park, H.S., Shin, U.S., Gong, M.S., and Kim, H.W. (2012). Size-dependent cellular toxicity of silver nanoparticles. J Biomed Mater Res A, 100(4), 1033-1043.

Larese, F.F., D'Agostin, F., Crosera, M., Adami, G., Renzi, N., Bovenzi, M., and Maina, G. (2009). Human skin penetration of silver nanoparticles through intact and damaged skin. Toxicology, 255(1), 33-37.

Lu, W., Senapati, D., Wang, S., Tovmachenko, O., Singh, A., Yu, H., and Ray, P. (2010). Effect of Surface Coating on the Toxicity of Silver Nanomaterials on Human Skin Keratinocytes. Chem Phys Lett, 487(1), 92-96.

Miethling-Graff, R., Rumpker, R., Richter, M., Verano-Braga, T., Kjeldsen, F., Brewer, J., Hoyland, J., Rubahn, H.-G.G., and Erdmann, H. (2014). Exposure to silver nanoparticles induces size- and dose-dependent oxidative stress and cytotoxicity in human colon carcinoma cells. Toxicol In Vitro, 28(7), 1280-1289.

Morar, N., Willis-Owen, S.A.G., and Moffatt, M.F. (2006). The genetics of atopic dermatitis. J Allergy Clin Immun, 118(1), 24-34.

Mossman, B.T., and Churg, A. (1998). Mechanisms in the pathogenesis of asbestosis and silicosis. Am J Respir Crit Care Med, 157(5), 1666-1680.

Murray, A.R., Kisin, E., Inman, A., Young, S.-H., Muhammed, M., Burks, T., Uheida, A., Tkach, A., Waltz, M., and Castranova, V. (2013). Oxidative stress and dermal toxicity of iron oxide nanoparticles in vitro. Cell Biochem Biophys, 67(2), 461-476.

Noursadeghi, M., Tsang, J., Haustein, T., Miller, R.F., Chain, B.M., and Katz, D.R. (2008). Quantitative imaging assay for NF-kappaB nuclear translocation in primary human macrophages. J Immunol Methods 329(1), 194-200.

Nowack, B., and Bucheli, T. (2007). Occurrence, behavior and effects of nanoparticles in the environment. Environ Pollut, 150(1), 5-22.

Nowack, B., Krug, H., and Height, M. (2011). 120 years of nanosilver history: implications for policy makers. Environ Sci Technol 45(4), 1177-1183.

Orlowski, P., Krzyzowska, M., Zdanowski, R., Winnicka, A., Nowakowska, J., Stankiewicz, W., Tomaszewska, E., Celichowski, G., and Grobelny, J. (2013). Assessment of in vitro cellular responses of monocytes and keratinocytes to tannic acid modified silver nanoparticles. Toxicol in Vitro, 27(6), 1798-1808.

Pang, C., Brunelli, A., Zhu, C., Hristozov, D., Liu, Y., Semenzin, E., Wang, W., Tao, W., Liang, J., Marcomini, A., et al. (2015). Demonstrating approaches to chemically modify the surface of Ag nanoparticles in order to influence their cytotoxicity and biodistribution after single dose acute intravenous administration. Nanotoxicology, 1-11.

Park, E.-J.J., Choi, K., and Park, K. (2011a). Induction of inflammatory responses and gene expression by intratracheal instillation of silver nanoparticles in mice. Arch Pharm Res, 34(2), 299-307.

Park, J., Lim, D.-H.H., Lim, H.-J.J., Kwon, T., Choi, J.-s.S., Jeong, S., Choi, I.-H.H., and Cheon, J. (2011b). Size dependent macrophage responses and toxicological effects of Ag nanoparticles. Chem Commun (Camb), 47(15), 4382-4384.

Parnsamut, C., and Brimson, S. (2015). Effects of silver nanoparticles and gold nanoparticles on IL-2, IL-6, and TNF-α production via MAPK pathway in leukemic cell lines. Genet Mol Res, 14(2), 3650.

Rossi, D., and Zlotnik, A. (2000). The biology of chemokines and their receptors. Annu Rev Immunol, 18(1), 217-242.

Ryan, S.M.M., Mantovani, G., Wang, X., Haddleton, D.M., and Brayden, D.J. (2008). Advances in PEGylation of important biotech molecules: delivery aspects. Expert Opin Drug Deliv, 5(4), 371-383.

Samberg, M.E., Oldenburg, S.J., and Monteiro-Riviere, N.A. (2010). Evaluation of Silver Nanoparticle Toxicity in Skin in Vivo and Keratinocytes in Vitro. Environ Health Perspect, 118(3), 407.

Schinwald, A., Murphy, F., Prina-Mello, A., Poland, C., Byrne, F., Glass, J., ... & MacNee, W. (2012). The threshold length for fibre-induced acute pleural inflammation: shedding light on the early events in asbestos-induced mesothelioma. Toxicol Sci, kfs171.

Schoemaker, M.H., Ros, J.E., Homan, M., and Trautwein, C. (2002). Cytokine regulation of pro-and anti-apoptotic genes in rat hepatocytes: NF-κB-regulated inhibitor of apoptosis protein 2 (cIAP2) prevents apoptosis. J Hepatol, 36(6), 742-750.

Sharma, V., Yngard, R., and Lin, Y. (2009). Silver nanoparticles: green synthesis and their antimicrobial activities. Adv Colloid Interface Sci, 145(1), 83-96.

Shi, J., Sun, X., Lin, Y., Zou, X., Li, Z., Liao, Y., Du, M., and Zhang, H. (2014). Endothelial cell injury and dysfunction induced by silver nanoparticles through oxidative stress via IKK/NF-κB pathways. Biomaterials, 35(24), 6657-6666.

Suliman Y, A., Ali, D., Alarifi, S., Harrath, A., Mansour, L., and Alwasel, S. (2013a). Evaluation of cytotoxic, oxidative stress, proinflammatory and genotoxic effect of silver nanoparticles in human lung epithelial cells. Environ Toxicol, 30(2), 149-160.

Suliman Y, A.O., Ali, D., Alarifi, S., Harrath, A.H., Mansour, L., and Alwasel, S.H. (2013b). Evaluation of cytotoxic, oxidative stress, proinflammatory and genotoxic effect of silver nanoparticles in human lung epithelial cells. Environ Toxicol, 30(2), 149-160.

Tejamaya, M., Römer, I., Merrifield, R., and Lead, J. (2012). Stability of citrate, PVP, and PEG coated silver nanoparticles in ecotoxicology media. Environ Sci Technol 46(13), 7011-7017.

Thorley, A.J., and Tetley, T.D. (2013). New perspectives in nanomedicine. Pharmacol Therapeut, 140(2), 176-185.

Tolaymat, T.M., El Badawy, A.M., Genaidy, A., Scheckel, K.G., Luxton, T.P., and Suidan, M. (2010). An evidence-based environmental perspective of manufactured silver nanoparticle in syntheses and applications: a systematic review and critical appraisal of peer-reviewed scientific papers. Sci Total Environ, 408(5), 999-1006.

Twentyman, P., and Luscombe, M. (1987). A study of some variables in a tetrazolium dye (MTT) based assay for cell growth and chemosensitivity. Br J Cancer 56(3), 279.

Vance, M.E., Kuiken, T., Vejerano, E.P., McGinnis, S.P., Hochella Jr, M.F., Rejeski, D., & Hull, M.S. (2015). Nanotechnology in the real world: Redeveloping the nanomaterial consumer products inventory. Beilstein J Nanotechnol, 6(1), 1769-1780.

Wang, X., Ji, Z., Chang, C., Zhang, H., Wang, M., Liao, Y.-P., Lin, S., Meng, H., Li, R., Sun, B., et al. (2014). Use of coated silver nanoparticles to understand the relationship of particle dissolution and bioavailability to cell and lung toxicological potential. Small, 10(2), 385-398.

Wong, K.K., Cheung, S.O., Huang, L., Niu, J., Tao, C., Ho, C.-M.M., Che, C.-M.M., and Tam,

P.K. (2009). Further evidence of the anti-inflammatory effects of silver nanoparticles. ChemMedChem 4(7), 1129-1135.
Wullaert, A., Bonnet, M.C., and Pasparakis, M. (2011). NF-κB in the regulation of epithelial homeostasis and inflammation. Cell Res 21(1), 146-158.
Yang, E.-J.J., Jang, J., Lim, D.-H.H., and Choi, I.-H.H. (2012). Enzyme-linked immunosorbent assay of IL-8 production in response to silver nanoparticles. Methods Mol Biol, 131-139.
Yarilin, A.A., and Belyakov, I.M. (2004). Cytokines in the thymus: production and biological effects. Curr Med Chem, 11(4), 447-464.
Yen, H.-J., Hsu, S.-H., and Tsai, C.-L. (2009). Cytotoxicity and immunological response of gold and silver nanoparticles of different sizes. Small, 5(13), 1553-1561.
Yoshizumi, M., Nakamura, T., Kato, M., Ishioka, T., Kozawa, K., Wakamatsu, K., and Kimura, H. (2008). Release of cytokines/chemokines and cell death in UVB-irradiated human keratinocytes, HaCaT. Cell Biol Int, 32(11), 1405-1411.
Zhang, L.W., Yu, W.W., Colvin, V.L., and Monteiro-Riviere, N.A. (2008). Biological interactions of quantum dot nanoparticles in skin and in human epidermal keratinocytes. Toxicol Appl Pharmacol, 228(2), 200-211.

Chapter 4

Genotoxicity of citrate-coated silver nanoparticles to human keratinocytes assessed by the comet assay and cytokinesis blocked micronucleus assay

Genotoxicity of citrate-coated silver nanoparticles to human keratinocytes assessed by the comet assay and cytokinesis blocked micronucleus assay

Bastos V.[1], Duarte IF.[2], Santos C.[1,3] and Oliveira H.[1]

[1]*CESAM & Laboratory of Biotechnology and Cytomics, Department of Biology, University of Aveiro, 3810-193 Aveiro, Portugal*
[2]*CICECO, Department of Chemistry, University of Aveiro, Aveiro, Portugal*
[3]Department of Biology, Faculty of Sciences, University of Porto, Rua do Campo Alegre, Porto, *corresponding author: csantos@fc.up.pt

Keywords: Silver nanoparticles (AgNPs), CBMN, Comet assay, Genotoxicity, HaCaT cells, Nanotoxicology, Skin, Viability.

Abstract

Silver nanoparticles (AgNPs) are widely used in industrial, cosmetic and biomedical products, skin frequently being the first exposed organ. It is widely recognized that the characteristics of AgNPs (e.g .size, coating) may influence their cytotoxic effects, but their correlation with DNA damage and mitotic disorders remains poorly explored. In this study, human keratinocytes (HaCaT cell line) were exposed to well-characterized 30 nm AgNPs coated with citrate and their effects on viability, DNA fragmentation (assessed by the Comet assay) and micronuclei (MNi) induction (assessed by the cytokinesis-block micronucleus cytome assays, CBMN) were investigated. The results showed that 10 and 40 µg/mL AgNPs decreased cell proliferation and viability and induced a significant genetic damage. This was observed by an increase of DNA amount in comet tail which linearly correlated with dose and time of exposure. Also, cytostaticity (increase of mononucleated cells) and MNi rates increased in treated cells. Contrarily, no significant changes were observed in nucleoplasmatic bridges (NPBs) nor in nuclear buds (NBUDs), although an increasing trend was observed in NBUDs in all conditions and periods. The cytostatic effects on HaCaT cells were also shown by the decrease of their nuclear division index. Thus, both comet and CBMN assays supported the observation that citrate-AgNPs induced genotoxic effects on HaCaT cells. Considering that AgNPs are present in a vast number of consumer products, for e.g. nanomedicine skin applications and formulations, more research is needed to determine the properties that confer less toxicity of AgNPs to different cell lines.

Introduction

Nanomaterials have great prospects for development of new products and applications in various sectors, thus making nanotechnology an increasingly important field. According to the inventory of nanotechnology-based consumer products compiled by the Project on Emerging Nanotechnologies (http://www.nanotechproject.org/cpi), nanosilver-containing products represent ~24% of all commercially available nanoproducts. Due to their physicochemical and biological properties, namely the efficient antimicrobial activity, silver nanoparticles (AgNPs) are often used in medicine, industry, and a vast range of consumer products, including clothing and cosmetics (Abdelhalim &Jarrar 2011, Behra et al. 2013, Benn &Westerhoff 2008, Eckhardt et al. 2013, Nowack et al. 2011). However, their impressive and useful characteristics and their rapid dissemination may become problematic in a toxicological perspective. In the last decade, serious concerns about their possible impacts on the environment and human health have emerged (Dusinska et al. 2013, Hillegass et al. 2010, Nowack &Bucheli 2007, Promtong 2015, Pumera 2011). The routes of human exposure to AgNPs may include dermal absorption, ingestion, inhalation and injection (Ahamed et al. 2010, Chen &Schluesener 2008), skin being a major entry route of AgNPs into the body.

There are many *in vitro* studies focused on the cytotoxicity of AgNPs (Li et al. 2014, Smita et al. 2012, Souza et al. 2016, Zhang et al. 2014), but the mechanisms of AgNPs-induced genotoxicity are not completely understood (Browning et al. 2013). Furthermore, subtle effects not necessarily causing cell death should be taken into account. One important effect is damage to DNA, as genetic instability is associated with cancer development (Karlsson 2010). Nanoparticles may induce DNA damage through different mechanisms: it was shown that they may cause oxidative stress, increasing the number of reactive oxygen species (ROS) either by generating oxidants such as the reactive hydroxyl radical ($OH^{\cdot}$) and/or by stimulating cells to produce oxidants/genotoxic compounds, which may eventually affect mitochondrial electron transport (e.g. inducing cytochrome P450 enzymes) (Vrček et al. 2014). Particles ability to cause inflammation and thus secondary formation of oxidants by inflammatory cells was also demonstrated (Knaapen et al. 2004b). Moreover, their eventual direct access to DNA via transport into the nucleus must not be excluded, despite being unlikely to occur since nuclear pore complex is less than 8 nm in diameter (Knaapen et al. 2004a, Terry et al. 2007). However, nanoparticles may contact with DNA during mitosis, when the nuclear membrane breaks down, enabling direct interactions with DNA. For example, it was demonstrated that AgNPs interference with microtubules during mitosis could give rise to aneuploidy cells (Gonzalez et al. 2008). Particles or intracellular metal ions from particles can also enhance the permeability of the lysosomal membrane. This permeability may lead to the release of DNase into the

cytoplasm and possibly into the nucleus, where it could cut DNA (Banasik et al. 2005).

Different methods have been used to assess the genotoxicity of nanomaterials (Butler et al. 2015, Gonzalez et al. 2008, Landsiedel et al. 2009, Singh et al. 2009). In their review on nanoparticles genotoxicity, Landsiedel et al (2009) stressed the usefulness of the comet assay to assess genotoxicity of several nanoparticles (e.g. TiO_2NP, AuNP, SiNP, CoCr, Carbon nanotube, Ni and Co nanopowder). More recently, other studies used the comet assay to demonstrate AgNPs genotoxicity on human peripheral blood mononuclear cells (Orta-García et al 2015), untransformed fibroblasts (AgNPs were more toxic that CeO2 or TiO2) (Franchi et al 2015), hepatoma and leukemia cells and dermal and pulmonary fibroblasts (Ávalos et al 2015), and human microvascular endothelial cells (Castiglioni et al 2015). Also, AgNPs induced DNA damage (due to oxidative stress) in human epithelial embryonic cells, but the authors reported that it was a transient effect, likely due to DNA repair (Rinna et al 2005). Additionally, a Comet chip technology was used to address multiple NP genotoxicity in both suspension human lymphoblastoid (TK6) and adherent Chinese hamster ovary (H9T3) cell lines (Watson et al 2014). Micronuclei (MNi) are induced by several genotoxic carcinogens and are indicative of numerical and/or structural chromosomal aberrations (Landsiedal et al 2009). Using the CBMN technique, TiO_2NPs were shown to cause an increase in micronucleated binuclear cells in WIL2-NS human B-cell lymphoblastoids (Wang et al 2007). Also, Gurr et al (2005) showed that TiO2 anatase particles induced oxidation and micronuclei formation in human bronchial epithelial cells. More recently, Li and co-workers (2013) found dose-dependent increases of micronucleation in primary Syrian hamster embryo (SHE) cells after exposure to AgNPs, suggesting AgNPs-induced genotoxicity. Also, low doses of polyethylenimine-coated AgNPs induced a chromosomal aberration effect and an increase of MNi in HepG2 cells (Kawata et al. 2009). Jiang et al (2013) reported an induction of MNi in Chinese hamster ovary cells (CHO-K1) after exposure to BSA-AgNPs. AgNP-induced micronuclei formation has also been shown inhuman lung fibroblast cells (IMR-90), human glioblastoma cells (U251) (AshaRani et al 2009), and HeLa cells (Xu et al 2012), the latter being affected via the JAK-STAT signal transduction pathway. For HaCat cells, the only data available has been reported by Zanette et al (2011), who found long-lasting inhibition of cell growth after exposure to PVP-coated AgNPs, confirming an antiproliferative effect of this type of AgNPs. However, no information is available regarding citrate-coated AgNPs, one of the most widely used types of AgNPs. In this work, we have used methods providing multiparametric information, namely the single-cell gel electrophoresis (comet) assay and the cytokinesis blocked micronucleus (CBMNs) assay, to determine the genotoxicity potential of citrate- AgNPs on a human keratinocyte cell line (HaCaT).

Material and methods

Chemicals

Sterile, purified and endotoxin-free silver nanoparticles (Biopure AgNPs 1.0 mg/mL), with a diameter of 30 nm and a citrate surface, were purchased from Nanocomposix Europe (Prague, Czech Republic). This AgNPs have a hydrodynamic diameter (Z-average size) of 43.3 ± 0.5 in water and 64.8 ± 0.4 in cell culture medium. Their polydispersity index (PdI) is 0.25-0.26 and their zeta potential (ζ) -42.7 ± 2.7. Dulbecco's modified Eagle's medium (DMEM), fetal bovine serum (FBS), antibiotics and phosphate buffer saline (PBS, pH 7.4) were purchased from Life Technologies (Carlsbad, CA, USA). 3-(4,5-dimethylthiazol-2-yl)-2,5-diphenyltetrazolium bromide (MTT) and dimethyl sulfoxide (DMSO) were obtained from Sigma-Aldrich (St. Louis, MO, USA). H_2O_2 were purchased from Sigma-Aldrich, St. Louis, MO. Cytochalasin B was from AppliChem, Darmstadt, Germany.

Cell Culture

The HaCaT cell line, a non-tumorigenic immortalized human keratinocyte cell line (Boukamp et al. 1988), was obtained from Cell Lines Services (Eppelheim, Germany). Cells were grown in complete medium, i.e., Dulbecco's modified Eagle's medium, supplemented with 10% fetal bovine serum (FBS), 2 mM L-glutamine, 100 U/mL penicillin, 100 µg/mL streptomycin and 250 µg/mL fungizone at 37°C in 5% CO_2 humidified atmosphere. Cells were daily observed under an inverted phase-contrast Eclipse TS100 microscope (Nikon, Tokyo, Japan). For each experiment, cells were allowed to adhere for 24h and then medium was replaced with fresh medium containing citrate-coated AgNPs. The effects were measured after 24 and 48h. Throughout the experiments, cultures were routinely visualized for confluence and cell morphology.

Viability assay

Cell viability was determined by the colorimetric 3-(4,5- dimethyl-2-thiazolyl)-2,5-diphenyl tetrazolium bromide (MTT) assay (Twentyman &Luscombe 1987). Cells were seeded in 96-well plates and cultured as described above. Cells were exposed to citrate-coated AgNPs at 0, 10 and 40 µg/mL (corresponding to IC20 and IC50, respectively). Cell viability was measured after 24 and 48h. Briefly, 50 µL of MTT (1 mg/mL) in phosphate buffered saline (PBS) were added to each well and incubated for 4h at 37°C, 5% CO_2. Medium was then removed and 150 µL of DMSO were added for solubilization of formazan crystals. The optical density of reduced MTT was measured at 570 nm in a microtiter plate reader (Synergy HT Multi-Mode, BioTeK, Winooski, VT). Three independent assays were performed with at least 2 technical replicates

each. The concentrations used of AgNPs in this study were higher than the Ag^+ concentration released from citrate-coated AgNPs at time 0h: 3.77% in 10µg/mL AgNPs (Fig. 2.2; Chapter 2), corresponding to 0.377 µg/mL of Ag^+, an Ag^+ dose which did not cause significant cytotoxicity, as assessed by MTT (Fig. 2.4; Chapter 2).

Comet assay

The Comet assay was performed according to Singh et al (1998) and Tice et al (2000). Briefly, cells were seeded in 6-well plates and, after exposure, they were washed, detached, centrifuged for 300g during 4 min and the pellets ressuspended in PBS. For a positive control, cells were ressuspended in 100 µM H_2O_2 for 5 min, centrifuged at 300 g for 5 min and ressuspended in PBS. 50 µL of cell suspension and 50 µL of low melting point agarose were added to slides previously prepared with normal melting point agarose. A coverslip was immediately added and the slides were placed at 4ºC for 10 min. After agarose solidification, the coverslip was removed and the slides were immersed in a lysis solution (2.5 M NaCl, 100 mM Na_2EDTA, 10 mM Tris-base, 10 M NaOH, 2% Triton X-100) cooled at 4◦C for at least 1h. Slides were then placed in cold electrophoretic buffer (200 mM Na_2EDTA, 10 mM NaOH, pH 13), in darkness for 20 min, and electrophoresis was performed for 30min at 0.8V/cm, 300mA. The slides were washed two times during 10 min in cold PBS, pH 7.4 (as a neutralizing buffer) and dried at room temperature, in darkness. For comet scoring, slides were rehydrated with dH_2O for 30 min, stained with ethidium bromide (20 µg/mL) using a Pasteur pipette (flooding the slide) for 20 min and water excess was removed with dH_2O during 20 min. The slides dried overnight at room temperature and at the moment of visualization they were rehydrated with one drop of dH_2O, covered with a coverslip. Slides were observed under the fluorescence microscope Eclipse 80i (Nikon, Tokyo, Japan). For each treatment, 2 gels from each sample were analyzed by visual scoring of 100 comets per duplicate gel, quantified by visual classification of nucleoids into five comet classes (Fig. 4.1), according to the tail intensity and length, from 0 (no tail) to 4 (almost all DNA in tail). The total score was calculated on a scale of 0-400 arbitrary units according to Collins (2004) by multiplying the percentage of nucleoids in each class by the corresponding factor, according to this formula: GDI (genetic damage indicator) = [(%nucleoids class 0)x0] + [(%nucleoids class 1)x1] + [(%nucleoids class 2)x2] + [(%nucleoids class 3)x3] + [(%nucleoids class 4)x4].

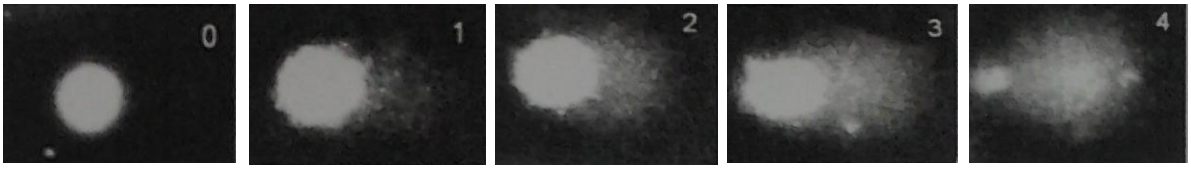

Figure 4.1: Examples of the five comet classes for the nucleoids visual scoring quantification.

Cytokinesis-block micronucleus (CBMN) assay

The cytokinesis-block micronucleus assay (CBMN) was performed according to Fenech (2007). Briefly, cells were seeded on coverslips inside 6-well plates incubated for 24h and, after exposure, cytochalasin B at 3.5µg/ml was added to each well and incubated during 29 h, in order to block cytokinesis. Cells were then fixed with absolute methanol cooled at 4ºC during 15 min and removed from the 6-well plates. Samples were stained with acridine orange (Merck, Darmstadt, Germany), and mounted in slides. These samples were scored for nuclear division index (NDI), micronuclei (MNi), nucleoplasmic bridges (NPBs) and nuclear buds (NBUDs) (Fig. 4.2). NDI was calculated by scoring at least 500 cells for the presence of 1, 2, 3, or 4 nuclei, through the formula: NDI = (M1 + 2 x M2 + 3 x M3 + 4 x M4)/N, where M1–M4 is the number of cells with 1–4 nuclei, and N is the total number of cells scored. The NDI and the proportion of binucleated cells provide the information about mitogenic response and cytostatic effects of AgNPs. MNi, NPBs and NBUDs were scored in 1000 binucleated cells per replicate (2 replicates per concentration) and MNi was examined for the presence of 1, 2, or more MNi.

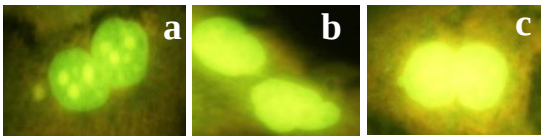

Figure 4.2: Examples of a) micronuclei (MNi), b) nucleoplasmic bridges (NPBs) and c) nuclear buds (NBUDs).

Statistical analysis

The results are reported as mean ± standard deviation (SD) of 2 technical replicates in each of the 3 independent experiments. For the MTT assay, the statistical significance between control and exposed cells was assessed by one-way ANOVA, followed by Dunnet or Dunn's method (parametric and non-parametric tests, respectively), using Sigma Plot 12.5 software (Systat Software Inc.). For the other assays, results were compared using two-way ANOVA, followed by Holm-Sidak test using also Sigma Plot 12.5 software (Systat Software Inc.). The differences were considered statistically significant for $p < 0.05$.

Results

Cell Viability

The viability of HaCaT cells was negatively affected by citrate- AgNPs (Fig. 4.3). Relatively to controls, the viability of exposed cells was significantly reduced ($p < 0.01$) upon exposure to AgNPs at both times, 24 and 48h, and both concentrations, 10 and 40 µg/mL. The effect was more severe in cells exposed to 40 µg/mL of AgNPs with a viability reduction of ~50%.

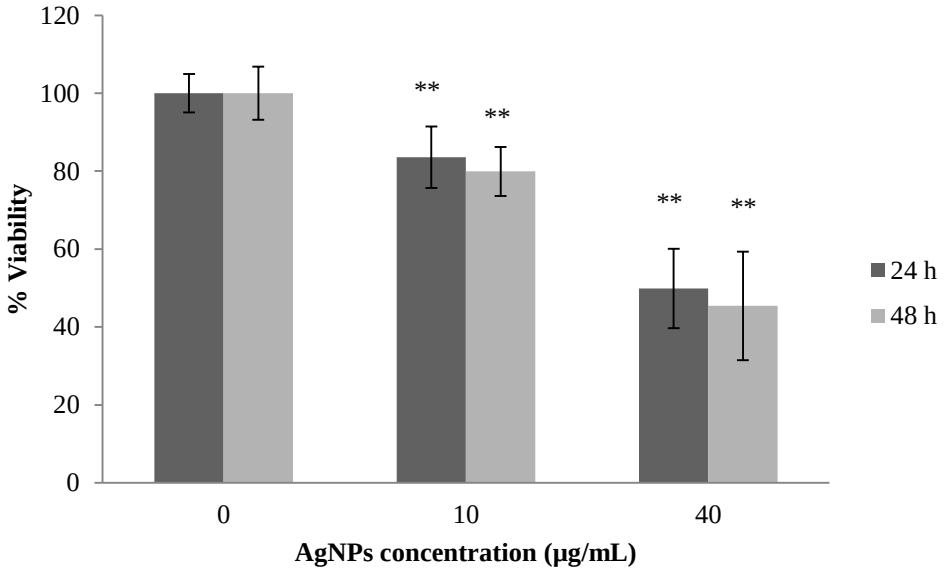

Figure 4.3: Relative cell viability (%) of HaCaT after exposure to 10 and 40 µg/mL AgNPs, measured by MTT assay, for 24h and 48h. Data expressed as mean and standard deviation. ** indicate significant differences between control at $p < 0.01$.

Comet assay

Negative control cells showed a predominance of cells in class 0 (~40% after 24h and ~25% after 48h) and class 1 (~55% after 24h and ~70% after 48h), and in both periods less 5% of cells showed nucleoids at class 2 or higher.

In AgNP-exposed cells, the genetic damage indicator (GDI) significantly increased ($p < 0.05$) for both times and concentrations, the effects being more pronounced after 48h (Fig. 4.4). Regarding individual DNA damage level (Fig. 4.5), the amount of nucleoids at class 0 significantly decreased after exposure to AgNPs for both times ($p < 0.01$). There was no difference between the amounts of cells at class 1 after both exposure times, however the amount of cells at class 2 significantly increased for both concentrations after 48h. Concerning the amount of cells at classes 3 and 4, which have a greater increase in DNA in tail, there was a significant increase for the higher concentration, 40 µg/mL, at both exposure times.

Comparatively to the 24h exposure, the 48h exposure of AgNPs induced a significant decrease of cells at class 0 and a significant increase of cells at class 3. For the higher concentration, 40 µg/mL, the amount of cells at class 1 and 2 was significantly increased after 48h compared to 24h exposure

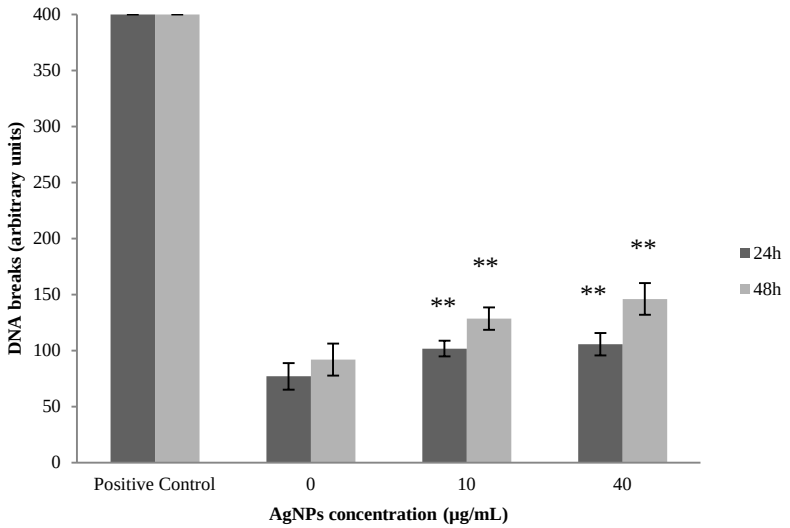

Figure 4.4: Mean values of genetic damage indicator (GDI) measured by the standard (alkaline) comet assay of HaCaT cells after exposure to 10 and 40µg/mL citrate- AgNPs 30 nm during 24h and 48h. The results were expressed as the mean +/- SD versus control. ** indicate significant differences between control at $p < 0.01$.

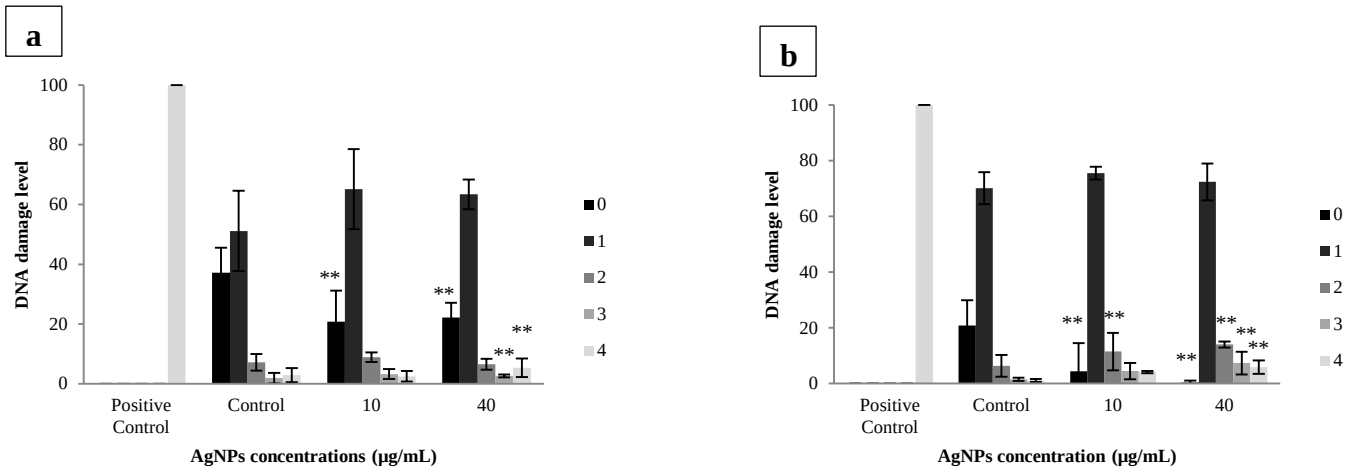

Figure 4.5: Individual DNA damage classes of HaCaT after exposure to 10 and 40µg/mL of citrate-AgNPs 30 nm during a) 24h and b) 48h. The results were expressed as the mean +/- SD versus control. ** indicate significant differences between control at $p < 0.01$.

Cytokinesis-block micronucleus (CBMN) assay

Negative control cells showed typical binucleated cells, indicative of normal cell division, occurrence of MNi (was only found one per binucleated cell) around or below 10% and NPBs or NBUDs lower than 5%. Also, a slight increase was found after 48h in MNi, but the amount of NPBs and NBUDs remained residual. The amount of HaCaT cells with MNi significantly

increased after AgNPs exposure for both times and concentrations ($p < 0.01$), and this increase was generally more pronounced after 48h (Fig. 4.6). The amount of NBUDs also had a tendency to increase after AgNPs exposure at both times and concentrations, although not reaching statistical significance.

Moreover, a significant increase of mononucleated cells (M1) and a significant decrease of binucleated (M2) cells after AgNPs exposure was found for both times and concentrations (Fig. 4.7). These results indicate a cytostatic effect induced by AgNPs exposure. The nuclear division index (NDI) significantly decreased for both exposure times and concentrations of AgNPs, which confirms the cytostatic effect of AgNPs on HaCaT cells (Fig. 4.8).

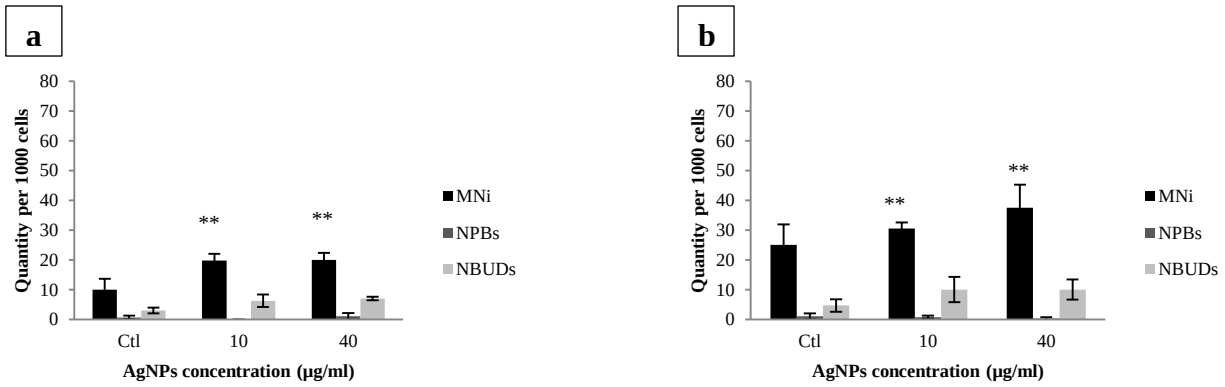

Figure 4.6: MNi, NPBs and NBUDs score of HaCaT after exporure to 10 and 40µg/mL of citrate- AgNPs 30 nm during a) 24h and b) 48h. The results were expressed as the mean +/- SD versus control. ** indicate significant differences between control at $p < 0.01$.

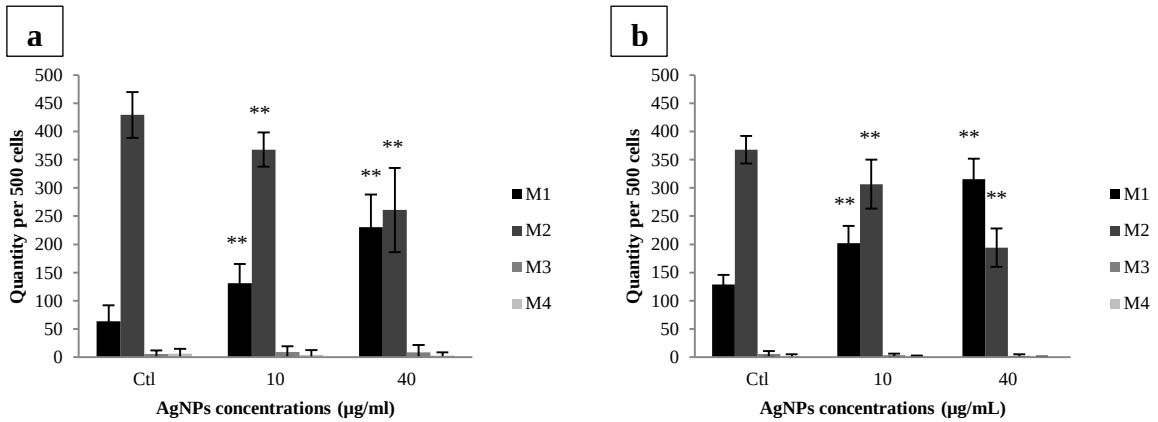

Figure 4.7: Quantity per 500 cells of M1(mononucleated cells), M2 (Binucleated cells), M3 (Trinucleated cells) and M4 (Tetranucleated cells) of HaCaT after exporure to 10 and 40µg/mL of AgNPs during a) 24h and b) 48h. The results were expressed as the mean +/- SD versus control. ** indicate significant differences between control at $p < 0.01$.

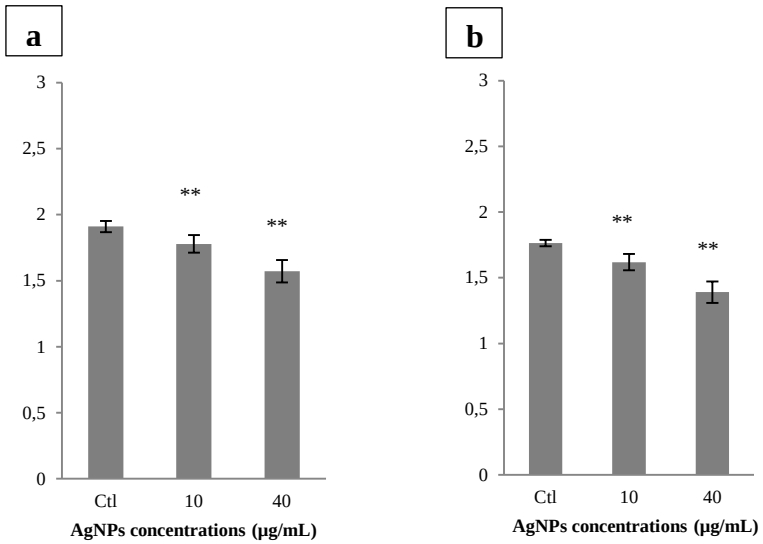

Figure 4.8: Nuclear divisin index (NDI) of HaCaT cells after exporure to 10 and 40µg/mL AgNPs during a) 24h and b) 48h. The results were expressed as the mean +/- SD versus control. ** indicate significant differences between control at $p < 0.01$.

Discussion

In this work, we have investigated the cytotoxic and genotoxic potential of citrate-coated AgNPs in human keratinocytes, motivated by the wide usage of these nanoparticles in several applications, namely in cosmetic products (Tolaymat et al. 2010), and the need to improve current understanding of their biological effects towards human skin.

The MTT viability results showed that the keratinocytes viability decreased even at the lowest concentration of AgNPs. This decrease is in line with the described loss of viability induced by this type of NPs in other cell lines. For example, a significant decrease in the viability of lung epithelial BEAS-2B cells was observed upon exposure to 20 nm citrate-coated AgNPs at 6.25-50 µg/mL after 24h (Wang et al. 2014). Also, Milić et al. (2015) found a significant viability decrease of mammalian kidney cells after exposure to citrate-coated AgNPs at concentrations above 25 µg/mL.

We further demonstrated, for the first time to our knowledge, that these citrate-coated AgNPs induced DNA damage in keratinocyte cells, even for the lower concentration and as soon as 24h. These genotoxic effects were evident by a significant increase of classes 3 and 4 (which are the classes with the greater amount of DNA in the tail) in exposed cells, at expenses of decreased class 0. This effect was higher for higher doses and longer periods (48h). These results are in line with other genotoxic information provided for these cell lines exposed to SiO2 nanoparticles (15, 30, and 100 nm at doses <10 µg/mL) (Gong et al. 2012), which support the sensitivity of these keratinocytes as *in vitro* models for this type of NP assays. In addition, AgNPs were reported to induce DNA breakage in other cell lines using the comet assay

(AshaRani et al. 2009, Eom &Choi 2010, Hackenberg et al. 2011, Kawata et al. 2009, Liu et al. 2011, Piao et al. 2011).

The interference of AgNPs with signaling cascades in keratinocytes is a current matter of debate, especially given the relevance of skin as an entry portal for AgNPs. Comfort et al (2014) demonstrated that 50 nm AgNPs affected the epidermal growth factor (EGF) signal transduction in HaCaT cell line (initially obstructed due to the dissolution of particles into silver ions). It was demonstrated that human keratinocytes undergo apoptosis when incubated with the blocking EGFR agents (Stoll et al. 1998), and that this receptor provides protection to normal human keratinocytes against apoptosis. It's over activation has also been reported as involved in modulating DNA repair after radiation-induced damage (Liccardi et al. 2011). Kuroda et al (2014) also demonstrated that epidermal growth factor receptor (EGFR)-targeted hybrid plasmatic magnetic nanoparticles (225-NP) – with a gold layer-, induced DNA damage and abrogates G2/M phase of the cell cycle, leading to cellular apoptosis in a EGFR-mutant HCC827 cell line. It has been proposed that some metal NP may drastically affect the redox regulation of protein tyrosine phosphatases (involved in transduction pathways of cell cycle regulation and differentiation) via the inhibition of MAPK and EGFR. Here, we hypothesise that pathways mediated by these phosphatases may be at least partially involved in the increased DNA damage observed in the AgNPs exposed HaCaT cells. It was demonstrated elsewhere that the highly reactive cysteine residues of protein tyrosine phosphatases are predisposed to oxidative stress in the form of H_2O_2, free radicals or changes in intracellular thiol/dissulfide redox state (Manke et al. 2013). Indeed, we have recently demonstrated by Nuclear Magnetic Resonance (NMR) metabolomics that AgNPs-exposed HaCaT cells displayed upregulated glutathione-based antioxidant protection, increased glutaminolysis, downregulated tricarboxylic acid (TCA) cycle activity, energy depletion and cell membrane modification (Carrola et al. 2016). The upregulation of the antioxidant battery was also supported by increased oxidative stress through ROS production (Chapter 2), pointing to their involvement on redox regulation of protein tyrosine phosphatases, which could be related to the DNA damage observed in the HaCaT exposed to AgNPs.

Concerning the micronucleus assay, there was a significant increase of cells with MNi, a biomarker of chromosome breakage and/or whole chromosome loss (Fenech 2007). We could also observe a significant increase of mononucleated cells and a significant decrease of binucleated cells, meaning that citrate-coated AgNPs had a cytostatic effect. This result was confirmed by the decrease of the nuclear division observed in the cells exposed to both AgNPs concentrations, for 24 and 48h. Using other type of AgNPs (Ag–ginger and Ag–coffee NPs), Chunyan and Valiyaveettil (2013) showed an arrest at G2/M in HepG2 cells, rather than induction of apoptosis or necrosis. In agreement with those authors, we suggest that these delays

and cell proliferation decreases act as a mechanism to allow cells to repair DNA damage prior the chromosomes segregation. Despite the observed MNi increase and nuclear division index (NDI) decrease, changes in nucleoplasmatic bridges (NPBs) were not apparent from the results hereby presented. According to Fenech (2007), NPB may be used as a biomarker of DNA misrepair and/or telomere end-fusions. On other hand, we found a non-significant trend for nuclear buds (NBUDs) to increase with AgNP exposure. This putative increase deserves further attention as NBUDs are used to evaluate the elimination of amplified DNA and/or DNA repair complexes. Finally, it is evident by this assay that the tested doses induced cytostatic effects in HaCaT cells, which were measured via the proportion of mono-, bi- and multinucleated cells and by cytotoxicity via necrotic and/or apoptotic cell ratios, confirmed elsewhere to be mainly due to an arrest at G2/M transition (Chapter 2).

Conclusions

In sum, our study demonstrates that the largely used citrate-coated AgNPs decreased cellular viability and induced DNA damage in HaCaT cells. Furthermore, these particles induced MNi formation, increased mononucleated cells and decreased binucleated cells and the nuclear division index, thus pointing to clear cytostatic effects. Thus, we conclude that 30 nm citrate-coated AgNPs have marked genotoxicity on HaCaT cells, even at a low dose (~IC20) and after a short period of exposure (24h). Overall, we demonstrate the validity of performing pre-clinical tests using HaCat cells as a model for skin toxicity evaluation, and we show that both Comet and CBMN assays are sensitive means for assessing genotoxicity. Considering that AgNPs are present in a vast number of consumer products and also in nanomedicine skin applications, this study highlights the need to investigate possible ways to reduce the genotoxic potential of AgNPs.

Acknowledgments

This work was developed in the scope of the projects CICECO-Aveiro Institute of Materials (Ref. FCT UID/CTM/50011/2013) and CESAM (Ref. FCT UID/AMB/50017/2013), financed by national funds through the FCT/MEC and when applicable co-financed by the European Regional Development Fund (FEDER) under the PT2020 Partnership Agreement. Funding to the project FCOMP-01-0124-FEDER-021456 (Ref. FCT PTDC/SAU-TOX/120953/2010) by FEDER through COMPETE and by national funds through FCT, and the FCT-awarded grants (SFRH/BD/81792/2011; SFRH/BPD/48853/2008) are acknowledged. I.F.D and A.L.D.S. acknowledge FCT/MCTES for the research contracts under the Program ‘Investigador FCT’ 2014.

Contributions

V.B. participated in the design experiment with the supervisors and did all laboratorial experiments and statistical data analyses. Also had a key role in the data analyses integration, and together with the supervisors wrote and revised the manuscripts. C.S. and H.O. planned the experimental design, contributed to data analyses and integration of all data, and in the manuscript preparation. I.F.D. coordinated NPs analyses and revised the manuscript.

References

Abdelhalim MAK, Jarrar BM (2011) Renal tissue alterations were size-dependent with smaller ones induced more effects and related with time exposure of gold nanoparticles. Lipids Health Dis 10(1), 1

Ahamed M, Alsalhi M, Siddiqui M (2010) Silver nanoparticle applications and human health. Clin Chim Acta 411(23), 1841-1848

AshaRani PV, Low Kah Mun G, Hande MP, Valiyaveettil S (2009) Cytotoxicity and genotoxicity of silver nanoparticles in human cells. ACS nano 3(2), 279-290

Ávalos A, Haza AI, Morales P (2015) Manufactured silver nanoparticles of different sizes induced DNA strand breaks and oxidative DNA damage in hepatoma and leukaemia cells and in dermal and pulmonary fibroblasts. Folia Biol (Praha), 61, 33-42.

Banasik A, Lankoff A, Piskulak A, Adamowska K, Lisowska H, Wojcik A (2005) Aluminum-induced micronuclei and apoptosis in human peripheral-blood lymphocytes treated during different phases of the cell cycle. Environmental toxicology 20(4), 402-406

Behra R, Sigg L, Clift M, Herzog F, Minghetti M, Johnston B, Petri-Fink A, Rothen-Rutishauser B (2013) Bioavailability of silver nanoparticles and ions: from a chemical and biochemical perspective. J R Soc Interface 10(87), 20130396

Benn T, Westerhoff P (2008) Nanoparticle silver released into water from commercially available sock fabrics. Environ Sci Technol 42(11), 4133-4139. Boukamp P, Petrussevska R, Breitkreutz D, Hornung J, Markham A, Fusenig N (1988) Normal keratinization in a spontaneously immortalized aneuploid human keratinocyte cell line. J Cell Biol 106(3), 761-771

Browning L, Lee K, Nallathamby P, Xu X-HN (2013) Silver nanoparticles incite size- and dose-dependent developmental phenotypes and nanotoxicity in zebrafish embryos. Chem Res Toxicol, 26(10), 1503-1513

Butler KS, Peeler DJ, Casey BJ, Dair BJ, Elespuru RK (2015) Silver nanoparticles: correlating nanoparticle size and cellular uptake with genotoxicity. Mutagenesis 30(4), 577-591

Carrola J, Bastos V, Ferreira de Oliveira JMM, Oliveira H, Santos C, Gil AM, Duarte IF (2016) Insights into the impact of silver nanoparticles on human keratinocytes metabolism through NMR metabolomics. Arch Biochem Biophys 589, 53-61

Casals E, Pfaller T, Duschl A, Oostingh GJ, Puntes V (2010) Time evolution of the nanoparticle protein corona. ACS Nano 4(7), 3623-3632

Castiglioni S, Caspani C, Cazzaniga A, Maier JA (2014) Short-and long-term effects of silver nanoparticles on human microvascular endothelial cells. World J Biol Chem 5(4), 457.

Chen X, Schluesener H (2008) Nanosilver: a nanoproduct in medical application. Toxicol Lett 176, 1-12

Chunyan W, Valiyaveettil S (2013) Correlation of biocapping agents with cytotoxic effects of silver nanoparticles on human tumor cells. RSC Advances, 3(34), 14329-14338.

Collins AR (2004) The comet assay for DNA damage and repair: principles, applications, and limitations. Mol Biotechnol 26(3), 249-261

Comfort KK, Maurer EI, Hussain SM (2014) Slow release of ions from internalized silver

nanoparticles modifies the epidermal growth factor signaling response. Colloids Surf B Biointerfaces 123, 136-142
Dusinska M, Magdolenova Z, Fjellsbø LM (2013) Toxicological aspects for nanomaterial in humans. Methods Mol Biol 948, 1-12
Eckhardt S, Brunetto P, Gagnon J, Priebe M, Giese B, Fromm K (2013) Nanobio silver: its interactions with peptides and bacteria, and its uses in medicine. Chem Rev 113(7), 4708-4754
El Badawy AM, Scheckel KG, Suidan M, Tolaymat T (2012) The impact of stabilization mechanism on the aggregation kinetics of silver nanoparticles. Sci Total Environ 429, 325-331
Eom H-JJ, Choi J (2010) p38 MAPK activation, DNA damage, cell cycle arrest and apoptosis as mechanisms of toxicity of silver nanoparticles in Jurkat T cells. Environ Sci Technol 44(21), 8337-8342
Fenech M (2007) Cytokinesis-block micronucleus cytome assay. Nat Protoc 2(5), 1084-1104
Franchi LP, Manshian BB, de Souza TA, Soenen SJ, Matsubara EY, Rosolen JM, Takahashi CS (2015) Cyto-and genotoxic effects of metallic nanoparticles in untransformed human fibroblast. Toxicol In Vitro 29(7), 1319-1331.
Gong C, Tao G, Yang L, Liu J, He H, Zhuang Z (2012) The role of reactive oxygen species in silicon dioxide nanoparticle-induced cytotoxicity and DNA damage in HaCaT cells. Mol Biol Rep, 39(4), 4915-4925
Gonzalez L, Lison D, Kirsch-Volders M (2008) Genotoxicity of engineered nanomaterials: A critical review. Nanotoxicology 2(4), 252-273
Gurr JR, Wang AS, Chen CH, Jan KY (2005) Ultrafine titanium dioxide particles in the absence of photoactivation can induce oxidative damage to human bronchial epithelial cells. Toxicology 213(1), 66-73.
Hackenberg S, Scherzed A, Kessler M, Hummel S, Technau A, Froelich K, Ginzkey C, Koehler C, Hagen R, Kleinsasser N (2011) Silver nanoparticles: evaluation of DNA damage, toxicity and functional impairment in human mesenchymal stem cells. Toxicol Lett 201(1), 27-33
Hillegass JM, Shukla A, Lathrop SA, MacPherson MB, Fukagawa NK, Mossman BT (2010) Assessing nanotoxicity in cells in vitro. Wiley Interdiscip Rev Nanomed Nanobiotechnol 2(3), 219-231
Jiang X, Foldbjerg R, Miclaus T, Wang L, Singh R, Hayashi Y, Sutherland D, Chen C, Autrup H, Beer C (2013) Multi-platform genotoxicity analysis of silver nanoparticles in the model cell line CHO-K1. Toxicol Lett 222(1), 55-63
Karlsson HL (2010) The comet assay in nanotoxicology research. Anal Bioanal Chem 398(2), 651-666
Kawata K, Osawa M, Okabe S (2009) In vitro toxicity of silver nanoparticles at noncytotoxic doses to HepG2 human hepatoma cells. Environ Sci Technol 43(15), 6046-6051
Knaapen AM, Borm PJA, Albrecht C (2004a) Inhaled particles and lung cancer. Part A: Mechanisms. International Journal of Cancer, 109(6), 799-809
Knaapen AM, Borm PJA, Albrecht C, Schins RPF (2004b): Inhaled particles and lung cancer. Part A: Mechanisms. Int J Cancer 109(6), 799-809
Kuroda S, Tam J, Roth JA, Sokolov K, Ramesh R (2014) EGFR-targeted plasmonic magnetic nanoparticles suppress lung tumor growth by abrogating G2/M cell-cycle arrest and inducing DNA damage. Int J Nanomed 9, 3825-3839
Landsiedel R, Kapp MD, Schulz M, Wiench K (2009) Genotoxicity investigations on nanomaterials: methods, preparation and characterization of test material, potential artifacts and limitations many questions, some answers. Mutat Res, 681(2), 241-258.
Li X, Lenhart JJ, Walker HW (2012) Aggregation kinetics and dissolution of coated silver nanoparticles. Langmuir 28(2), 1095-1104
Li X, Xu L, Shao A, Wu G, Hanagata N (2013) Cytotoxic and genotoxic effects of silver nanoparticles on primary Syrian hamster embryo (SHE) cells. J Nanosci Nanotechnol

13(1), 161-170
Li Y, Zhang Y, Yan B (2014) Nanotoxicity overview: nano-threat to susceptible populations. Int J Mol Sci 15(3), 3671-3697
Liccardi G, Hartley JA, Hochhauser D (2011) EGFR nuclear translocation modulates DNA repair following cisplatin and ionizing radiation treatment. Cancer Res 71(3), 1103-1114
Liu P, Guan R, Ye X, Jiang J, Liu M (2011) Toxicity of nano-and micro-sized silver particles in human hepatocyte cell line L02. In Journal of Physics: Conference Series (Vol. 304, No. 1, p. 012036). IOP Publishing
Maiorano G, Sabella S, Sorce B, Brunetti V, Malvindi MA, Cingolani R, Pompa PP (2010) Effects of cell culture media on the dynamic formation of protein-nanoparticle complexes and influence on the cellular response. ACS Nano 4(12), 7481-7491
Manke A, Wang L, Rojanasakul Y (2013) Mechanisms of nanoparticle-induced oxidative stress and toxicity. Biomed Res Int 942916
Milić M, Leitinger G, Pavičić I, Zebić Avdičević M, Dobrović S, Goessler W, Vinković Vrček I (2015) Cellular uptake and toxicity effects of silver nanoparticles in mammalian kidney cells. J Appl Toxicol 35(6), 581-592
Nowack B, Bucheli T (2007) Occurrence, behavior and effects of nanoparticles in the environment. Environ Pollut 150(1), 5-22.
Nowack B, Krug H, Height M (2011) 120 years of nanosilver history: implications for policy makers. Environ Sci Technol 45(4), 1177-1183
Orta- García ST, Plascencia- Villa G, Ochoa- Martínez AC, Ruiz- Vera T, Pérez- Vázquez FJ, Velázquez- Salazar JJ, Yacamán MJ, Navarro-Contreras HR, Pérez-Maldonado IN (2015) Analysis of cytotoxic effects of silver nanoclusters on human peripheral blood mononuclear cells 'in vitro'. J Appl Toxicol 35(10), 1189-1199
Piao MJ, Kang KA, Lee IK, Kim HS, Kim S, Choi JY, Choi J, Hyun JW (2011) Silver nanoparticles induce oxidative cell damage in human liver cells through inhibition of reduced glutathione and induction of mitochondria-involved apoptosis. Toxicol Lett 201(1), 92-100
Promtong P (2015) Determinants of Silver Nanoparticle Toxicity. Dissertation, University of Manchester
Pumera M (2011) Nanotoxicology: the molecular science point of view. Chem Asian J, 6(2), 340-348.
Rinna A, Magdolenova Z, Hudecova A, Kruszewski M, Refsnes M, Dusinska M (2015) Effect of silver nanoparticles on mitogen-activated protein kinases activation: role of reactive oxygen species and implication in DNA damage. Mutagenesis 30(1), 59-66.
Robert IM (2010) Colloidal stability of silver nanoparticles in biologically relevant conditions. J Nanopart Res, 13(7), 2893-2908
Singh N, Manshian B, Jenkins GJS, Griffiths SM (2009) NanoGenotoxicology: the DNA damaging potential of engineered nanomaterials. Biomaterials, 30(23), 3891-3914.
Smita S, Gupta S, Bartonova A, Dusinska M, Gutleb A, Rahman Q (2012) Nanoparticles in the environment: assessment using the causal diagram approach. Environ Health, 11(Suppl 1), S13
Souza TA, Franchi LP, Rosa LR, da Veiga MAA, Takahashi CS (2016) Cytotoxicity and genotoxicity of silver nanoparticles of different sizes in CHO-K1 and CHO-XRS5 cell lines. Mutat Res Genet Toxicol Environ Mutagen 795, 70-83
Stoll SW, Benedict M, Mitra R, Hiniker A, Elder JT, Nuñez G (1998) EGF receptor signaling inhibits keratinocyte apoptosis: evidence for mediation by Bcl-XL. Oncogene 16(11), 1493-1499
Terry LJ, Shows EB, Wente SR (2007) Crossing the nuclear envelope: hierarchical regulation of nucleocytoplasmic transport. Science 318(5855), 1412-1416
Tolaymat TM, El Badawy AM, Genaidy A, Scheckel KG, Luxton TP, Suidan M (2010) An evidence-based environmental perspective of manufactured silver nanoparticle in

syntheses and applications: a systematic review and critical appraisal of peer-reviewed scientific papers. Sci Total Environ 408(5), 999-1006

Twentyman P, Luscombe M (1987) A study of some variables in a tetrazolium dye (MTT) based assay for cell growth and chemosensitivity. Br J Cancer 56(3), 279-285

Vrček IV, Zuntar I, Petlevski R, Pavičić I, Dutour Sikirić M, Curlin M, Goessler W (2014) Comparison of in vitro toxicity of silver ions and silver nanoparticles on human hepatoma cells. Environmental toxicology

Wang X, Ji Z, Chang CH, Zhang H, Wang M, Liao Y-PP, Lin S, Meng H, Li R, Sun B, Winkle LV, Pinkerton KE, Zink JI, Xia T, Nel AE (2014) Use of coated silver nanoparticles to understand the relationship of particle dissolution and bioavailability to cell and lung toxicological potential. Small 10(2), 385-398

Wang JJ, Sanderson BJ, Wang H (2007) Cyto-and genotoxicity of ultrafine TiO 2 particles in cultured human lymphoblastoid cells. Mutat Res 628(2), 99-106

Watson C, Ge J, Cohen J, Pyrgiotakis G, Engelward BP, Demokritou P (2014) High-throughput screening platform for engineered nanoparticle-mediated genotoxicity using CometChip technology. ACS nano 8(3), 2118-2133

Xu L, Li X, Takemura T, Hanagata N, Wu G, Chou LL (2012) Genotoxicity and molecular response of silver nanoparticle (NP)-based hydrogel. J Nanobiotechnology 10(16), 1-11

Zanette C, Pelin M, Crosera M, Adami G, Bovenzi M, Larese FF, Florio C (2011) Silver nanoparticles exert a long-lasting antiproliferative effect on human keratinocyte HaCaT cell line. Toxicol In Vitro 25(5), 1053-1060

Zhang T, Wang L, Chen Q, Chen C (2014) Cytotoxic potential of silver nanoparticles. Yonsei Med J 55(2), 283-291

Chapter 5

Coating independent cytotoxicity of citrate- and PEG-coated silver nanoparticles on a human hepatoma cell line

Part of this chapter was submitted as:

Bastos V., Ferreira de Oliveira J. M. P., Duarte I.F., Santos C. and Oliveira H. (2016) Coating independent cytotoxicity of citrate- and PEG-coated silver nanoparticles on a human hepatoma cell line. Journal of Environmental Sciences. *Accepted*

Coating independent cytotoxicity of Citrate- and PEG-coated silver nanoparticles on a human hepatoma cell line

Bastos V.[1], Ferreira de Oliveira J. M. P.[1], Duarte I.F.[2], Santos C.[1,3*] and Oliveira H.[1]

[1]*CESAM & Laboratory of Biotechnology and Cytomics, Department of Biology, University of Aveiro, 3810-193 Aveiro, Portugal*
[2]*CICECO, Department of Chemistry, University of Aveiro, Aveiro, Portugal*
[3]*Department of Biology, Faculty of Sciences, University of Porto, Rua do Campo Alegre, Porto, Portugal*

*corresponding author: csantos@fc.up.pt

Abstract

The antibacterial potential of silver nanoparticles (AgNPs) resulted in their increasing incorporation into consumer, industrial and biomedical products. Therefore, human and environmental exposure to AgNPs (either as an engineered product or a contaminant) supports the emergent research on the features conferring them different toxicity profiles. In this study, 30 nm AgNPs coated with citrate or poly(ethylene glycol) (PEG) were used to assess the influence of coating on the effects produced on a human hepatoma cell line (HepG2), namely in terms of viability, apoptosis, apoptotic related genes, cell cycle and cyclins gene expression. Both types of coated AgNPs decreased cell proliferation and viability with a similar toxicity profile. At the concentrations used (11 µg/mL and 5 µg/mL corresponding to IC50 and ~ IC10 levels, respectively) the amount of cells undergoing apoptosis was not significant and the apoptotic related genes BCL2 and BAX were both downregulated. Moreover, both AgNPs affected HepG2 cell cycle progression at the higher concentration (11 µg/mL) by increasing the % of cells in S and G2 phases. Considering the cell-cycle related genes, the expression of CCNB1 (cyclin B1) and CCNE1 (cyclin E1) was decreased. Thus, this work has shown that citrate- and PEG-coated AgNPs impact on HepG2 apoptotic gene expression, cell cycle dynamics and cyclin regulation in a similar way. More research is needed to determine the properties that confer AgNPs a lower toxicity, since their use has proved helpful in several industrial and biomedical contexts.

Keywords: Silver nanoparticles (AgNPs), Citrate, Poly(ethylene glycol) (PEG), Cytotoxicity, Apoptosis, Cell cycle, Cyclins, Gene expression, HepG2 cells, Nanotoxicology.

Introduction

AgNPs are being extensively used in a wide range of applications, from medicine and industry to the most common consumer products (Behra et al., 2013; Eckhardt et al., 2013; EPA, 2010;

Franci et al., 2015; Rai et al., 2015). Consequently, the possible risks associated with their release into the environment and human exposure has also increased. Indeed, while researchers have stressed the need to establish whether the presence of nanosilver in those products is essential (Nowack and Bucheli, 2007), and several studies showed the toxic potential of AgNPs, their usage remains widespread (Chen et al., 2015; Dusinska et al., 2013; McShan et al., 2014).

Previous studies have shown that the physico-chemical characteristics of AgNPs will influence cellular uptake, intracellular fate and, consequently, the toxicity of these NPs (Caballero-Díaz et al., 2013; Gliga et al., 2014; Wang et al., 2014b; Zhang et al., 2015; Zhang et al., 2014). In particular, the size (Gliga et al., 2014; Kim et al., 2012; Park et al., 2011) and surface chemistry (Lu et al., 2010), as well as the type of formulation (Boonkaew et al., 2014), period of exposure (Comfort et al., 2014) and storage conditions (Ahlberg et al., 2014) have all been shown to play a determinant role in AgNPs toxicity.

AgNPs are often coated to promote stability and avoid aggregation. Citrate is the most common reducing agent used to stabilize AgNPs, providing the particles a negative surface charge (Gutierrez et al., 2015; Pillai and Kamat, 2004; Sharma et al., 2009). Several other agents have also been employed to coat AgNPs, such as polyvinyl pyrrolidone (PVP) (Haberl et al., 2013; Nymark et al., 2013; Wang et al., 2014a), polyacrylates (Panacek et al., 2014), poly(vinyl)alcohol (PVA), polyacrylamide, poly(oxyethylene)-segmented imide (POEM), poly(styrene-co-maleic anhydride)-grafting poly(oxyalkylene) (SMA), poly(ethylene glycol) (PEG) (Fernández-López et al., 2009; Xu et al., 2007), and peptides (Haase et al., 2012; Nair and Laurencin, 2007). Polyethylene glycol (PEG) is another popular coating, especially concerning biomedical applications, due to its biocompatible nature and the high stability conferred to the particles (Ryan et al., 2008). Ginn and co-workers (2014) refer that in the years to come we will see an increase in the number of novel site-directed PEGylation chemistries and a shift in its application to a wider range of therapeutic molecules, including NPs for therapeutic and diagnostic purposes, becoming increasingly essential more studies with this coating. PEG coating improved the biopharmaceutical properties of drugs, increased stability and resistance to proteolytic inactivation, increased circulatory lives, and showed low toxicity (Ginn et al., 2014; Jain and Jain, 2008; Ryan et al., 2008). Moreover, it has been argued that PEG coating decreases AgNPs toxicity by reducing their cellular uptake (Brandenberger et al., 2010; Caballero-Díaz et al., 2013; Pang et al., 2015).

As liver is the most important organ for xenobiotic metabolism (Roberts et al., 2014), liver cell lines have been amply used in biomedical research involving the testing of drugs or other toxicants. The cytotoxicity of AgNPs towards liver cells has also been demonstrated in a few previous studies. Faedmaleki and collegues (2014) showed that 20-40nm AgNPs decreased HepG2 viability in a concentration-dependent manner. Also, Nowrouzi and co-workers (2010)

studied the cytotoxicity of AgNPs on HepG2 and obtained IC50 value of 2.75-3 µg/mL for HepG2 after exposure to 5-10 nm AgNPs. Moreover, by determining changes in the activity of lactate dehydrogenase, alanine aminotransferase, aspartate aminotransferase, glutathione peroxidase, superoxide dismutase, lipid peroxidation and cytochrome c content, that same work provided evidence for the involvement of oxidative alterations upon exposure to low doses of AgNPs. Recently, Xin and co-workers (2015) also found dose-dependent cytotoxicity of AgNPs in HepG2 cells, which was attributed to the interplay of oxidative stress, DNA damage and mitochondrial injury. Consistently, Xue et al. (2015), suggested the cellular toxicological mechanism of AgNPs to be related with oxidative stress induced by the generation of ROS, leading to mitochondria injury and induction of apoptosis. However, there are few studies comparing the coating influence on AgNPs cytotoxicity to liver cells. Kennedy et al (2014) studied the cytotoxicity potential of carbohydrate functionalization of ~54 nm AgNPs to HepG2 and neuronal-line Neuro 2A cells and found that particles functionalized with ethylenglycol, glucose and citrate coated nanoparticles show a similar toxicity, while galactose and mannose functionalized AgNPs were significant less toxic to HepG2 cell line. Other studies comparing the influence of coating on AgNPs cytotoxicity have been addressed to other cell lines. Gliga et al. (2014) compared the cytoxicity of uncoated, PVP- and citrate-coated AgNPs in bronchial BEAS-2B cells and found no coating-dependent differences in cytotoxicity. Caballero-Díaz et al. (2013) reported that pegylation of AgNPs reduced cellular uptake and their toxicity in NIH/3T3 (mouse embryonic fibroblasts), compared to AgNPs coated with other polymers. The conflicting existing information addressed the need to deeply study surface coating AgNPs cytotoxicity, in order to aware if or which NPs are more cytotoxic to the different cell lines.

Thus, in this study we aimed to compare the influence of coating (citrate *vs* PEG) on the cytotoxicity of AgNPs in liver cells, using the human hepatoma cell line HepG2 as an in vitro model. HepG2 cells were exposed to citrate- and PEG-coated AgNPs of 30 nm diameter and the effects on cell viability, apoptosis induction, apoptotic expression genes, cell cycle profile and cyclins gene expression were assessed.

Material and methods

Chemicals

Sterile, purified and endotoxin-free AgNPs (Biopure AgNPs 1.0 mg/mL), with 30-nm diameter and a citrate or polyethyleneglycol (PEG) surface, designated from now on as Cit30 and PEG30 NPs, were purchased from Nanocomposix Europe (Prague, Czech Republic). Dulbecco's modified Eagle's medium (DMEM), fetal bovine serum (FBS), antibiotics and phosphate buffer saline (PBS, pH 7.4) were purchased from Life Technologies (Carlsbad, CA, USA). 3-(4,5-

dimethylthiazol-2-yl)-2,5-diphenyltetrazolium bromide (MTT) and dimethyl sulfoxide (DMSO) were obtained from Sigma-Aldrich (St. Louis, MO, USA). RNase and propidium iodide (PI) were both from Sigma-Aldrich, St. Louis, MO-USA.

Physicochemical characterization of AgNPs

The morphology and size of AgNPs was assessed by scanning transmission electron microscopy (STEM) using a scanning electron microscope Hitachi SU-70 (Hitachi High-Technologies Europe GmbH, Germany) operating at 30 kV. Samples for STEM analysis were prepared by evaporating dilute suspensions of the nanoparticles on a copper grid coated with an amorphous carbon film. The hydrodynamic diameter and polydispersity index (PDI) of the nanoparticles were measured by dynamic light scattering (DLS) and the zeta potential was assessed by electrophoretic mobility, both measurements using a Zetasizer Nano ZS (Malvern Instruments, UK).

Silver quantification measurements were performed by inductively coupled plasma optical emission spectrometry (ICP-OES) in an Activa M Radial spectrometer (Horiba Jobin Yvon), employing a charge coupled device (CCD) array detector, with a wavelength range of 166–847 nm and radial plasma view. Samples were introduced into the ICP plasma using an HF resistant sample introduction system including a Burgener nebulizer, a cyclonic spray chamber and a quartz torch with aluminum injector. Samples for ICP-OES were prepared by addition of 10 µL AgNPs (1.0 mg/mL) to 990 µL of either ultrapure water or complete culture medium, incubation for variable periods (0, 4, 24 or 48h), followed by centrifugation at 40000 rcf for 120 min at 4ºC (in accordance with the manufacturer's recommendations) to deposit the nanoparticles and separate the supernatant (with dissolved ionic silver). Acid digestion of the supernatant was then performed by mixing 500 µL with 100 µL of acids (HCl:HNO3 2:1 v/v) and 400 µL of ultrapure water. The % dissolution of AgNPs to ionic silver was calculated as 100×F×[Ag]/Ci, where F is the dilution factor, Ci the initial concentration of AgNPs and [Ag] the concentration of silver determined by ICP-OES.

Cell Culture

The HepG2 cell line, a liver hepatocellular carcinoma cell line, was obtained from European Collection of Authenticated Cell Cultures (ECACC) and supplied by Sigma. Cell culture reagents were purchased from Life Technologies (Carlsbad, CA, USA). The cells were grown in complete medium, i.e., Dulbecco's modified Eagle's medium, supplemented with 10% fetal bovine serum (FBS), 2 mM L-glutamine, 100 U/mL penicillin, 100 µg/mL streptomycin, 250 µg/mL fungizone and 1 mM sodium pyruvate at 37°C in 5% CO_2 humidified atmosphere. Cells

were daily observed under an inverted phase-contrast Eclipse TS100 microscope (Nikon, Tokyo, Japan). For each experiment, cells were allowed to adhere for 24h and then medium was replaced with fresh medium containing Cit30 or PEG30 AgNPs. The effects were measured after 24 and 48h. Throughout the experiments, cultures were routinely visualized for confluence and cell morphology.

Exposure and Viability assay

Cell viability was determined by the colorimetric 3-(4,5- dimethyl-2-thiazolyl)-2,5-diphenyl tetrazolium bromide (MTT) assay, which measures the formation of purple formazan in viable cells (Twentyman and Luscombe, 1987). Cells were seeded in 96-well plates and after 24h, medium was replaced with fresh medium containing coated AgNPs.

Cells were exposed to Cit30 or PEG30AgNPs at 0, 1, 5, 10, 15, 25 and 50 µg/mL AgNPs. Cell viability was measured after 24h and 48h. Fifty microliters of MTT reagent (1 mg/mL) in phosphate buffered saline (PBS) were added to each well, and incubated for 4h at 37 °C, 5% CO_2. Medium was then removed, and 150 µL of DMSO were added to each well for crystal solubilization. The optical density of reduced MTT was measured at 570 nm in a microtiter plate reader (Synergy HT Multi-Mode, BioTeK, Winooski, VT), and the cell metabolic activity (MA, a usual marker for cell viability) was calculated as: MA = [(Sample Abs –DMSO Abs) / (Control Abs – DMSO Abs)]*100. Three independent assays were performed with at least 2 technical replicates each and the results compared with the control (no exposure). From the MTT results, the IC50 values were similar for cells exposed to Cit30 and to PEG30, around 11 µg/mL at 24h. Therefore, 11 µg/mL was selected as the higher dose, and a lower dose corresponding to minimal loss of viability (~IC10 ~ 5 µg/mL) was also selected. The following studies were then performed with cell exposure during 24h to 5 µg/mL and 11 µg/mL of Cit30 and PEG30 AgNPs.

Uptake potential by flow cytometry

Uptake potential of Cit30 and PEG30 AgNPs by HepG2 cells was assessed by flow cytometery (FCM), as previously described by Suzuki et al (2007). Briefly, cells were seeded in 6-well plates and after AgNPs exposure they were trypsinized, collected to FCM tubes and analyzed by FCM. Both parameters, forward scatter (FS), which give information on the particle's size, and side scatter (SS), information on complexity of particles, were measured in a Coulter XL Flow Cytometer (Beckman Coulter, Hialeah, FL-USA) equipped with an argon laser (15 mW, 488 nm). Acquisitions were made using SYSTEM II software v. 3.0 (Beckman Coulter, Hialeah, FL). For each sample, 5000–20000 cells were analyzed at a flow rate of about 1000 cells/s.

Annexin V

Apoptosis and cell viability were measured by flow cytometry (FCM) in a Coulter XL Flow Cytometer (Beckman Coulter, Hialeah, FL-USA), with the FITC Annexin V Apoptosis Detection Kit (BD Pharmingen, San Diego, CA-USA) according to manufacturer. Briefly, cells were detached and washed with PBS, then cells were resuspended in diluted binding buffer provided with the kit (1:10 in distilled water) at 1×10^6 cells/ml. To stain cell suspension, 5µL of FITC-Annexin V and 5µL of propidium iodide were added for 15 min at room temperature in the dark, after which each sample was diluted in 400µL binding buffer. For each sample, 10000 events were analyzed using the SYSTEM II (v. 2.5) software (Beckman Coulter, Hialeah, FL-USA). The cytogram of FITC florescence versus PI florescence allows the identification of live intact cells (Annexin V-FITC negative, PI negative), exclusively early apoptotic cells (Annexin V-FITC positive, PI negative), predominantly late apoptotic/necrotic cells (Annexin V-FITC positive, PI positive), and predominantly dead cells (Annexin V-FITC negative, PI positive). FCM data were analyzed by FlowJo software (Tree Star Inc., Ashland, OR).

Cell cycle and clastogenicity analysis

Cell cycle and putative clastogenic effects were analyzed by flow cytometry according to the method previously described (Oliveira et al., 2014). Briefly, cells were seeded in 6-well plates and after exposure they were washed with PBS, harvested using Trypsin-EDTA and centrifuged twice at 300 xg for 5 min. Cells were then fixed with 85% cold ethanol and kept at -20 ºC until analysis. At the time of analysis cells were centrifuged at 300 g for 5 min, resuspended in PBS and filtered through a 35-µm nylon mesh to separate aggregates. Then, 50 µL RNase (1mg/mL) and 50 µL PI (1mg/mL) were added to each sample which were then incubated for 20 min in darkness at room temperature until analysis. The relative fluorescence intensity of the stained nuclei was measured in a Coulter XL Flow Cytometer (Beckman Coulter, Hialeah, FL-USA) equipped with an argon laser (15 mW, 488 nm). Acquisitions were made using SYSTEM II software v. 3.0 (Beckman Coulter, Hialeah, FL). For each sample, the number of nuclei analyzed was approximately 5,000. The percentage of nuclei in each phase of the cell cycle (G0/G1, S and G2 phases) was analyzed using the FlowJo software (Tree Star Inc., Ashland, Oregon, USA). In order to assess the putative clastogenic effects of the two coated AgNPs and the silver ion, as described by (Misra and Easton, 1999), the coefficient of variation (CV) of the G0/G1 peak was determined.

Apoptosis and Cyclin Gene Expression

Gene-specific primer pairs (Table 5.1) were designed using the program Primer3 (REF) and confirmed for specificity by the UCSC In-Silico PCR Genome Browser (http://genome.

ucsc.edu/cgi-bin/hgPcr).

Total RNA of control and exposed cells was extracted using the TRIzol method. Organic phase separation was achieved in Phase-Lock Gel Heavy tubes (5 Prime 3 Prime, Inc., Boulder, CO). The aqueous phase was mixed with 1 vol 70% ethanol and RNA was purified using RNeasy Mini Kit columns (Qiagen, Hilden, Germany). Synthesis of cDNAs was performed by a reverse transcriptase (RT) reaction: 2 µg total RNA were pre-incubated with DNase I (Sigma Aldrich, St. Louis, MO) and reverse-transcribed with 1 µM Oligo dT18, using the Omniscript RT Kit (Qiagen, Hilden, Germany). The cDNA samples were prediluted in ultrapure MilliQ water (1:20). The final individual qPCR reactions contained iQ SYBR Green Supermix (BioRad, Hercules, CA-USA), 0.15 µM each gene-specific primer and 1:4 (v/v) prediluted cDNA (1:20). Primers were designed using the program Primer3 (Rozen and Skaletsky 2000) and confirmed for specificity by the UCSC In-Silico PCR Genome Browser (http://genome.ucsc.edu/cgi-bin/hgPcr). The qPCR program included 1 min denaturation at 95 °C, followed by 40 cycles at 94 °C for 5 s, 58 °C for 15 s, and 72 °C for 15 s. After qPCR, a melting temperature program was performed. At least two technical replicates per sample of qPCR were performed from each of three independent biological replicates. Average PCR and cycle thresholds were determined from the fluorescence data using the algorithm Real-Time PCR Miner (Zhao and Fernald 2005). Gene expression of *BAX* and *BCL2* and cyclins B1 (*CCNB1*), and E1 (*CCNE1*) were normalized with the GAPDH reference gene and expressed relative to control cells, calculated from the average efficiencies and cycle thresholds using the Pfaffl method (Pfaffl 2001).

Table 5.1: Oligonucleotide primer sequences used for qPCR.

Gene	Forward primer (5' – 3')	Reverse primer (5' – 3')
BAX	GACGGCCTCCTCTCCTACTT	CAGCCCATCTTCTTCCAGAT
BCL2	GGAGGATTGTGGCCTTCTTT	GCCGGTTCAGGTACTCAGTC
CCNB1	GCTGAAAATAAGGCGAAGATCAA	ACCAATGTCCCCAAGAGCTG
CCNE1	CAGCCTTGGGACAATAATGC	GAGGCTTGCACGTTGAGTTT
GAPDH	ACACCCACTCCTCCACCTTT	TACTCCTTGGAGGCCATGTG

Statistical analysis

The results are reported as mean ± standard deviation (SD) of 2 technical replicates in each of the 3 independent experiments. For MTT assay, the statistical significance between control and exposed cells was performed by one way ANOVA, followed by Dunnet and Dunn's method (as parametric and non-parametric test, respectively), using Sigma Plot 12.5 software (Systat Software Inc.). For the other assays, the results were compared using two-way ANOVA, followed by Holm-Sidak method, using also Sigma Plot 12.5 software (Systat Software Inc.). The differences were considered statistically significant for $p < 0.05$.

Results

Physicochemical characterization of AgNPs dispersed in water and in cell culture medium

The characteristics of Cit30 and PEG30 AgNPs dispersed in water or in culture medium are summarized in Table 5.2, including hydrodynamic diameter of 43.3 ± 0.5 for Cit30 and 62.1±0.5 for PEG30; polydispersity index (PdI) of 0.25-0.26 for Cit30 and 0.15-0.16 for PEG30; zeta potential (ζ) -42.7 ± 2.7 for Cit30 and -12.1±0.5 for PEG30; ionic silver dissolution in ultrapure water at 0h of Cit30 3.3±0.04% and PEG30 0.63±0.01%; and also ionic silver dissolution in DMEM at 0, 4, 24 and 48h of Cit30 3.8±0.04%, 5.5±0.07%, 5.7±0.03%, 7.6±0.1%, respectively and PEG30 3.2±0.03%, 6.0±0.06%, 7.0±0.07%, 7.2±0.06%, respectively.

Effects on cell growth, morphology and viability

In control conditions, HepG2 cells showed typical morphology (Fig. 5.1a, and 5.2a). When they were exposed to Cit30 and PEG30 AgNPs, their confluence decreased, especially for the higher concentration (11 µg/mL) (Fig. 5.1c and 5.2c). No morphological alterations were observed in AgNP-exposed cells, independently of the coating and concentration. The viability of exposed cells was significantly reduced ($p < 0.05$) upon exposure to Cit30 and PEG30 at concentrations higher than 5 µg/mL after 48h and 10 µg/mL after 24h for Cit30; and concentrations higher than 5 µg/mL after 24 and 48h for PEG30 (Fig. 5.3a-b).

Table 5.2: Physicochemical properties of AgNPs.

	Citrate- AgNPs	**PEG- AgNPs**
D (nm)[a]	32.7±4.8	31.8±3.2
D (nm)[b]	29.1±3.9	26.8±5.3
D_h (nm)[c]	43.3±0.5	62.1±0.5
PdI[c]	0.25-0.26	0.15-0.16
ζ (mV)[d]	-42.7±2.7	-12.1±0.5
λ_{max}[e] (nm)	408	411
$\%Ag^+$ in water 0h[f]	3.3±0.04	0.63±0.01
$\%Ag^+$ in DMEM 0h[f]	3.8±0.04	3.2±0.03
$\%Ag^+$ in DMEM 4h[f]	5.5±0.07	6.0±0.06
$\%Ag^+$ in DMEM 24h[f]	5.7±0.03	7.0±0.07
$\%Ag^+$ in DMEM 48h[f]	7.6±0.1	7.2±0.06

[a]Diameter indicated by the manufacturer; [b]Diameter measured by TEM; [c]Hydrodynamic diameter and polydispersity index (PdI) measured by DLS; [d]Zeta potential assessed by electrophoretic mobility (in cell culture medium); [e]Wavelength of maximum absorbance peak in the UV-Vis spectrum; [f]Percentage of ionic silver in the AgNP suspension (10 µg/mL). Standard deviations calculated for Dh, ζ and $\%Ag^+$ correspond to 3 replicate measurements.

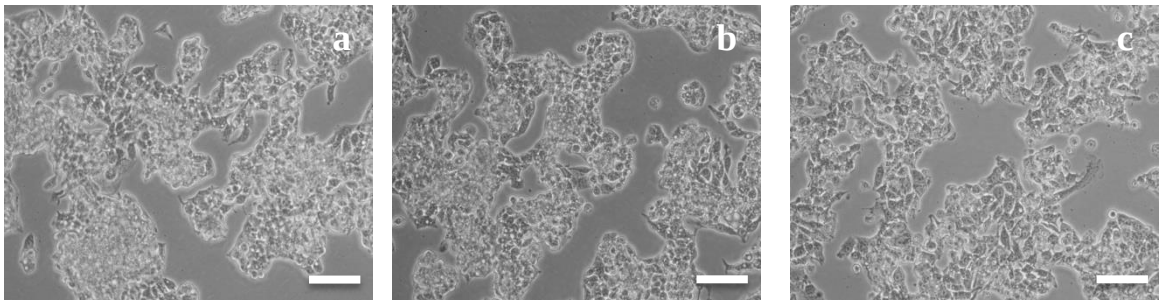

Figure 5.1: Light microscopy images (100X) of HepG2 cells exposed to citrate- AgNPs for: 24h - a) 0, b) 5 µg/mL and c) 11 µg/mL. Bar corresponds to 100 µm.

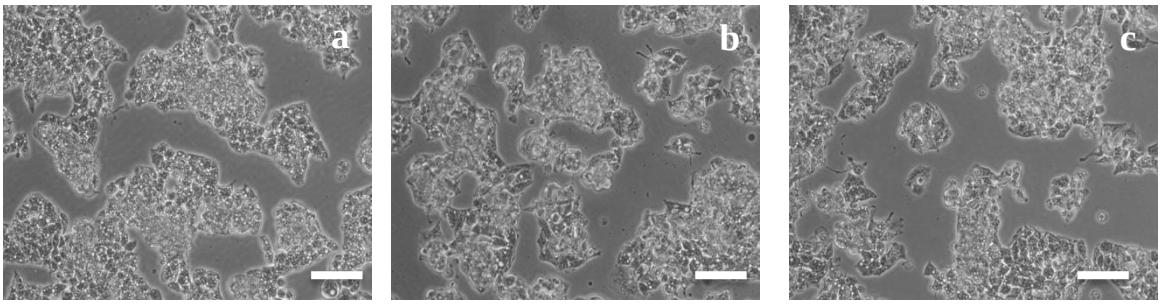

Figure 5.2: Light microscopy images (100X) of HepG2 cells exposed to PEG- AgNPs for: 24h - a) 0, b) 5 µg/mL and c) 11 µg/mL. Bar corresponds to 100 µm.

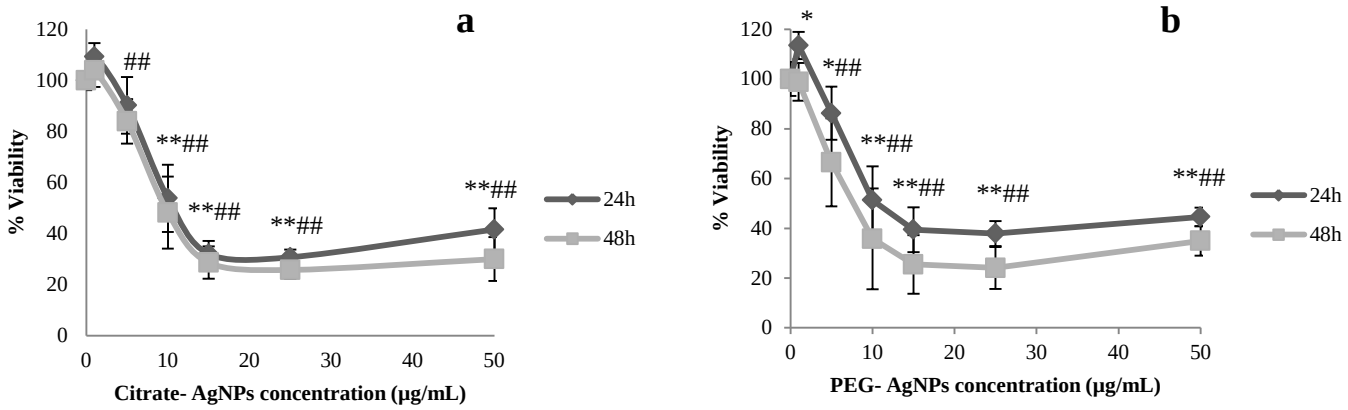

Figure 5.3: Relative cell viability of HepG2 (%), measured by MTT assay, for 24h and 48h. a) 30 nm citrate-coated AgNPs; b) 30 nm PEG coated AgNPs. Data expressed as mean and standard deviation. * indicate significant differences between control at $p < 0.05$ and ** at $p < 0.01$ for 24h; and # indicate significant differences between control at $p < 0.05$ and ## at $p < 0.01$ for 48h.

Nanoparticle uptake measured by flow cytometry

The uptake of both Cit30 and PEG30 AgNPs by HepG2 cells is shown in Figure 5.4. Both concentrations (5 and 11 µg/mL) of both AgNPs induce an increase in side scatter intensity without change of forward scatter intensity of HepG2 cells, which means particles taken up by cells. The uptake potential was significant only for the highest concentration (11 µg/mL) and no significant difference was observed when comparing cells exposed to Cit30 *vs* PEG30 AgNPs.

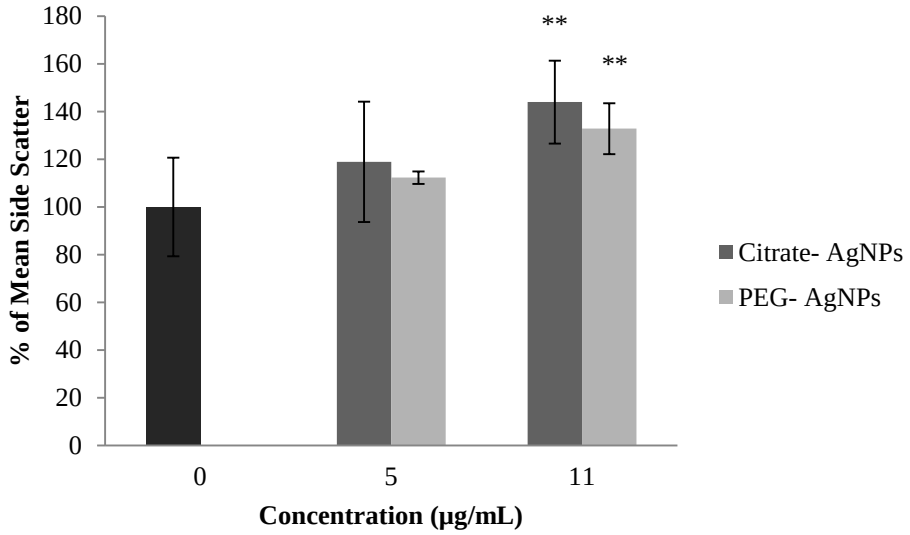

Figure 5.4: Uptake of AgNP by HepG2 cells after 24h exposure to 5 and 11 µg/mL of citrate- AgNPs and PEG- AgNPs assessed by the side scattered light by flow cytometry. The results were expressed as the mean +/- SD versus control. ** indicate significant differences between control at $p < 0.01$.

Apoptotic markers

The Annexin V assay was performed in order to evaluate the potential of AgNPs to induce apoptosis in HepG2 cells. Although exposure to Cit30 NPs at the IC50 concentration caused a small non-significant increase in the % late apoptotic cells (Fig. 5.5), there were no statistically significant differences in relation to controls. Both concentration of Cit30 and PEG30 AgNPs decreased the expression levels of selected genes involved in the apoptotic cascade, BCL2 and BAX, after 24h (Fig. 5.6). Cit30 induced a significant decrease of antiapoptotic BCL2 expression levels for the higher concentration tested and of BAX expression levels for 5 µg/mL. PEG30 induced a significant decrease of BCL2 expression levels for both concentrations used.

Cell cycle analysis

Figure 5.7 shows the effect of Cit30 and PEG30 AgNPs on the cell cycle of HepG2 cells. Cit30 in both doses decreased the percentage of cells in G0/G1 (significant at the higher concentration) and increased the percentage of cells in G2, this effect being visible for both concentrations, but more pronounced for 11 µg/mL ($p < 0.01$) (Fig. 5.7a). An increase in the percentage of cells in the S phase was also observed for the higher concentration.

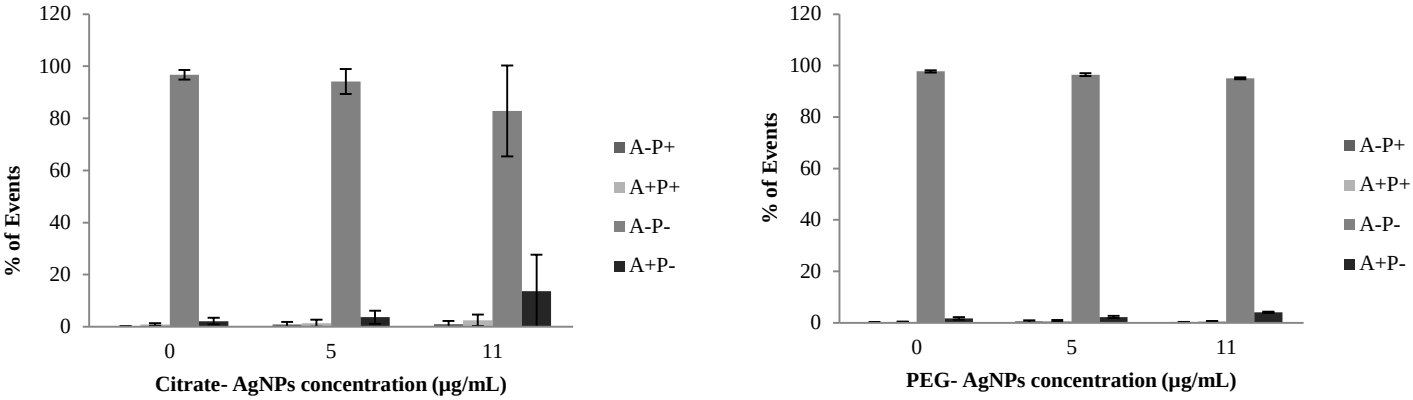

Figure 5.5: Citrate- and PEG- AgNPs effects on HepG2 cells exposed to 5 and 11 µg/mL after 24h, measured by annexin V assay. Intact cells are represented by "A-P-", dead cells "A-P+", early apoptotic cells "A+P-" and late apoptotic/necrotic cells "A+P+". The results were expressed as the mean +/- SD versus control.

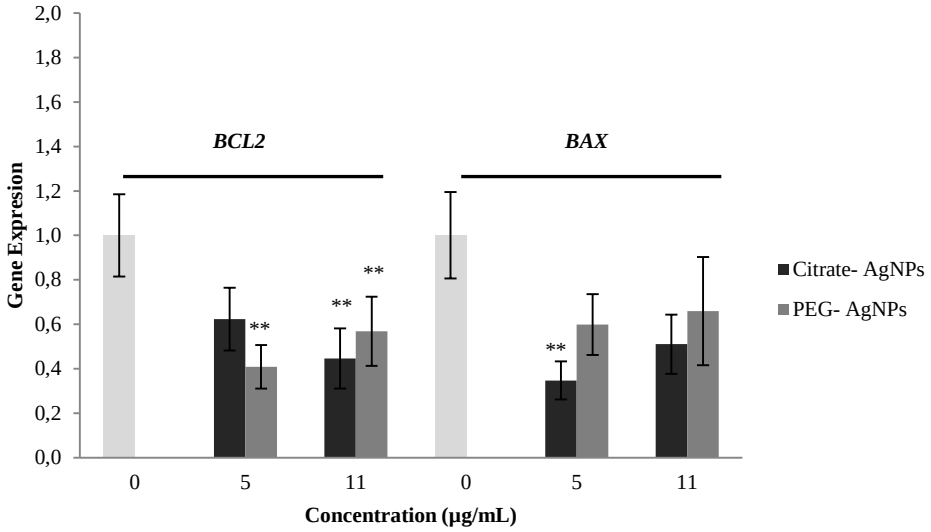

Figure 5.6: HepG2 gene expression of apoptotic genes, for 24h: a) Citrate-coated AgNPs; and b) PEG-coated AgNPs The results were expressed as mean relative to control cells (normalized with the GAPDH reference gene) and standard deviation. ** indicate significant differences between control at $p < 0.01$.

PEG30 showed a similar trend, but decreased the percentage of cells at G0/G1 only at the higher concentration (11 µg/mL). The increase of the percentage of cells at G2 and S phases was pronounced at the higher concentration; for the lower concentration, only the populations at G2 increased. The coefficient of variation (CV) of the G0/G1 peak did not change significantly with exposure to AgNPs, comparatively to their counterparts in the control (Fig. 5.8). When

comparing cell cycle profiles upon exposure to both types of AgNPs, significant differences were found for the lowest concentration (5 µg/mL) at G0/G1 and S phases: the percentage of cells in G0/G1 phase was higher for PEG-AgNPs exposed cells; and the percentage of cells in S phase was higher for the Cit30 AgNPs.

Finally, it should also be stressed that both exposures increased the percentage of subpopulations at channel >600 and channel >800 corresponding to superG2 subpopulations (Fig. 5.8).

In addition to changing the cell cycle distribution, exposure to AgNPs downregulated the expression of genes involved in G1/S (cyclin E1) and G2/M (cyclin B1) phase transitions (Fig. 5.9). Both concentrations of Cit30 AgNPs downregulated the expression of cyclin B1 gene (*CCNB1*), though only significantly for 11 µg/mL ($p < 0.01$). HepG2 cells exposed to PEG30 AgNPs showed a similar profile of CCNB1, where the expression was significantly decreased for 11 µg/mL ($p < 0.01$). In HepG2 exposed to Cit30 the expression of *CCNE1* gene was decreased for both concentrations, while cells exposed to PEG30 did not show differences for the higher concentration, showing a significant decrease of *CCNE1* expression levels after exposure to 5 µg/mL ($p < 0.05$).

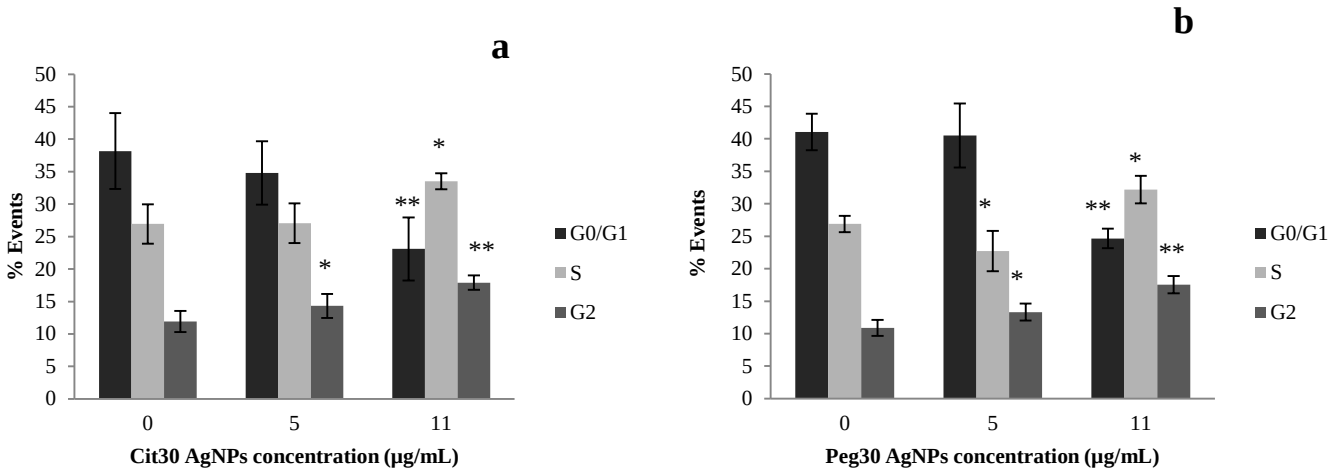

Figure 5.7: Effects of AgNPs on cell cycle dynamics, measured by flow cytometry: a) citrate-coated AgNPs; and b) PEG-coated AgNPs. The results were expressed as mean and standard deviation. * indicate significant differences between control at $p < 0.05$ and ** at $p < 0.01$.

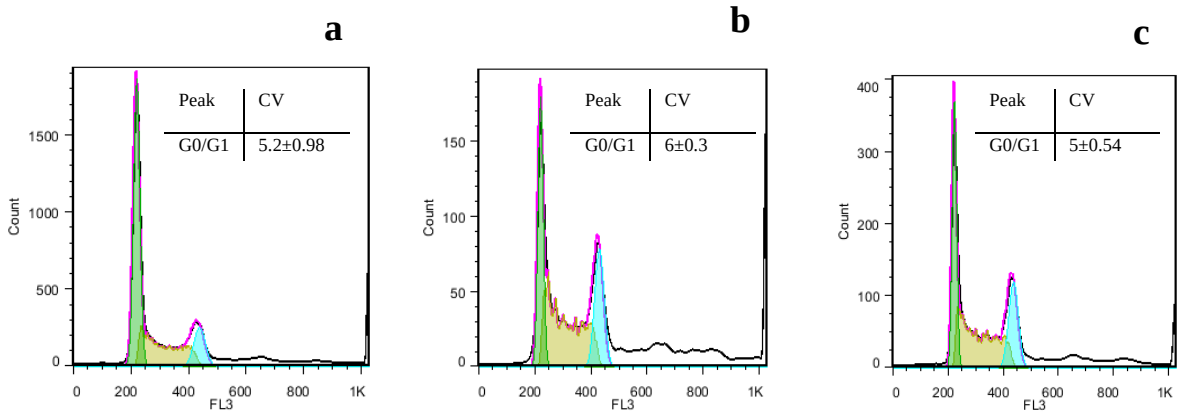

Figure 5.8: Examples of HepG2 cell cycle histograms obtained after 24h of AgNPs exposure, measured by flow cytometry. a) Control; b) 11 µg/mL of citrate- AgNPs; and c) 11 µg/mL of PEG- AgNPs. In each histogram are represented the coefficient of variation (CV) values of the respective conditions.

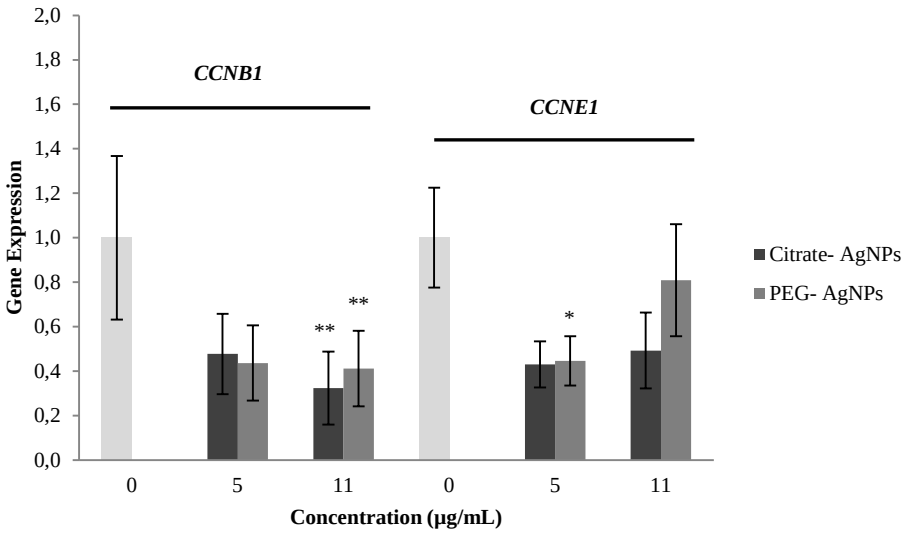

Figure 5.9: HepG2 gene expression of cell cycle genes, for 24h: a) Citrate-coated AgNPs; and b) PEG-coated AgNPs The results were expressed as mean relative to control cells (normalized with the GAPDH reference gene) and standard deviation. ** indicate significant differences between control at $p < 0.01$ and * $p < 0.05$.

Discussion

Citrate- AgNPs are widely used, e.g. as antimicrobial agents in industry (Tolaymat et al., 2010), while the use of PEG-coated AgNPs is still emerging, particularly in e.g. nanomedical applications (Ginn et al., 2014; Ryan et al., 2008; Thorley and Tetley, 2013). Despite data

supporting some cytotoxic effects of AgNPs on different cell lines have been reported, these effects are dependent on multiple aspects such as external factors (e.g. storage conditions, dispersion medium) and NP characteristics (e.g. size and coating). In particular, research on the coating properties that may confer AgNPs less toxicity is essential, namely the evaluation of cyto- and genotoxic potential.

This study focused on the comparison between citrate- and PEG- coated AgNPs cytotoxicity to human liver cells. As discussed elsewhere (Chapter 2) coating deeply influences AgNPs physicochemical properties, with citrate coating providing a more negative and, hence, potentially more reactive surface. It has been reported that nanoparticle coating, media composition and ionic strength influences the surface chemistry, shape, aggregation state and dissolution, which can impact toxicological determinations by altering concentration, dissolved ionic silver, aggregation and shape, consequently affecting NP uptake (Tejamaya et al., 2012). The same authors reported that charge-stabilized particles (e.g. by citrate) were more unstable and aggregated more than sterically stabilized particles (e.g. by PEG); which could induce different levels of cytotoxicity (Wang et al., 2014b).

In this study, citrate-coated AgNPs and PEG-coated AgNPs (both 30 nm nanospheres) yielded approximately the same viability profile, up to IC50 concentrations, indicating that particle coating did not greatly influence the AgNPs cytotoxicity potential on HepG2 cell line. Considering the literature (Caballero-Díaz et al., 2013), it was expected that citrate- AgNPs would induce higher cell death compared to PEG-AgNPs. For example, our previous results on human keratinocytes HaCaT cell line showed that citrate-AgNPs had higher cytotoxicity than PEG- AgNPs (Chapter 2). Lu and colleagues (2010) found that citrate-coated silver nanopowder was cytotoxic, whereas PVP-coated silver nanoprisms or NPs were not. The authors also highlighted the importance of replacing, in daily life applications, citrate-coating with other biocompatible and functionalized formulations such as PVP. Pang and co-workers (2015) demonstrated that the toxicity of AgNPs on murine hepatoma cells (Hepa1c1c7) depended on the surface chemistry of NPs. They suggested that PEG-AgNPs have better biocompatibility, with an optimal biological inertia, and could effectively resist opsonization or non-specific binding to protein in mice. Also, Caballero-Díaz et al (2013) reported that pegylation of AgNPs reduced cellular uptake and their toxicity to NIH/3T3 (mouse embryonic fibroblasts). Also, when evaluating the uptake rates of gold NPs on human alveolar epithelial cells (A549), Brandenberger et al (2010) observed that significantly more plain NPs (i.e., stabilized with citrate buffer) could enter the cells than PEG-coated gold NPs. However, from our uptake results there was not a statistical difference between cells exposed to Cit30 AgNPs and cells exposed to PEG30 AgNPs.

We have previously tested these AgNPs in other cell lines and demonstrated that the IC50

for keratinocytes (HaCaT) was 40 µg/mL, above the values herein found for the HepG2 cells. The cytotoxicity of these AgNPs is thus dependent on the cell type, with keratinocytes demonstrating higher tolerance than liver cells. PEG-coated AgNPs induced a similarly decrease on the viability of liver cells (HL-7702) in a dose- and time-dependent manner at doses from 6.25 µg/mL (Song et al., 2012). Faedmaleki and collegues (2014) obtained IC50 value of 2.764 µg/mL for HepG2 when exposed to 20-40 nm AgNPs. Similarly, Nowrouzi and co-workers (2010) obtained IC50 value of 2.75-3 µg/mL for HepG2 after exposure to 5-10 nm AgNPs. However, Xin and co-workers (2015) observed lower cytotoxicity of 20-50 nm AgNPs to HepG2 cells, where viability decreased with concentrations ranging from 25 to 200 µg/mL. The same authors found a viability decrease of A549 cells after exposure to 20-50 nm AgNPs within concentrations ranging from 12.5 to 200 µg/mL.

Regarding apoptosis, our results did not show significant differences between control and exposed cells after 24h. Urbańska and co-workers (2015) determined the occurrence of apoptosis on glioblastoma multiforme (GBM) cells cultured in an *in ovo* model (tumor cell implantation of GBM cells, line U-87, placed on chicken embryo membrane on fertilized chicken eggs in order to study tumors growth rate, angiogenic potential, and metastatic capability) treated with colloidal 70 nm AgNPs (40 µg/ml). Through TUNEL assay, the authors observed no induction of apoptosis as well, despite the increased level of immunohistochemical caspase 3 and 9. The authors suggested that malignant tumor cells, such as GBM, are extremely resistant to apoptosis and particularly resistant to radiation and chemotherapy (Kuriyama et al., 2002). Also, Xue et al (2015) determined the apoptotic potential of 15 nm AgNPs in HepG2 cells and did not find significant differences between control and 40 µg/mL exposed cells after 24h. However, a study using 1 and 50 µM of PVA- AgNPs obtained significant apoptotic effects on HepG2 after 24h (Paino and Zucolotto, 2015). In terms of apoptotic gene expression, we have found that both AgNPs downregulated *BAX* and *BCL2* gene expression. Cit30 AgNPs significantly decreased BAX (pro-apoptotic) gene expression for the lowest concentration (5 µg/mL) and *BCL2* (anti-apoptotic) gene expression for the higher concentration (11 µg/mL). On the other hand, PEG30 decreased significantly *BCL2* gene expression for both concentrations. *BCL2* is an anti-apoptotic protein coding gene that prevents the opening of the mitochondrial membrane pore, while *BAX* – pro-apoptotic coding gene - accelerates it. Mitochondrial membrane pore opening induces the release of cytochrome c from mitochondria. Piao and co-workers (2011), observed that AgNPs downregulated *BCL2* expression and upregulated *BAX* expression in Human Chang liver cells, resulting in the disruption of mitochondrial membrane potential, followed by cytochrome c release from the mitochondria, resulting in mitochondria-dependent apoptotic pathway. Furthermore, Jeyaraj and co-workers (2015) found an upregulation of *BAX*, caspases-6 and -9 and downregulation of *BCL2* on HeLa cells after

exposure to AgNPs.

Cell cycle dynamics was evaluated in HepG2 cells exposed to Cit30 and PEG30 AgNPs. For both AgNPs, there were changes on the cell cycle of HepG2 cells. Cit30 and PEG30 induced an increase in the percentage of cells in G2, indicating an arrest at this phase, visible for both concentrations. Also, both AgNPs significantly increased the percentage of cells at S phase for the higher concentration used (11 µg/mL) pointing to an S-phase delay. An S phase delay was also observed by Liu et al. (2010) in HepG2 cells exposed to PVP-coated AgNPs. However, Song et al. (2012) found an increase in the percentage of cells at G2/M phase on HL-7702 cells (human liver cell line) exposed to 100 µg/mL mPEG-SH coated AgNPs after 24h. Indeed, cell cycle arrest at G2 was also previously observed as a result of AgNP exposure (AshaRani et al., 2009; Kang et al., 2012; Lee et al., 2011; Wei et al., 2010). Xue and colleagues (2015) found that no significant changes were observed on HepG2 after exposure to 40 and 80 µg/mL AgNPs for 24h. In our study, both exposures promoted the appearance of superG2 subpopulations. This suggests that exposure to AgNPs stimulates the proliferation of the hyperdiploid karyotype subpopulations (ATCC 2015; http://www.hepg2.com/) over the typical diploid profile, meaning an increase of the heterogeneity of this culture, and the consequences of this increase remain unknown, as well as the behavior of each subpopulation individually.

Expression of two selected cell cycle regulator genes was also assessed in this study. Cyclin B1, encoded by the *CCNB1* gene, is a regulatory protein which complexes with Cdk1 and both play a determinant role in G2/M phase transition of the cell cycle. Cyclin E1, encoded by the *CCNE1* gene, forms a complex with Cdk2, which accumulates at the G1-S phase and is degraded as cells progress through the S phase. From our results, both AgNPs decreased the *CCNB1* and *CCNE1* gene expression for both concentrations used. *CCNE1* gene expression was decreased after exposure to both AgNPs, especially at the lowest concentration (5 µg/mL), although it was significantly decreased only for PEG- AgNPs. This agrees with the increase in the percentage of cells in S-phase observed for both AgNPs. There are other studies on AgNPs cytotoxicity in agreement with our results: Foldbjerg et al (2012) found a downregulation of *CCNB1* and Cdk1 for A549 cell line; and also AshaRani et al (2012) reported a downregulation of *CCNB1* and also of *CCNE1* in normal human lung cells IMR-90 and human brain cancer cells.

Conclusions

In sum, our study demonstrates that citrate-coated and PEG- coated AgNPs have similar profiles in decreasing the viability of HepG2 cells. Thus, and contrarily to what we have found in other cell lines such as keratinocytes where citrate coating was generally more toxic, in HepG2 cells

the cytotoxicity of AgNPs was independent of the studied coatings. Despite leading to low proliferation, AgNPs did not induced apoptosis for the studied concentrations and the apoptotic related genes *BCL2* and *BAX* were downregulated, supporting that the decrease of proliferation may be due to both cytostatic effects and/or necrotic events. HepG2 showed the same profile of cell cycle dynamics after exposure to both AgNPs, where, for the higher concentration, there was an increase of the percentage of cells at S and G2 phases. Cyclins gene expressions *CCNB1* and *CCNE1* were also downregulated, which supports cytostatic effects of these coated AgNPs on this cell line. Also, both type of nanoparticles induced higher heterogeneity of the population (increase % of cells at super G2).

This study supports the claim for more thorough studies on different cell lines before a decision can be reached on the toxicity of each type of nanoparticles on humans. For this reason, more research is needed to complement the existing information about the cell lines response to different physicochemical features of AgNPs currently used in industrial, consumer products and nanomedicines.

Acknowledgments

This work was developed in the scope of the projects CICECO-Aveiro Institute of Materials (Ref. FCT UID/CTM/50011/2013) and CESAM (Ref. FCT UID/AMB/50017/2013), financed by national funds through the FCT/MEC and when applicable co-financed by the European Regional Development Fund (FEDER) under the PT2020 Partnership Agreement. Funding to the project FCOMP-01-0124-FEDER-021456 (Ref. FCT PTDC/SAU-TOX/120953/2010) by FEDER through COMPETE and by national funds through FCT, and the FCT-awarded grants (SFRH/BD/81792/2011; SFRH/BPD/48853/2008; SFRH/BPD/74868/2010) are acknowledged. I.F.D and A.L.D.S. acknowledge FCT/MCTES for the research contracts under the Program ‘Investigador FCT’ 2014.

Contributions

V.B. participated in the design experiment with the supervisors and did all laboratorial experiments and statistical data analyses. Also had a key role in the data analyses integration, and together with the supervisors wrote and revised the manuscripts. C.S. and H.O. planned the experimental design, contributed to data analyses and integration of all data, and in the manuscript preparation. I.F.D. coordinated NPs analyses and revised the manuscript. J.M.P.O. coordinated gene expression and revised the manuscript.

References

Abdelhalim, M.A.K., and Jarrar, B.M. (2011). Renal tissue alterations were size-dependent with smaller ones induced more effects and related with time exposure of gold nanoparticles. Lipids Health Dis, 10(1), 1.

Ahlberg, S., Meinke, M.C., Werner, L., Epple, M., Diendorf, J., Blume-Peytavi, U., Lademann, J., Vogt, A., and Rancan, F. (2014). Comparison of silver nanoparticles stored under air or argon with respect to the induction of intracellular free radicals and toxic effects toward keratinocytes. Eur J Pharm Biopharm, 88(3), 651-657.

AshaRani, P., Low Kah Mun, G., Hande, M., and Valiyaveettil, S. (2009). Cytotoxicity and genotoxicity of silver nanoparticles in human cells. ACS nano, 3(2), 279-290.

Behra, R., Sigg, L., Clift, M., Herzog, F., Minghetti, M., Johnston, B., Petri-Fink, A., and Rothen-Rutishauser, B. (2013). Bioavailability of silver nanoparticles and ions: from a chemical and biochemical perspective. J R Soc Interface, 10(87), 20130396.

Benn, T., and Westerhoff, P. (2008). Nanoparticle silver released into water from commercially available sock fabrics. Environ Sci Technol, 42(11), 4133-4139.

Boonkaew, B., Kempf, M., Kimble, R., and Cuttle, L. (2014). Cytotoxicity testing of silver-containing burn treatments using primary and immortal skin cells. Burns, 40(8), 1562-1569.

Brandenberger, C., Mühlfeld, C., Ali, Z., Lenz, A.-G.G., Schmid, O., Parak, W.J., Gehr, P., and Rothen-Rutishauser, B. (2010). Quantitative evaluation of cellular uptake and trafficking of plain and polyethylene glycol-coated gold nanoparticles. Small, 6(15), 1669-1678.

Caballero-Díaz, E., Pfeiffer, C., Kastl, L., Gil, P., Simonet, B., Valcárcel, M., Lamana, J., Laborda, F., and Parak, W.J. (2013). The toxicity of silver nanoparticles depends on their uptake by cells and thus on their surface chemistry. Part Part Syst Charact, 30(12), 1079-1085.

Chen, L.Q., Fang, L., Ling, J., Ding, C.Z., Kang, B., and Huang, C.Z. (2015). Nanotoxicity of silver nanoparticles to red blood cells: size dependent adsorption, uptake, and hemolytic activity. Chem Res Toxicol, 28(3), 501-509.

Comfort, K.K., Maurer, E.I., and Hussain, S.M. (2014). Slow release of ions from internalized silver nanoparticles modifies the epidermal growth factor signaling response. Colloids Surf B Biointerfaces, 123, 136-142.

Dusinska, M., Magdolenova, Z., and Fjellsbø, L.M. (2013). Toxicological aspects for nanomaterial in humans. Methods Mol Biol, 1-12.

Eckhardt, S., Brunetto, P., Gagnon, J., Priebe, M., Giese, B., and Fromm, K. (2013). Nanobio silver: its interactions with peptides and bacteria, and its uses in medicine. Chem Rev 113(7), 4708-4754.

EPA, E.P.A. (2010). State of the Science Literature Review: Everything Nanosilver and More. Scientific, Technical, Research, Engineering and Modeling Support Final Report.

Faedmaleki, F., H Shirazi, F., Salarian, A.-A.A., Ahmadi Ashtiani, H., and Rastegar, H. (2014). Toxicity Effect of Silver Nanoparticles on Mice Liver Primary Cell Culture and HepG2 Cell Line. Iran J Pharm Res, 13(1), 235-242.

Fernández-López, C., Mateo-Mateo, C., Alvarez-Puebla, R., Pérez-Juste, J., Pastoriza-Santos, I., and Liz-Marzán, L. (2009). Highly controlled silica coating of PEG-capped metal nanoparticles and preparation of SERS-encoded particles. Langmuir, 25(24), 13894-13899.

Franci, G., Falanga, A., Galdiero, S., Palomba, L., Rai, M., Morelli, G., and Galdiero, M. (2015). Silver nanoparticles as potential antibacterial agents. Molecules, 20(5), 8856-8874.

Ginn, C., Khalili, H., Lever, R., and Brocchini, S. (2014). PEGylation and its impact on the design of new protein-based medicines. Future Med Chem, 6(16), 1829-1846.

Gliga, A., Skoglund, S., Odnevall Wallinder, I., Fadeel, B., and Karlsson, H. (2014). Size-

dependent cytotoxicity of silver nanoparticles in human lung cells: the role of cellular uptake, agglomeration and Ag release. Part Fibre Toxicol, 11(1), 1.

Gutierrez, L., Aubry, C., Cornejo, M., and Croue, J.P. (2015). Citrate-coated silver nanoparticles interactions with effluent organic matter: influence of capping agent and solution conditions. Langmuir, 31(32), 8865-8872.

Haase, A., Mantion, A., Graf, P., Plendl, J., Thuenemann, A.F., Meier, W., Taubert, A., and Luch, A. (2012). A novel type of silver nanoparticles and their advantages in toxicity testing in cell culture systems. Arch Toxicol, 86(7), 1089-1098.

Haberl, N., Hirn, S., Wenk, A., Diendorf, J., Epple, M., Johnston, B., Krombach, F., Kreyling, W., and Schleh, C. (2013). Cytotoxic and proinflammatory effects of PVP-coated silver nanoparticles after intratracheal instillation in rats. Beilstein J Nanotechnol, 4(1), 933-940.

Jain, A., and Jain, S.K. (2008). PEGylation: an approach for drug delivery. A review. Crit Rev Ther Drug Carrier Syst, 25(5), 403-447.

Jeyaraj, M., Renganathan, A., and Sathishkumar, G. (2015). Biogenic metal nanoformulations induce Bax/Bcl2 and caspase mediated mitochondrial dysfunction in human breast cancer cells (MCF 7). RSC Advances, 5(3), 2159-2166.

Kang, S., Lee, Y., Lee, E.-K., and Kwak, M.-K. (2012). Silver nanoparticles-mediated G2/M cycle arrest of renal epithelial cells is associated with NRF2-GSH signaling. Toxicol Lett, 211(3), 334-341.

Kennedy, D. C., Orts-Gil, G., Lai, C. H., Müller, L., Haase, A., Luch, A., & Seeberger, P. H. (2014). Carbohydrate functionalization of silver nanoparticles modulates cytotoxicity and cellular uptake. J Nanobiotechnology, 12(1), 59.

Kim, T.H., Kim, M., Park, H.S., Shin, U.S., Gong, M.S., and Kim, H.W. (2012). Size-dependent cellular toxicity of silver nanoparticles. J Biomed Mater Res A, 100(4), 1033-1043.

Kuriyama, H., Lamborn, K.R., O'Fallon, J.R., Iturria, N., Sebo, T., Schaefer, P.L., Scheithauer, B.W., Buckner, J.C., Kuriyama, N., Jenkins, R.B., et al. (2002). Prognostic significance of an apoptotic index and apoptosis/proliferation ratio for patients with high-grade astrocytomas. Neuro-oncology 4(3), 179-186.

Lee, Y., Kim, D., Oh, J., Yoon, S., Choi, M., Lee, S., Kim, J., Lee, K., and Song, C.-W. (2011). Silver nanoparticles induce apoptosis and G2/M arrest via PKCζ-dependent signaling in A549 lung cells. Arch Toxicol 85(12), 1529-1540.

Liu, W., Wu, Y., Wang, C., Li, H., Wang, T., Liao, C., Cui, L., Zhou, Q., Yan, B., and Jiang, G. (2010). Impact of silver nanoparticles on human cells: effect of particle size. Nanotoxicology 4(3), 319-330.

Lu, W., Senapati, D., Wang, S., Tovmachenko, O., Singh, A.K., Yu, H., and Ray, P.C. (2010). Effect of Surface Coating on the Toxicity of Silver Nanomaterials on Human Skin Keratinocytes. Chem Phys Lett 487(1), 92-96.

McShan, D., Ray, P.C., and Yu, H. (2014). Molecular toxicity mechanism of nanosilver. J Food Drug Anal 22(1), 116-127.

Misra, R., and Easton, M. (1999). Comment on analyzing flow cytometric data for comparison of mean values of the coefficient of variation of the G1 peak. Cytometry 36(2), 112-116.

Nair, L.S., and Laurencin, C.T. (2007). Silver nanoparticles: synthesis and therapeutic applications. J Biomed Nanotechnol 3(4), 301-316.

Nowack, B., and Bucheli, T. (2007). Occurrence, behavior and effects of nanoparticles in the environment. Environ Pollut 150(1), 5-22.

Nowack, B., Krug, H., and Height, M. (2011). 120 years of nanosilver history: implications for policy makers. Environ Sci Technol 45(4), 1177-1183.

Nowrouzi, A., Meghrazi, K., Golmohammadi, T., Golestani, A., Ahmadian, S., Shafiezadeh, M., Shajary, Z., Khaghani, S., and Amiri, A.N. (2010). Cytotoxicity of subtoxic AgNP in human hepatoma cell line (HepG2) after long-term exposure. Iran Biomed J 14(1/2), 23-32.

Nymark, P., Catalán, J., Suhonen, S., Järventaus, H., Birkedal, R., Clausen, P., Jensen, K., Vippola, M., Savolainen, K., and Norppa, H. (2013). Genotoxicity of polyvinylpyrrolidone-coated silver nanoparticles in BEAS 2B cells. Toxicology 313(1), 38-48.

Oliveira, H., Monteiro, C., Pinho, F., Pinho, S., Ferreira de Oliveira, J.M., and Santos, C. (2014). Cadmium-induced genotoxicity in human osteoblast-like cells. Mutat Res Genet Toxicol Environ Mutagen 775-776, 38-47.

Paino, I.M.M.M., and Zucolotto, V. (2015). Poly(vinyl alcohol)-coated silver nanoparticles: activation of neutrophils and nanotoxicology effects in human hepatocarcinoma and mononuclear cells. Environ Toxicol Pharmacol 39(2), 614-621.

Panacek, A., Prucek, R., Hrbac, J., na, T.j., Steffkova, J., Zboril, R., and tek, L. (2014). Polyacrylate-Assisted Size Control of Silver Nanoparticles and Their Catalytic Activity. Chem Mat 26(3), 1332-1339.

Pang, C., Brunelli, A., Zhu, C., Hristozov, D., Liu, Y., Semenzin, E., Wang, W., Tao, W., Liang, J., Marcomini, A., et al. (2015). Demonstrating approaches to chemically modify the surface of Ag nanoparticles in order to influence their cytotoxicity and biodistribution after single dose acute intravenous administration. Nanotoxicology, 1-11.

Park, J., Lim, D.-H.H., Lim, H.-J.J., Kwon, T., Choi, J.-s.S., Jeong, S., Choi, I.-H.H., and Cheon, J. (2011). Size dependent macrophage responses and toxicological effects of Ag nanoparticles. Chem Commun (Camb) 47(15), 4382-4384.

Piao, M.J., Kang, K.A., Lee, I.K., Kim, H.S., Kim, S., Choi, J.Y., Choi, J., and Hyun, J.W. (2011). Silver nanoparticles induce oxidative cell damage in human liver cells through inhibition of reduced glutathione and induction of mitochondria-involved apoptosis. Toxicol Lett 201(1), 92-100.

Pillai, Z.S., and Kamat, P.V. (2004). What factors control the size and shape of silver nanoparticles in the citrate ion reduction method? J Phys Chem B 108(3), 945-951.

Rai, M., Ingle, A.P., Birla, S., Yadav, A., and Santos, C.A. (2015). Strategic role of selected noble metal nanoparticles in medicine. Crit Rev Microbiol, 1-24.

Roberts, S. M., James, R. C., & Williams, P. L. (2014). Principles of toxicology: environmental and industrial applications. John Wiley & Sons

Ryan, S.M.M., Mantovani, G., Wang, X., Haddleton, D.M., and Brayden, D.J. (2008). Advances in PEGylation of important biotech molecules: delivery aspects. Expert Opin Drug Deliv 5(4), 371-383.

Sharma, V., Yngard, R., and Lin, Y. (2009). Silver nanoparticles: green synthesis and their antimicrobial activities. Adv Colloid Interface Sci 145(1), 83-96.

Song, X.-l., Li, B., Xu, K., Liu, J., Ju, W., Wang, J., Liu, X.-d., Li, J., and Qi, Y.-f. (2012). Cytotoxicity of water-soluble mPEG-SH-coated silver nanoparticles in HL-7702 cells. Cell Biol Toxicol 28(4), 225-237.

Suzuki H, Toyooka T, Ibuki Y. (2007). Simple and easy method to evaluate uptake potential of nanoparticles in mammalian cells using a flow cytometric light scatter analysis. Environ Sci Technol 41(8), 3018–3024.

Tejamaya, M., Römer, I., Merrifield, R., and Lead, J. (2012). Stability of citrate, PVP, and PEG coated silver nanoparticles in ecotoxicology media. Environ Sci Technol 46(3), 7011-7017.

Thorley, A.J., and Tetley, T.D. (2013). New perspectives in nanomedicine. Pharmacol Ther 140(2), 176-185.

Tolaymat, T.M., El Badawy, A.M., Genaidy, A., Scheckel, K.G., Luxton, T.P., and Suidan, M. (2010). An evidence-based environmental perspective of manufactured silver nanoparticle in syntheses and applications: a systematic review and critical appraisal of peer-reviewed scientific papers. Sci Total Environ 408(5), 999-1006.

Twentyman, P., and Luscombe, M. (1987). A study of some variables in a tetrazolium dye (MTT) based assay for cell growth and chemosensitivity. Br J Cancer 56(3), 279-285.

Urbańska, K., Pająk, B., and Orzechowski, A. (2015). The effect of silver nanoparticles (AgNPs) on proliferation and apoptosis of in ovo cultured glioblastoma multiforme (GBM) cells. Nanoscale Res Lett, 10(1), 1-11.

Wang, X., Ji, Z., Chang, C., Zhang, H., Wang, M., Liao, Y.-P., Lin, S., Meng, H., Li, R., Sun, B., et al. (2014a). Use of coated silver nanoparticles to understand the relationship of particle dissolution and bioavailability to cell and lung toxicological potential. Small 10(2), 385-398.

Wei, L., Tang, J., Zhang, Z., Chen, Y., Zhou, G., and Xi, T. (2010). Investigation of the cytotoxicity mechanism of silver nanoparticles in vitro. Biomed Mater 5(4), 44103.

Xin, L., Wang, J., Fan, G., Che, B., Wu, Y., Guo, S., and Tong, J. (2015). Oxidative stress and mitochondrial injury-mediated cytotoxicity induced by silver nanoparticles in human A549 and HepG2 cells. Environ Toxicol

Xu, T., Zhang, N., Nichols, H. L., Shi, D., & Wen, X. (2007). Modification of nanostructured materials for biomedical applications. Mater Sci Eng C, 27(3), 579-594.

Xue, Y., Zhang, T., Zhang, B., Gong, F., Huang, Y., and Tang, M. (2016). Cytotoxicity and apoptosis induced by silver nanoparticles in human liver HepG2 cells in different dispersion media. J Appl Toxicol, 36(3), 352-360.

Zhang, F., Durham, P., Sayes, C.M., Lau, B.L., and Bruce, E.D. (2015). Particle uptake efficiency is significantly affected by type of capping agent and cell line. J Appl Toxicol 35(10), 1114-1121.

Zhang, T., Wang, L., Chen, Q., and Chen, C. (2014). Cytotoxic potential of silver nanoparticles. Yonsei Med J 55(2), 283-291.

Chapter 6

Effects of citrate- silver nanoparticles on RAW 264.7 cell line using a toolbox of cytotoxic endpoints

Effects of Citrate- silver nanoparticles on RAW 264.7 cell line using a toolbox of cytotoxic endpoints

Bastos V.[1], Duarte I.F.[2], Santos C.[1,3] and Oliveira H.[1]

[1]*CESAM & Laboratory of Biotechnology and Cytomics, Department of Biology, University of Aveiro, 3810-193 Aveiro, Portugal*
[2]*CICECO, Department of Chemistry, University of Aveiro, Aveiro, Portugal*
[3]*Department of Biology, Faculty of Sciences, University of Porto, Rua do Campo Alegre, Porto, Portugal*
*corresponding author: csantos@fc.up.pt

Abstract

The influence of coating on the induced toxicity of nanoparticles (NPs) has emerged in the last year among the scientific community. Citrate coated silver nanoparticles (citrate-AgNPs) are among the most commonly used nanomaterials, widely present in industrial and biomedical products. In this study, the cytotoxicity of 30 nm AgNPs, coated with citrate, on the macrophage cell line RAW 264.7 was evaluated, using a battery of cytotoxicity endpoints (viability, oxidative stress and cytostaticity/clastogenicity). After 24 and 48h, viability, oxidative stress and cell cycle dynamics were assessed. Citrate-AgNPs decreased cell proliferation and viability only at 75 µg/mL, suggesting a low sensitivity of RAW cells to lower doses of these AgNPs. After 24h exposure, ROS content decreased in cells exposed to 60 µg/mL AgNPs (IC20 value), and the putative involvement with the high tolerance of these cells to citrate- AgNPs is discussed here. However, these cells suffered an impairment of the cell cycle, while an increase of cells at Sub-G1 phase is observed. This increase of the subG1 population is correlated with an increase of DNA fragmentation which suggests an increase of apoptosis in these cells. Regarding literature, these cells present a high IC20 for these AgNPs when compared with other cells, which may be related with the function of these cells *in vivo*.

Keywords: Cell cycle, Citrate- silver nanoparticles, Nanotoxicology, RAW 264.7, ROS, Viability.

Introduction

Nanotechnology revolution poses advantages in many fields as engineering, information technology and diagnostics. The antibacterial effects of silver nanoparticles (AgNPs) are well known rendering wide range of applications from medicine and industry to household and personal care products or clothing (Abdelhalim and Jarrar, 2011; Behra et al., 2013; Benn and Westerhoff, 2008; Eckhardt et al., 2013; EPA, 2010; Nowack et al., 2011).This extensive use of AgNPs raises the concern about safety and their possible impacts on the environment and

human health (Nowack and Bucheli, 2007; Oberdorster et al., 2005). Thus, their toxic effects on biological system should be investigated in order to monitor putative influence on health caused by chronic or acute exposure (Pumera, 2011). The widespread use of silver nanoparticles makes human exposure inevitable. It is therefore important to understand the mechanisms of toxicity of these nanoparticles, in particular in to mammalian cells. Several *in vitro* studies have reported toxic effects of AgNPs towards different types of human cells (Li et al., 2014; Smita et al., 2012; Zhang et al., 2014), but the mechanisms of AgNPs-induced toxicity are not completely understood (Browning et al., 2013). Also, the susceptibility of different cell types to AgNPs should be more deeply investigated (Zhang et al., 2015). The cell dependent toxicity could reflect, besides inherent characteristics of the cells, differences in the Ag^+ dissolution from the AgNP, cellular uptake, bioavailability or the generation of oxidative stress (AshaRani et al., 2009; Avalos et al., 2014; Wang et al., 2014).

As often reported, AgNPs are coated to promote stability and avoid aggregation, being citrate the most commonly used reducing agent and stabilizer conferring the NPs a negative charge (Sharma et al., 2009). Zhang and co-workers (2014) reported that citrate coating improves the stability of AgNPs while decreasing their toxicity. Nevertheless, other studies found that after 24h, citrate-coated AgNPs (20 and 10 nm) can be cytotoxic to human bronchial epithelial cells at concentrations ≥ 6.25 μg/mL (Wang et al., 2014) and to rat brain endothelial cells at concentrations ≥ 10 μg/mL (Grosse et al., 2013). However, more research on this field is needed to determine the cytotoxic potential of AgNPs with different physico-chemical characteristics in different cell types.

The response of macrophages to nanoparticles is an important area of investigation since these cells represent the major pathway by which early-stage defense barriers are established in skin, lungs, and mucosal systems to counteract foreign molecules (Park et al., 2011). Macrophages among the most phagocytic cell lines in the human body constitute the first line of defense upon nanosilver intake by humans and other mammals.

In this report we aimed to evaluate the effects of well characterized and sized defined citrate coated AgNPs on macrophage's viability, intracellular ROS production and cell cycle profile. For that, the RAW 264.7 cell line was exposed to 30 nm citrate-coated AgNPs. The mouse macrophage RAW 264.7 cell line is a model macrophage cell type, which is commonly used for hazard assessment and mechanistic studies in nanotoxicology (Munusamy et al., 2015; Orr et al., 2011).

Material and methods

Chemicals

Sterile, purified and endotoxin-free silver nanoparticles (Biopure AgNPs 1.0 mg/mL), with a diameter of 30 nm and a citrate surface, Cit30, were purchased from Nanocomposix Europe (Prague, Czech Republic). Dulbecco's modified Eagle's medium (DMEM), fetal bovine serum (FBS), antibiotics and phosphate buffer saline (PBS, pH 7.4) were purchased from Life Technologies (Carlsbad, CA, USA). 3-(4,5-dimethylthiazol-2-yl)-2,5-diphenyltetrazolium bromide (MTT) and dimethyl sulfoxide (DMSO) were obtained from Sigma-Aldrich (St. Louis, MO, USA). Dichlorodihydrofluorescein diacetate (DCFH2-DA) was purchased from Sigma-Aldrich, St. Louis, MO-USA. RNase and propidium iodide (PI) used in cell cycle assay was purchased from Sigma-Aldrich, St. Louis, MO-USA.

Cell Culture

The RAW 264.7 cell line, a macrophage-like cell line, was obtained from European Collection of Authenticated Cell Cultures (ECACC) and supplied by Sigma. Cell culture reagents were purchased from Life Technologies (Carlsbad, CA, USA). The cells were grown in complete medium, i.e., Dulbecco's modified Eagle's medium, supplemented with 10% fetal bovine serum (FBS), 2 mM L-glutamine, 100 U/mL penicillin, 100 µg/mL streptomycin and 250 µg/mL fungizone at 37°C in 5% CO_2 humidified atmosphere. Cells were daily observed under an inverted phase-contrast Eclipse TS100 microscope (Nikon, Tokyo, Japan). For each experiment, cells were allowed to adhere for 24h and then medium was replaced with fresh new medium containing citrate- AgNPs. The effects were measured after 24 and 48h. Throughout the experiments, cultures were routinely visualized for confluence and cell morphology.

Viability assay

Cell viability was determined by the colorimetric 3-(4,5- dimethyl-2-thiazolyl)-2,5-diphenyl tetrazolium bromide (MTT) assay (Twentyman and Luscombe, 1987). Cells were seeded in 96-well plates and cultured as described above. Cell viability was measured after 24h and 48h of citrate- AgNPs exposure at the concentrations 0, 0.5, 5, 10, 25, 50, and 75 µg/mL. Fifty microliters of MTT (1 mg/mL) in phosphate buffered saline (PBS) were then added to each well, and incubated for 4h at 37°C, 5% CO_2. Medium was then removed and 150 µL of DMSO were added to each well for solubilization of formazan crystals. The optical density of reduced MTT was measured at 570 nm in a microtiter plate reader (Synergy HT Multi-Mode, BioTeK, Winooski, VT). Three independent assays were performed with at least 2 technical replicates each and the results compared with the control (no exposure). From the MTT results, the IC50

(calculated through SigmaPlot) and IC20 was 87 µg/mL and 60 µg/mL at 24h of exposure and 79.8 µg/mL and 61.4 µg/mL at 48h of exposure, respectively. Therefore, the 24h exposure and the concentration of citrate- AgNPs corresponding IC20 was selected for the following assays.

Intracellular ROS Formation

Intracellular ROS production was assessed by flow cytometry (FCM) with the use of dichlorodihydrofluorescein diacetate (DCFH2-DA) fluorescent probe, as described previously (Ferreira de Oliveira et al., 2014). This probe enters the cells and is deacetylated by cellular esterases producing non-fluorescent DCFH2 and diacetate. In the cytosol DCFH2 is quickly oxidized to fluorescent DCF by intracellular ROS. Cells were plated in 6-well plates and after AgNPs exposure, medium was discarded and cells were incubated for 30 min, at 37ºC, in the dark with serum-free DMEM containing 10 mM DCFH2-DA. Cells were washed with PBS, trypsinised and collected for analysis. Acquisitions were made using a Coulter EPICS XL flow cytometer (Coulter Electronics, Hialeah, Florida, USA) equipped with an argon laser (15 mW, 488 nm). Acquisitions were made using SYSTEM II software v. 3.0 (Beckman Coulter, Hialeah, FL). ROS formation was estimated from the median fluorescence intensity (MFI) of DCF using the FlowJo software (Tree Star Inc., Ashland, OR-USA). For each sample, the number of events reached at least 10000.

Cell cycle and clastogenicity analysis

Cell cycle and putative clastogenic effects were analyzed by FCM according to the method previously described (Oliveira et al., 2014). Briefly, cells were seeded in 6-well plates and after exposure, they were harvested through scrapping and centrifuged twice at 300 xg for 5 min. Cells were then fixed with 85% cold ethanol and kept at -20 ºC until analysis. At the time of analysis cells were centrifuged at 300 g for 5 min, resuspended in PBS and filtered through a 35-µm nylon mesh to separate aggregates. Then, 50 µL RNase (1mg/mL) and 50 µL propidium iodide (PI) (1mg/mL) were added to each sample which were then incubated for 20 min in darkness at room temperature until analysis. The relative fluorescence intensity of the stained nuclei was measured in a Coulter XL Flow Cytometer (Beckman Coulter, Hialeah, FL-USA) equipped with an argon laser (15 mW, 488 nm). Acquisitions were made using SYSTEM II software v. 3.0 (Beckman Coulter, Hialeah, FL). For each sample, the number of nuclei analyzed was approximately 5,000. The percentage of nuclei in each phase of the cell cycle (G0/G1, S and G2 phases) was analyzed using the FlowJo software (Tree Star Inc., Ashland, Oregon, USA). In order to assess the putative clastogenic effects of Cit30 AgNPs, as described by (Misra and Easton, 1999), the coefficient of variation (CV) of the G0/G1 peak was determined.

Statistical analysis

The results are reported as mean ± standard deviation (SD) of 2 technical replicates in each of the 3 independent experiments. For all the assays, the statistical significance between control and exposed cells was performed by one-way ANOVA, followed by Dunnet and Dunn's method (as parametric and non-parametric test, respectively), using Sigma Plot 12.5 software (Systat Software Inc.). The differences were considered statistically significant from $p < 0.05$.

Results

Physicochemical characterization of AgNPs

The characteristics of water or medium solubilized citrate-AgNPs are summarized in Table 6.1, including hydrodynamic diameter (Dh), polydispersity index (PDI) and zeta potential (ζ). The three parameters increase when AgNPs were solubilized in DMEM: hydrodynamic diameter from 43.3 to 64.8 nm; polydispersity index from 0.25 to 0.4; and zeta potential from -42.7 to –8.5 mV.

Table 6.1: Hydrodynamic diameter D_h (with respective polydispersity index PdI), and zeta potential (ζ) of citrate- AgNPs (30 nm nominal diameter) dispersed in ultrapure water or in DMEM culture medium (10 µg/ml). Standard deviations calculated from 3 replicate measurements.

	D_h (nm)	PdI	ζ (mV)
In water	43.3 ± 0.5	0.25-0.26	-42.7 ± 2.7
In DMEM	64.8 ± 0.4	0.40-0.41	-8.5 ± 0.4

Effects on cell growth, viability and ROS

RAW 264.7 cells in control conditions showed typical confluence profile and morphology (Fig. 6.1a and 6.1c). When cells were exposed to 60 µg/mL citrate-coated AgNPs, their confluence decreased (Fig. 6.1b and 6.1d), especially after 48h of exposure (Fig. 6.1d). In exposed cells, some alterations on cells morphology, semblance of phagosomes, after exposure to AgNPs were noticed, including an increase of granularity and darker aspect (Fig. 6.1b and 6.1d).

The viability of RAW cells was negatively affected by citrate- AgNPs (Fig. 6.2). Relatively to controls, the viability of exposed cells was significantly reduced ($p < 0.05$) upon exposure to citrate- AgNPs at 75 µg/mL after both time exposures.

The intracellular ROS production is shown in Fig 6.3. Citrate- AgNPs significantly decrease ROS production in RAW 264.7 cells at the concentration of 60 µg/mL after 24h exposure.

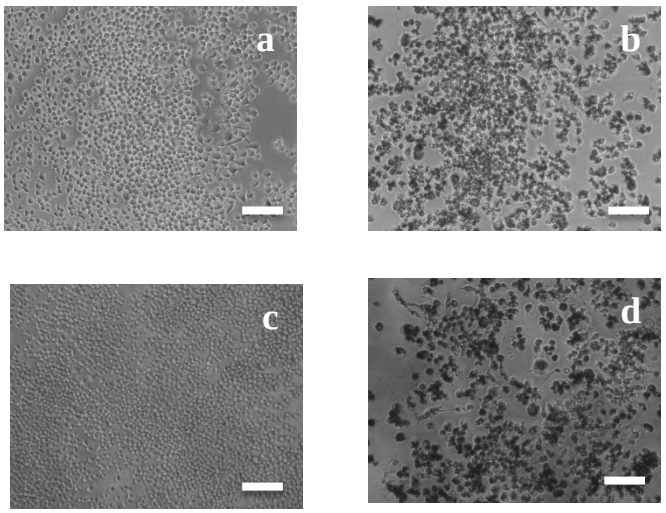

Figure 6.1: Light microscopy images (100X) of RAW 264.7 cells exposed to citrate- AgNPs for: 24h - a) 0, b) 75 µg/mL of citrate- AgNPs; and for 48h – c) 0, d) 75 µg/mL of citrate- AgNPs. Bar corresponds to 100 µm.

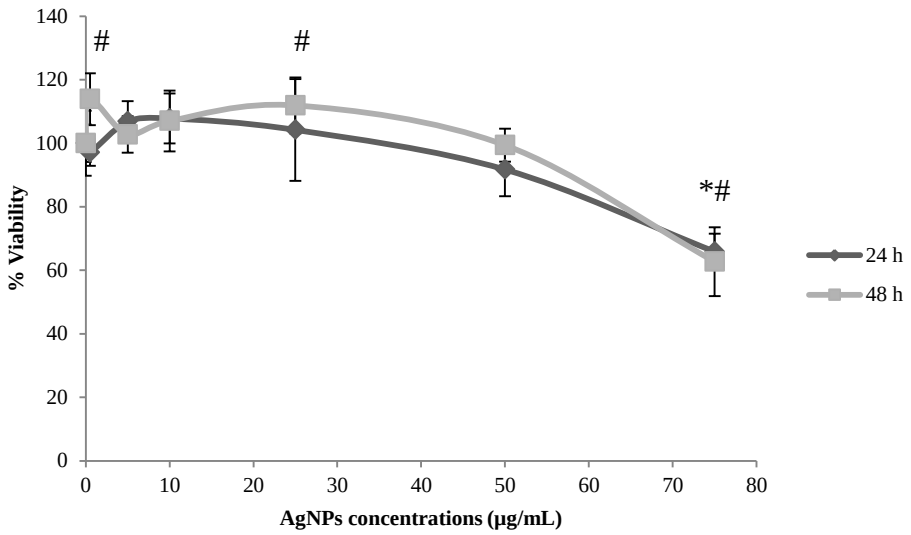

Figure 6.2: Relative cell viability (%) of RAW 264.7 after exposure to 30 nm citrate- AgNPs for 24h and 48h, measured by MTT assay. Data expressed as mean and standard deviation. * indicate significant differences between control at $p < 0.05$ for 24h and # indicate significant differences between control at $p < 0.05$ for 48h.

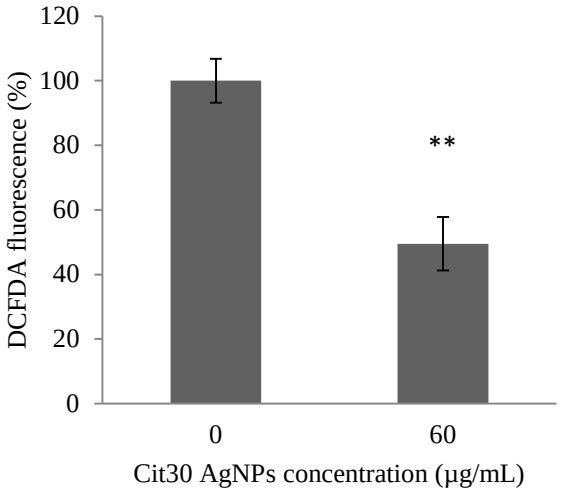

Figure 6.3: Characterization of intracellular ROS production of RAW 264.7 after exposure to citrate-AgNPs for 24h, using the DCFDA assay. The results were expressed as the mean +/- SD versus control. ** indicate significant differences between control at $p < 0.01$.

Cell cycle and clastogenicity

Figure 6.4 shows the effect of IC20 citrate- AgNPs on the cell cycle of RAW 264.7 cells. Citrate- AgNPs induced a significant increase in the percentage of cells in Sub G1 phase and a significant decrease in the percentage of cells in S and G2 ($p < 0.05$). Beyond, there is a significant increase of the coefficient of variation (CV) corresponding to G1 peak after exposure to citrate- AgNPs ($p < 0.01$). An example of histograms obtained for control cells and after 24h of exposure to 60 µg/mL citrate- AgNPs are represent in figure 6.5.

Discussion

The influence of coating has to be considered in studies of AgNPs cytoxicity, despite several publications still omit the description of coating used. Citrate-coated AgNPs have been demonstrated to exert some cytotoxic effects in some cells/tissues such as keratinocytes and liver cells (Chapter 2 and 5). This toxicity has been poorly explored in macrophages with few exceptions (eg Hamilton et al., (2014), Shannahan and Sowrirajan (2015)).

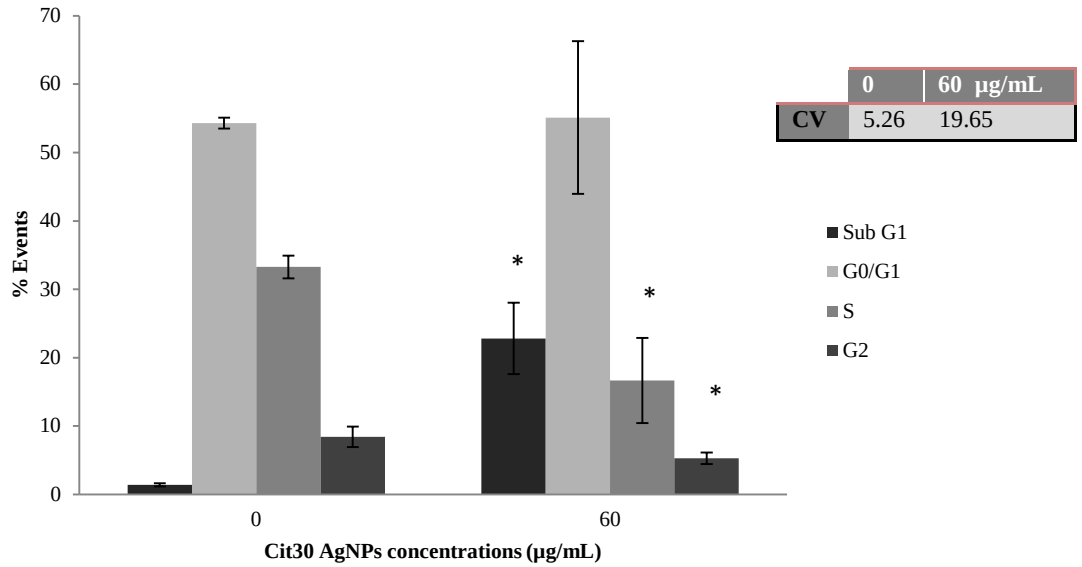

Figure 6.4: Effects of AgNPs on cell cycle dynamics, Sub G1 population and coefficient of variation (CV), measured by flow cytometry, exposed during 24h. The results were expressed as mean and standard deviation. * indicate significant differences between control at $p < 0.05$.

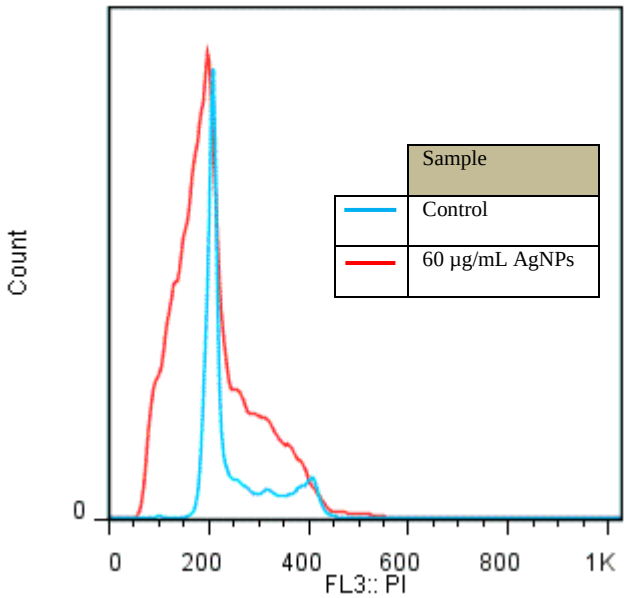

Figure 6.5: Examples of RAW 264.7 cell cycle histograms obtained after 24h of Cit30 AgNPs exposure, measured by flow cytometry.

Hamilton et al (2014) showed that smaller AgNPs (20 nm) were, regardless of coating (citrate-coated or PVP-coated) more toxic and most active in THP-1 macrophages than larger AgNPs. It was also demonstrated that macrophages internalize AgNPs agglomerates via actin-dependent

endocytosis mediated by scavenger receptors (Wang et al., 2012), but the influence of the coating on this process remains unknown. For mouse macrophage cell line RAW 264.7 and bone marrow-derived macrophages (BMDM) exposed to 20 nm citrate-coated AgNPs it was demonstrated an up-regulation expression of some inflammatory related transcripts (Aldossari et al., 2015).

Our data contributes to clarify the influence of AgNPs coated with citrate on macrophages cells, where a toolbox of cellular function endpoints were employed to determine if low citrate-AgNPs toxic concentrations (IC20) have effects on vital macrophage functions in vitro.

Different cells have different roles in our body and thus it is expectable that they behave differently to AgNPs exposure. White blood cells have greater capacity to destroy or remove foreign matter from the body since they are the cells of the immune system. More specifically macrophages actively perform phagocytic functions engulfing the particles creating phagosomes where enzymes are released into it by lysosomes. The acidic environment in the lysosomes can further contribute to dissolve the Ag ions from the AgNP. Our results showed that RAW 264.7 cells only reduced 20% of viability after exposure of 60 µg/mL Cit30 AgNPs, supporting that macrophage cells may present higher tolerance towards AgNP mediated toxicity than other cell lines. This hypothesis is in agreement with Kaur et al (2013) who found that RAW macrophages presented the least cell viability reduction (21% cell death) at 100 µg/ml of TSNPs (AgNPs synthesized by reduction with tannic acid) compared with A431 (skin epithelial) and A549 (lung epithelial). They also concluded that RAW cells "engulf" silver nanoparticles and thus resist any toxic response. Zhang et al (2015) exposed RAW 264.7 cells to a range of citrate-AgNPs concentrations (0.1-50 µg/mL) and also obtained less than 20% of viability reduction. Otherwise, a study on the cytotoxic potential of tannic acid modified AgNPs (13, 33 and 46 nm) reported a significantly decrease on RAW 264.7 cells viability after exposure to 2.5 µg/mL AgNPs (Orlowski et al., 2013). Other study on toxicity of Ag/SiO2 particles in murine macrophage RAW 264.7 highlighted the influence of size and their release of Ag^{+} ions on their toxicity potential (Pratsinis et al., 2013). The authors obtained significant viability decrease after exposure to ~ 20 nm Ag/SiO2 particles for concentrations ≥ 20 µg/mL, while for ~ 10 nm Ag/SiO2 particles significant decrease begins at concentrations ≥ 10 µg/mL. On the other hand, a study on the cytotoxic effects of AgNPs coated with a peptide layer on a human macrophage cell line (THP-1) obtained IC50 values of 110 µg/mL for 20nm AgNPs and 140 µg/mL for 40 nm AgNPs after 24h of exposure, while after 48h was 18 µg/mL for 20 nm AgNPs and 30 µg/mL for 40 nm AgNPs, stressing the size and time dependent toxicity (Hasse et al., 2011).

Although the induction of ROS is a common in vitro response to AgNPs exposure (Arora et al., 2008; Hussain et al., 2005), in our work we could not find evidences of ROS induction, and on the contrary, a 50% decrease in the ROS levels was detected for Raw cells exposed to AgNPs at

IC20. Other studies also failed to present evidences of ROS increase upon AgNPs exposure. For instance, Gliga et al (2014) investigated the ROS formation upon exposure to AgNPs of 10-75 nm uncoated or coated with PVP or citrate and found no changes in ROS generation in BEAS-2B cells. In another study Kaur et al (2013) found that TSNPs (AgNPs synthesized by reduction with tannic acid) at 50 µg/mL did not induce significant ROS generation in RAW macrophages while increasing in more sensitive cells (lung cell line A549 and epidermoid carcinoma cell line A431).

Also, the observed decrease of ROS levels in macrophages exposed to such low levels of AgNPs supports the hypothesis that these cells present a good adaptive mechanism to cope with AgNPs inside the cell. This may involve an induction of the total antioxidant battery in response to exposure this low dose of AgNPs, reducing the ROS intracellular content.

A significant increase in the sub-G0/G1 population was observed in RAW cell exposed to AgNPs. The increase in Sub G1 population may be related to DNA fragmentation often associated with apoptosis (Kajstura et al., 2007). Park et al (2010) after exposure RAW 264.7 cells to 1.6 µg/mL AgNPs also obtained a significant increase of cells at Sub G1 phase suggesting, as in our results, the occurrence of apoptosis. Concerning cell cycle dynamics, RAW 264.7 cells were extremely affected by AgNPs exposure. Moreover, the significant increase of the coefficient of variation could be related to clastogenic potential of citrate-AgNPs on RAW 264.7 cells (Misra and Easton 1999). On other hand, the arrest at G0/G1 phase may support the observed decreases of cells in both S and G2 phases. Sasidharan et al (2011) obtained similar histograms for nasopharyngeal carcinoma cell line (KB) cells after 24h exposure of 200 and 300 µM ZnO nanocrystals (NCs). Similarly, RAW 264.7 cells showed a decrease in S phase and increases of cells in G0/G1 and sub G1 after exposure to 0.01 µg/mL of SiO2 NPs (10 nm). The authors indicated that although there was no decrease in cell viability, a subpopulation of cells (between 12% and 15% at sub G1) underwent apoptosis (Bancos et al., 2015).

Comparing to our previous studies on cytotoxic potential of the same citrate- AgNPs on human keratinocyte cell line (HaCaT) and hepatocellular carcinoma cell line (HepG2), RAW 264.7 cell line was, undoubtable the less sensible, with the higher IC20 value (60 µg/mL) (Chapter 2 and 5), which demonstrates that different cell types have different susceptibility to AgNPs and that the toxicological profile of AgNPs must not be generalized for individual nanoparticles.

In conclusion, our study demonstrates that the widely used citrate-coated AgNPs only induced a significant decrease on viability of RAW at higher concentrations (75 µg/mL). In addiction citrate-AgNPs did not induce ROS production, in opposition, decreased ROS production on RAW 264.7 cell line. However, AgNPs have a great impact on cell cycle progression of RAW cells. Beyond the apparent cytostatic effect, AgNPs induced a population at Sub G1 phase,

associated with apoptosis/necrosis. Thus, and reporting our previous works, we can conclude that toxicity of AgNPs varies with the cell type and their toxicological profile could not be generalized for individual nanoparticles. Instead, a long data based should be done to determine the toxicity profile of the different sized and coated AgNPs in each cell type.

Acknowledgments

This work was developed in the scope of the projects CICECO-Aveiro Institute of Materials (Ref. FCT UID/CTM/50011/2013) and CESAM (Ref. FCT UID/AMB/50017/2013), financed by national funds through the FCT/MEC and when applicable co-financed by the European Regional Development Fund (FEDER) under the PT2020 Partnership Agreement. Funding to the project FCOMP-01-0124-FEDER-021456 (Ref. FCT PTDC/SAU-TOX/120953/2010) by FEDER through COMPETE and by national funds through FCT, and the FCT-awarded grants (SFRH/BD/81792/2011; SFRH/BPD/48853/2008) are acknowledged. I.F.D and A.L.D.S. acknowledge FCT/MCTES for the research contracts under the Program 'Investigador FCT' 2014.

Contributions

V.B. participated in the design experiment with the supervisors and did all laboratorial experiments and statistical data analyses. Also had a key role in the data analyses integration, and together with the supervisors wrote and revised the manuscripts. C.S. and H.O. planned the experimental design, contributed to data analyses and integration of all data, and in the manuscript preparation. I.F.D. coordinated NPs analyses and revised the manuscript.

References

Abdelhalim, M.A.K., and Jarrar, B.M. (2011). Renal tissue alterations were size-dependent with smaller ones induced more effects and related with time exposure of gold nanoparticles. Lipids Health Dis, 10(1), 1.

Aldossari, A.A., Shannahan, J.H., and Podila, R. (2015). Scavenger receptor B1 facilitates macrophage uptake of silver nanoparticles and cellular activation. J Nanopart Res 17(7), 1-14.

Arora, S., Jain, J., Rajwade, J. M., & Paknikar, K. M. (2008). Cellular responses induced by silver nanoparticles: in vitro studies. Toxicol Lett, 179(2), 93-100.

AshaRani, P., Low Kah Mun, G., Hande, M., and Valiyaveettil, S. (2009). Cytotoxicity and genotoxicity of silver nanoparticles in human cells. ACS nano, 3(2), 279-290.

Avalos, A., Haza, A.I., Mateo, D., and Morales, P. (2014). Cytotoxicity and ROS production of manufactured silver nanoparticles of different sizes in hepatoma and leukemia cells. J Appl Toxicol 34(4), 413-423.

Bancos, S., Stevens, D.L., and Tyner, K.M. (2015). Effect of silica and gold nanoparticles on macrophage proliferation, activation markers, cytokine production, and phagocytosis in vitro. Int J Nanomed 10, 183-206.

Behra, R., Sigg, L., Clift, M., Herzog, F., Minghetti, M., Johnston, B., Petri-Fink, A., and Rothen-Rutishauser, B. (2013). Bioavailability of silver nanoparticles and ions: from a chemical and biochemical perspective. J R Soc Interface, 10(87), 20130396.

Benn, T., and Westerhoff, P. (2008). Nanoparticle silver released into water from commercially available sock fabrics. Environ Sci Technol, 42(11), 4133-4139.

Browning, L., Lee, K., Nallathamby, P., and Xu, X.-H.N. (2013). Silver nanoparticles incite size- and dose-dependent developmental phenotypes and nanotoxicity in zebrafish embryos. Chem Res Toxicol 26(10), 1503-1513.

Eckhardt, S., Brunetto, P., Gagnon, J., Priebe, M., Giese, B., and Fromm, K. (2013). Nanobio silver: its interactions with peptides and bacteria, and its uses in medicine. Chem Rev 113(7), 4708-4754.

EPA, E.P.A. (2010). State of the Science Literature Review: Everything Nanosilver and More. Scientific, Technical, Research, Engineering and Modeling Support Final Report.

Ferreira de Oliveira JM, Costa M, Pedrosa T, Pinto P, Remédios C, Oliveira H, Pimentel F, Almeida L, Santos C. (2014). Sulforaphane induces oxidative stress and death by p53-independent mechanism: implication of impaired glutathione recycling. PloS one, 9(3), e92980.

Gliga, A., Skoglund, S., Odnevall Wallinder, I., Fadeel, B., and Karlsson, H. (2014). Size-dependent cytotoxicity of silver nanoparticles in human lung cells: the role of cellular uptake, agglomeration and Ag release. Part Fibre Toxicol, 11(1), 1.

Grosse, S., Evje, L., and Syversen, T. (2013). Silver nanoparticle-induced cytotoxicity in rat brain endothelial cell culture. Toxicol In Vitro 27(1), 305-313.

Haase, A., Tentschert, J., Jungnickel, H., Graf, P., Mantion, A., Draude, F., Plendl, J., Goetz, M.E., Galla, S., Masic, A., Thuenemann, A.F., Taubert, A., Arlinghaus, H.F. and Luch, A., (2011). Toxicity of silver nanoparticles in human macrophages: uptake, intracellular distribution and cellular responses. J. Phys.: Conf. Ser (Vol. 304, No. 1, p. 012030). IOP Publishing.

Hamilton, R.F., Buckingham, S., and Holian, A. (2014). The effect of size on Ag nanosphere toxicity in macrophage cell models and lung epithelial cell lines is dependent on particle dissolution. Int J Mol Sci 15(4), 6815-6830.

Hussain, S. M., Hess, K. L., Gearhart, J. M., Geiss, K. T., & Schlager, J. J. (2005). In vitro toxicity of nanoparticles in BRL 3A rat liver cells. Toxicol In Vitro, 19(7), 975-983.

Kajstura, M., Halicka, H.D., Pryjma, J., and Darzynkiewicz, Z. (2007). Discontinuous fragmentation of nuclear DNA during apoptosis revealed by discrete "sub-G1" peaks on DNA content histograms. Cytometry A 71(3), 125-131.

Kaur, J., and Tikoo, K. (2013). Evaluating cell specific cytotoxicity of differentially charged silver nanoparticles. Food Chem Toxicol 51, 1-14.

Li, Y., Zhang, Y., and Yan, B. (2014). Nanotoxicity overview: nano-threat to susceptible populations. Int J Mol Sci 15(3), 3671-3697.

Misra, R., and Easton, M. (1999). Comment on analyzing flow cytometric data for comparison of mean values of the coefficient of variation of the G1 peak. Cytometry 36(2), 112-116.

Munusamy, P., Wang, C., Engelhard, M.H., Baer, D.R., Smith J.N., Liu C., Kodali V., Thrall B.D., Chen S., Porter A.E., and Ryan M.P.. (2015). Comparison of 20 nm silver nanoparticles synthesized with and without a gold core: Structure, dissolution in cell culture media, and biological impact on macrophages. Biointerphases, 10(3), 031003.

Nowack, B., and Bucheli, T. (2007). Occurrence, behavior and effects of nanoparticles in the environment. Environ Pollut 150(1), 5-22.

Nowack, B., Krug, H., and Height, M. (2011). 120 years of nanosilver history: implications for policy makers. Environ Sci Technol 45(4), 1177-1183.

Oberdorster, G., Maynard, A., Donaldson, K., Castranova, V., Fitzpatrick, J., Ausman, K., Carter, J., Karn, B., Kreyling, W., Lai, D., et al. (2005). Principles for characterizing the potential human health effects from exposure to nanomaterials: elements of a screening

strategy. Part Fibre Toxicol 2, 8.
Oliveira, H., Monteiro, C., Pinho, F., Pinho, S., Ferreira de Oliveira, J.M., and Santos, C. (2014). Cadmium-induced genotoxicity in human osteoblast-like cells. Mutat Res Genet Toxicol Environ Mutagen 775-776, 38-47.
Orlowski, P., Krzyzowska, M., Zdanowski, R., Winnicka, A., Nowakowska, J., Stankiewicz, W., Tomaszewska, E., Celichowski, G., and Grobelny, J. (2013). Assessment of in vitro cellular responses of monocytes and keratinocytes to tannic acid modified silver nanoparticles. Toxicol In Vitro 27(6), 1798-1808.
Orr, G.A., Chrisler, W.B., Cassens, K.J., Tan, R., Tarasevich, B.J., Markillie, L.M., Zangar, R.C., and Thrall, B.D. (2011). Cellular recognition and trafficking of amorphous silica nanoparticles by macrophage scavenger receptor A. Nanotoxicology 5(3), 296-311.
Park, E.-J.J., Yi, J., Kim, Y., Choi, K., and Park, K. (2010). Silver nanoparticles induce cytotoxicity by a Trojan-horse type mechanism. Toxicol InVitro 24(3), 872-878.
Park, J., Lim, D.-H.H., Lim, H.-J.J., Kwon, T., Choi, J.-s.S., Jeong, S., Choi, I.-H.H., and Cheon, J. (2011). Size dependent macrophage responses and toxicological effects of Ag nanoparticles. Chem Commun (Camb) 47(15), 4382-4384.
Pratsinis, A., Hervella, P., Leroux, J. C., Pratsinis, S. E., & Sotiriou, G. A. (2013). Toxicity of silver nanoparticles in macrophages. Small, 9(15), 2576-2584.
Pumera, M. (2011). Nanotoxicology: the molecular science point of view. Chem Asian J 6(2), 340-348.
Sasidharan, A., Chandran, P., Menon, D., Raman, S., Nair, S., and Koyakutty, M. (2011). Rapid dissolution of ZnO nanocrystals in acidic cancer microenvironment leading to preferential apoptosis. Nanoscale 3(9), 3657-3669.
Shannahan, J.H., and Sowrirajan, H. (2015). Impact of Silver and Iron Nanoparticle Exposure on Cholesterol Uptake by Macrophages. J Nanomater 501,127235.
Sharma, V., Yngard, R., and Lin, Y. (2009). Silver nanoparticles: green synthesis and their antimicrobial activities. Adv Colloid Interface Sci 145(1), 83-96.
Smita, S., Gupta, S., Bartonova, A., Dusinska, M., Gutleb, A., and Rahman, Q. (2012). Nanoparticles in the environment: assessment using the causal diagram approach. Environ Health. 11(Suppl 1), S13
Twentyman, P., and Luscombe, M. (1987). A study of some variables in a tetrazolium dye (MTT) based assay for cell growth and chemosensitivity. Br J Cancer 56(3), 279-285.
Wang, H., Wu, L., and Reinhard, B.M.M. (2012). Scavenger receptor mediated endocytosis of silver nanoparticles into J774A.1 macrophages is heterogeneous. ACS Nano 6(8), 7122-7132.
Wang, X., Ji, Z., Chang, C., Zhang, H., Wang, M., Liao, Y.-P., Lin, S., Meng, H., Li, R., Sun, B., et al. (2014a). Use of coated silver nanoparticles to understand the relationship of particle dissolution and bioavailability to cell and lung toxicological potential. Small 10(2), 385-398.
Zhang, H., Wang, X., Wang, M., Li, L., Chang, C.H., Ji, Z., Xia, T., and Nel, A.E. (2015). Mammalian Cells Exhibit a Range of Sensitivities to Silver Nanoparticles that are Partially Explicable by Variations in Antioxidant Defense and Metallothionein Expression. Small 11(31), 3797-3805.
Zhang, T., Wang, L., Chen, Q., and Chen, C. (2014). Cytotoxic potential of silver nanoparticles. Yonsei Med J 55(2), 283-291.

Chapter 7

General Conclusions

General Conclusions

At the beginning of this study, we assessed size dependent cytotoxicity of citrate- AgNPs (10 nm, 30 nm and 60 nm AgNPs) to HaCaT cells, through MTT assay (Fig. A1 and A2; Annex). We found that the decrease of viability was higher for 30 nm AgNPs exposed cells, thus we preceded the studies using 30 nm AgNPs. AgNPs with 10 nm was only used at inflammatory responses study in order to determine the influence of the size.

In this work, we have investigated the cellular effects of well-characterized AgNPs with different coatings (citrate and PEG) and the same nominal diameter (30 nm or 10 nm), in order to address the influence of NP surface on biological outcomes, assessing cell proliferation and viability, oxidative stress, inflammatory responses, apoptosis, cytostaticity, DNA damage, micronuclei (MNi) induction, and the less commonly reported changes in cell cycle dynamics. Further motivation arose from the growing interest in using PEG-coated NPs in nanomedicine applications (Povoski et al., 2013; Thorley and Tetley, 2013), thus making it timely and useful to report on the cytotoxic effects of such particles.

Our study has shown that largely used citrate-coated AgNPs decreased the viability of the keratinocytes cells (HaCaT) more severely than the emerging PEG-coated AgNPs. This difference was not due to putative effects of the coating molecules *per se* (as they produced no cytotoxicity), neither to the extent of extracellular release of ionic silver. However, our study demonstrates that citrate-coated and PEG- coated AgNPs decrease viability of hepatoma cells (HepG2) in a similar way. Thus, for HepG2 cells the cytotoxicity of AgNPs is independent of the studied coatings.

The differently coated AgNPs produced in HaCaT distinct effects regarding the mode of cell death and cell cycle progression. While Cit30 AgNPs clearly induced apoptotic death, cells exposed to PEG30 AgNPs appeared to be at an earlier phase of apoptosis mechanisms, as supported by gene expression analysis. Concerning the impact on cell cycle progression, both Cit30 and PEG30 AgNPs affected cell cycle regulation of HaCaT cells, but, again, citrate-coating induced more drastic effects, showing earlier downregulation of cyclin B1 gene and blockage of cells at G2. However, both AgNPs increased similarly the amount of ROS produced by HaCaT cells.

Concerning the effects of citrate- and PEG- AgNPs on HepG2, both AgNPs did not induced apoptosis for the studied concentrations and the apoptotic related genes BCL2 and BAX were downregulated. HepG2 showed the same profile of cell cycle dynamics after exposure to both AgNPs, where, for the higher concentration, there was an increase of the percentage of cells at S and G2 phases. Gene expressions of cyclins CCNB1 and CCNE1 were also downregulated.

PEG10 AgNPs at high concentrations inactivate the transcription factor, NF-kB, in HaCaT cells

and putative correlation with anti-inflammatory and antiapoptotic homeostasis should be further explored. It was demonstrated that, independently of the coating, 10 nm and 30 nm AgNPs do maintain cytokins release at undetectable levels, and decreases MCP-1 release, which is in line with part of the literature, though this remains a controversial topic, most probably due to the complex varieties involved.

Our study also demonstrates that citrate- AgNPs induced DNA damage to HaCaT cells increasing their genetic damage. Also, these NPs induced MNi, increased mononucleated cells and decreased binucleated cells, being, thus, cytostatic for HaCaT cells by decreasing their nuclear division index.

However, our study showed that the widely used citrate-coated AgNPs only induced a significant decrease on viability of mouse monocyte/macrophage cells (RAW 264.7) at higher concentrations (75 µg/mL). In addition citrate- AgNPs did not induce ROS production, in opposition, decreased ROS production on RAW 264.7 cell line. However, AgNPs have a great impact on cell cycle progression of RAW cells. Beyond the apparent cytostatic effect, AgNPs induced a population at Sub G1 phase, commonly associated to apoptosis/necrosis.

Therefore, we can conclude that toxicity of AgNPs varies within the cell type, since, HepG2 was more sensitive to AgNPs, followed by HaCaT cells and finally RAW 264.7 cells. These last ones have the greatest IC20 value comparing to HaCaT and HepG2 cells, and this fact could be due to a good adaptative mechanism to cope with AgNPs inside the cell by macrophages, since it has been proposed elsewhere that they may "engulf" silver nanoparticles and thus resist any toxic response.

Thus, we can conclude that AgNPs toxicological profile could not be generalized for individual nanoparticles. Instead, a long data based should be done to determine the toxicity profile of the different sized and coated AgNPs in each cell type.

Considering that AgNPs are present in a vast number of consumer products, it is important to determine if or which NPs are more cytotoxic. Our study suggests that PEG-coating can be regarded as a good alternative to citrate stabilization of AgNPs used in industrial and medical applications towards human skin cells. However, for hepatocyte cells, AgNPs cytotoxic potential was coating independent for these studied conditions.

As future work, additional cytotoxic studies, including metabolomics and other –omics approaches, could be performed to better understand the mechanisms of AgNPs toxicity and their underlying pathways of toxicity/cell resistance.

In order to get a better knowledge on what might be happening in all the human body, other cell lines should be used to determine the cytotoxic potential of AgNPs representing other human

organs, supporting laboratory *in vivo* assays. Also, the characterization of AgNPs effects in inflammatory responses is at its infancy and deserves further studies, combining multiple analyses, *omics* and *in vitro vs in vivo* assays.

Finally, a major conclusion from our work points that the largely used citrate AgNPs are cytotoxic, and further studies to find effective coating alternatives for health/cosmetic industry must be performed to search for AgNPs less toxic to human health (as PEG has demonstrated to be *in vitro*).

References

Povoski, S.P., Davis, P.D., Colcher, D., and Martin, E.W. (2013). Single molecular weight discrete PEG compounds: emerging roles in molecular diagnostics, imaging and therapeutics. Expert Rev Mol Diagn 13(4), 315-319.

Thorley, A.J., and Tetley, T.D. (2013). New perspectives in nanomedicine. Pharmacol Ther 140(2), 176-185.

Annex

Annex

Results from a preliminary assay where 10 nm citrate- AgNPs and 60 nm citrate- AgNPs were used, together with 30 nm citrate- AgNPs (Fig. 2.4a, Chapter 2), to assess the size dependent cytotoxicity in HaCaT cells in order to continue the other assays using the size that induced the higher reduction on viability (30 nm).

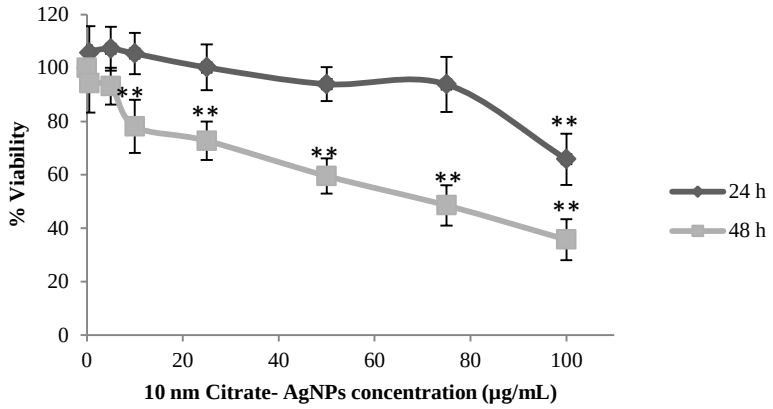

Figure A1: Relative cell viability (%) of HaCaT after exposure to 10 nm citrate- AgNPs for 24h and 48h, measured by MTT assay. Data expressed as mean and standard deviation. ** indicate significant differences between control at $p < 0.01$.

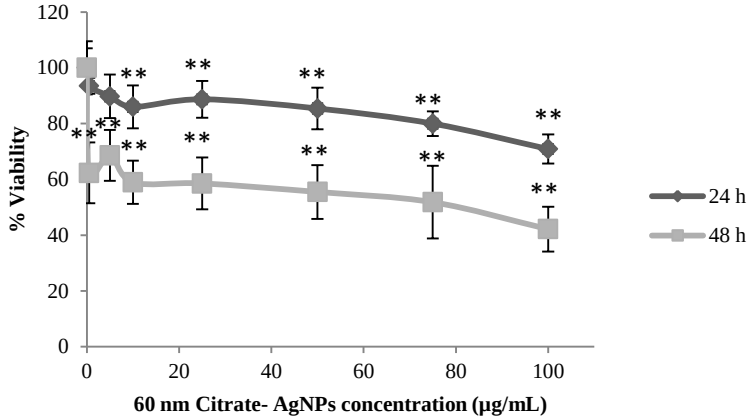

Figure A2: Relative cell viability (%) of HaCaT after exposure to 60 nm citrate- AgNPs for 24h and 48h, measured by MTT assay. Data expressed as mean and standard deviation. ** indicate significant differences between control at $p < 0.01$